PLACE IN RETURN BOX to remove this checkout from your record.
TO AVOID FINES return on or before date due.

DATE DUE	DATE DUE	DATE DUE

A NUMERICAL METHOD FOR THE SOLUTION OF PLANE STEADY-STATE THERMOELASTIC FRACTURE MECHANICS PROBLEMS

By

Nengquan Liu

A DISSERTATION

Submitted to

Michigan State University

in partial fulfillment of the requirements

for the degree of

DOCTOR OF PHILOSOPHY

Department of Metallurgy, Mechanics and Materials Science

1991

ABSTRACT

A NUMERICAL METHOD FOR THE SOLUTION OF PLANE STEADY-STATE THERMOELASTIC FRACTURE MECHANICS PROBLEMS

By

Nengquan Liu

An efficient numerical technique is developed for plane, homogeneous, isotropic, steady-state thermoelasticy problems involving arbitrary internal smooth and/or kinked cracks. The thermal stress intensity factors and relative crack surface displacements due to steady-state temperature distributions are determined and compared to available solutions obtained by other methods. In these analyses, the thermal boundary conditions across the crack surface are assumed to be insulated. The present approach involves coupling the direct boundary-integral equations to newly-developed crack integral equations.

This new method has distinct advantages over the Finite Element Methods (FEM) and Boundary Element Methods (BEM), since the FEM treatment requires fine discretization in the vicinity of crack tips or the use of special crack-tip elements, and the BEM treatment requires division of the body into two regions and solution the coupled problems. Both treatments require continual remeshing for crack propagation studies.

To my father and mother.

Acknowledgments

I would like to express my appreciation to my advisor Professor Nicholas J. Altiero, Associate Dean of Engineering, for his excellent support and valuable assistance throughout this work. I also would like to thank, the members of my guidance committee, Professor Thomas J. Pence, Professor Yvonne Jasiuk and Professor David Y. S. Yen, for their support and assistance. A final note of appreciation must go to my father and mother for their great support and encouragement throughout all these years.

Funding of this research by the State of Michigan Research Excellence Fund is most gratefully acknowledged.

Table of Contents

List of Tables

List of Figures

Chapter 1 Introduction and Background 1

Chapter 2 Mode I and Mode II Crack Problems

2.1 Cracks 7

2.1.1 Theoretical Development 8

2.1.2 Numerical Treatment 14

2.1.2.1 A Single Smooth or Kinked Crack 14

2.1.2.2 A Branch Crack or Multiple Cracks 19

2.1.3 Results 33

2.2 Edge Cracks 68

2.2.1 Theoretical Development 68

2.2.2 Numerical Treatment 72

2.2.2.1 A Single Edge Crack 72

2.2.2.2 An Edge Branch Crack 76

2.2.3 Results 83

Chapter 3 Model III Crack Problems: Internal Cracks

3.1 Theoretical Development 92

3.2 Numerical Treatment 94

3.2.1 A Single Smooth or Kinked Crack 94

3.2.2 A Branch Crack or Multiple Cracks 98

3.3 Results 107

Chapter 4 Thermoelastic Problems Involving Cracks

4.1 Theoretical Development 123

4.2 Numerical Treatment 128

4.3 Results 137

Chapter 5 Conclusions 147

References 148

Appendix A In-plane Elasticity Influence Functions 159

Appendix B Complementary Elasticity Influence Functions 161

Appendix C Anti-plane Elasticity Influence Functions 164

Appendix D Reduction of Domain Integrals to Boundary Integrals 165

Appendix E Heat Transfer Influence Functions 168

Appendix F Computer Program for Matrices 170

List of Tables

Table 2.1 Stress intensity factors for a straight central crack in a finite plate.

Table 2.2 Stress intensity factors for a straight central slant crack in a finite plate $\gamma = 22.5^{\circ}$.

Table 2.3 Stress intensity factors for a straight central slant crack in a finite plate $\gamma = 45.0^{\circ}$.

Table 2.4 Stress intensity factors for a straight central slant crack in a finite plate $\gamma = 67.5^{\circ}$.

Table 2.5 Stress intensity factors for the Z-shaped crack of Figure 17 in a finite plate.

Table 2.6 Stress intensity factors for the Z-shaped crack of Figure 18 in a finite plate.

Table 2.7 Stress intensity factors for two equal-length collinear cracks in a finite plate.

Table 2.8 Stress intensity factors for two equal-length offset cracks in a finite plate, tip A.

Table 2.9 Stress intensity factors for two equal-length offset cracks in a finite plate, tip B.

Table 2.10 Stress intensity factors for two equal-length offset cracks in a finite plate, tip C.

Table 2.11 Stress intensity factors for two equal-length offset cracks in a finite plate, tip D.

Table 2.12 Stress intensity factors for a straight crack and a kinked crack in a finite plate.

Table 2.13 Stress intensity factors for a branch crack in a finite plate, h/w=1.0, 2a/w=0.5.

Table 2.14 Stress intensity factors for a branch crack in a finite plate, $\alpha=45^{o}$, h/w=1.0.

Table 2.15 Stress intensity factors for a branch crack in a finite plate, $\alpha=45^{o}$, 2a/w=0.5.

Table 2.16 Stress intensity factors for a single edge cracked plate under uniform tension.

Table 2.17 Stress intensity factors for a single edge cracked plate under uniform tension, L/w=1.0.

Table 2.18 Stress intensity factors for a single slanted edge cracked plate.

Table 2.19 Stress intensity factors for a single edge cracked plate as shown in Figure 2.34.

Table 3.1 Stress intensity factors for a straight central crack under a uniformly distributed shear stress as shown in Figure 3.1.

Table 3.2 Stress intensity factors for a straight central crack with fixed edges parallel to the crack as shown in Figure 3.2.

Table 3.3 Stress intensity factors for a straight central crack with fixed edges perpendicular to the crack as shown in Figure 3.3.

Table 3.4 Stress intensity factors for a straight central crack with four fixed edges as shown in Figure 3.4.

Table 3.5 Stress intensity factors for a symmetric V-shaped crack under a uniformly distributed shear stress as shown in Figure 3.5.

Table 3.6 Stress intensity factors for an asymmetric kinked crack under a uniformly distributed shear stress as shown in Figure 3.7.

Table 3.7 Stress intensity factors for an anti-symmetric kinked crack under a uniformly distributed shear stress as shown in Figure 3.9.

Table 4.1 Thermal stress intensity factors $K_{II} / \alpha_t ET (w)^{1/2}$ for an insulated straight central crack.

List of Figures

Figure 2.1 Source point, $\overline{\mathbf{x}}$, and field point, $\mathbf{x}$, in an infinite plane.

Figure 2.2 Plane elastic region containing a crack.

Figure 2.3 Plane elastic region containing a branch crack.

Figure 2.4 Plane elastic region containing multiple cracks.

Figure 2.5 Discretized plane region containing a discretized crack.

Figure 2.6 Discretized plane region containing a discretized branch crack.

Figure 2.7 Discretized plane region containing discretized multiple cracks.

Figure 2.8 Discretization for a straight crack.

Figure 2.9 Geometry and loading for a straight central crack in a finite plate.

Figure 2.10 Geometry and loading for a straight central slant crack in a finite plate.

Figure 2.11 Geometry and loading for a symmetric V-shaped crack in a finite plate.

Figure 2.12 Relative crack surface displacement Δu_1 for a body containing a symmetric V-shaped crack and subjected to pure shear.

Figure 2.13 Relative crack surface displacement Δu_2 for a body containing a symmetric V-shaped crack and subjected to pure shear.

Figure 2.14 Geometry and loading for a non-symmetric V-shaped crack in a finite plate.

Figure 2.15 Relative crack surface displacement Δu_n for a body containing a non-symmetric V-shaped crack and subjected to uniform uniaxial tensile stress.

Figure 2.16 Relative crack surface displacement Δu_t for a body containing a non-symmetric V-shaped crack and subjected to uniform uniaxial tensile stress.

Figure 2.17 Geometry and loading for a Z-shaped crack in a finite plate, case 1.

Figure 2.18 Geometry and loading for a Z-shaped crack in a finite plate, case 2.

Figure 2.19 Discretization for a Z-shaped crack.

Figure 2.20 Relative crack surface displacement Δu_1 for a body containing a Z-shaped crack as shown in Figure 2.17.

Figure 2.21 Relative crack surface displacement Δu_2 for a body containing a Z-shaped crack as shown in Figure 2.17.

Figure 2.22 Geometry and loading for two equal-length collinear cracks in a finite plate.

Figure 2.23 Geometry and loading for two equal-length offset cracks in a finite plate.

Figure 2.24 Geometry and loading for a straight crack and a kinked crack in a finite plate.

Figure 2.25 Geometry and loading for a branch crack in a finite plate.

Figure 2.26 Relative crack surface displacement Δu_1 for a body containing a branch crack and subjected to uniform uniaxial stress.

Figure 2.27 Relative crack surface displacement Δu_2 for a body containing a branch crack and subjected to uniform uniaxial stress.

Figure 2.28 Half-plane elastic region containing a single edge crack.

Figure 2.29 Half-plane elastic region containing an edge branch crack.

Figure 2.30 Discretized half-plane region containing a discretized single edge crack.

Figure 2.31 Discretized half-plane region containing a discretized edge branch crack.

Figure 2.32 Geometry and loading of a rectangular plate with a single edge crack.

Figure 2.33 Geometry and loading of a rectangular plate with a single slanted edge crack.

Figure 2.34 Geometry and loading of a rectangular plate with a single edge crack.

Figure 3.1 Geometry and loading for a straight central crack in a finite sheet under a uniformly distributed shear stress.

Figure 3.2 Geometry and loading for a straight central crack in a finite sheet with fixed edges parallel to the crack.

Figure 3.3 Geometry and loading for a straight central crack in a finite sheet with fixed edges perpendicular to the crack.

Figure 3.4 Geometry and loading for a straight central crack in a finite sheet with four fixed edges.

Figure 3.5 Geometry and loading for a symmetric V-shaped crack in a finite sheet under a uniformly distributed transverse shear stress.

Figure 3.6 Relative crack surface displacement Δu_3 for a symmetric V-shaped crack.

Figure 3.7 Geometry and loading for an asymmetric kinked crack in a finite sheet under a uniformly distributed transverse shear stress.

Figure 3.8 Relative crack surface displacement Δu_3 for an asymmetric kinked crack.

Figure 3.9 Geometry and loading for an anti-symmetric kinked crack in a finite sheet under a uniformly distributed transverse shear stress.

Figure 3.10 Relative crack surface displacement Δu_3 for an anti-symmetric kinked crack.

Figure 4.1 Heat transfer problem involving a crack.

Figure 4.2 Thermoelasticity problem involving a crack.

Figure 4.3 Geometry and thermal loading for an insulated straight central crack in a finite plate.

Figure 4.4 Relative crack surface thermal displacement Δu_t for a body containing an insulated straight central crack, a/w=0.1.

Figure 4.5 Relative crack surface thermal displacement Δu_t for a body containing an insulated straight central crack, a/w=0.2.

Figure 4.6 Relative crack surface thermal displacement Δu_t for a body containing an insulated straight central crack, a/w=0.3.

Figure 4.7 Relative crack surface thermal displacement Δu_t for a body containing an insulated straight central crack, a/w=0.4.

Figure 4.8 Relative crack surface thermal displacement Δu_t for a body containing an insulated straight central crack, a/w=0.5.

Figure 4.9 Relative crack surface thermal displacement Δu_t for a body containing an insulated straight central crack, a/w=0.6.

Chapter 1

Introduction and Background

During the last three decades powerful methods have been developed for numerical analysis. The most popular and efficient ones are Finite Element Methods (FEM), Finite Difference Methods (FDM), Boundary Element Methods (BEM) and coupled techniques. In recent years, the BEM has received considerable attention for analysis of many practical problems in science and engineering. The effort has been particularly intense in the area of stress analysis and thermal analysis of cracks where the FEM treatment requires fine discretization in the vicinity of crack tips or the use of special crack-tip elements. Such an approach is cumbersome if one seeks to model crack propagation since the special element must move with the crack tip and continual re-meshing is required. However, direct application of the BEM is not without problems. The most popular approach has been to divide the body into two regions (with the crack located along the interface of these regions) and then to solve the coupled problems. This technique suffers the same shortcomings as FEM, i.e. crack propagation studies would require continual redefinition of the coupled regions and associated re-meshing.

Many investigators have reported that the temperature field is disturbed and thermal stresses are induced if a body having cracks or rigid ribbonlike inclusions is subjected to heat flow. The thermoelastic problem of an infinite plate with a crack [1,2] or a rigid ribbonlike inclusion [2,3] has been considered. That of an infinite solid with a penny-shaped crack [4,5] was also analyzed. In these analyses, the thermal boundary conditions assumed at the flaw are insulation [1,3,4], prescribed surface temperature [1,5], or prescribed heat flux across the surface [2,5]. Solutions for the corresponding external crack problems have also been developed [6-8]. Solutions for the case in which heat is generated at the crack, giving a temperature field symmetrical with respect to the crack plane have been given [9]. Solutions were presented for the corresponding temperature field [10] and the stress field [11] in a large solid containing an imperfectly conducting, penny-shaped crack, where the heat flux between the crack surfaces is assumed to be proportional to the local temperature difference.

Thermoelastic crack solutions have been developed rapidly because of various technical applications. Solutions were presented for the thermal fracture problem of a uniform heat flow disturbed by an insulated circumferential edge crack in an infinite circular cylinder of finite radius [12], in an infinite cylindrical cavity [13], and in an infinite spherical cavity [14-16]. In these analyses, the surface of the crack and the cylinder or the cavity are assumed to be insulated and the heat flow is perpendicular to the crack surface. The heat conduction problem is first reduced to that of solving a singular integral equation of the first kind. Next, by the use of the potential of thermoelastic displacement, the thermoelastic problems reduced to the isothermal elastic problem of solving a similar singular integral equation, in which the solution of the integral equation for the first heat conduction problem appears as a known function.

In recent years there has been great interest in the calculation of thermal stress in the neighborhood of a crack in the interior of an elastic solid, mainly because of its importance in the theory of brittle fracture. Most of the work has been concerned with steady thermal stress problems, but a few transient thermal stresses in an elastic solid having a crack have been considered. Solutions have been obtained for the transient thermal stress field in a semi-infinite body containing an edge crack [17] and containing an internal crack [18-20]. Solutions have been given for the transient thermal stress problem involving a circumferentially cracked hollow cylinder [21], in an edge-cracked plate [22] and in a thin plate with a Griffith crack [23-24]. However, in [17,21,22], it was assumed that the thermal disturbance in the vicinity of the crack may be neglected. In [23], it was assumed that the surface temperature at a crack is prescribed and there was a heat exchange by convection from the flat surfaces. In [24], the elastic medium was assumed to be cooled by time- and position-dependent temperature on the external crack surfaces.

Many thermal stress problems for isotropic, transversely isotropic, orthotropic and anisotropic bodies containing many kinds of cracks have been treated. Any linear thermoelastic problem of an infinite isotropic medium can be resolved into symmetrical and antisymmetrical problems by the method of dual integral equations [4-5]. The steady thermal problems of a transversely isotropic materials with a penny-shaped crack [25-28] and with an annular crack [29] have been investigated. The transient thermoelastic crack problem in a transverse isotropic infinite solid with an annular crack has been developed [30], where the crack was subjected to time- and position-dependent heat absorption and heat exchange on the crack surface. The antisymmetrical thermoelastic stress problems of an orthotropic plate containing a pair of central cracks [31] and a single central crack [32] were investigated. The symmetrical thermal fracture problem of an orthotropic plate containing a pair of coplanar central cracks was presented [33]. For anisotropic materials, the thermal and elastic properties were described for metallic substances [34] and for composite materials [35].

The early BEM work to solve steady-state thermoelasticity went back to [36-37]. The approach consisted of two steps. In the first step, the boundary element formulation of steady-state heat conduction was employed to determine the surface temperature and heat flux distribution. In the second step, the resulting temperatures were applied as body forces in an elastostatic BEM to obtain deformation and stress. General properties of the steady-state temperature field were exploited to transfer the thermal body force domain integral to surface integrals involving the known boundary temperatures and heat flux. Thus, the entire two step process required only surface discretization. A collection of fundamental solutions were presented, in both Laplace transform and time domains, under the classifications of coupled, uncoupled, transient and quasistatic thermoelasticity in [38-42], but there was no numerical implementation. Tanaka and Tanaka [43] presented a reciprocal theorem and the corresponding boundary element formulation for the time-domain coupled problem, but kernal functions were not discussed and no numerical results were included. Later, the formulation used by Tanaka *et al.*[44-46] required the evaluation of a domain integral. Not only is the calculation of domain integrals undesirable, but also such schemes require that special care be taken when evaluating the integral close to the singularity. Chaudouet [47] again resorted to the volume-based approach, while Masinda [48] and Sharp and Crouch [49] have made efforts for transferring the thermal body force domain integral to a surface integral. Masida presented some formulations for three-dimensional problems, but stopped short of attempting an implementation. On the other hand, Sharp and Crouch developed an approach for two-dimensional quasistatic thermoelasticity using time-dependent Green's functions, but domain integrals were used in the time marching algorithm. Banerjee *et al*. presented the boundary element formulation in 2D for transient ground water flow [50], steady-state heat conduction [51] and time-dependent thermoelasticity [52]. Those of transient thermoelasticity were developed in [53-54]. Among these papers, domain discretization was completely eliminated in [52-54].

Several attempts have been made to determine thermal stress intensity factors (TSIFs) [1,43,55-61]. Among these developments, Sladek *et al.* [43] determined TSIFs for various line cracks by employing BEM. Sumi [57] obtained the TSIFs for Griffith cracks with steady temperature distribution in finite rectangular plates by using the modified mapping collocation method. Thereafter, Emmel *et a*l. [58] applied the FEM to the same model as Sumi's and compared his numerical solutions with Sumi's. Sladek *et al.* [59] transformed area integral for body force term in BEM to line integral and calculated the TSIFs for edge cracks. Lee *et al.* [60] determined the TSIFs for cusp cracks in infinite bodies by using a complex variable approach. Lee *et al.* [61] computed the TSIFs for the same model as Sumi's in finite bodies as well as cusp cracks in infinite bodies by using BEM with the linearized body force term.

The application of the BEM for solving boundary value problems with body forces, time dependent effects or certain classes of non-linearities generally lead to integral equations which contains domain integrals [62]. Although these integrals do not introduce any new unknowns they detract from the elegance of the formulation and affect the efficiency of the method as integrations over the whole volume are required. Hence, a substantial amount of research has been carried out to find a general and efficient method of transforming domain integrals into equivalent boundary ones. The approaches which have so far been proposed can be divided into four groups. The first approach, the Dual Reciprocity Method, was developed in [63,64] and later extended to a variety of problems [65,66]. It has been shown that the Dual Reciprocity Method permits one to solve a wide range of problems and is very accurate [67-69]. The second approach was based on the expansion of the source term into a Fourier series to deal with potential and elasticity problems [70]. It has also been successfully applied for solving neutron diffusion problems [71]. The third approach was the use of particular solutions which can convert domain integrals into boundary integrals. This technique offers some specific advantages over the previous approaches in some specific applications [72]. The Multiple Reciprocity Method can be thought of as an extension of the idea of Dual Reciprocity Method. However, instead of approximating the source term by a set of coordinate functions, a sequence of functions related to the fundamental solution is introduced [73,74]. The Multiple Reciprocity Method is essentially different from the Dual Reciprocity Method. While the latter applies the same fundamental solution throughout the process of transformation of domain integrals into boundary integrals, the Multiple Reciprocity Method uses increasingly higher order fundamental solutions. The fourth approach, the method of particular integrals, was presented in [75]. The method was the use of particular integrals which is based on the well-known concept of developing the solution of an inhomogeneous differential equation by means of a complementary solution and a particular integral. This completely general approach does not require any volume or additional surface integration to solve the general body force problem.

In Chapter 2, the crack integral-equation representation developed in [76] is coupled to the direct boundary-element method and applied to finite plane bodies containing internal cracks and edge cracks. The method is developed for in-plane (modes I and II) loadings only. In Chapter 3, the technique is adapted to mode III problems involving internal cracks. In Chapter 4, the method is extended for application to steady-state thermal fields disturbed by internal insulated cracks in finite plane regions. The numerical treatment is quite straightforward, yet the results are shown to be extremely accurate.

Chapter 2

Mode I and Mode II Crack Problems

2.1 Internal Cracks

Recent attention has been focused on the development of integral-equation representations of cracks which can be coupled to the well-known boundary-integral equations for the treatment of cracks in finite bodies. In [80,81], a crack integral-equation representation is written in terms of the crack surface tractions. The unknowns in this representation are the dislocation densities along the crack line. While this formulation is shown to be quite effective for curved cracks, the equations are shown to be invalid when the crack contains a kink. In [82-84], a crack integral-equation representation is written in terms of the resultant forces along the crack line. It is shown that, unlike the previous formulation, this one can handle kinked cracks. However, the unknowns in this representation are still the dislocation densities. Since these densities are singular at the crack tips and weakly-singular at kinks, a rather cumbersome numerical treatment is required.

The crack integral-equation representation presented in [76] contains, as unknowns, the displacement discontinuities along the crack line. Since these are zero at crack tips and continuous at kinks, the numerical treatment of these equations need be no more complicated than the treatment of the boundary-integral equations themselves.

In this section, the crack integral-equation representation developed in [76] is coupled the direct boundary-integral equation method with a novel "displacement-discontinuity" representation of the internal and edge crack. It is shown that the analysis of such complex crack geometries is straightforward with this technique and several examples are reported to demonstrate method accuracy.

2.1.1 Theoretical Development

Consider an infinite isotropic elastic plane in which there is a point, $\bar{\mathbf{x}}$, at which some "source" of stress is located and a point, $\mathbf{x}$, at which the stresses are to be computed. At each of these points, we will be referring to internal "surfaces", as shown in Figure 2.1, described by unit normals $\bar{\mathbf{n}}$ and $\mathbf{n}$, respectively, and we will employ the following influence functions:

$(uR)_{ij}(\mathbf{x}, \bar{\mathbf{x}})$ = the displacement in the i direction at $\mathbf{x}$ due to a unit force applied in the j direction at $\bar{\mathbf{x}}$ in the infinite plane,

$(uc)_{ij}(\mathbf{x}, \bar{\mathbf{x}})$ = the displacement in the i direction at $\mathbf{x}$ due to a unit displacement discontinuity applied in the j direction at $\bar{\mathbf{x}}$ in the infinite plane,

$(\pi R)_{ij}(\mathbf{x}, \bar{\mathbf{x}})$ = the value of π_i at $\mathbf{x}$ due to a unit force applied in the j direction at $\bar{\mathbf{x}}$ in the infinite plane,

$(\pi c)_{ij}(\mathbf{x}, \bar{\mathbf{x}})$ = the value of π_i at $\mathbf{x}$ due to a unit displacement discontinuity applied in the j direction at $\bar{\mathbf{x}}$ in the infinite plane,

where π_i are stress functions defined such that the stress components are

$$\sigma_{11} = \frac{\partial \pi_1}{\partial x_2}, \qquad \sigma_{22} = -\frac{\partial \pi_2}{\partial x_1}, \qquad \sigma_{12} = -\frac{\partial \pi_1}{\partial x_1} = \frac{\partial \pi_2}{\partial x_2} \quad . \tag{2.1.1}$$

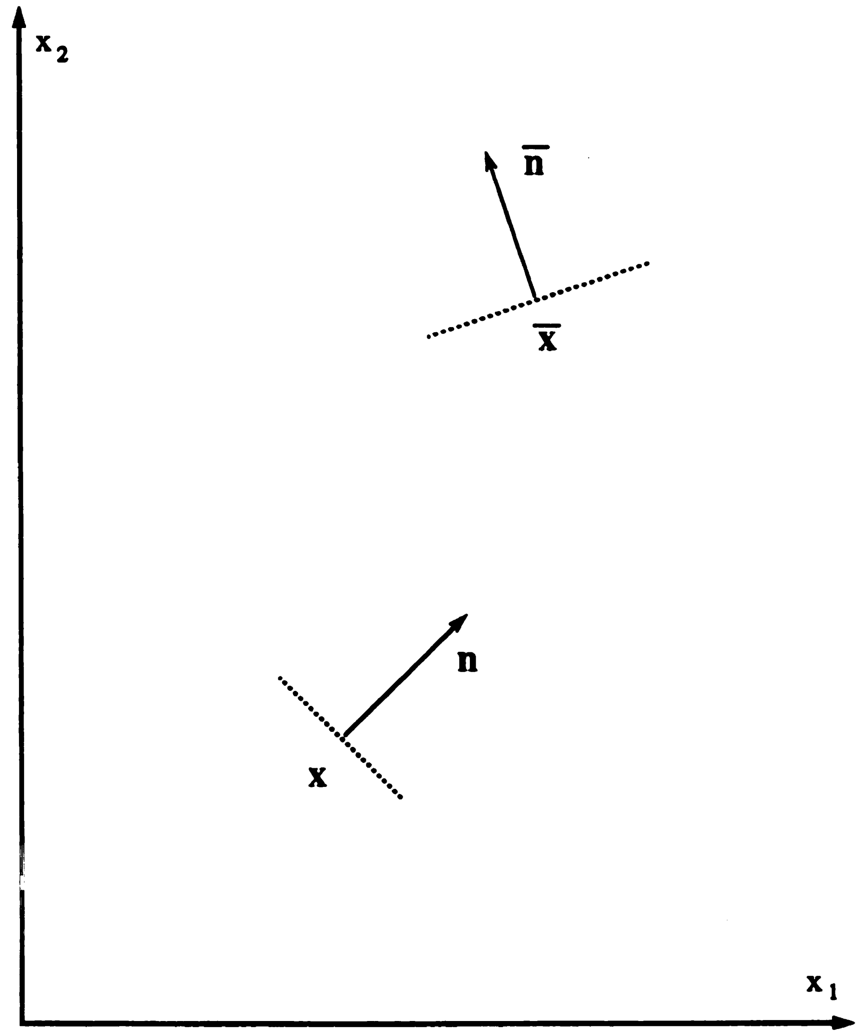

Figure 2.1 Source point, $\overline{x}$, and field point, x, in an infinite plane.

The influence functions are given in the Appendix A.

A plane elastic region Ω, with external boundary Γ_b, containing an internal piece-wise smooth crack Γ_c, as shown in Figure 2.2, or an internal piece-wise smooth branch crack or multiple cracks composed of Γ_{c1} and Γ_{c2}, as shown in Figures 2.3 and 2.4, respectively, is loaded by prescribed tractions t_j on some part of the external boundary and prescribed displacements u_j on the remainder of the external boundary. Then the direct boundary-integral equations and the integral equations developed in [76] can be coupled as follow.

For a single smooth or kinked crack:

$$\begin{aligned} c_{ij}(\mathbf{x})\, u_j(\mathbf{x}) &= \oint_{\Gamma_b} (uR)_{ij}(\mathbf{x}, \bar{\mathbf{x}})\, t_j(\bar{\mathbf{x}})\, ds(\bar{\mathbf{x}}) - \oint_{\Gamma_b} (uc)_{ij}(\mathbf{x}, \bar{\mathbf{x}})\, u_j(\bar{\mathbf{x}})\, ds(\bar{\mathbf{x}}) \\ &\quad + \int_{\Gamma_c} (uc)_{ij}(\mathbf{x}, \bar{\mathbf{x}})\, \Delta u_j(\bar{\mathbf{x}})\, ds(\bar{\mathbf{x}}) \qquad \mathbf{x} \text{ on } \Gamma_b \\ \pi_i(\mathbf{x}) &= \oint_{\Gamma_b} (\pi R)_{ij}(\mathbf{x}, \bar{\mathbf{x}})\, t_j(\bar{\mathbf{x}})\, ds(\bar{\mathbf{x}}) - \oint_{\Gamma_b} (\pi c)_{ij}(\mathbf{x}, \bar{\mathbf{x}})\, u_j(\bar{\mathbf{x}})\, ds(\bar{\mathbf{x}}) \\ &\quad + \int_{\Gamma_c} (\pi c)_{ij}(\mathbf{x}, \bar{\mathbf{x}})\, \Delta u_j(\bar{\mathbf{x}})\, ds(\bar{\mathbf{x}}) \qquad \mathbf{x} \text{ on } \Gamma_c \ . \end{aligned} \tag{2.1.2}$$

For a branch crack or multiple cracks:

$$c_{ij}(\mathbf{x})\, u_j(\mathbf{x}) = \oint_{\Gamma_b} (uR)_{ij}(\mathbf{x}, \bar{\mathbf{x}})\, t_j(\bar{\mathbf{x}})\, ds(\bar{\mathbf{x}}) - \oint_{\Gamma_b} (uc)_{ij}(\mathbf{x}, \bar{\mathbf{x}})\, u_j(\bar{\mathbf{x}})\, ds(\bar{\mathbf{x}})$$

$$+ \sum_{k=1}^{2} \int_{\Gamma_{ck}} (uc)_{ij}(\mathbf{x}, \bar{\mathbf{x}})\, \Delta u_j(\bar{\mathbf{x}})\, ds(\bar{\mathbf{x}}) \qquad \mathbf{x} \text{ on } \Gamma_b$$

$$\pi_i(\mathbf{x}) = \oint_{\Gamma_b} (\pi R)_{ij}(\mathbf{x}, \bar{\mathbf{x}})\, t_j(\bar{\mathbf{x}})\, ds(\bar{\mathbf{x}}) - \oint_{\Gamma_b} (\pi c)_{ij}(\mathbf{x}, \bar{\mathbf{x}})\, u_j(\bar{\mathbf{x}})\, ds(\bar{\mathbf{x}})$$

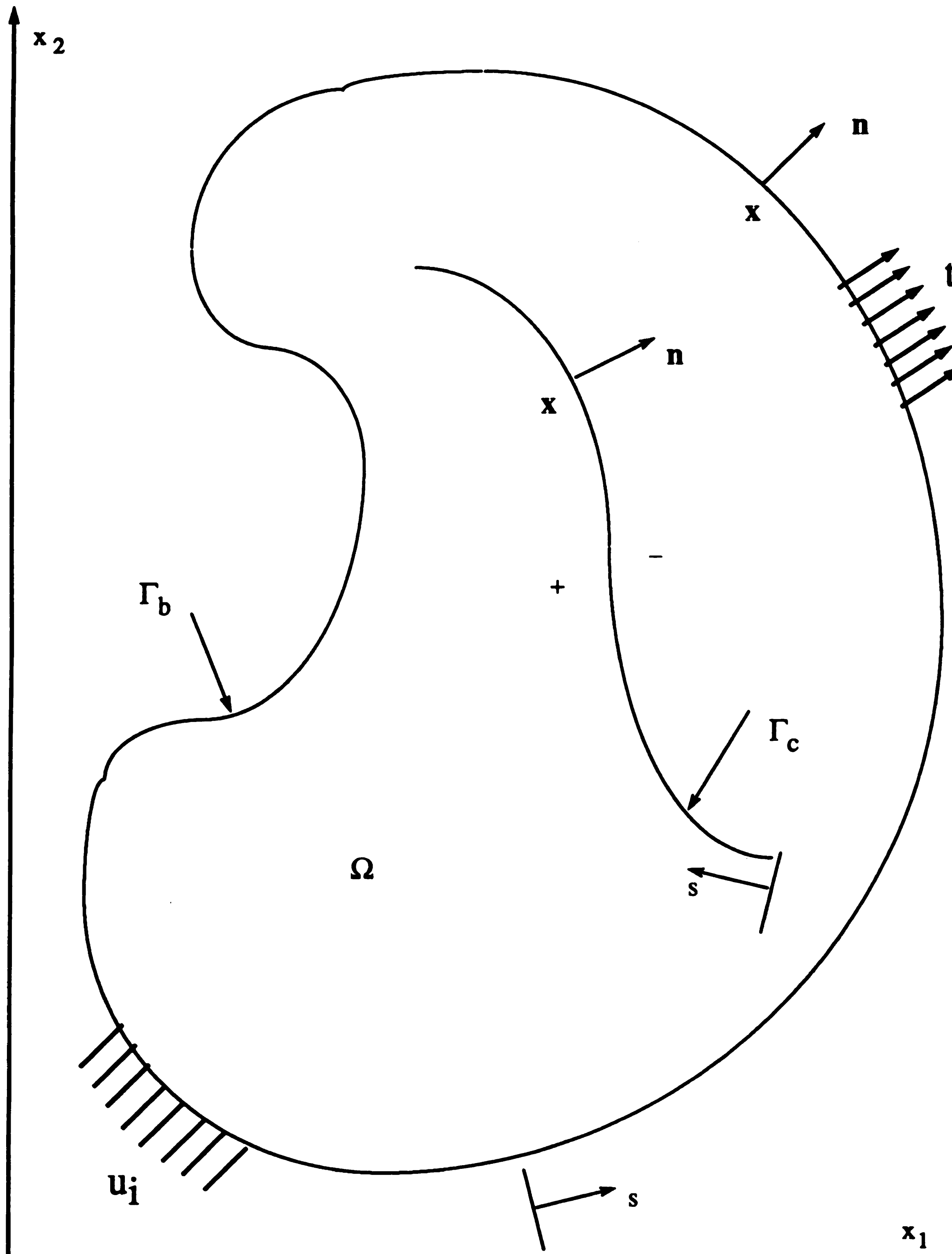

Figure 2.2 Plane elastic region containing a crack.

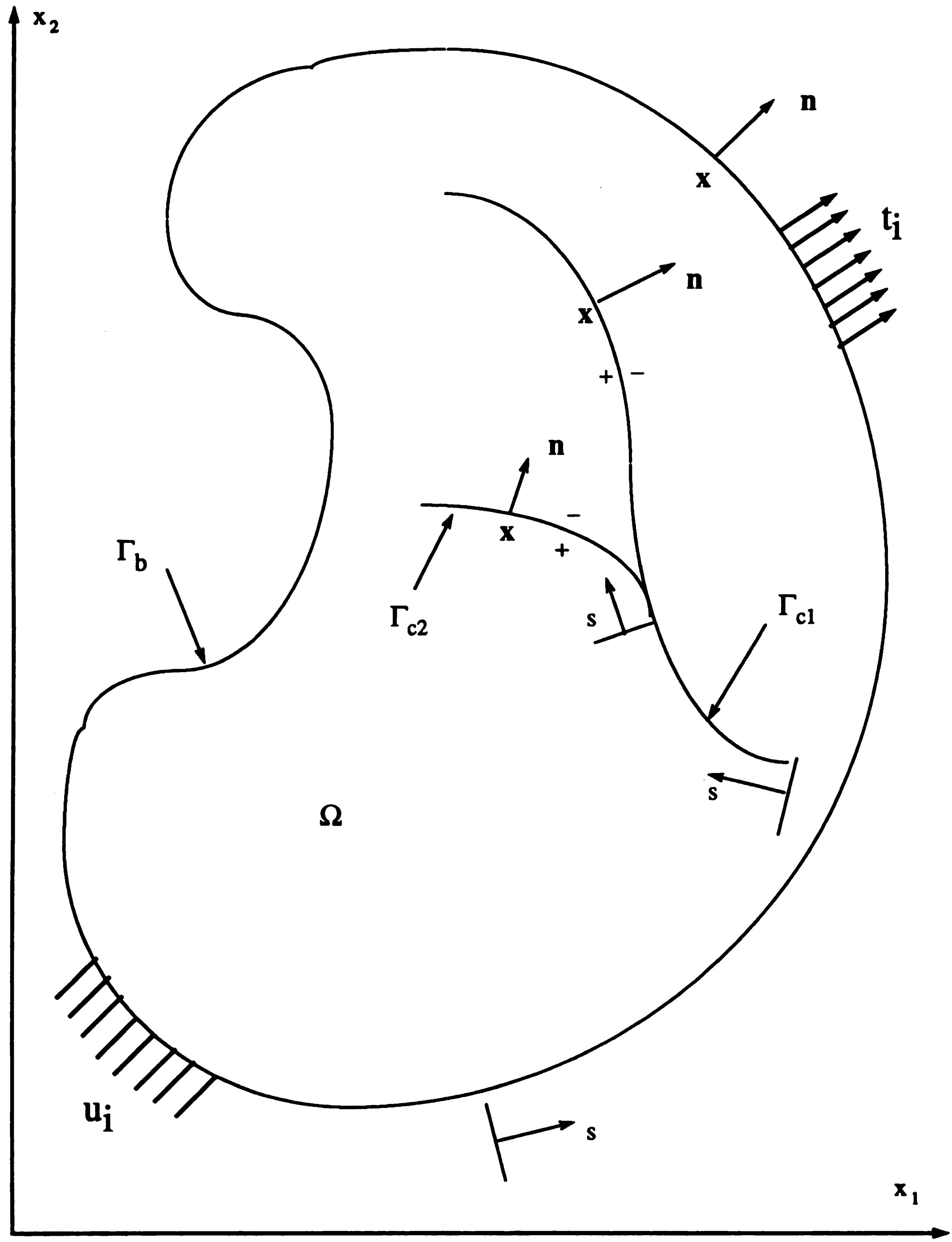

Figure 2.3 Plane elastic region containing a branch crack.

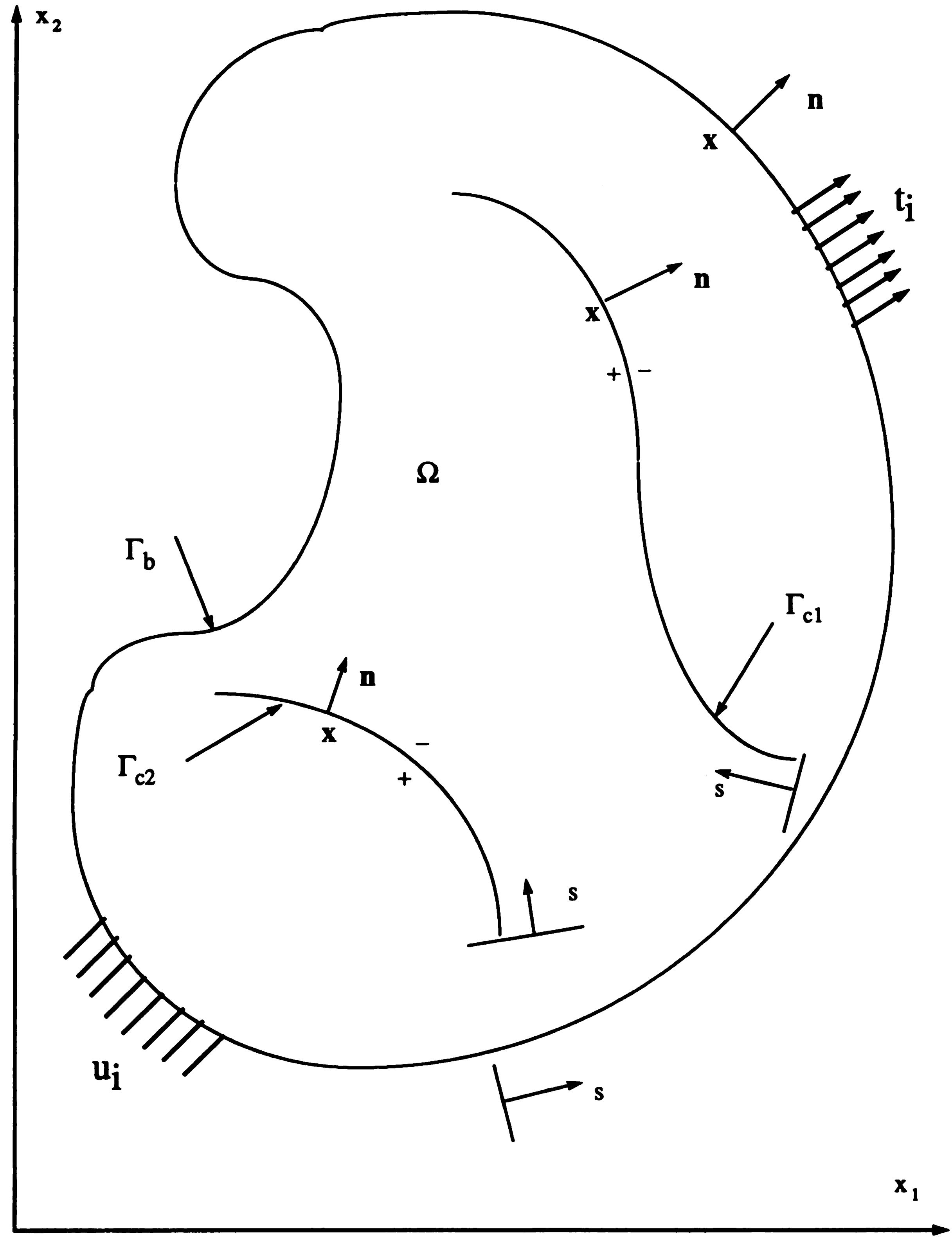

Figure 2.4 Plane elastic region containing multiple cracks.

$\pi_i(x)$

In ec

Δu_j

2.1

2.

A

b

n

$$+ \sum_{k=1}^{2} \int_{\Gamma_{ck}} (\pi c)_{ij}(\mathbf{x}, \overline{\mathbf{x}})\, \Delta u_j(\overline{\mathbf{x}})\, ds(\overline{\mathbf{x}}) \qquad \mathbf{x} \text{ on } \Gamma_{c1} \qquad (2.1.3)$$

$$\pi_i(\mathbf{x}) = \oint_{\Gamma_b} (\pi R)_{ij}(\mathbf{x}, \overline{\mathbf{x}})\, t_j(\overline{\mathbf{x}})\, ds(\overline{\mathbf{x}}) - \oint_{\Gamma_b} (\pi c)_{ij}(\mathbf{x}, \overline{\mathbf{x}})\, u_j(\overline{\mathbf{x}})\, ds(\overline{\mathbf{x}})$$

$$+ \sum_{k=1}^{2} \int_{\Gamma_{ck}} (\pi c)_{ij}(\mathbf{x}, \overline{\mathbf{x}})\, \Delta u_j(\overline{\mathbf{x}})\, ds(\overline{\mathbf{x}}) \qquad \mathbf{x} \text{ on } \Gamma_{c2} \ .$$

In eqs.(2.1.2) and (2.1.3), i=1, 2, j=1, 2, summation on repeated indices is implied, and $\Delta u_j = u_j^- - u_j^+$ are the relative crack surface displacements.

2.1.2 Numerical Treatment

2.1.2.1 A single smooth or kinked crack

A simple numerical treatment of eqs.(2.1.2) is presented here in which the external boundary is approximated by M_b straight elements and the crack by M_c straight elements, as shown in Figure 2.5. Eqs.(2.1.2) can then be written as

$$c_{ij}(\mathbf{x})\, u_j(\mathbf{x}) = \sum_{m=1}^{M_b} \int_m [\, (uR)_{ij}(\mathbf{x}, \overline{\mathbf{x}})\, t_j(\overline{\mathbf{x}}) - (uc)_{ij}(\mathbf{x}, \overline{\mathbf{x}})\, u_j(\overline{\mathbf{x}})\,]\, ds(\overline{\mathbf{x}})$$

$$+ \sum_{m=M_b+1}^{M_b+M_c} \int_m (uc)_{ij}(\mathbf{x}, \overline{\mathbf{x}})\, \Delta u_j(\overline{\mathbf{x}})\, ds(\overline{\mathbf{x}}) \qquad \mathbf{x} \text{ on } \Gamma_b$$

(2.1.4)

$$\pi_i(\mathbf{x}) = \sum_{m=1}^{M_b} \int_m [\, (\pi R)_{ij}(\mathbf{x}, \overline{\mathbf{x}})\, t_j(\overline{\mathbf{x}}) - (\pi c)_{ij}(\mathbf{x}, \overline{\mathbf{x}})\, u_j(\overline{\mathbf{x}})\,]\, ds(\overline{\mathbf{x}})$$

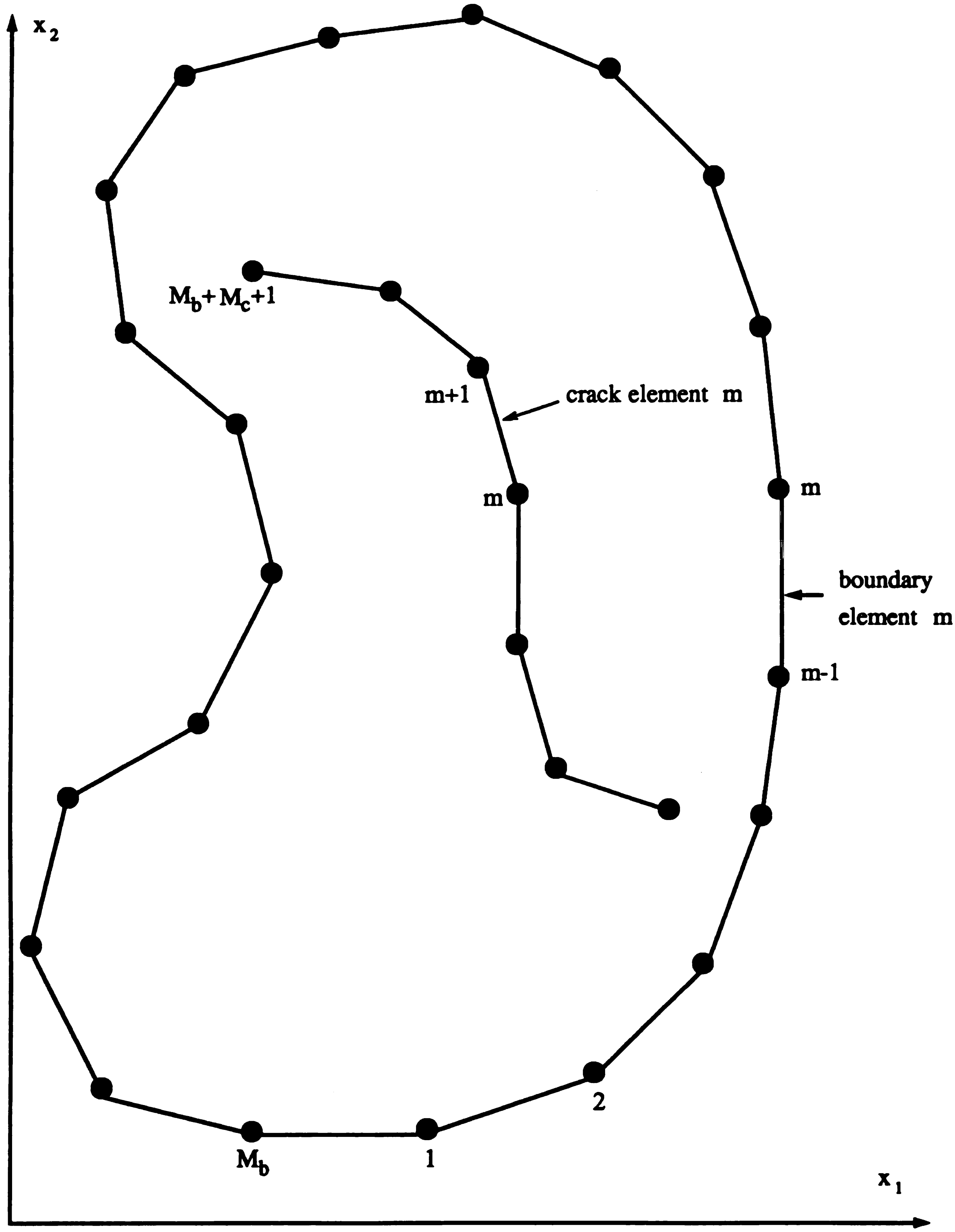

Figure 2.5 Discretized plane region containing a discretized crack.

$$+\sum_{m=M_b+1}^{M_b+M_c}\int_m (\pi c)_{ij}(\mathbf{x},\bar{\mathbf{x}})\,\Delta u_j(\bar{\mathbf{x}})\,ds(\bar{\mathbf{x}}) \qquad \mathbf{x} \text{ on } \Gamma_c \ .$$

The displacements, tractions and displacement discontinuities on each element can be linearly approximated by

$$
\begin{aligned}
u_j(\bar{\mathbf{x}}) &= N_1(\xi)u_j^{(m-1)} + N_2(\xi)u_j^{(m)} && \bar{\mathbf{x}} \text{ on element } m \text{ of } \Gamma_b \\
t_j(\bar{\mathbf{x}}) &= N_1(\xi)t_j^{(2m-1)} + N_2(\xi)t_j^{(2m)} && \bar{\mathbf{x}} \text{ on element } m \text{ of } \Gamma_b \qquad (2.1.5) \\
\Delta u_j(\bar{\mathbf{x}}) &= N_1(\xi)\Delta u_j^{(m)} + N_2(\xi)\Delta u_j^{(m+1)} && \bar{\mathbf{x}} \text{ on element } m \text{ of } \Gamma_c
\end{aligned}
$$

where $u_j^{(m)}$, $t_j^{(2m)}$, $t_j^{(2m+1)}$ are values at the external boundary nodal point m (m=1, ... M_b), $\Delta u_j^{(m)}$ are values at the crack nodal point m (m=M_b+2, ... M_b+M_c), and

$$N_1(\xi) = (1-\xi)/2 \qquad N_2(\xi) = (1+\xi)/2 \qquad -1 \le \xi \le 1 \ . \qquad (2.1.6)$$

Furthermore

$$\bar{\mathbf{x}} = \begin{cases} N_1(\xi)\mathbf{x}^{(m-1)} + N_2(\xi)\mathbf{x}^{(m)} & \bar{\mathbf{x}} \text{ on element m of } \Gamma_b \\ N_1(\xi)\mathbf{x}^{(m)} + N_2(\xi)\mathbf{x}^{(m+1)} & \bar{\mathbf{x}} \text{ on element m of } \Gamma_{c1} \text{ or } \Gamma_{c2} \end{cases} \qquad (2.1.7)$$

$$ds(\bar{\mathbf{x}}) = \begin{cases} [(s_b^{(m)} - s_b^{(m-1)})/2]\,d\xi = [\Delta s_b^m/2]\,d\xi & \bar{\mathbf{x}} \text{ on element m of } \Gamma_b \\ [(s_c^{(m+1)} - s_c^{(m)})/2]\,d\xi = [\Delta s_c^m/2]\,d\xi & \bar{\mathbf{x}} \text{ on elemeent m of } \Gamma_{c1} \text{ or } \Gamma_{c2} \end{cases} \qquad (2.1.8)$$

where Δs_b^m is the length of the external boundary element m and Δs_c^m is the length of the crack element m.

Inserting eqs.(2.1.5) through (2.1.8) into eqs.(2.1.4), we obtain

$$
\begin{aligned}
c_{ij}^{(n)}u_j^{(n)} = & \sum_{m=1}^{M_b} \Delta s_b^m/4 \ [\int_m (1-\xi)(uR)_{ij}(\mathbf{x}^{(n)}, \xi)d\xi \ ] \ t_j^{(2m-1)} \\
& + \sum_{m=1}^{M_b} \Delta s_b^m/4 \ [\int_m (1+\xi)(uR)_{ij}(\mathbf{x}^{(n)}, \xi)d\xi \ ] \ t_j^{(2m)} \\
& - \sum_{m=1}^{M_b} \Delta s_b^m/4 \ [\int_m (1-\xi)(uc)_{ij}(\mathbf{x}^{(n)}, \xi)d\xi \ ] \ u_j^{(m-1)} \\
& - \sum_{m=1}^{M_b} \Delta s_b^m/4 \ [\int_m (1+\xi)(uc)_{ij}(\mathbf{x}^{(n)}, \xi)d\xi \ ] \ u_j^{(m)} \\
& + \sum_{m=M_b+2}^{M_b+M_c} \Delta s_c^m/4 \ [\int_m (1-\xi)(uc)_{ij}(\mathbf{x}^{(n)}, \xi)d\xi \ ] \ \Delta u_j^{(m)} \\
& + \sum_{m=M_b+1}^{M_b+M_c-1} \Delta s_c^m/4 \ [\int_m (1+\xi)(uc)_{ij}(\mathbf{x}^{(n)}, \xi)d\xi \ ] \ \Delta u_j^{(m+1)}
\end{aligned}
\tag{2.1.9}
$$

$$
\begin{aligned}
\pi_i^{(n)} = & \sum_{m=1}^{M_b} \Delta s_b^m/4 \ [\int_m (1-\xi)(\pi R)_{ij}(\mathbf{x}^{(n)}, \xi)d\xi \ ] \ t_j^{(2m-1)} \\
& + \sum_{m=1}^{M_b} \Delta s_b^m/4 \ [\int_m (1+\xi)(\pi R)_{ij}(\mathbf{x}^{(n)}, \xi)d\xi \ ] \ t_j^{(2m)} \\
& - \sum_{m=1}^{M_b} \Delta s_b^m/4 \ [\int_m (1-\xi)(\pi c)_{ij}(\mathbf{x}^{(n)}, \xi)d\xi \ ] \ u_j^{(m-1)} \\
& - \sum_{m=1}^{M_b} \Delta s_b^m/4 \ [\int_m (1+\xi)(\pi c)_{ij}(\mathbf{x}^{(n)}, \xi)d\xi \ ] \ u_j^{(m)} \\
& + \sum_{m=M_b+2}^{M_b+M_c} \Delta s_c^m/4 \ [\int_m (1-\xi)(\pi c)_{ij}(\mathbf{x}^{(n)}, \xi)d\xi \ ] \ \Delta u_j^{(m)}
\end{aligned}
$$

wh

(n=

n.

E

$$+ \sum_{m=M_b+1}^{M_b+M_c-1} \Delta s_c^m/4 \left[\int_m (1+\xi)(\pi c)_{ij}(x^{(n)}, \xi) d\xi \right] \Delta u_j^{(m+1)}$$

where $u_j^{(n)} = u_j(x^{(n)})$, $x^{(n)}$ being the location of the external boundary nodal point n, (n=1, ... M_b), and $\pi_i^{(n)} = \pi_i(x^{(n)})$, $x^{(n)}$ being the location of the crack element mid-point n, (n= M_b+1, ... M_b+M_c).

Eqs.(2.1.9) can be written in the following matrix form:

$$[UC]\left\{ u \right\} - [Q]\left\{ \Delta u \right\} = [UR]\left\{ t \right\}$$

$$[PC]\left\{ u \right\} - [X]\left\{ \Delta u \right\} = [PR]\left\{ t \right\} - \left\{ \pi \right\} \tag{2.1.10}$$

where [UC] is $2M_b$ x $2M_b$, [Q] is $2M_b$ x $2(M_c-1)$, [UR] is $2M_b$ x $4M_b$, [PC] is $2M_c$ x $2M_b$, [X] is $2M_c$ x $2(M_c-1)$ and [PR] is $2M_c$ x $4M_b$.

Thus

$$\begin{bmatrix} [UC] & -[Q] \\ [\Gamma_2][PC] & -[\Gamma_2][X] \end{bmatrix} \begin{Bmatrix} u \\ \Delta u \end{Bmatrix} = \begin{bmatrix} [UR] & [0] \\ [\Gamma_2][PR] & [I] \end{bmatrix} \begin{Bmatrix} t \\ F \end{Bmatrix} \tag{2.1.11}$$

where, as in [76], we have defined a nodal force matrix on the crack by

F

wh

[T

I

$$\left\{ F \right\} = [\Gamma_2] \left\{ \pi \right\} \tag{2.1.12}$$

where

$$[\Gamma_2] = \begin{bmatrix} -I & I & 0 & 0 & 0 & 0 & 0 \\ 0 & -I & I & 0 & 0 & 0 & 0 \\ 0 & 0 & -I & I & 0 & 0 & 0 \\ \cdot & \cdot & \cdot & \cdot & \cdot & \cdot & \cdot \\ \cdot & \cdot & \cdot & \cdot & \cdot & \cdot & \cdot \\ 0 & 0 & 0 & 0 & 0 & -I & I \end{bmatrix} \tag{2.1.13}$$

I represents a 2x2 identity matrix, and $[\Gamma_2]$ is $2(M_c-1) \times 2M_c$.

2.1.2.2 A branch crack or multiple cracks

A simple numerical treatment of eqs.(2.1.3) is presented here in which the external boundary is approximated by M_b straight elements and the branch crack or multiple cracks by M_{c1}, M_{c2} straight elements, as shown in Figures 2.6 and 2.7, respectively. Eqs.(2.1.3) can then be written as

$$\begin{aligned} c_{ij}(\mathbf{x})\, u_j(\mathbf{x}) = & \sum_{m=1}^{M_b} \int_m [\, (uR)_{ij}(\mathbf{x}, \bar{\mathbf{x}})\, t_j(\bar{\mathbf{x}}) - (uc)_{ij}(\mathbf{x}, \bar{\mathbf{x}})\, u_j(\bar{\mathbf{x}}) \,]\, ds(\bar{\mathbf{x}}) \\ & + \sum_{m=M_b+1}^{M_b+M_{c1}} \int_m (uc)_{ij}(\mathbf{x}, \bar{\mathbf{x}})\, \Delta u_j(\bar{\mathbf{x}})\, ds(\bar{\mathbf{x}}) \\ & + \sum_{m=M_b+M_{c1}+2}^{M_b+M_{c1}+M_{c2}+1} \int_m (uc)_{ij}(\mathbf{x}, \bar{\mathbf{x}})\, \Delta u_j(\bar{\mathbf{x}})\, ds(\bar{\mathbf{x}}) \qquad \mathbf{x} \text{ on } \Gamma_b \end{aligned}$$

$$\pi_i(\mathbf{x}) = \sum_{m=1}^{M_b} \int_m [\, (\pi R)_{ij}(\mathbf{x}, \bar{\mathbf{x}})\, t_j(\bar{\mathbf{x}}) - (\pi c)_{ij}(\mathbf{x}, \bar{\mathbf{x}})\, u_j(\bar{\mathbf{x}}) \,]\, ds(\bar{\mathbf{x}})$$

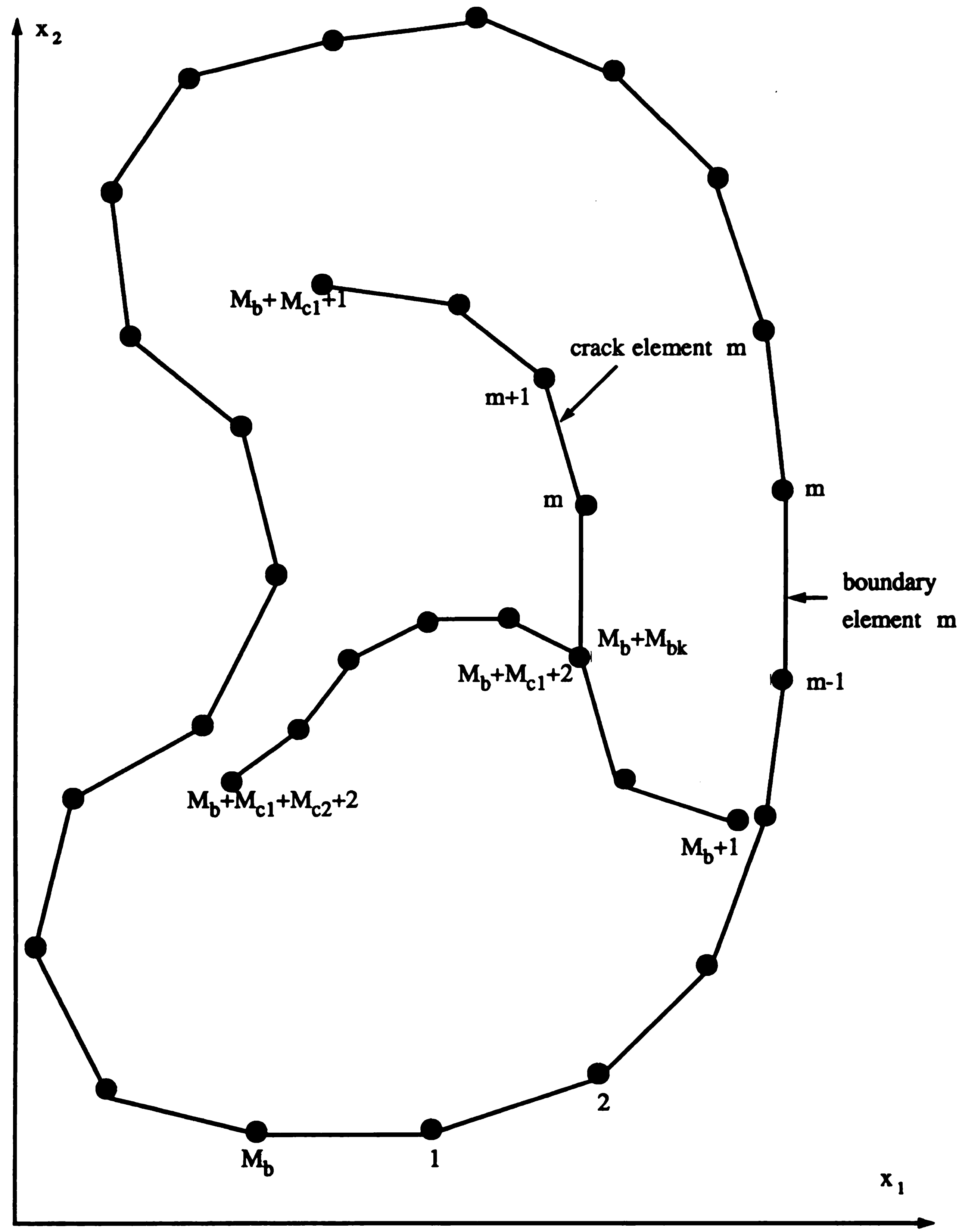

Figure 2.6 Discretized plane region containing a discretized branch crack.

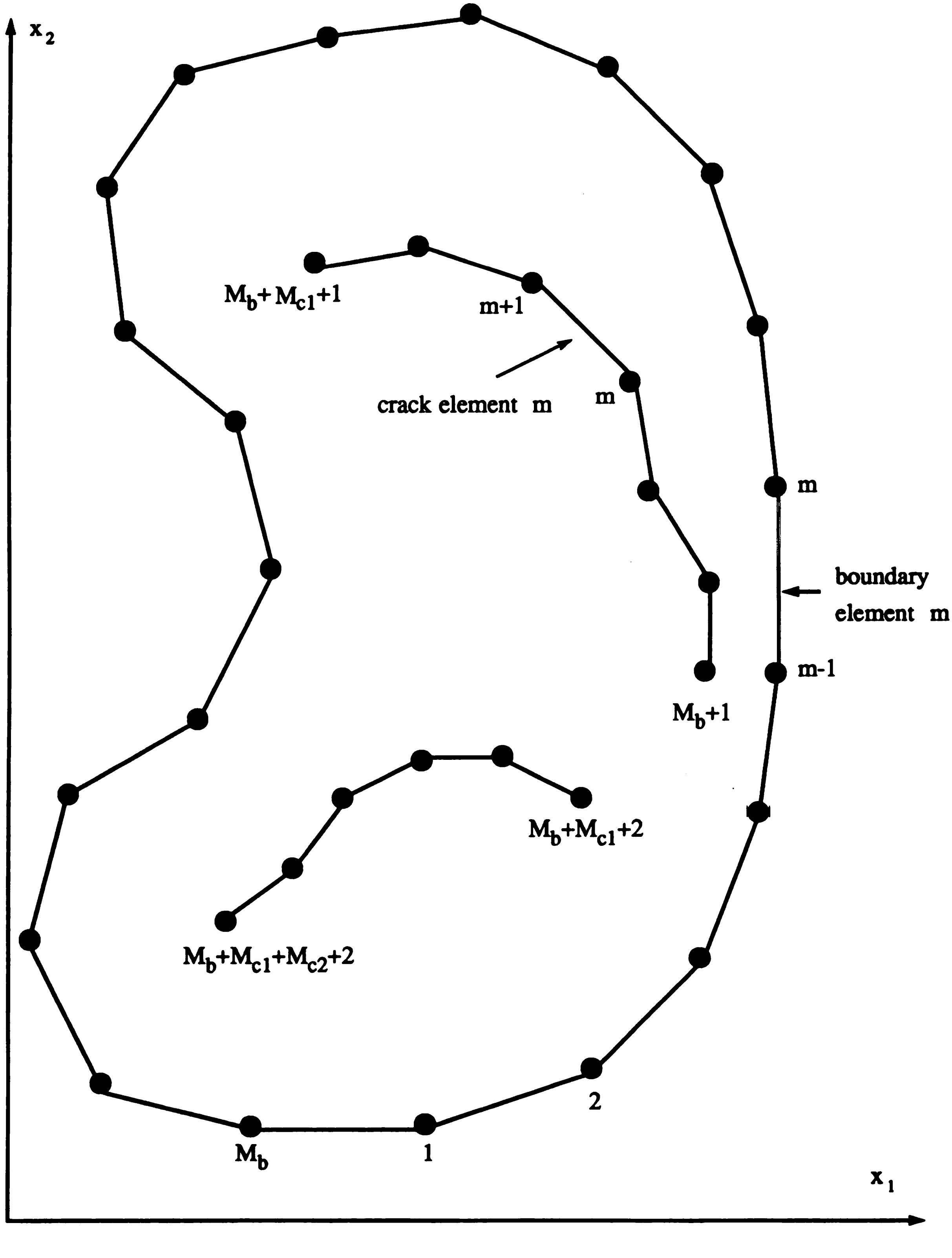

Figure 2.7 Discretized plane region containing discretized multiple cracks.

$$+ \sum_{m=M_b+1}^{M_b+M_{c1}} \int_m (\pi c)_{ij}(\mathbf{x}, \bar{\mathbf{x}})\, \Delta u_j(\bar{\mathbf{x}})\, ds(\bar{\mathbf{x}}) \tag{2.1.14}$$

$$+ \sum_{m=M_b+M_{c1}+2}^{M_b+M_{c1}+M_{c2}+1} \int_m (\pi c)_{ij}(\mathbf{x}, \bar{\mathbf{x}})\, \Delta u_j(\bar{\mathbf{x}})\, ds(\bar{\mathbf{x}}) \qquad \mathbf{x} \text{ on } \Gamma_{c1}$$

$$\pi_i(\mathbf{x}) = \sum_{m=1}^{M_b} \int_m [\, (\pi R)_{ij}(\mathbf{x}, \bar{\mathbf{x}})\, t_j(\bar{\mathbf{x}}) - (\pi c)_{ij}(\mathbf{x}, \bar{\mathbf{x}})\, u_j(\bar{\mathbf{x}})\,]\, ds(\bar{\mathbf{x}})$$

$$+ \sum_{m=M_b+1}^{M_b+M_{c1}} \int_m (\pi c)_{ij}(\mathbf{x}, \bar{\mathbf{x}})\, \Delta u_j(\bar{\mathbf{x}})\, ds(\bar{\mathbf{x}})$$

$$+ \sum_{m=M_b+M_{c1}+2}^{M_b+M_{c1}+M_{c2}+1} \int_m (\pi c)_{ij}(\mathbf{x}, \bar{\mathbf{x}})\, \Delta u_j(\bar{\mathbf{x}})\, ds(\bar{\mathbf{x}}) \qquad \mathbf{x} \text{ on } \Gamma_{c2}\,.$$

The displacements, tractions and displacement discontinuities on each element can be linearly approximated by

$$
\begin{aligned}
u_j(\bar{\mathbf{x}}) &= N_1(\xi)u_j^{(m-1)} + N_2(\xi)u_j^{(m)} && \bar{\mathbf{x}} \text{ on element m of } \Gamma_b \\
t_j(\bar{\mathbf{x}}) &= N_1(\xi)t_j^{(2m-1)} + N_2(\xi)t_j^{(2m)} && \bar{\mathbf{x}} \text{ on element m of } \Gamma_b \\
\Delta u_j(\bar{\mathbf{x}}) &= N_1(\xi)\Delta u_j^{(m)} + N_2(\xi)\Delta u_j^{(m+1)} && \bar{\mathbf{x}} \text{ on element m of } \Gamma_{c1} \text{ or } \Gamma_{c2}
\end{aligned}
\tag{2.1.15}
$$

where $u_j^{(m)}$, $t_j^{(2m)}$, $t_j^{(2m+1)}$ are values at the external boundary nodal point m (m=1, ... M_b) and $\Delta u_j^{(m)}$ are values at the crack nodal point m. For multiple cracks, m=M_b+2, ... M_b+M_{c1} , M_b+M_{c1}+3, ... $M_b+M_{c1}+M_{c2}$+1. For a branch crack, m=M_b+2, ... M_b+M_{c1} , M_b+M_{c1}+2, ... $M_b+M_{c1}+M_{c2}$+1.

Furthermore

$$\bar{\mathbf{x}} = \begin{cases} N_1(\xi)\mathbf{x}^{(m-1)} + N_2(\xi)\mathbf{x}^{(m)} & \bar{\mathbf{x}} \text{ on element m of } \Gamma_b \\ N_1(\xi)\mathbf{x}^{(m)} + N_2(\xi)\mathbf{x}^{(m+1)} & \bar{\mathbf{x}} \text{ on element m of } \Gamma_{c1} \text{ or } \Gamma_{c2} \end{cases} \tag{2.1.16}$$

$$ds(\bar{\mathbf{x}}) = \begin{cases} [(s_b^{(m)} - s_b^{(m-1)})/2]\, d\xi = [\Delta s_b^m/2]\, d\xi & \bar{\mathbf{x}} \text{ on element m of } \Gamma_b \\ [(s_c^{(m+1)} - s_c^{(m)})/2]\, d\xi = [\Delta s_c^m/2]\, d\xi & \bar{\mathbf{x}} \text{ on element m of } \Gamma_{c1} \text{ or } \Gamma_{c2} \end{cases} \tag{2.1.17}$$

where Δs_b^m is the length of the external boundary element m and Δs_c^m is the length of the crack element m.

Inserting eqs.(2.1.15) through (2.1.17) into eqs.(2.1.14), we obtain

$$\begin{aligned} c_{ij}^{(n)}u_j^{(n)} = & \sum_{m=1}^{M_b} \Delta s_b^m/4\ [\textstyle\int_m (1-\xi)(uR)_{ij}(\mathbf{x}^{(n)}, \xi)d\xi\ ]\ t_j^{(2m-1)} \\ & + \sum_{m=1}^{M_b} \Delta s_b^m/4\ [\textstyle\int_m (1+\xi)(uR)_{ij}(\mathbf{x}^{(n)}, \xi)d\xi\ ]\ t_j^{(2m)} \\ & - \sum_{m=1}^{M_b} \Delta s_b^m/4\ [\textstyle\int_m (1-\xi)(uc)_{ij}(\mathbf{x}^{(n)}, \xi)d\xi\ ]\ u_j^{(m-1)} \\ & - \sum_{m=1}^{M_b} \Delta s_b^m/4\ [\textstyle\int_m (1+\xi)(uc)_{ij}(\mathbf{x}^{(n)}, \xi)d\xi\ ]\ u_j^{(m)} \\ & + \sum_{m=M_b+2}^{M_b+M_{c1}} \Delta s_c^m/4\ [\textstyle\int_m (1-\xi)(uc)_{ij}(\mathbf{x}^{(n)}, \xi)d\xi\ ]\ \Delta u_j^{(m)} \\ & + \sum_{m=M_b+1}^{M_b+M_{c1}-1} \Delta s_c^m/4\ [\textstyle\int_m (1+\xi)(uc)_{ij}(\mathbf{x}^{(n)}, \xi)d\xi\ ]\ \Delta u_j^{(m+1)} \end{aligned}$$

$$+ \sum_{m=M_b+M_{c1}+2}^{M_b+M_{c1}+M_{c2}+1} \Delta s_c^m/4 \; [\int_m (1-\xi)(uc)_{ij}(\mathbf{x}^{(n)}, \xi)d\xi \;] \; \Delta u_j^{(m)}$$

$$+ \sum_{m=M_b+M_{c1}+2}^{M_b+M_{c1}+M_{c2}} \Delta s_c^m/4 \; [\int_m (1+\xi)(uc)_{ij}(\mathbf{x}^{(n)}, \xi)d\xi \;] \; \Delta u_j^{(m+1)}$$

$$\begin{aligned}
\pi_i^{(n)} = & \sum_{m=1}^{M_b} \Delta s_b^m/4 \; [\int_m (1-\xi)(\pi R)_{ij}(\mathbf{x}^{(n)}, \xi)d\xi \;] \; t_j^{(2m-1)} \\
& + \sum_{m=1}^{M_b} \Delta s_b^m/4 \; [\int_m (1+\xi)(\pi R)_{ij}(\mathbf{x}^{(n)}, \xi)d\xi \;] \; t_j^{(2m)} \\
& - \sum_{m=1}^{M_b} \Delta s_b^m/4 \; [\int_m (1-\xi)(\pi c)_{ij}(\mathbf{x}^{(n)}, \xi)d\xi \;] \; u_j^{(m-1)} \\
& - \sum_{m=1}^{M_b} \Delta s_b^m/4 \; [\int_m (1+\xi)(\pi c)_{ij}(\mathbf{x}^{(n)}, \xi)d\xi \;] \; u_j^{(m)} \\
& + \sum_{m=M_b+2}^{M_b+M_{c1}} \Delta s_c^m/4 \; [\int_m (1-\xi)(\pi c)_{ij}(\mathbf{x}^{(n)}, \xi)d\xi \;] \; \Delta u_j^{(m)} \\
& + \sum_{m=M_b+1}^{M_b+M_{c1}-1} \Delta s_c^m/4 \; [\int_m (1+\xi)(\pi c)_{ij}(\mathbf{x}^{(n)}, \xi)d\xi \;] \; \Delta u_j^{(m+1)} \qquad (2.1.18) \\
& + \sum_{m=M_b+M_{c1}+2}^{M_b+M_{c1}+M_{c2}+1} \Delta s_c^m/4 \; [\int_m (1-\xi)(\pi c)_{ij}(\mathbf{x}^{(n)}, \xi)d\xi \;] \; \Delta u_j^{(m)} \\
& + \sum_{m=M_b+M_{c1}+2}^{M_b+M_{c1}+M_{c2}} \Delta s_c^m/4 \; [\int_m (1+\xi)(\pi c)_{ij}(\mathbf{x}^{(n)}, \xi)d\xi \;] \; \Delta u_j^{(m+1)}
\end{aligned}$$

$$\begin{aligned}
\pi_i^{(n)} = & \sum_{m=1}^{M_b} \Delta s_b^m/4 \; [\int_m (1-\xi)(\pi R)_{ij}(\mathbf{x}^{(n)}, \xi)d\xi \;] \; t_j^{(2m-1)} \\
& + \sum_{m=1}^{M_b} \Delta s_b^m/4 \; [\int_m (1+\xi)(\pi R)_{ij}(\mathbf{x}^{(n)}, \xi)d\xi \;] \; t_j^{(2m)} \\
& - \sum_{m=1}^{M_b} \Delta s_b^m/4 \; [\int_m (1-\xi)(\pi c)_{ij}(\mathbf{x}^{(n)}, \xi)d\xi \;] \; u_j^{(m-1)}
\end{aligned}$$

$$- \sum_{m=1}^{M_b} \Delta s_b^m/4 \; [\int_m (1+\xi)(\pi c)_{ij}(x^{(n)}, \xi) d\xi \;] \; u_j^{(m)}$$

$$+ \sum_{m=M_b+2}^{M_b+M_{c1}} \Delta s_c^m/4 \; [\int_m (1-\xi)(\pi c)_{ij}(x^{(n)}, \xi) d\xi \;] \; \Delta u_j^{(m)}$$

$$+ \sum_{m=M_b+1}^{M_b+M_{c1}-1} \Delta s_c^m/4 \; [\int_m (1+\xi)(\pi c)_{ij}(x^{(n)}, \xi) d\xi \;] \; \Delta u_j^{(m+1)}$$

$$+ \sum_{m=M_b+M_{c1}+2}^{M_b+M_{c1}+M_{c2}+1} \Delta s_c^m/4 \; [\int_m (1-\xi)(\pi c)_{ij}(x^{(n)}, \xi) d\xi \;] \; \Delta u_j^{(m)}$$

$$+ \sum_{m=M_b+M_{c1}+2}^{M_b+M_{c1}+M_{c2}} \Delta s_c^m/4 \; [\int_m (1+\xi)(\pi c)_{ij}(x^{(n)}, \xi) d\xi \;] \; \Delta u_j^{(m+1)}$$

where $u_j^{(n)} = u_j(x^{(n)})$, $x^{(n)}$ being the location of the external boundary nodal point n, (n=1, ... M_b), and $\pi_i^{(n)} = \pi_i(x^{(n)})$, $x^{(n)}$ being the location of the crack element mid-point n. For multiple and branch cracks, n= M_b+1, ... M_b+M_{c1}, $M_b+M_{c1}+2$, ... $M_b+M_{c1}+M_{c2}+1$. In addition, for a branch crack, we add a nodal point n= $M_b+M_{c1}+2$.

Eqs.(2.1.18) can be written in the following matrix form:

$$\begin{aligned}
&[UC]\left\{ u \right\} - [Q]\left\{ \Delta u^1 \right\} - [Q_1]\left\{ \Delta u^2 \right\} = [UR]\left\{ t \right\} \\
&[PC]\left\{ u \right\} - [X]\left\{ \Delta u^1 \right\} - [X_{12}]\left\{ \Delta u^2 \right\} = [PR]\left\{ t \right\} - \left\{ \pi^1 \right\} \qquad (2.1.19) \\
&[PC_1]\left\{ u \right\} - [X_{21}]\left\{ \Delta u^1 \right\} - [X_2]\left\{ \Delta u^2 \right\} = [PR_1]\left\{ t \right\} - \left\{ \pi^2 \right\}.
\end{aligned}$$

For multiple cracks, the matrices in eqs.(2.1.19) have the following dimensions:

[UC] is $2M_b$ x $2M_b$, [Q] is $2M_b$ x $2(M_{c1}-1)$, [Q_1] is $2M_b$ x $2(M_{c2}-1)$, [UR] is $2M_b$ x $4M_b$, [PC] is $2M_{c1}$ x $2M_b$, [X] is $2M_{c1}$ x $2(M_{c1}-1)$, [X_{12}] is $2M_{c1}$ x $2(M_{c2}-1)$, [PR] is $2M_{c1}$ x $4M_b$, [PC_1] is $2M_{c2}$ x $2M_b$, [X_{21}] is $2M_{c2}$ x $2(M_{c1}-1)$, [X_2] is $2M_{c2}$ x $2(M_{c2}-1)$, [PR_1] is $2M_{c2}$ x $4M_b$, and

$$\left\{ \Delta u^1 \right\} = \left\{ \begin{array}{c} \Delta u^{(M_b+2)} \\ \Delta u^{(M_b+3)} \\ \cdot \\ \cdot \\ \Delta u^{(M_b+M_{c1})} \end{array} \right\} \qquad \left\{ \pi^1 \right\} = \left\{ \begin{array}{c} \pi^{(M_b+1)} \\ \pi^{(M_b+2)} \\ \pi^{(M_b+3)} \\ \cdot \\ \cdot \\ \pi^{(M_b+M_{c1})} \end{array} \right\}$$

$$\left\{ \Delta u^2 \right\} = \left\{ \begin{array}{c} \Delta u^{(M_b+M_{c1}+3)} \\ \cdot \\ \cdot \\ \Delta u^{(M_b+M_{c1}+M_{c2}+1)} \end{array} \right\} \qquad \left\{ \pi^2 \right\} = \left\{ \begin{array}{c} \pi^{(M_b+M_{c1}+2)} \\ \pi^{(M_b+M_{c1}+3)} \\ \cdot \\ \cdot \\ \pi^{(M_b+M_{c1}+M_{c2}+1)} \end{array} \right\} .$$

For a branch crack, the matrices in eqs.(2.1.19) have the following dimensions:

[UC] is $2M_b$ x $2M_b$, [Q] is $2M_b$ x $2(M_{c1}-1)$, [Q_1] is $2M_b$ x $2M_{c2}$, [UR] is $2M_b$ x $4M_b$, [PC] is $2M_{c1}$ x $2M_b$, [X] is $2M_{c1}$ x $2(M_{c1}-1)$, [X_{12}] is $2M_{c1}$ x $2M_{c2}$, [PR] is $2M_{c1}$ x $4M_b$, [PC_1] is $2(M_{c2}+1)$ x $2M_b$, [X_{21}] is $2(M_{c2}+1)$ x $2(M_{c1}-1)$, [X_2] is $2(M_{c2}+1)$ x $2M_{c2}$, [PR_1] is $2(M_{c2}+1)$ x $4M_b$, and

$$\left\{\Delta u^1\right\} = \left\{\begin{array}{c} \Delta u^{(M_b+2)} \\ \Delta u^{(M_b+3)} \\ \cdot \\ \cdot \\ \Delta u^{(M_b+M_{bk}+1)} \\ \cdot \\ \cdot \\ \Delta u^{(M_b+M_{c1})} \end{array}\right\} \qquad \left\{\pi^1\right\} = \left\{\begin{array}{c} \pi^{(M_b+1)} \\ \pi^{(M_b+2)} \\ \pi^{(M_b+3)} \\ \cdot \\ \cdot \\ \pi^{(M_b+M_{bk}+1)} \\ \cdot \\ \cdot \\ \pi^{(M_b+M_{c1})} \end{array}\right\}$$

$$\left\{\Delta u^2\right\} = \left\{\begin{array}{c} \Delta u^{(M_b+M_{c1}+2)} \\ \Delta u^{(M_b+M_{c1}+3)} \\ \cdot \\ \cdot \\ \Delta u^{(M_b+M_{c1}+M_{c2}+1)} \end{array}\right\} \qquad \left\{\pi^2\right\} = \left\{\begin{array}{c} \pi^{(M_b+M_{c1}+2)} \\ \pi^{(M_b+M_{c1}+2)} \\ \pi^{(M_b+M_{c1}+3)} \\ \cdot \\ \cdot \\ \pi^{(M_b+M_{c1}+M_{c2}+1)} \end{array}\right\} .$$

Thus

$$\begin{bmatrix} [UC] & -[Q] & -[Q_1] \\ [\Gamma_2][PC] & -[\Gamma_2][X] & -[\Gamma_2][X_{12}] \\ [\Gamma_{21}][PC_1] & -[\Gamma_{21}][X_{21}] & -[\Gamma_{21}][X_2] \end{bmatrix} \begin{Bmatrix} u \\ \Delta u^1 \\ \Delta u^2 \end{Bmatrix} = \begin{bmatrix} [UR] & [0] & [0] \\ [\Gamma_2][PR] & [I] & [0] \\ [\Gamma_{21}][PR_1] & [0] & [I] \end{bmatrix} \begin{Bmatrix} t \\ F^1 \\ F^2 \end{Bmatrix} \tag{2.1.20}$$

where, as in [76], we have defined nodal force matrices on the crack by

$$\left\{F^1\right\} = [\Gamma_2]\left\{\pi^1\right\}$$

$$\left\{ F^2 \right\} = [\Gamma_{21}] \left\{ \pi^2 \right\} \tag{2.1.21}$$

where

$$[\Gamma_2] = [\Gamma_{21}] = \begin{bmatrix} -I & I & 0 & 0 & 0 & 0 & 0 \\ 0 & -I & I & 0 & 0 & 0 & 0 \\ 0 & 0 & -I & I & 0 & 0 & 0 \\ \cdot & \cdot & \cdot & \cdot & \cdot & \cdot & \cdot \\ \cdot & \cdot & \cdot & \cdot & \cdot & \cdot & \cdot \\ 0 & 0 & 0 & 0 & 0 & -I & I \end{bmatrix} \tag{2.1.22}$$

and I represents a 2x2 identity matrix. For multiple cracks, $[\Gamma_2]$ is $2(M_{c1}-1)\text{x}2M_{c1}$ and $[\Gamma_{21}]$ is $2(M_{c2}-1)\text{x}2M_{c2}$. For a branch crack, $[\Gamma_2]$ is $2M_{c1}\text{x}2(M_{c1}+1)$ and $[\Gamma_{21}]$ is $2M_{c2}\text{x}2(M_{c2}+1)$.

For multiple cracks, the matrices in eqs.(2.1.21) have the following dimensions:

$$\left\{ F^1 \right\} = \left\{ \begin{matrix} F^{(M_b+2)} \\ F^{(M_b+3)} \\ \cdot \\ \cdot \\ F^{(M_b+M_{c1})} \end{matrix} \right\} \qquad \left\{ F^2 \right\} = \left\{ \begin{matrix} F^{(M_b+M_{c1}+3)} \\ \cdot \\ \cdot \\ F^{(M_b+M_{c1}+M_{c2}+1)} \end{matrix} \right\} .$$

For a branch crack, the matrices in eqs.(2.1.21) have the following dimensions:

$$\left\{ F^1 \right\} = \left\{ \begin{array}{c} F^{(M_b+2)} \\ F^{(M_b+3)} \\ \vdots \\ F^{(M_b+M_{bk}+1)} \\ \vdots \\ F^{(M_b+M_{c1})} \end{array} \right\} \qquad \left\{ F^2 \right\} = \left\{ \begin{array}{c} F^{(M_b+M_{c1}+2)} \\ F^{(M_b+M_{c1}+3)} \\ \vdots \\ F^{(M_b+M_{c1}+M_{c2}+1)} \end{array} \right\} .$$

For a branch crack, we need to employ continuity conditions and equilibrium conditions, i.e.

$$\Delta u_j^{(M_b+M_{bk}+1)} = \Delta u_j^{(M_b+M_{c1}+2)} \tag{2.1.23}$$

$$F_j^{(M_b+M_{bk}+1)} = F_j^{(M_b+M_{bk}+1)} + F_j^{(M_b+M_{c1}+2)} \quad . \tag{2.1.24}$$

It is well-known that one can obtain the diagonal 2x2 blocks of [UC] in eqs.(2.1.11) or (2.1.20) from rigid-body considerations. If we apply a rigid-body displacement, i.e.

$$\begin{aligned} u_1^{(1)} = u_1^{(2)} = u_1^{(3)} = \; \ldots\ldots \; = u_1^{(M_b)} = u_1 \\ u_2^{(1)} = u_2^{(2)} = u_2^{(3)} = \; \ldots\ldots \; = u_2^{(M_b)} = u_2 \end{aligned} \tag{2.1.25}$$

then the body is stress-free. Thus

$$\left\{ t \right\} = \left\{ 0 \right\} \qquad \left\{ \Delta u \right\} = \left\{ 0 \right\}$$

and eqs.(2.1.11) or (2.1.20) reduce to

$$[UC]\begin{Bmatrix} u_1 \\ u_2 \\ u_1 \\ u_2 \\ \cdot \\ \cdot \\ u_1 \\ u_2 \end{Bmatrix} = \left\{ 0 \right\} \tag{2.1.26}$$

so that

$$UC^{(2i-1)(2i-1)} = -\sum_{\substack{j=1 \\ j\neq i}}^{M_b} UC^{(2i-1)(2j-1)}$$

$$UC^{(2i-1)(2i)} = -\sum_{\substack{j=1 \\ j\neq i}}^{M_b} UC^{(2i-1)(2j)}$$

(2.1.27)

$$UC^{(2i)(2i-1)} = -\sum_{\substack{j=1 \\ j\neq i}}^{M_b} UC^{(2i)(2j-1)}$$

$$UC^{(2i)(2i)} = -\sum_{\substack{j=1 \\ j\neq i}}^{M_b} UC^{(2i)(2j)} \quad .$$

Once eqs.(2.1.11) or (2.1.20) have been constructed, we must impose four conditions at each nodal point m on Γ_b involving the boundary values

$$u_1^{(m)}, \quad t_1^{(2m)}, \quad t_1^{(2m+1)},$$

$$u_2^{(m)}, \quad t_2^{(2m)}, \quad t_2^{(2m+1)},$$

and rearrange eqs.(2.1.11) or (2.1.20) accordingly to obtain

$$[A]\left\{ Z \right\} = \left\{ B \right\} \tag{2.1.28}$$

where $\{Z\}$ contains the unknown boundary displacements and tractions on Γ_b and the unknown matrix $\{\Delta u\}$.

Once we have obtained Δu_i at each crack nodal point, the displacement discontinuities normal and tangential to the crack surfaces at that point are

$$\Delta u_n = \Delta u_1 n_1 + \Delta u_2 n_2$$

$$(2.1.29)$$

$$\Delta u_t = \Delta u_2 n_1 - \Delta u_1 n_2$$

and the nondimensional stress intensity factors can be determined from

$$K_I|_{s=0} = \sqrt{\frac{\pi}{8\varepsilon}} G(1+\nu)\Delta u_n(\varepsilon)/\sigma\sqrt{\pi a}$$

$$K_{II}|_{s=0} = \sqrt{\frac{\pi}{8\varepsilon}} G(1+\nu)\Delta u_t(\varepsilon)/\sigma\sqrt{\pi a}$$

(2.1.30)

$$K_I|_{s=l} = \sqrt{\frac{\pi}{8\varepsilon}} G(1+\nu)\Delta u_n(l-\varepsilon)/\sigma\sqrt{\pi a}$$

$$K_{II}|_{s=l} = \sqrt{\frac{\pi}{8\varepsilon}} G(1+\nu)\Delta u_t(l-\varepsilon)/\sigma\sqrt{\pi a}$$

where $\varepsilon \to 0$, G, ν are the shear modulus and Possion's ratio, respectively, l is the length of the crack, σ is a reference load, and a is a reference length.

It should be noted that, for a problem involving a traction free crack, $\{F\}=\{0\}$ and eqs.(2.1.11) or (2.1.20) reduce to

$$\begin{bmatrix} [UC] & -[Q] \\ [\Gamma_2][PC] & -[\Gamma_2][X] \end{bmatrix} \begin{Bmatrix} u \\ \Delta u \end{Bmatrix} = \begin{bmatrix} [UR] \\ [\Gamma_2][PR] \end{bmatrix} \begin{Bmatrix} t \end{Bmatrix}. \qquad (2.1.31)$$

or

$$\begin{bmatrix} [UC] & -[Q] & -[Q_1] \\ [\Gamma_2][PC] & -[\Gamma_2][X] & -[\Gamma_2][X_{12}] \\ [\Gamma_{21}][PC_1] & -[\Gamma_{21}][X_{21}] & -[\Gamma_{21}][X_2] \end{bmatrix} \begin{Bmatrix} u \\ \Delta u^1 \\ \Delta u^2 \end{Bmatrix} = \begin{bmatrix} [UR] \\ [\Gamma_2][PR] \\ [\Gamma_{21}][PR_1] \end{bmatrix} \begin{Bmatrix} t \end{Bmatrix} \qquad (2.1.32)$$

respectively.

2.1.3 Results

Here we employ the coupled model to find numerical solutions for some finite domain problems.

1. Straight crack.

In all straight crack problems, the crack is modeled by 12 elements and the external boundary is modeled by 40 elements. The crack discretization is shown in Figure 2.8. The stress intensity factors, normalized with respect to $\sigma\sqrt{\pi a}$, as shown in eqs.(2.1.30), are calculated and are compared to those obtained in [84].

a) Straight central crack in a rectangular plate subjected to uniform uniaxial tensile stress.

A rectangular plate of height 2h and width 2b contains a central straight crack of length 2a. A uniform uniaxial stress, σ, perpendicular to the crack direction, acts over the ends of the plate as shown in Figure 2.9. In Table 2.1, the stress intensity factors are given for various ratios of a/b and h/b.

b) Straight central slant crack in a rectangular plate subjected to uniform uniaxial tensile stress.

A rectangular plate of height 2.5b and width 2b, containing a crack of length 2a, is subjected to a uniform uniaxial stress σ at the ends. The crack is located centrally at an angle γ to the direction of σ as shown in Figure 2.10. In Tables 2.2 through 2.4, the stress intensity factors are given for various

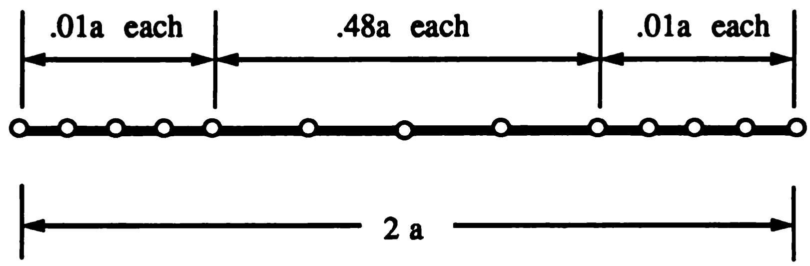

$\varepsilon = .01\,a$

Figure 2.8 Discretization for a straight crack.

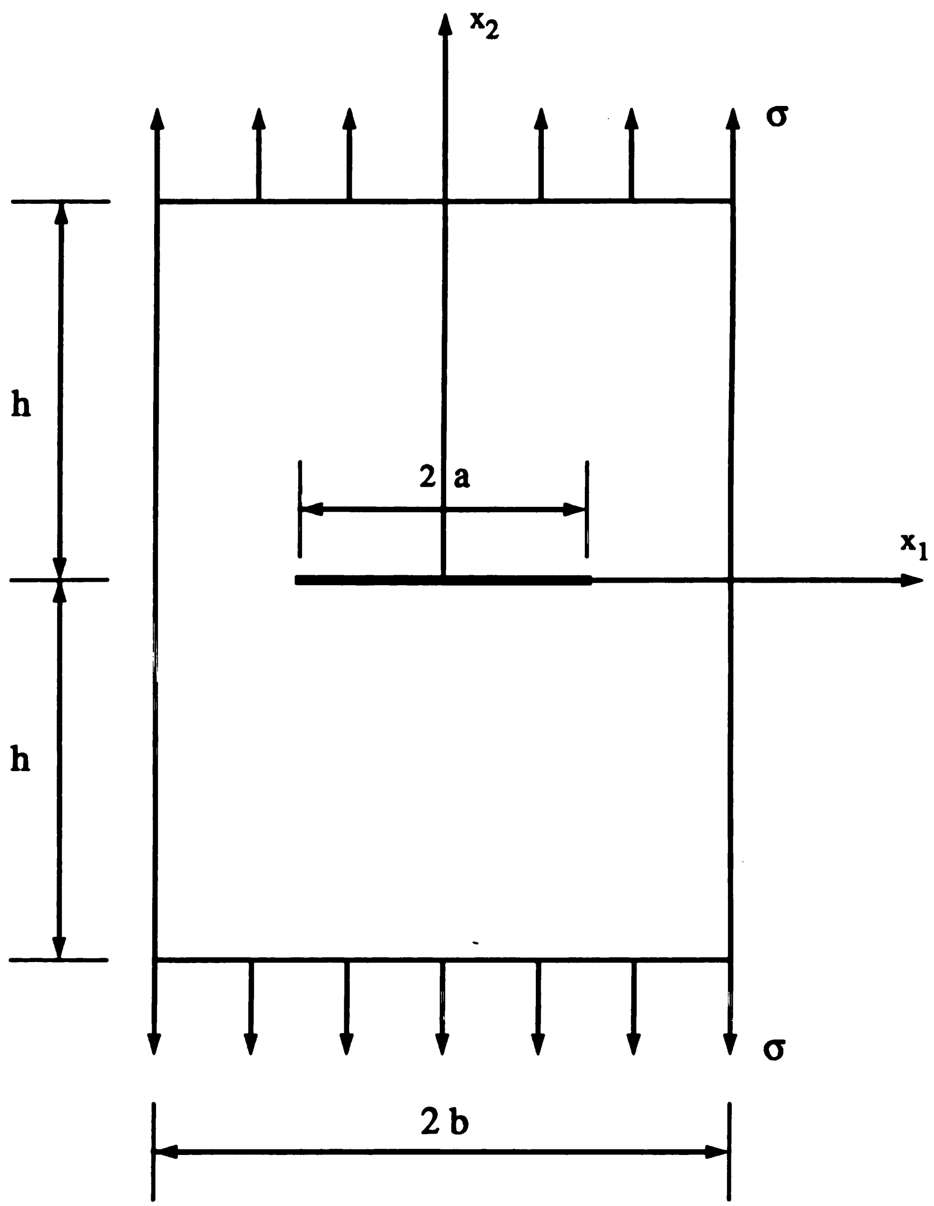

Figure 2.9 Geometry and loading for a straight central crack in a finite plate.

Table 2.1 Stress intensity factors for a straight central crack in a finite plate.

a/b	K_I (h/b=1.0)		K_I (h/b=0.4)	
	Present	**Ref. [84]**	**Present**	**Ref. [84]**
.2	1.07	1.07	1.25	1.25
.3	1.12	1.12	1.51	1.52
.4	1.21	1.21	1.83	1.84
.5	1.31	1.32	2.24	2.24
.6	1.47	1.47	2.80	2.80
.7	1.67	1.67	3.66	3.66

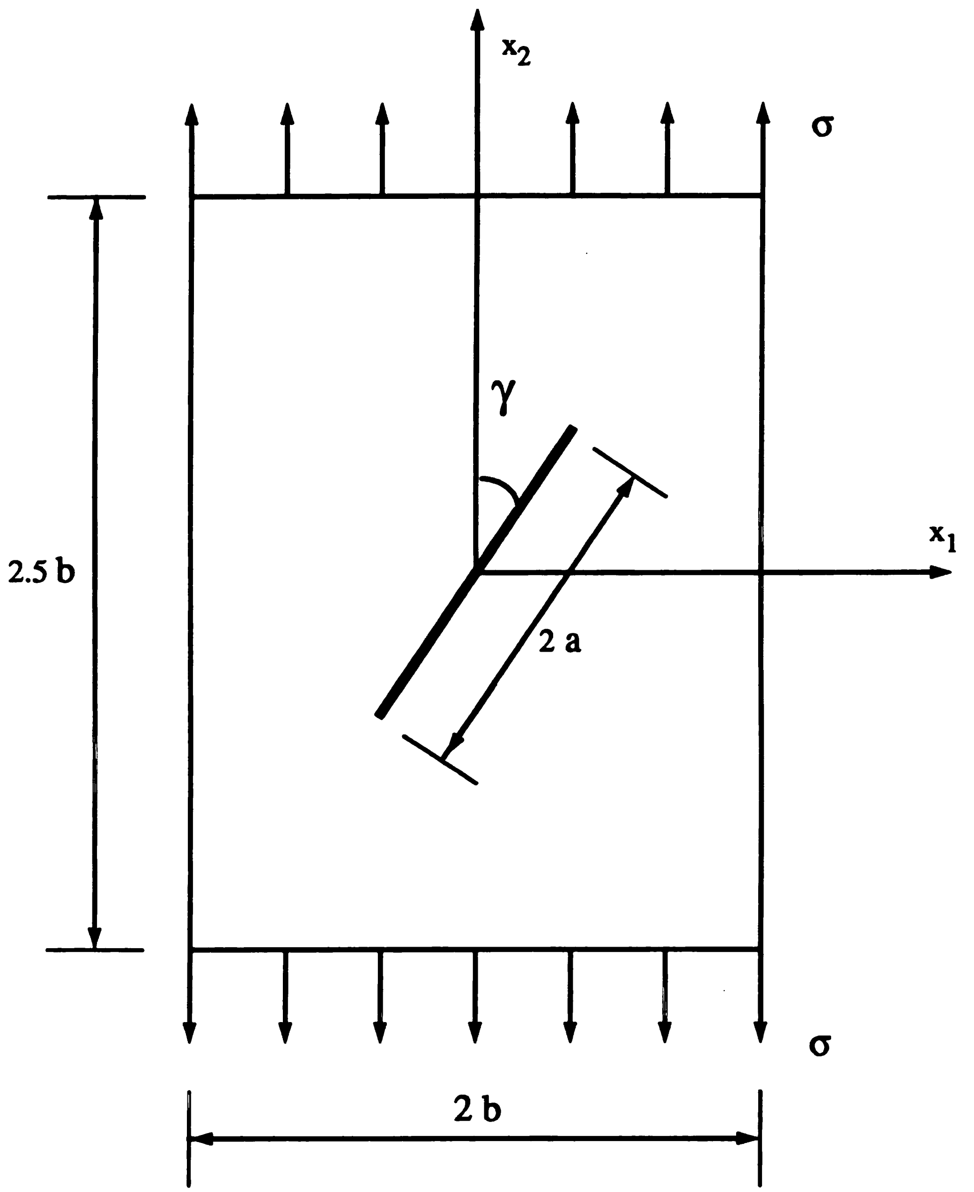

Figure 2.10 Geometry and loading for a straight central slant crack in a finite plate.

Table 2.2 Stress intensity factors for a straight central slant crack in a finite plate, γ=22.5°.

	K_I		K_{II}	
a/b	Present	Ref. [84]	Present	Ref. [84]
.1	.148	.148	.356	.358
.2	.154	.160	.367	.366
.3	.164	.164	.386	.367
.4	.180	.180	.413	.390
.5	.187	.188	.425	.404
.6	.200	.200	.439	.416

Table 2.3 Stress intensity factors for a straight central slant crack in a finite plate, γ=45.0°.

	K_I		K_{II}	
a/b	Present	Ref. [84]	Present	Ref. [84]
.1	.500	.500	.500	.500
.2	.513	.513	.506	.502
.3	.534	.538	.518	.510
.4	.550	.550	.522	.522
.5	.610	.618	.535	.538
.6	.616	.606	.551	.551

Table 2.4 Stress intensity factors for a straight central slant crack in a finite plate, γ=67.5°.

	K_I		K_{II}	
a/b	**Present**	**Ref. [84]**	**Present**	**Ref. [84]**
.1	0.861	0.868	.355	.351
.2	0.868	0.870	.354	.351
.3	0.900	0.900	.359	.356
.4	0.959	0.958	.374	.374
.5	1.002	1.003	.377	.369
.6	1.085	1.118	.388	.380

ratios a/b and various angles γ.

2. Kinked crack.

In the kinked crack problems, both stress intensity factors and relative crack surface displacements are reported. The material properties selected G, ν, are given in the following descriptions.

a) Symmetric V-shaped crack in a square plate.

This example involves a symmetric V-shaped crack in a square plate subjected to pure shear stress as shown in Figure 2.11. Each straight crack segment is modeled by 22 elements of equal length and the external boundary is modeled by 72 elements. In Figures 2.12 and 2.13, the relative crack surface displacements are plotted for $G/\sigma=78.85$, $\nu=0.3$.

b) Non-symmetric V-shaped crack in a square plate.

This example involves a non-symmetric V-shaped crack in a square plate subjected to uniform uniaxial tensile stress as shown in Figure 2.14. Each straight crack segment is modeled by 12 elements of equal length and the external boundary is modeled by 72 elements. In Figures 2.15 and 2.16, the relative crack surface displacements are plotted for $G/\sigma=76.92$, $\nu=0.3$.

c) Z-shaped crack in a rectangular plate.

The first example involves a Z-shaped crack in rectangular plate subjected to

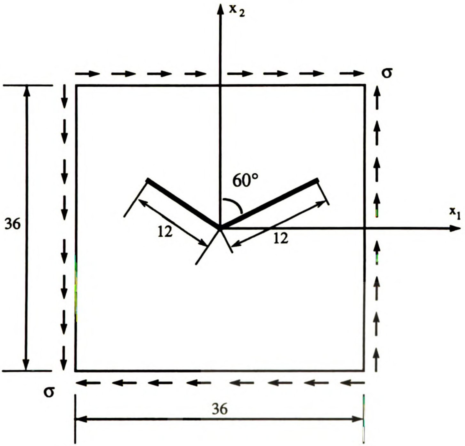

Figure 2.11 Geometry and loading for a symmetric V-shaped crack in a finite plate.

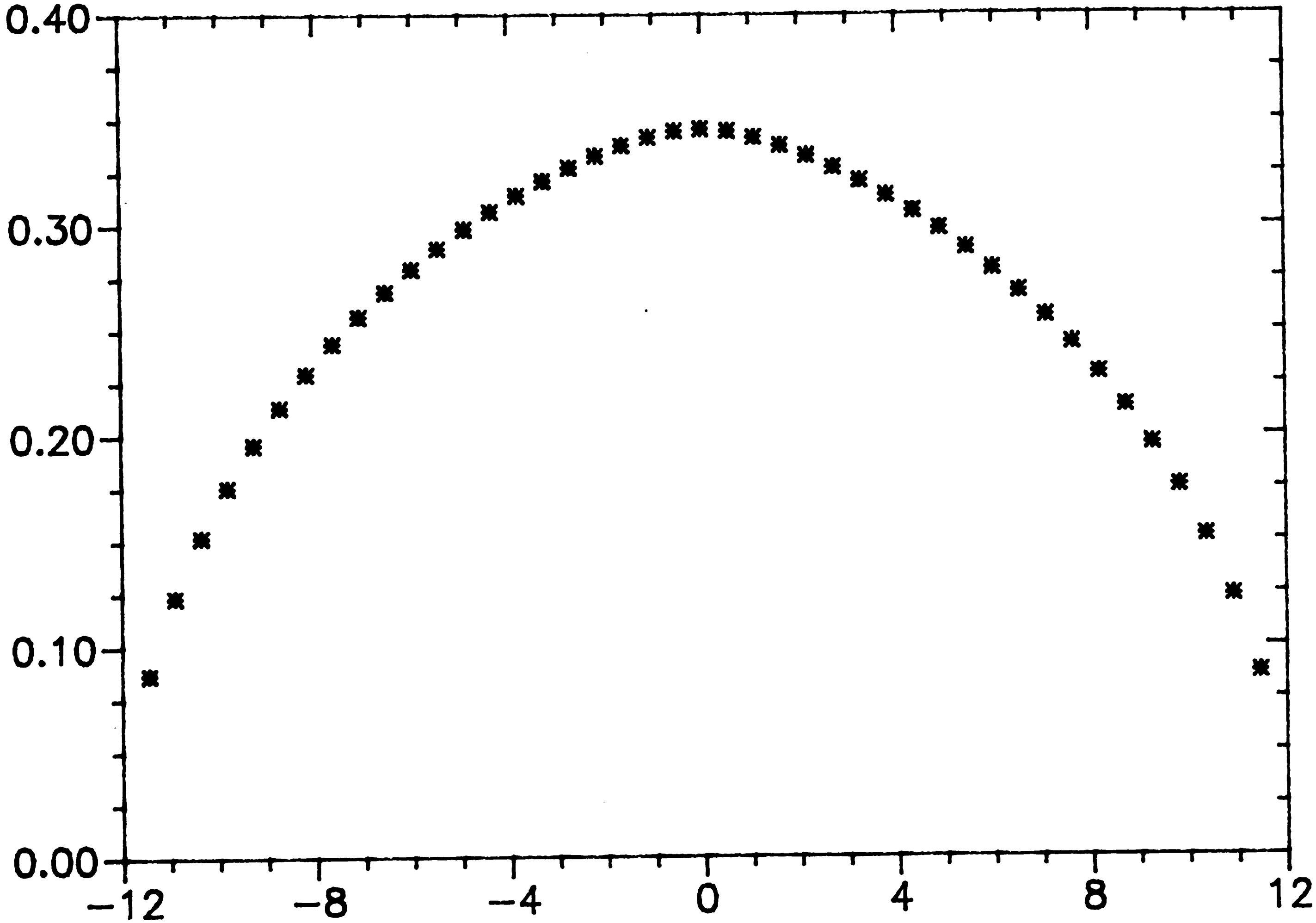

Figure 2.12 Relative crack surface displacement Δu_1 for a body containing a symmetric V–shaped crack and subjected to pure shear.

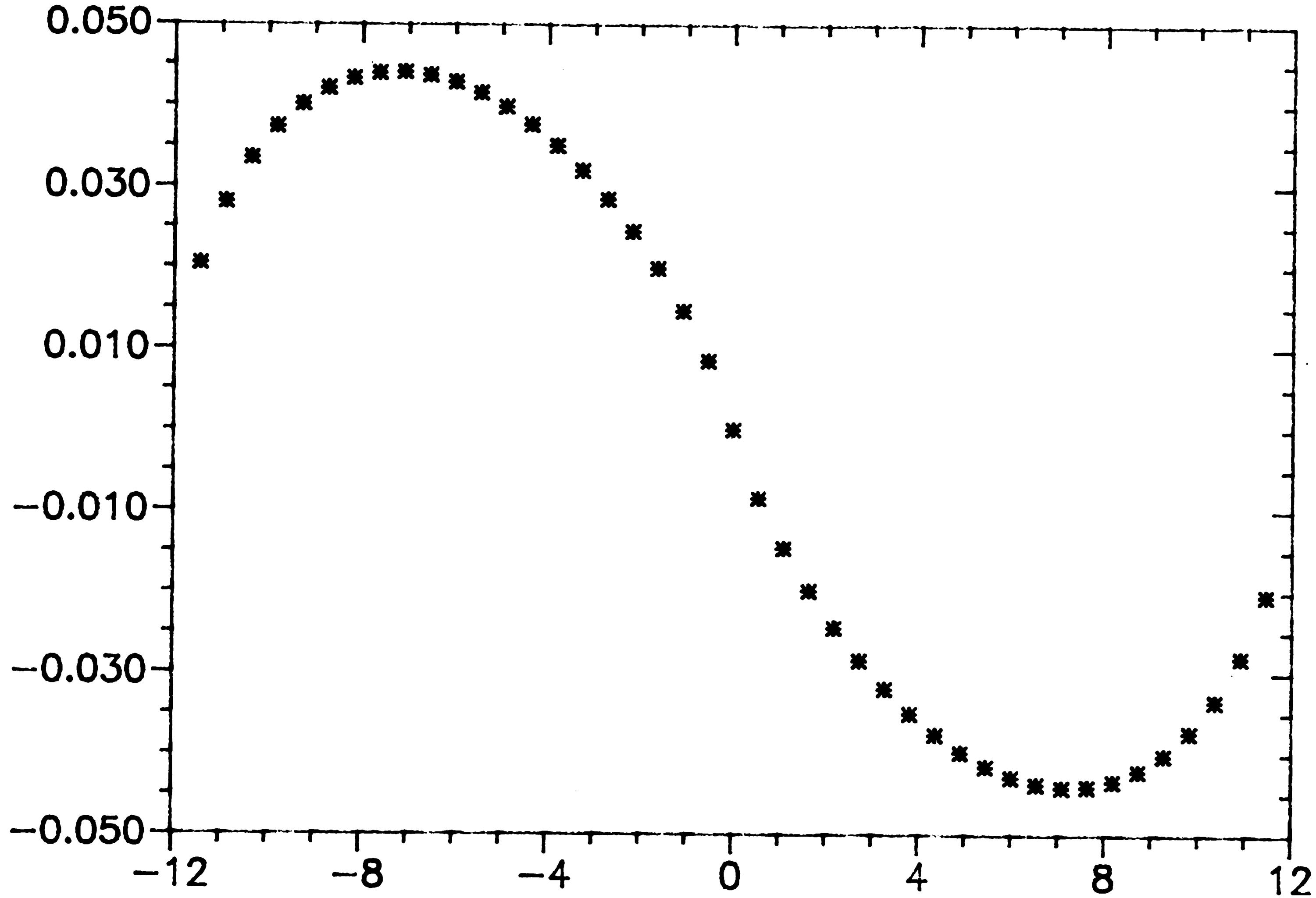

Figure 2.13 Relative crack surface displacement Δu_2 for a body containing a symmetric V−shaped crack and subjected to pure shear.

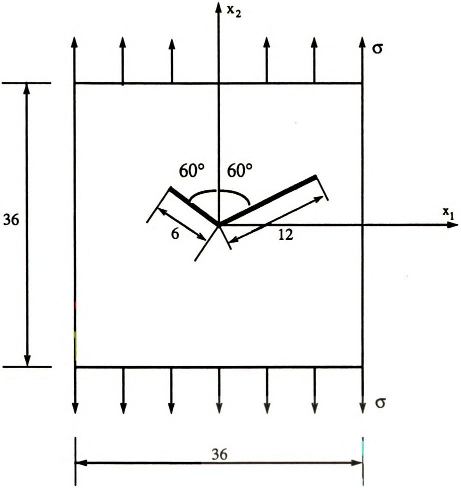

Figure 2.14 Geometry and loading for a non-symmetric V-shaped crack in a finite plate.

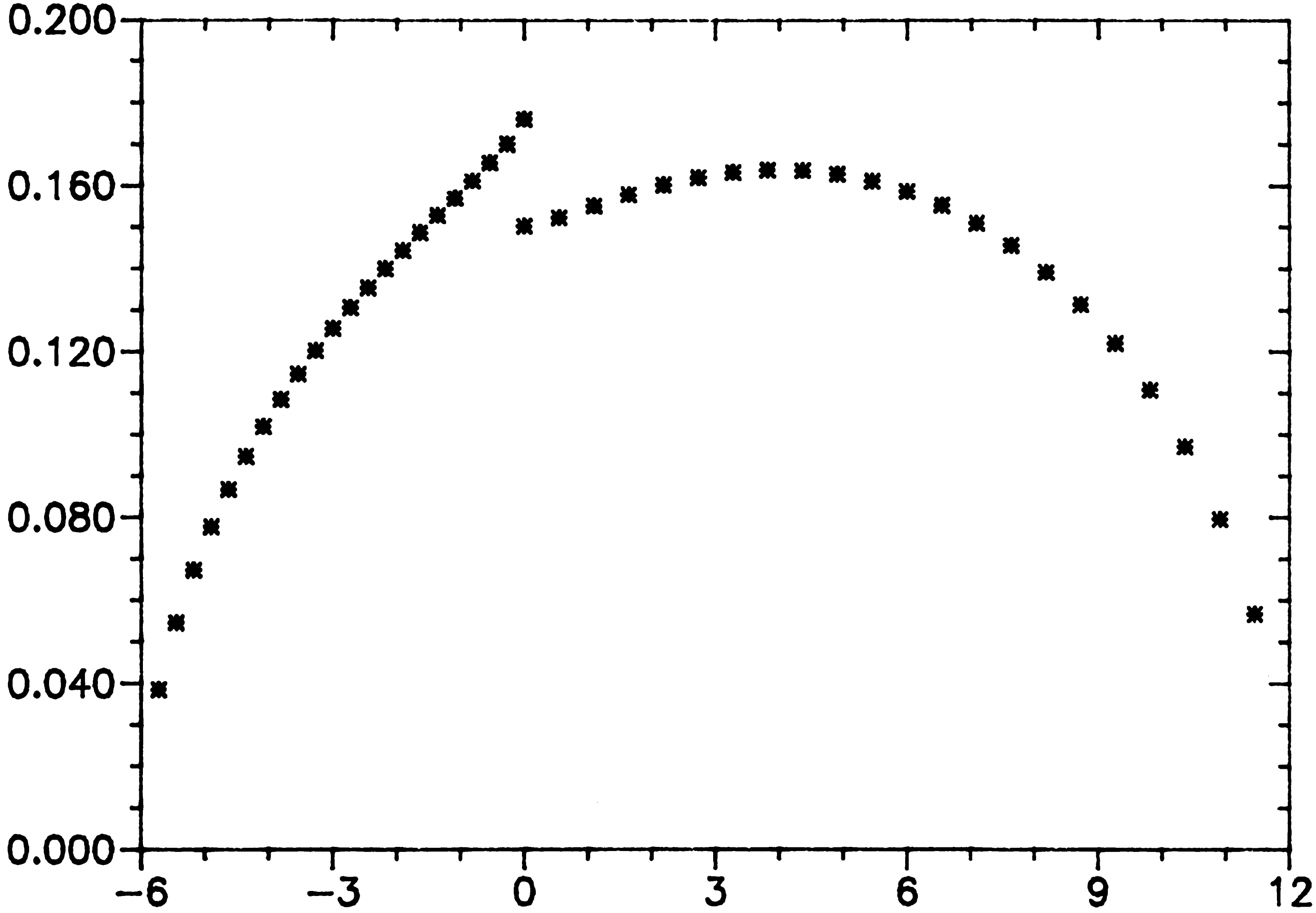

Figure 2.15 Relative crack surface displacement Δu_n for a body containing a non-symmetric V-shaped crack and subjected to uniform uniaxial tensile stress.

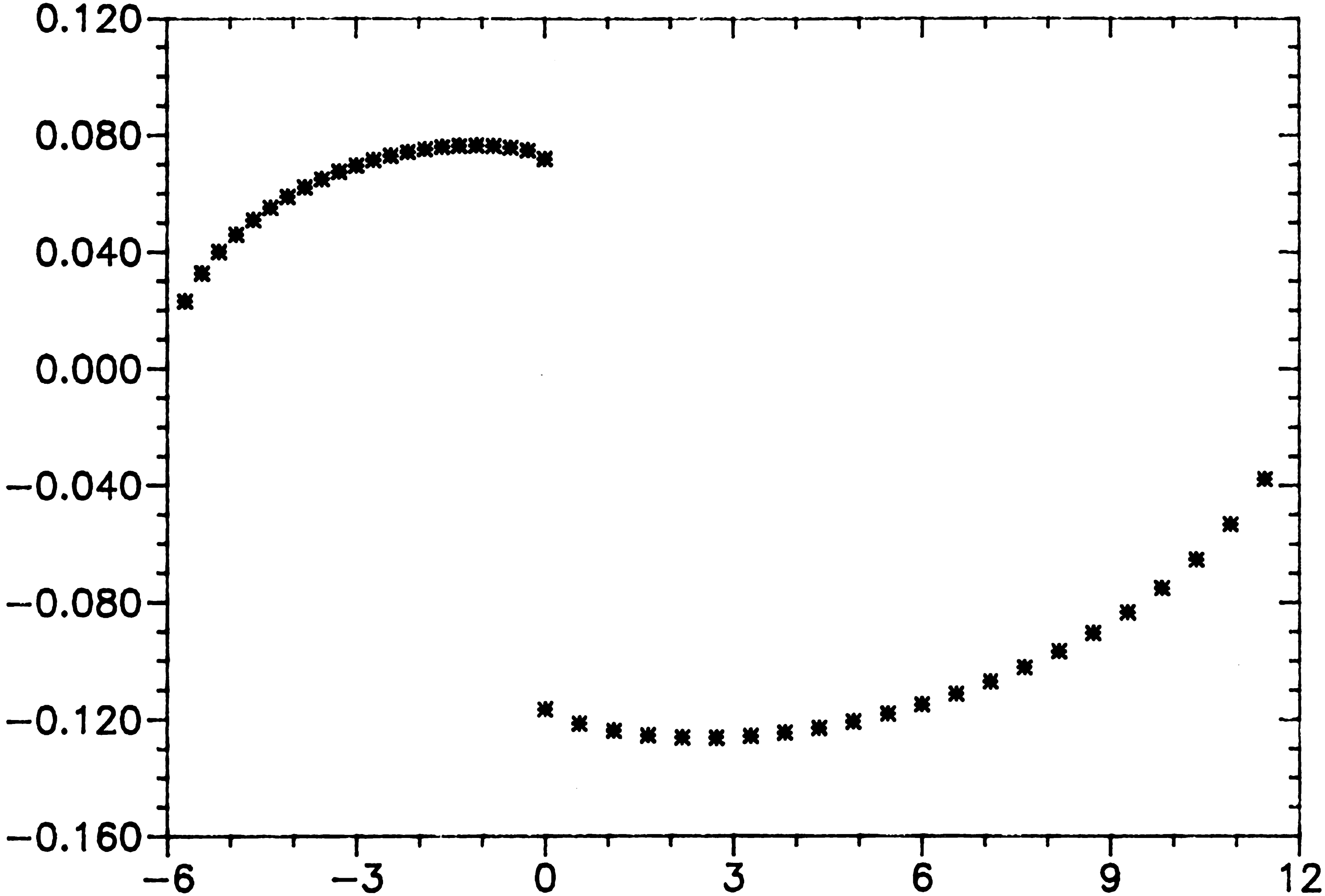

Figure 2.16 Relative crack surface displacement Δu_t for a body containing a non–symmetric V–shaped crack and subjected to uniform uniaxial tensile stress.

a uniform uniaxial tensile stress at one end and a sliding support on the opposite end as shown in Figure 2.17 and the second example involves uniaxial tensile stress as shown in Figure 2.18. The middle straight crack segment is modeled by 20 elements of equal length and each of the two other segments are modeled by 5 elements, as shown in Figure 2.19. The external boundary is modeled by 90 elements. In Figures 2.20 and 2.21, the relative crack surface displacements for the first example are plotted. In Tables 2.5 and 2.6, the stress intensity factors for the two examples are reported and compared to those obtained in [81,85] for $G/\sigma=78.85$, $\nu=0.3$.

3. Multiple cracks.

In the multiple crack problems, both stress intensity factors and relative crack surface displacements are reported. The material properties, G, ν, are given in the following descriptions.

a) Two equal length collinear cracks in a square plate subjected to uniform uniaxial tensile stress.

A square plate contains two equal length collinear cracks of length 2a. A uniform uniaxial stress, σ, acts at the ends as shown in Figure 2.22. Each straight crack segment is modeled by 9 equal elements and the external boundary is modeled by 40 elements. In Table 2.7, the stress intensity factors are given for various ratios 2a/b and compared to those obtained in [86-88]. ($G/\sigma = 4.$, $\nu = 0.25$)

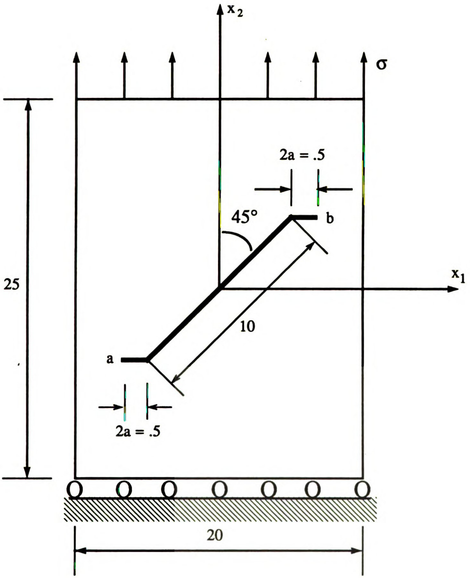

Figure 2.17 Geometry and loading for a Z-shaped crack in a finite plate, case 1.

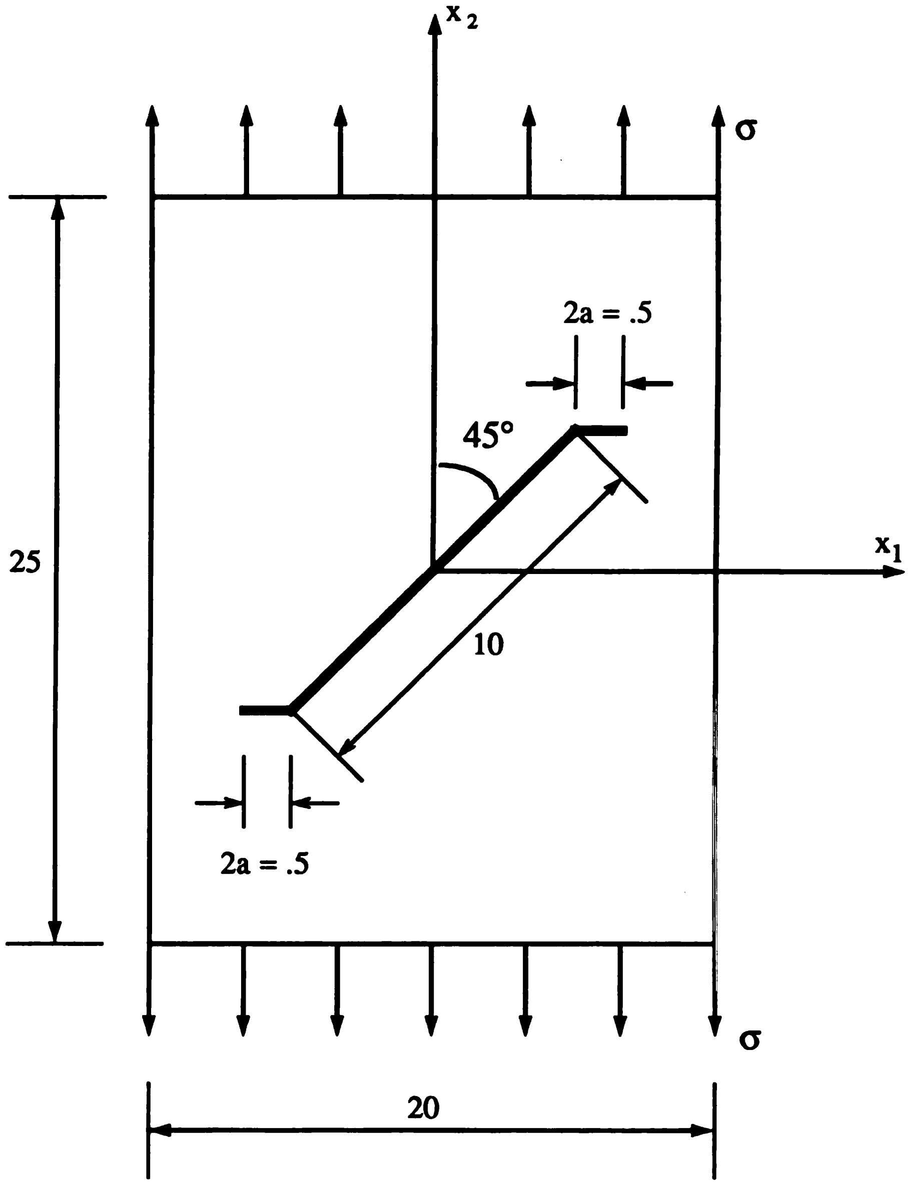

Figure 2.18 Geometry and loading for a Z-shaped crack in a finite plate, case 2.

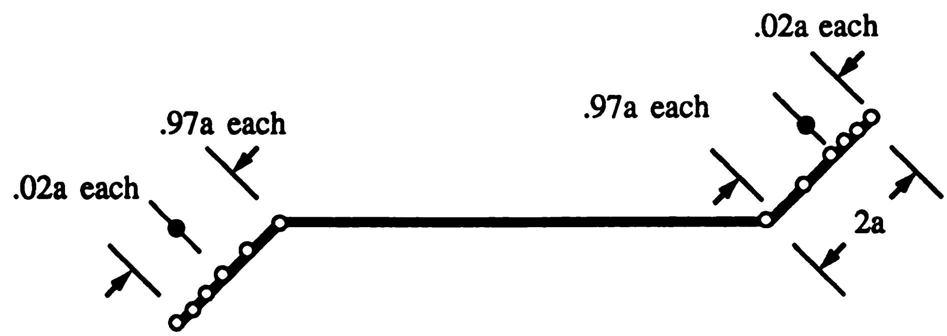

$\varepsilon = .02\ a$

Figure 2.19 Discretization for a Z-shaped crack.

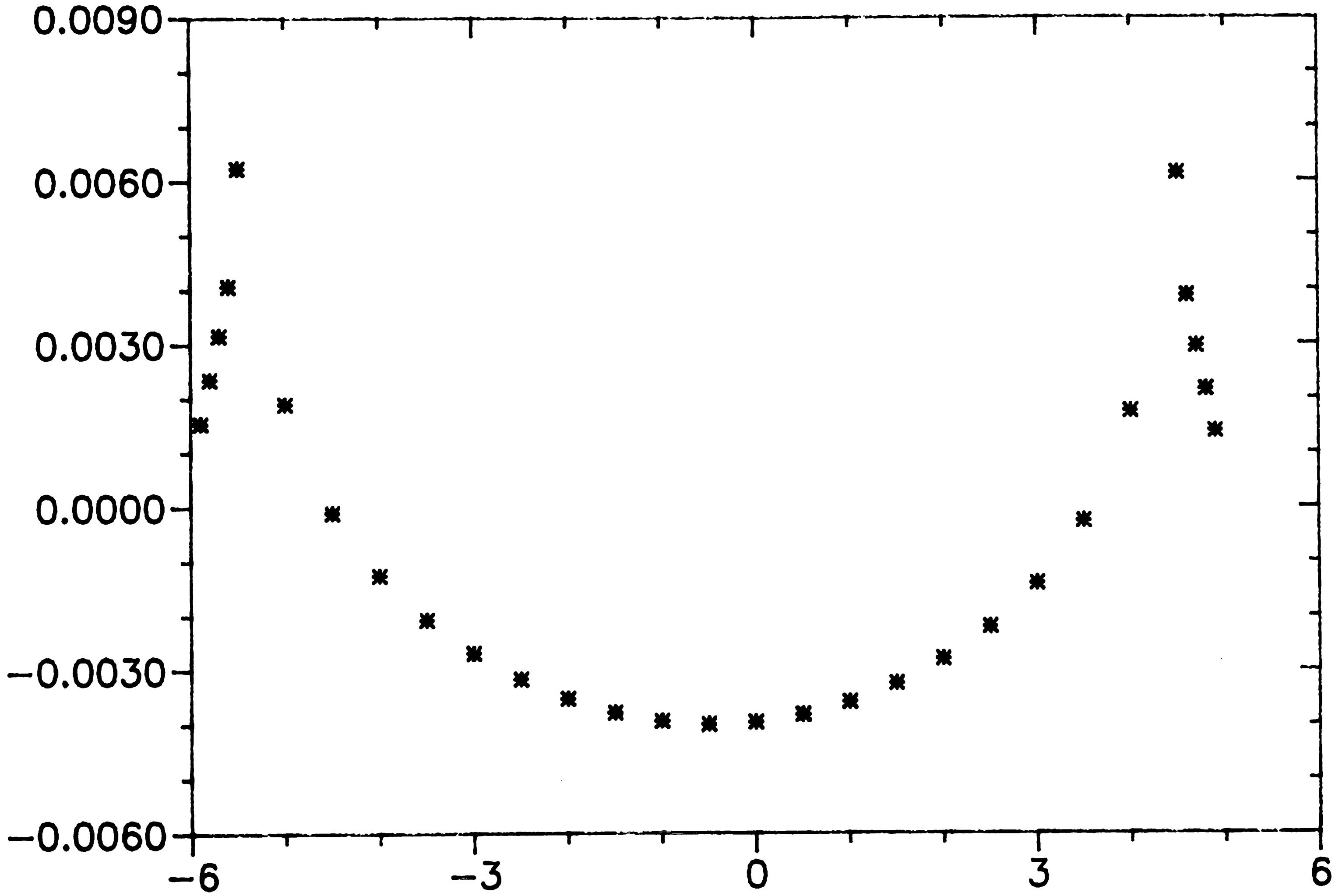

Figure 2.20 Relative crack surface displacement Δu_1 for a body containing a Z-shaped crack as shown in Figure 2.17.

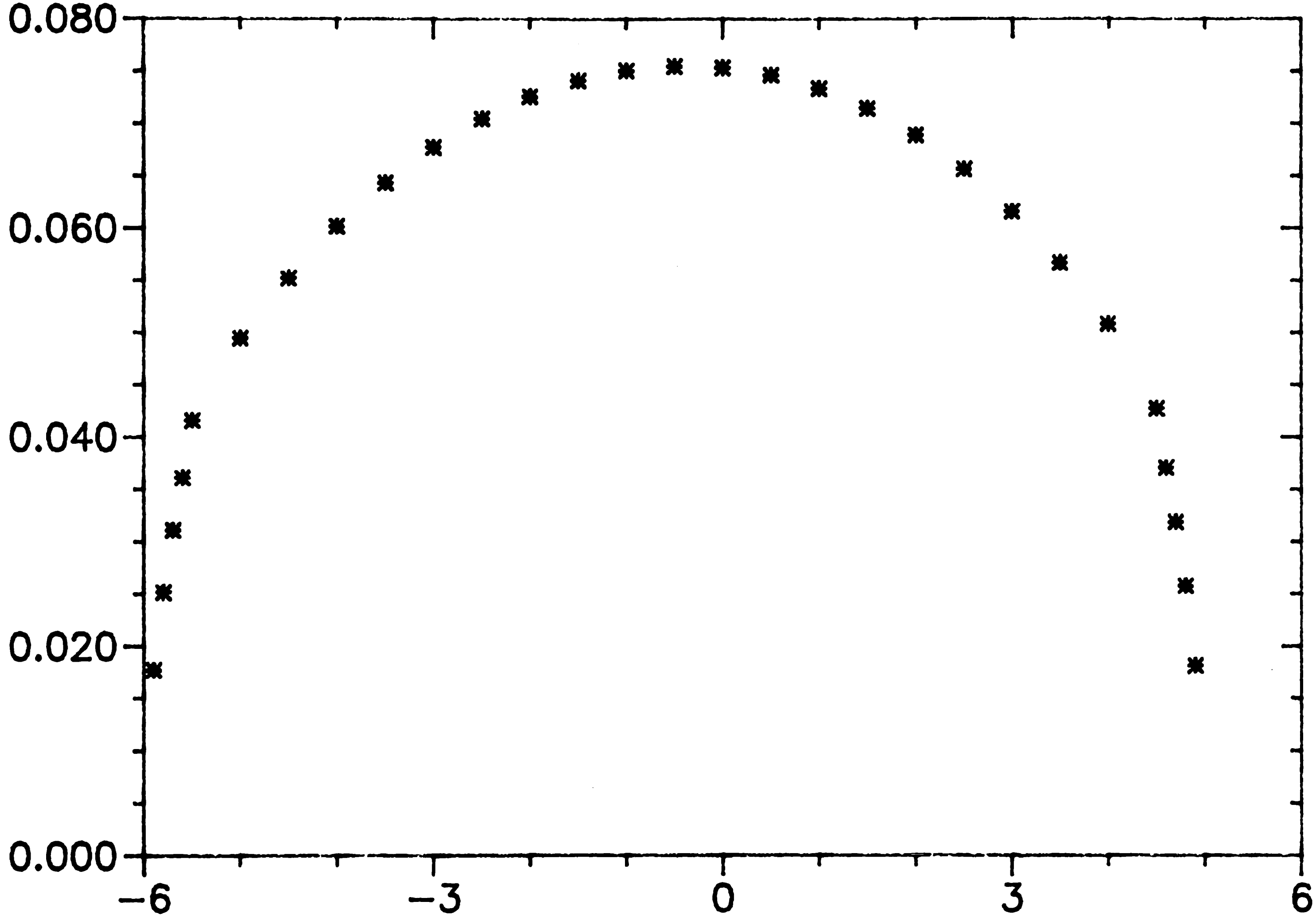

Figure 2.21 Relative crack surface displacement Δu_2 for a body containing a Z–shaped crack as shown in Figure 2.17.

Table 2.5 Stress intensity factors for the Z-shaped crack of Figure 17 in a finite plate.

	K_{Ia}	K_{Ib}	K_{IIa}	K_{IIb}
Present	4.516	.321	4.410	.363
Ref. [81]	4.502	.325	4.397	.405
Ref. [85]	4.555	.335		

Table 2.6 Stress intensity factors for the Z-shaped crack of Figure 18 in a finite plate.

	K_I	K_{II}
Present	4.592	.382
Ref. [81]	4.600	.410

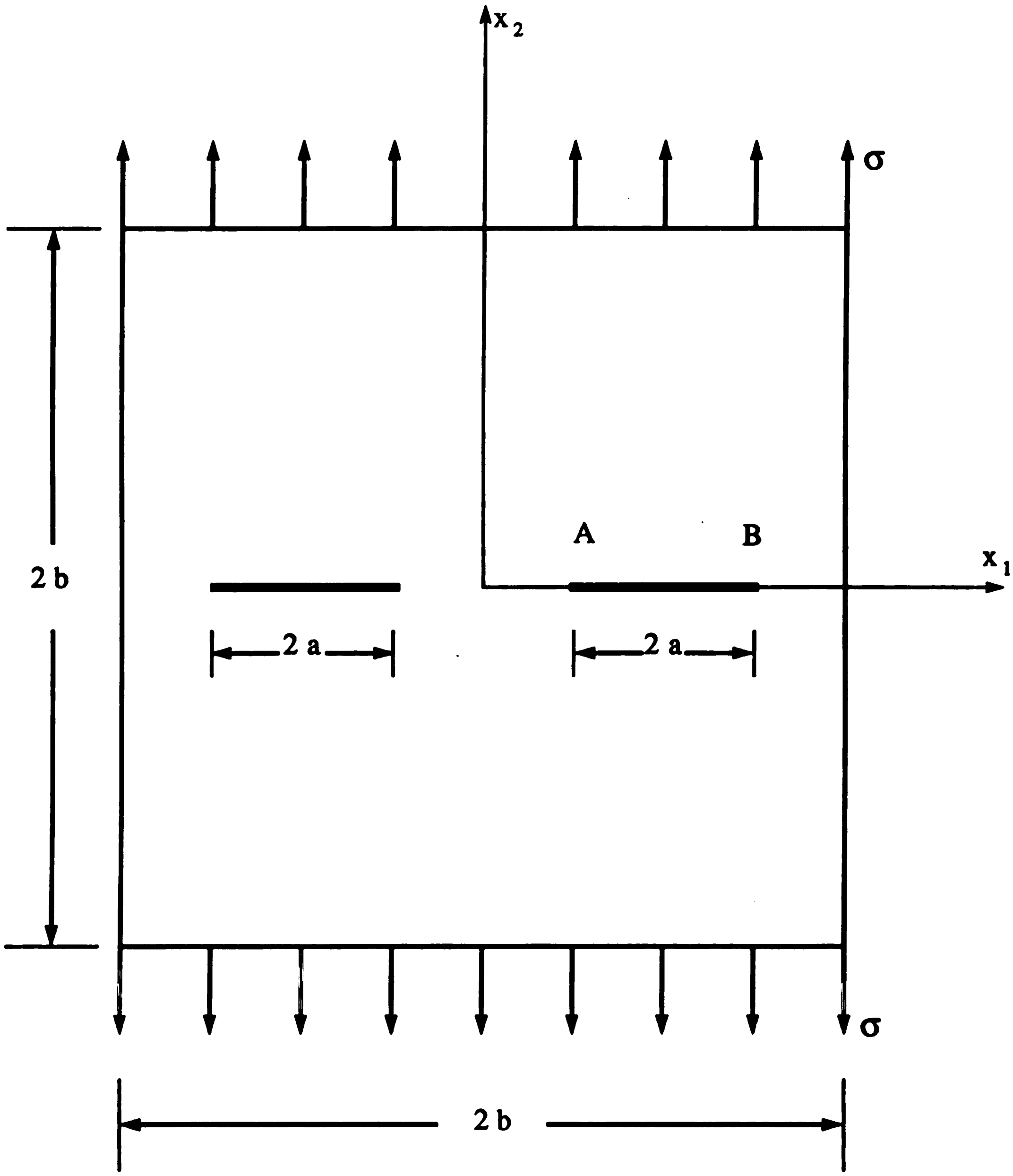

Figure 2.22 Geometry and loading for two equal-length collinear cracks in a finite plate.

Table 2.7 Stress intensity factors for two equal-length collinear cracks in a finite plate.

2a/b	Present		Ref. [86]		Ref. [87]		Ref. [88]	
	K_{IA}	K_{IB}	K_{IA}	K_{IB}	K_{IA}	K_{IB}	K_{IA}	K_{IB}
.1	1.0049	1.0049	1.0054	1.0053	1.0051	1.0044	1.006	1.005
.2	1.0219	1.0200	1.0223	1.0215	1.0223	1.0188	1.023	1.021
.3	1.0540	1.0480	1.0524	1.0497	1.0548	1.0458	1.056	1.048
.4	1.0999	1.0900	1.0989	1.0919	1.1066	1.0885	1.106	1.088
.5	1.1780	1.1500	1.1679	1.1521	1.1825	1.1508	1.181	1.142
.6	1.2800	1.2339	1.2699	1.2368	1.2871	1.2361	1.290	1.220
.7	1.4270	1.3500	1.4269	1.3603	1.4274	1.3488	1.450	1.340
.8	1.6779	1.5600	1.6926	1.5663	1.6244	1.5052	1.680	1.560
.9	2.2694	2.1102	2.2777	2.1195				

b) Two equal length offset cracks in a rectangular plate subjected to uniform uniaxial tensile stress.

A rectangular plate of height 15. inches and width 4.5 inches, containing two equal offset cracks of lenght 0.8 inches, is subjected to a uniform uniaxial stress σ at the ends as shown in Figure 2.23. Each straight crack segment is modeled by 9 equal elements and the external boundary is modeled by 24 elements. In tables 2.8 through 2.11, the stress intensity factors are given for various angles α and compared to those obtained in [89]. (G/σ = 1.257, ν = 0.38)

c) A straight crack and a kinked crack in a rectangular plate subjected to uniform uniaxial tensile stress.

A rectangular plate of height 15. inches and width 4.5 inches, containing two cracks, is subjected to a uniform uniaxial stress σ at the ends as shown in Figure 2.24. Each straight crack segment is modeled by 5 equal elements and the external boundary is modeled by 24 elements. In Table 2.12, the stress intensity factors are given for various distances h. (G/σ = 1.257, ν = 0.38)

4. Branch crack.

In all branch crack problems, each straight crack segment is modeled by 6 elements and the external boundary is modeled by 40 elements. The stress intensity factors, normalized with respect to $\sigma\sqrt{\pi a}$, as shown in eq.(2.1.30), are calculated and are compared to those obtained in [90]. (G/σ = 4., ν = 0.25)

Fig

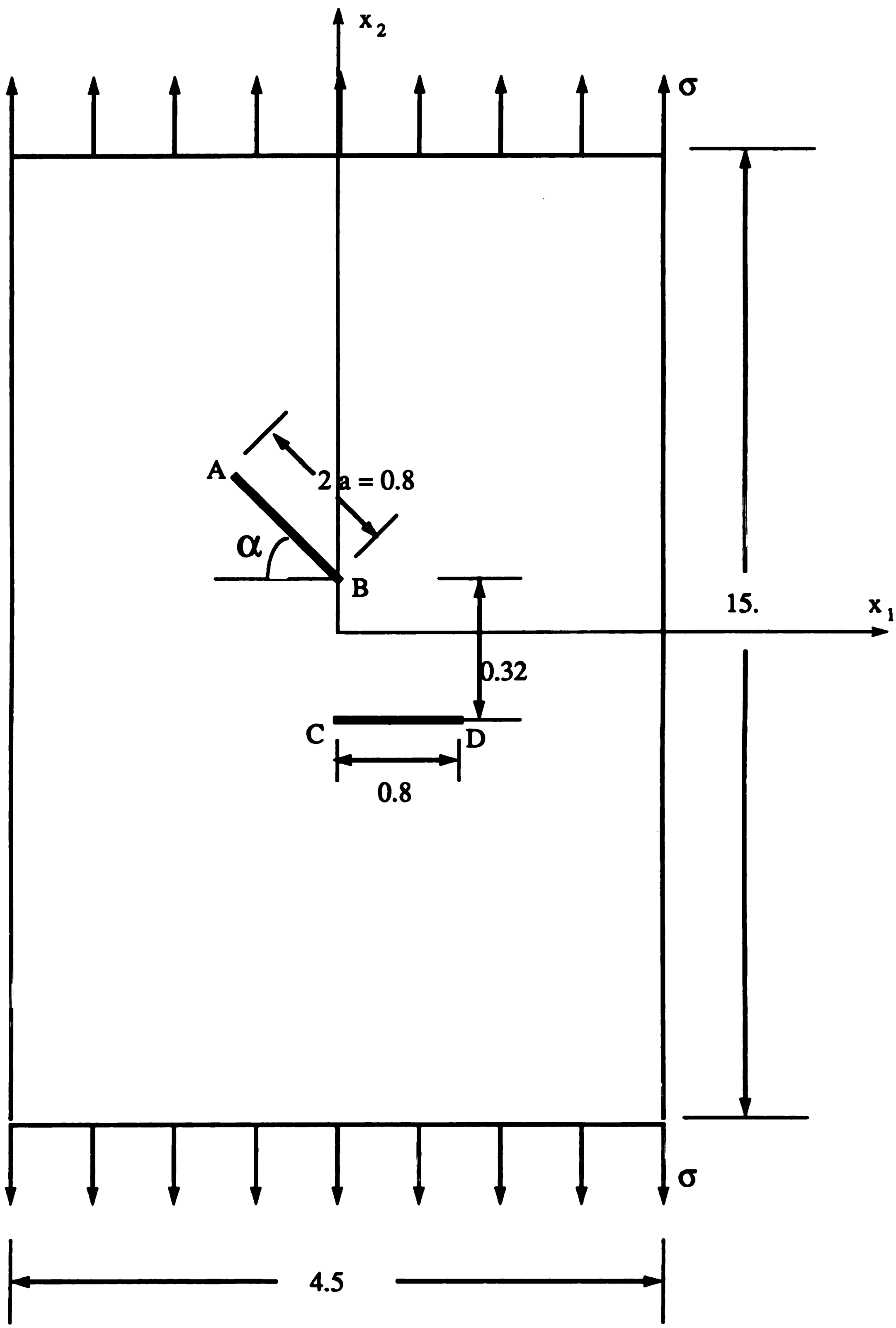

Figure 2.23 Geometry and loading for two equal-length offset cracks in a finite plate.

Table 2.8 Stress intensity factors for two equal length offset cracks in a finite plate, tip A.

	Present		Ref. [89]			
α^o	K_I	K_{II}	$K_I^{experimental}$	$K_{II}^{experimental}$	$K_I^{numerical}$	$K_{II}^{numerical}$
0	1.30	0.03	1.22	0.04	1.35	0.02
15	1.20	0.21	1.18	0.31	1.31	0.15
30	0.97	0.50	0.94	0.49	0.95	0.52
45	0.70	0.60	0.64	0.59	0.79	0.65
60	0.42	0.60	0.36	0.56	0.43	0.68
75	0.13	0.51	0.14	0.45	0.11	0.54
90	0.09	0.25			0.09	0.28

Table 2.9 Stress intensity factors for two equal length offset cracks in a finite plate, tip B.

	Present		Ref. [89]			
α^o	K_I	K_{II}	$K_I^{experimental}$	$K_{II}^{experimental}$	$K_I^{numerical}$	$K_{II}^{numerical}$
0	1.40	0.20	1.47	0.16	1.39	0.22
15	1.18	0.25	1.19	0.17	1.18	0.30
30	1.02	0.50	1.10	0.44	0.95	0.52
45	0.65	0.60	0.70	0.58	0.64	0.61
60	0.36	0.60	0.38	0.68	0.34	0.56
75	0.10	0.40	0.10	0.58	0.11	0.39
90	0.01	0.20	0.06	0.33	0.00	0.13

Table 2.10 Stress intensity factors for two equal length offset cracks in a finite plate, tip C.

	Present		Ref. [89]			
α^o	K_I	K_{II}	$K_I^{experimental}$	$K_{II}^{experimental}$	$K_I^{numerical}$	$K_{II}^{numerical}$
0	1.40	0.20	1.42	0.21	1.39	0.22
15	1.27	0.21	1.30	0.20	1.27	0.22
30	1.25	0.19	1.27	0.19	1.22	0.19
45	1.16	0.14	1.14	0.14	1.18	0.14
60	1.14	0.10	1.14	0.08	1.14	0.10
75	1.10	0.05	1.08	0.05	1.11	0.05
90	1.06	0.03	1.05	0.08	1.08	0.02

Table 2.11 Stress intensity factors for two equal length offset cracks in a finite plate, tip D.

	Present		Ref. [89]			
α^o	K_I	K_{II}	$K_I^{experimental}$	$K_{II}^{experimental}$	$K_I^{numerical}$	$K_{II}^{numerical}$
0	1.30	0.03	1.28	0.00	1.35	0.02
15	1.27	0.01	1.28	0.00	1.25	0.00
30	1.20	0.01	1.18	0.01	1.21	0.01
45	1.16	0.01	1.16	0.04	1.18	0.01
60	1.14	0.01	1.15	0.06	1.14	0.00
75	1.10	0.00	1.06	0.02	1.12	0.01
90	1.00	0.00	1.10	0.02	1.09	0.01

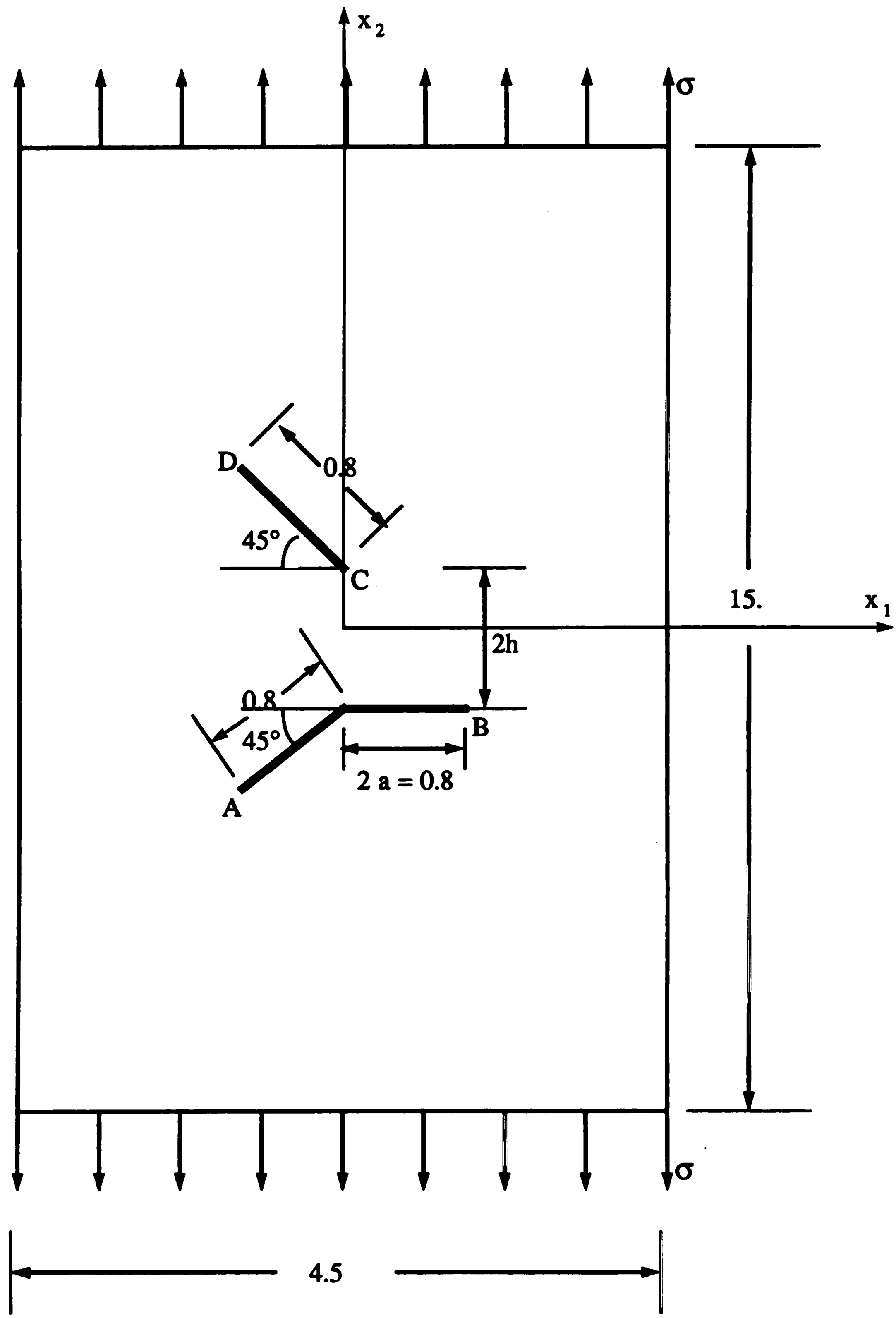

Figure 2.24 Geometry and loading for a straight crack and a kinked crack in a finite plate.

Table 2.12 Stress intensity factors for a straight crack and a kinked crack in a finite plate.

h	K_{IA}	K_{IIA}	K_{IB}	K_{IIB}	K_{IC}	K_{IIC}	K_{ID}	K_{IID}
0.02	1.1099	0.9021	2.0836	0.0114	0.8068	2.2328	0.0536	0.1832
0.04	1.1176	0.9140	2.0811	0.0148	0.7997	2.0923	0.0614	0.1764
0.06	1.1250	0.9241	2.0784	0.0169	0.7948	1.9731	0.0681	0.1704
0.08	1.1321	0.9330	2.0756	0.0183	0.7901	1.8756	0.0736	0.1652
0.10	1.1386	0.9407	2.0727	0.0191	0.7852	1.7973	0.0779	0.1607
0.12	1.1447	0.9475	2.0696	0.0196	0.7800	1.7351	0.0811	0.1568
0.14	1.1504	0.9534	2.0664	0.0198	0.7745	1.6862	0.0834	0.1535
0.16	1.1556	0.9586	2.0630	0.0197	0.7689	1.6486	0.0849	0.1508

a) A central symmetrically-branched crack in a square plate subjected to uniform uniaxial tensile stress.

A square plate, i.e. h=w, contains a branch crack. A uniform uniaxial stress, σ, acts at the ends as shown in Figure 2.25. In table 2.13, the stress intensity factors are given for various angles α. In Figures 2.26 and 2.27, the relatve crack surface displacements are plotted. In Table 2.14, the stress intensity factors are given for various ratios 2a/w.

b) A central symmetrically-branched crack in a rectangular plate subjected to uniform uniaxial tensile stress.

A rectangular plate contains a branch crack and is subjected to uniform uniaxial tensile tensile stress σ at the ends as shown in Figure 2.25. In Table 2.15, the stress intensity factors are given for various ratios h/w.

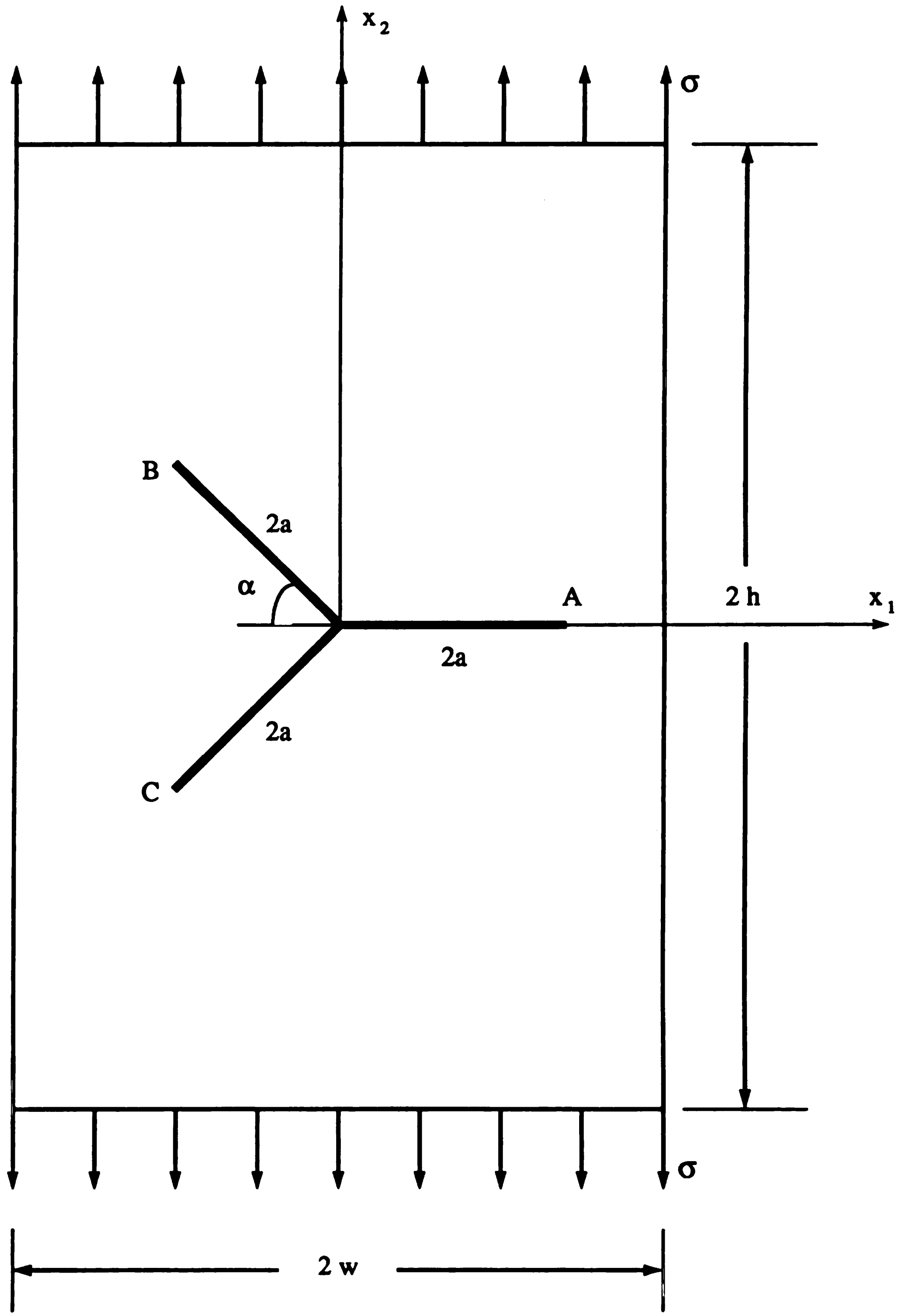

Figure 2.25 Geometry and loading for a branch crack in a finite plate.

Table 2.13 Stress intensity factors for a branch crack in a finite plate, h/w=1.0, 2a/w=0.5.

	Present			Ref. [90]		
α^o	K_{IA}	K_{IB}	K_{IIB}	K_{IA}	K_{IB}	K_{IIB}
10	0.87	0.61	0.12	0.87	0.62	0.12
20	0.92	0.58	0.24	0.92	0.58	0.24
30	0.90	0.49	0.35	0.91	0.50	0.35
45	0.87	0.33	0.50	0.87	0.33	0.50
60	0.82	0.12	0.52	0.81	0.12	0.52
70	0.77	-.08	0.50	0.77	-.08	0.50

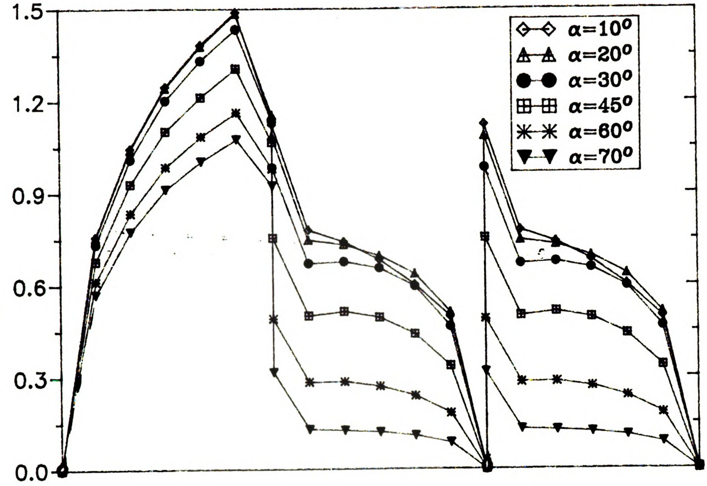

Figure 2.26 Relative crack surface displacement Δu_1 for a body aontaining a branch crack and subjected to uniform uniaxial stress.

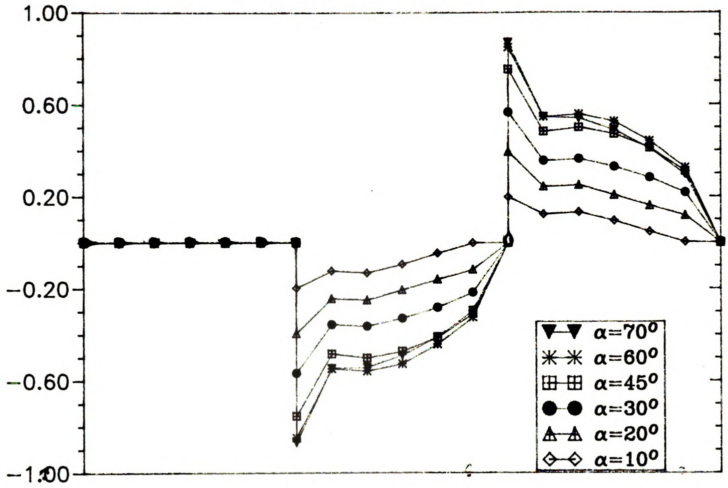

Figure 2.27 Relative crack surface displacement Δu_2 for a body containing a branch crack and subjected to uniform uniaxial stress.

Table 2.14 Stress intensity factors for a branch crack in a finite plate, α=45°, h/w=1.0.

	Present			**Ref. [90]**		
2a/w	K_{IA}	K_{IB}	K_{IIB}	K_{IA}	K_{IB}	K_{IIB}
.10	0.69	0.31	0.32	0.69	0.31	0.32
.25	0.73	0.32	0.34	0.74	0.31	0.34
.40	0.81	0.32	0.41	0.81	0.32	0.41
.50	0.87	0.33	0.50	0.87	0.33	0.50
.60	0.93	0.35	0.60	0.93	0.35	0.60

Table 2.15 Stress intensity factors for a branch crack in a finite plate, α=45°, 2a/w=0.5 .

	Present			**Ref. [90]**		
h/w	K_{IA}	K_{IB}	K_{IIB}	K_{IA}	K_{IB}	K_{IIb}
0.8	0.99	0.38	0.55	1.00	0.38	0.55
1.0	0.87	0.33	0.50	0.87	0.33	0.50
1.2	0.80	0.31	0.43	0.80	0.31	0.43
1.6	0.74	0.30	0.40	0.74	0.30	0.40
2.0	0.71	0.30	0.38	0.71	0.30	0.38
2.4	0.70	0.30	0.37	0.70	0.30	0.37

2.2 Edge Cracks

2.2.1 Theoretical Development

A plane elastic region Ω, with external boundary $\Gamma = \Gamma_{b1} + \Gamma_{b2}$, containing a piece-wise smooth edge crack Γ_c , as shown in Figure 2.28 or a piece-wise smooth edge branch crack, Γ_{c1} and Γ_{c2}, as shown in Figure 2.29, is loaded by prescribed tractions t_j on some part of the external boundary and prescribed displacements u_j on the remainder of the external boundary. Then the direct boundary-integral equations and the integral equations developed in [76] can be coupled as follows.

For a single edge crack:

$$c_{ij}(\mathbf{x})\, u_j(\mathbf{x}) = \int_{\Gamma_{b1}} [\, (uR)_{ij}^{h}(\mathbf{x}, \bar{\mathbf{x}})\, t_j(\bar{\mathbf{x}}) - (uc)_{ij}^{h}(\mathbf{x}, \bar{\mathbf{x}})\, u_j(\bar{\mathbf{x}})]\, ds(\bar{\mathbf{x}})$$

$$+ \int_{\Gamma_c} (uc)_{ij}^{h}(\mathbf{x}, \bar{\mathbf{x}})\, \Delta u_j(\bar{\mathbf{x}})\, ds(\bar{\mathbf{x}}) \qquad \mathbf{x} \text{ on } \Gamma_{b1}$$

$$(2.2.1)$$

$$\pi_i(\mathbf{x}) = \int_{\Gamma_{b1}} [\, (\pi R)_{ij}^{h}(\mathbf{x}, \bar{\mathbf{x}})\, t_j(\bar{\mathbf{x}}) - (\pi c)_{ij}^{h}(\mathbf{x}, \bar{\mathbf{x}})\, u_j(\bar{\mathbf{x}})]\, ds(\bar{\mathbf{x}})$$

$$+ \int_{\Gamma_c} (\pi c)_{ij}^{h}(\mathbf{x}, \bar{\mathbf{x}})\, \Delta u_j(\bar{\mathbf{x}})\, ds(\bar{\mathbf{x}}) \qquad \mathbf{x} \text{ on } \Gamma_c$$

For an edge branch crack:

$$c_{ij}(\mathbf{x})\, u_j(\mathbf{x}) = \int_{\Gamma_{b1}} [\, (uR)_{ij}^{h}(\mathbf{x}, \bar{\mathbf{x}})\, t_j(\bar{\mathbf{x}}) - (uc)_{ij}^{h}(\mathbf{x}, \bar{\mathbf{x}})\, u_j(\bar{\mathbf{x}})\,] ds(\bar{\mathbf{x}})$$

$$+ \sum_{k=1}^{2} \int_{\Gamma_{ck}} (uc)_{ij}^{h}(\mathbf{x}, \bar{\mathbf{x}})\, \Delta u_j(\bar{\mathbf{x}})\, ds(\bar{\mathbf{x}}) \qquad \mathbf{x} \text{ on } \Gamma_{b1}$$

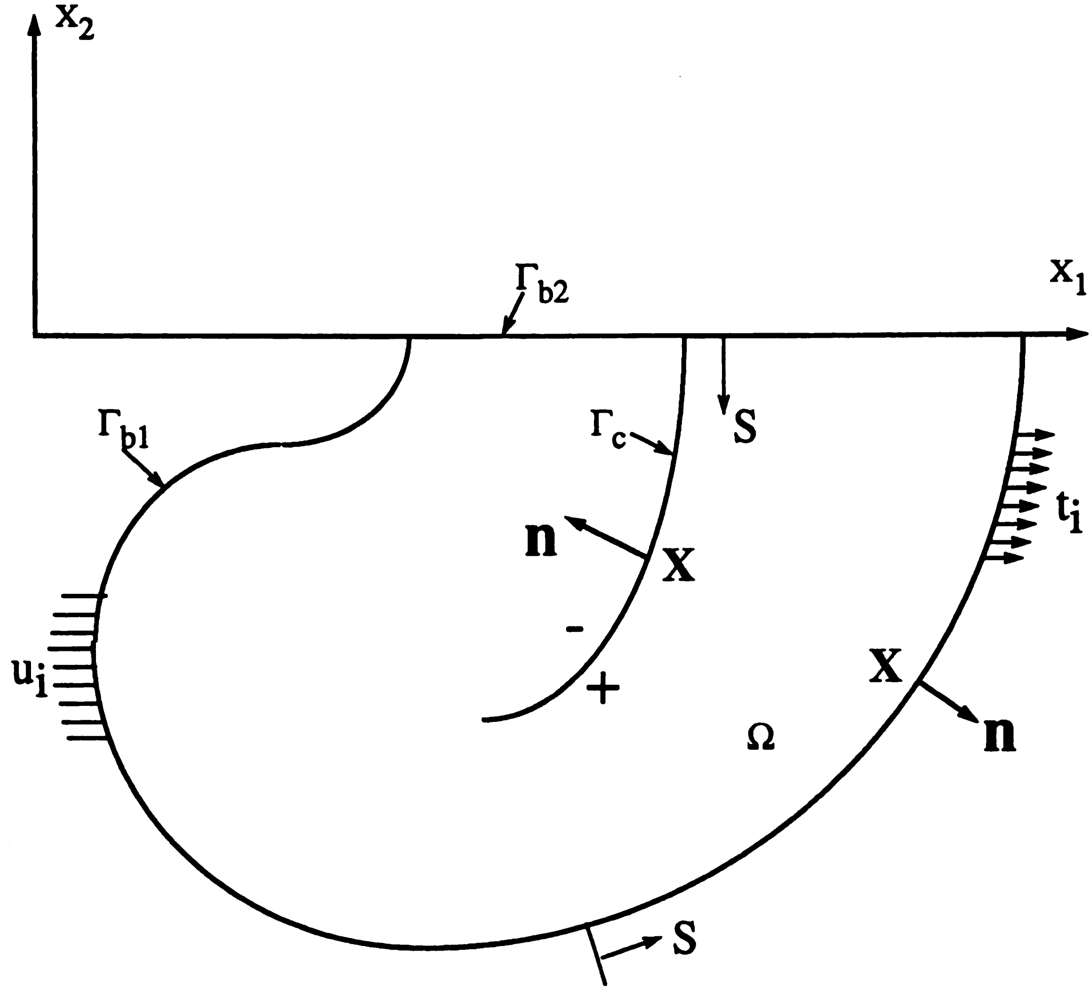

Figure 2.28 Half-hlane elastic region containing a single edge crack.

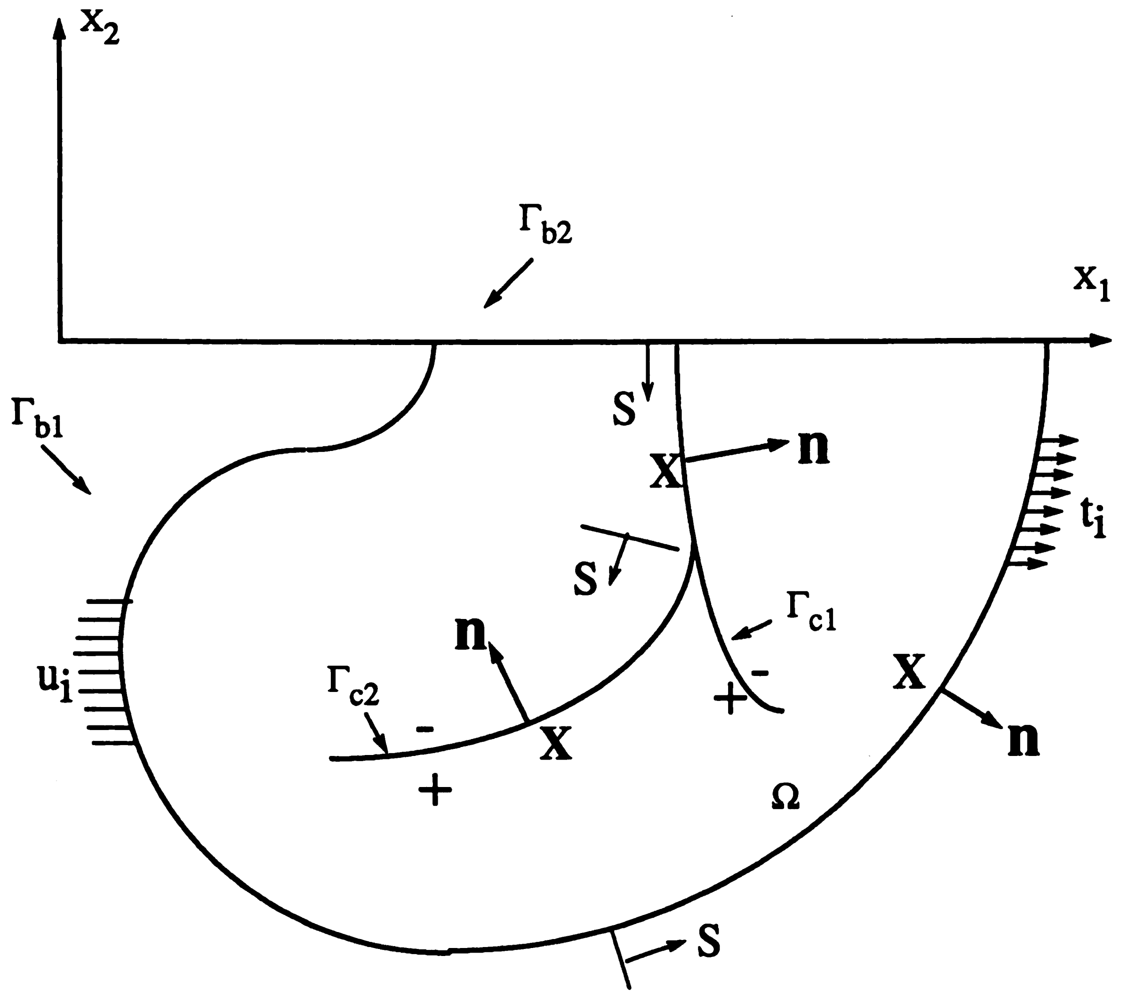

Figure 2.29 Half-plane elastic region containing an edge branch crack.

$$\pi_i(\mathbf{x}) = \int_{\Gamma_{b1}} [\, (\pi R)^h_{ij}(\mathbf{x}, \bar{\mathbf{x}})\, t_j(\bar{\mathbf{x}}) - (\pi c)^h_{ij}(\mathbf{x}, \bar{\mathbf{x}})\, u_j(\bar{\mathbf{x}})\,] ds(\bar{\mathbf{x}})$$

$$+ \sum_{k=1}^{2} \int_{\Gamma_{ck}} (\pi c)^h_{ij}(\mathbf{x}, \bar{\mathbf{x}})\, \Delta u_j(\bar{\mathbf{x}})\, ds(\bar{\mathbf{x}}) \qquad \mathbf{x} \text{ on } \Gamma_{c1} \qquad (2.2.2)$$

$$\pi_i(\mathbf{x}) = \int_{\Gamma_{b1}} [\, (\pi R)^h_{ij}(\mathbf{x}, \bar{\mathbf{x}})\, t_j(\bar{\mathbf{x}}) - (\pi c)^h_{ij}(\mathbf{x}, \bar{\mathbf{x}})\, u_j(\bar{\mathbf{x}})\,] ds(\bar{\mathbf{x}})$$

$$+ \sum_{k=1}^{2} \int_{\Gamma_{ck}} (\pi c)^h_{ij}(\mathbf{x}, \bar{\mathbf{x}})\, \Delta u_j(\bar{\mathbf{x}})\, ds(\bar{\mathbf{x}}) \qquad \mathbf{x} \text{ on } \Gamma_{c2} \;.$$

In eqs.(2.2.1) and (2.2.2), i=1, 2, j=1, 2, summation on repeated indices is implied, $\Delta u_j = u_j^- - u_j^+$ are the relative crack surface displacements, and π_i are stress functions defined such that the stress components

$$\sigma_{11} = \frac{\partial \pi_1}{\partial x_2} \;, \qquad \sigma_{22} = -\frac{\partial \pi_2}{\partial x_1} \;, \qquad \sigma_{12} = -\frac{\partial \pi_1}{\partial x_1} = \frac{\partial \pi_2}{\partial x_2} \;. \qquad (2.2.3)$$

It was shown in [91,92] that the half-plane fundamental solutions $(\;)^h$ can by represented by adding a complementary part $(\;)^c$ to the well-known two-dimensional Kelvin solutions ( ) as follows:

$$(uR)^h_{ij}(\mathbf{x},\bar{\mathbf{x}}) = (uR)_{ij}(\mathbf{x},\bar{\mathbf{x}}) + (uR)^c_{ij}(\mathbf{x},\bar{\mathbf{x}})$$

$$(uc)^h_{ij}(\mathbf{x},\bar{\mathbf{x}}) = (uc)_{ij}(\mathbf{x},\bar{\mathbf{x}}) + (uc)^c_{ij}(\mathbf{x},\bar{\mathbf{x}})$$

$$(2.2.4)$$

$$(\pi R)^h_{ij}(\mathbf{x},\bar{\mathbf{x}}) = (\pi R)_{ij}(\mathbf{x},\bar{\mathbf{x}}) + (\pi R)^c_{ij}(\mathbf{x},\bar{\mathbf{x}})$$

$$(\pi c)^h_{ij}(\mathbf{x},\bar{\mathbf{x}}) = (\pi c)_{ij}(\mathbf{x},\bar{\mathbf{x}}) + (\pi c)^c_{ij}(\mathbf{x},\bar{\mathbf{x}})$$

The Kelvin fundamental solutions and the corresponding complementary expressions are given in the Appendix A and Appendix B, respectively.

2.2.2 Numerical Treatment

2.2.2.1 A single edge crack

A simple numerical treatment of eqs.(2.2.1) is presented here in which the external boundary is approximated by M_b straight elements and the crack by M_c straight elements, as shown in Figure 2.30. Eqs.(2.2.1) can then be written as

$$c_{ij}(\mathbf{x})\, u_j(\mathbf{x}) = \sum_{m=2}^{M_b} \int_m [(uR)_{ij}^h(\mathbf{x}, \bar{\mathbf{x}})\, t_j(\bar{\mathbf{x}}) - (uc)_{ij}^h(\mathbf{x}, \bar{\mathbf{x}})\, u_j(\bar{\mathbf{x}})]\, ds(\bar{\mathbf{x}})$$

$$+ \sum_{m=M_b+1}^{M_b+M_c} \int_m (uc)_{ij}^h(\mathbf{x}, \bar{\mathbf{x}})\, \Delta u_j(\bar{\mathbf{x}})\, ds(\bar{\mathbf{x}}) \qquad \mathbf{x} \text{ on } \Gamma_{b1}$$

(2.2.5)

$$\pi_i(\mathbf{x}) = \sum_{m=2}^{M_b} \int_m [(\pi R)_{ij}^h(\mathbf{x}, \bar{\mathbf{x}})\, t_j(\bar{\mathbf{x}}) - (\pi c)_{ij}^h(\mathbf{x}, \bar{\mathbf{x}})\, u_j(\bar{\mathbf{x}})]\, ds(\bar{\mathbf{x}})$$

$$+ \sum_{m=M_b+1}^{M_b+M_c} \int_m (\pi c)_{ij}^h(\mathbf{x}, \bar{\mathbf{x}})\, \Delta u_j(\bar{\mathbf{x}})\, ds(\bar{\mathbf{x}}) \qquad \mathbf{x} \text{ on } \Gamma_c\ .$$

Following the same procedures as in previous section, eqs.(2.2.5) become

$$c_{ij}^{(n)} u_j^{(n)} = \sum_{m=2}^{M_b} \Delta s_b^m/4\ [\int_m (1-\xi)(uR)_{ij}^h(\mathbf{x}^{(n)}, \xi) d\xi\ ]\ t_j^{(2m-1)}$$

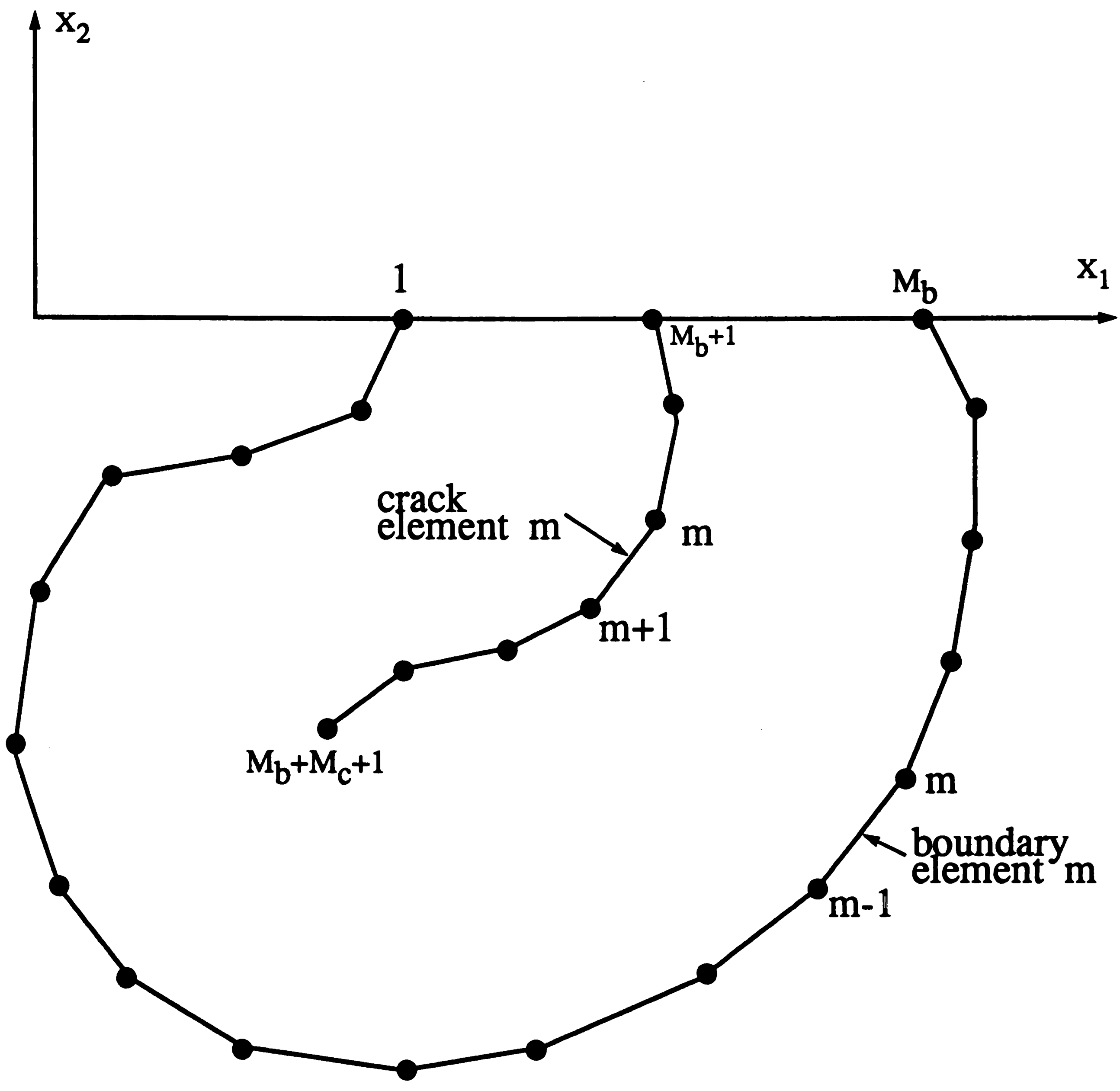

Figure 2.30 Discretized half-plane region containing a discretized single edge crack.

$$+ \sum_{m=2}^{M_b} \Delta s_b^m/4 \; [\int_m (1+\xi)(uR)_{ij}^h(\mathbf{x}^{(n)}, \xi)d\xi \;]\; t_j^{(2m)}$$

$$- \sum_{m=2}^{M_b} \Delta s_b^m/4 \; [\int_m (1-\xi)(uc)_{ij}^h(\mathbf{x}^{(n)}, \xi)d\xi \;]\; u_j^{(m-1)}$$

$$- \sum_{m=2}^{M_b} \Delta s_b^m/4 \; [\int_m (1+\xi)(uc)_{ij}^h(\mathbf{x}^{(n)}, \xi)d\xi \;]\; u_j^{(m)}$$

$$+ \sum_{m=M_b+1}^{M_b+M_c} \Delta s_c^m/4 \; [\int_m (1-\xi)(uc)_{ij}^h(\mathbf{x}^{(n)}, \xi)d\xi \;]\; \Delta u_j^{(m)}$$

$$+ \sum_{m=M_b+1}^{M_b+M_c-1} \Delta s_c^m/4 \; [\int_m (1+\xi)(uc)_{ij}^h(\mathbf{x}^{(n)}, \xi)d\xi \;]\; \Delta u_j^{(m+1)}$$

(2.2.6)

$$\pi_i^{(n)} = \sum_{m=2}^{M_b} \Delta s_b^m/4 \; [\int_m (1-\xi)(\pi R)_{ij}^h(\mathbf{x}^{(n)}, \xi)d\xi \;]\; t_j^{(2m-1)}$$

$$+ \sum_{m=2}^{M_b} \Delta s_b^m/4 \; [\int_m (1+\xi)(\pi R)_{ij}^h(\mathbf{x}^{(n)}, \xi)d\xi \;]\; t_j^{(2m)}$$

$$- \sum_{m=2}^{M_b} \Delta s_b^m/4 \; [\int_m (1-\xi)(\pi c)_{ij}^h(\mathbf{x}^{(n)}, \xi)d\xi \;]\; u_j^{(m-1)}$$

$$- \sum_{m=2}^{M_b} \Delta s_b^m/4 \; [\int_m (1+\xi)(\pi c)_{ij}^h(\mathbf{x}^{(n)}, \xi)d\xi \;]\; u_j^{(m)}$$

$$+ \sum_{m=M_b+1}^{M_b+M_c} \Delta s_c^m/4 \; [\int_m (1-\xi)(\pi c)_{ij}^h(\mathbf{x}^{(n)}, \xi)d\xi \;]\; \Delta u_j^{(m)}$$

$$+ \sum_{m=M_b+1}^{M_b+M_c-1} \Delta s_c^m/4 \; [\int_m (1+\xi)(\pi c)_{ij}^h(\mathbf{x}^{(n)}, \xi)d\xi \;]\; \Delta u_j^{(m+1)}$$

where $u_j^{(m)}$, $t_j^{(2m)}$, $t_j^{(2m+1)}$ are values at the external boundary nodal point m (m=1, ... M_b), $\Delta u_j^{(m)}$ are values at the crack nodal point m (m=M_b+1, ... M_b+M_c); $u_j^{(n)} = u_j(\mathbf{x}^{(n)})$, $\mathbf{x}^{(n)}$ being the location of the external boundary nodal point n, (n=1, ... M_b), and $\pi_i^{(n)}$ =

$\pi_i(\mathbf{x}^{(n)})$, $\mathbf{x}^{(n)}$ being the location of the crack element mid-point n, (n= M_b+1, ... M_b+M_c), in addition, we add a nodal point n= M_b+1.

Eqs.(2.2.6) can be written in the following matrix form:

$$[UC]\left\{ u \right\} - [Q]\left\{ \Delta u \right\} = [UR]\left\{ t \right\}$$

(2.2.7)

$$[PC]\left\{ u \right\} - [X]\left\{ \Delta u \right\} = [PR]\left\{ t \right\} - \left\{ \pi \right\}$$

where

[UC] is $2M_b \times 2M_b$, [Q] is $2M_b \times 2M_c$, [UR] is $2M_b \times 4(M_b-1)$, [PC] is $2(M_c+1) \times 2M_b$, [X] is $2(M_c+1) \times 2M_c$ and [PR] is $2(M_c+1) \times 4(M_b-1)$.

Thus

$$\begin{bmatrix} [UC] & -[Q] \\ [\Gamma_2][PC] & -[\Gamma_2][X] \end{bmatrix} \begin{Bmatrix} u \\ \Delta u \end{Bmatrix} = \begin{bmatrix} [UR] & [0] \\ [\Gamma_2][PR] & [I] \end{bmatrix} \begin{Bmatrix} t \\ F \end{Bmatrix} \tag{2.2.8}$$

where, as in [76], we have defined a nodal force matrix on the crack by

$$\left\{ F \right\} = [\Gamma_2]\left\{ \pi \right\} \tag{2.2.9}$$

where

$$[\Gamma_2] = \begin{bmatrix} -I & I & 0 & 0 & 0 & 0 & 0 \\ 0 & -I & I & 0 & 0 & 0 & 0 \\ 0 & 0 & -I & I & 0 & 0 & 0 \\ \cdot & \cdot & \cdot & \cdot & \cdot & \cdot & \cdot \\ \vdots & \vdots & \vdots & \vdots & \vdots & \vdots & \vdots \\ 0 & 0 & 0 & 0 & 0 & -I & I \end{bmatrix} \qquad (2.2.10)$$

I represents a 2x2 identity matrix, and $[\Gamma_2]$ is $2M_c$ x $2(M_c+1)$.

2.2.2.2 An edge branch crack

A simple numerical treatment of eqs.(2.2.2) is presented here in which the external boundary is approximated by M_b straight elements and the cracks by M_{c1}, M_{c2} straight elements, as shown in Figure 2.31. Eqs.(2.2.2) can then be written as

$$c_{ij}(x)\, u_j(x) = \sum_{m=2}^{M_b} \int_m [\, (uR)^h_{ij}(x, \bar{x})\, t_j(\bar{x}) - (uc)^h_{ij}(x, \bar{x})\, u_j(\bar{x})]\, ds(\bar{x})$$

$$+ \sum_{m=M_b+1}^{M_b+M_{c1}} \int_m (uc)_{ij}{}^h(x, \bar{x})\, \Delta u_j(\bar{x})\, ds(\bar{x})$$

$$+ \sum_{m=M_b+M_{c1}+2}^{M_b+M_{c1}+M_{c2}+1} \int_m (uc)^h_{ij}(x, \bar{x})\, \Delta u_j(\bar{x})\, ds(\bar{x})$$

$$\pi_i(x) = \sum_{m=2}^{M_b} \int_m [\, (\pi R)^h_{ij}(x, \bar{x})\, t_j(\bar{x}) - (\pi c)_{ij}{}^h(x, \bar{x})\, u_j(\bar{x})]\, ds(\bar{x})$$

$$+ \sum_{m=M_b+1}^{M_b+M_{c1}} \int_m (\pi c)^h_{ij}(x, \bar{x})\, \Delta u_j(\bar{x})\, ds(\bar{x}) \qquad (2.2.11)$$

$$+ \sum_{m=M_b+M_{c1}+2}^{M_b+M_{c1}+M_{c2}+1} \int_m (\pi c)^h_{ij}(x, \bar{x})\, \Delta u_j(\bar{x})\, ds(\bar{x}) \qquad x \text{ on } \Gamma_{c1}$$

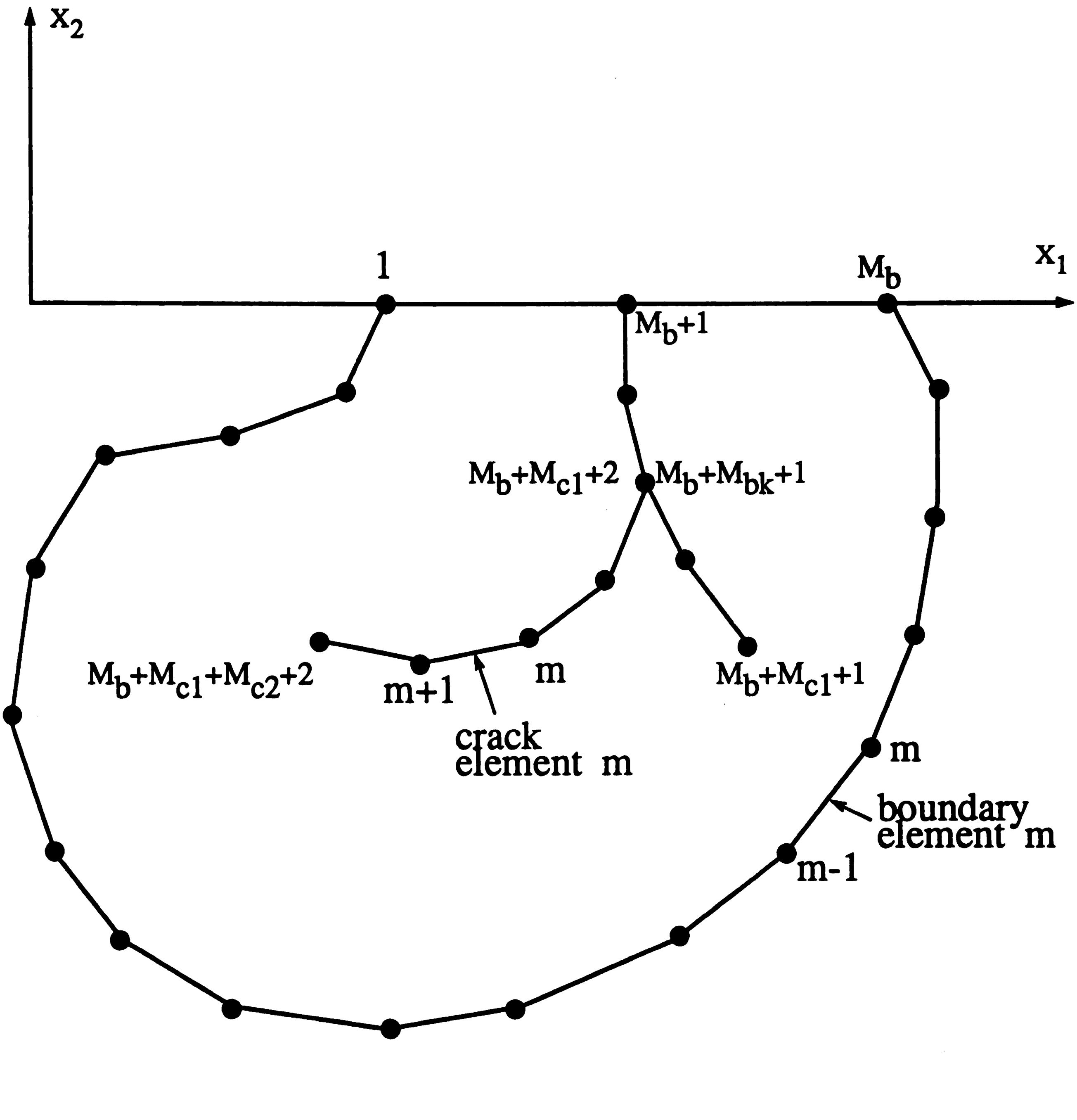

Figure 2.31 Discretized half-plane region containing a discretized edge branch crack.

$$\pi_i(\mathbf{x}) = \sum_{m=2}^{M_b} \int_m [\, (\pi R)_{ij}^h(\mathbf{x}, \bar{\mathbf{x}})\; t_j(\bar{\mathbf{x}}) - (\pi c)_{ij}^h(\mathbf{x}, \bar{\mathbf{x}})\; u_j(\bar{\mathbf{x}})]\; ds(\bar{\mathbf{x}})$$

$$+ \sum_{m=M_b+1}^{M_b+M_{c1}} \int_m (\pi c)_{ij}^h(\mathbf{x}, \bar{\mathbf{x}})\; \Delta u_j(\bar{\mathbf{x}})\; ds(\bar{\mathbf{x}})$$

$$+ \sum_{m=M_b+M_{c1}+2}^{M_b+M_{c1}+M_{c2}+1} \int_m (\pi c)_{ij}^h(\mathbf{x}, \bar{\mathbf{x}})\; \Delta u_j(\bar{\mathbf{x}})\; ds(\bar{\mathbf{x}}) \qquad \mathbf{x} \text{ on } \Gamma_{c2}\,.$$

Following the same procedures as in previous section, eqs.(2.2.11) become

$$c_{ij}^{(n)}u_j^{(n)} = \sum_{m=2}^{M_b} \Delta s_b^m/4\; [\int_m (1-\xi)(uR)_{ij}^h(\mathbf{x}^{(n)}, \xi)d\xi\;]\; t_j^{(2m-1)}$$

$$+ \sum_{m=2}^{M_b} \Delta s_b^m/4\; [\int_m (1+\xi)(uR)_{ij}^h(\mathbf{x}^{(n)}, \xi)d\xi\;]\; t_j^{(2m)}$$

$$- \sum_{m=2}^{M_b} \Delta s_b^m/4\; [\int_m (1-\xi)(uc)_{ij}^h(\mathbf{x}^{(n)}, \xi)d\xi\;]\; u_j^{(m-1)}$$

$$- \sum_{m=2}^{M_b} \Delta s_b^m/4\; [\int_m (1+\xi)(uc)_{ij}^h(\mathbf{x}^{(n)}, \xi)d\xi\;]\; u_j^{(m)}$$

$$+ \sum_{m=M_b+1}^{M_b+M_{c1}} \Delta s_c^m/4\; [\int_m (1-\xi)(uc)_{ij}^h(\mathbf{x}^{(n)}, \xi)d\xi\;]\; \Delta u_j^{(m)}$$

$$+ \sum_{m=M_b+1}^{M_b+M_{c1}-1} \Delta s_c^m/4\; [\int_m (1+\xi)(uc)_{ij}^h(\mathbf{x}^{(n)}, \xi)d\xi\;]\; \Delta u_j^{(m+1)}$$

$$+ \sum_{m=M_b+M_{c1}+2}^{M_b+M_{c1}+M_{c2}+1} \Delta s_c^m/4\; [\int_m (1-\xi)(uc)_{ij}^h(\mathbf{x}^{(n)}, \xi)d\xi\;]\; \Delta u_j^{(m)}$$

$$+ \sum_{m=M_b+M_{c1}+2}^{M_b+M_{c1}+M_{c2}} \Delta s_c^m/4\; [\int_m (1+\xi)(uc)_{ij}^h(\mathbf{x}^{(n)}, \xi)d\xi\;]\; \Delta u_j^{(m+1)}$$

$$\pi_i^{(n)} = \sum_{m=2}^{M_b} \Delta s_b^m/4\; [\int_m (1-\xi)(\pi R)_{ij}^h(\mathbf{x}^{(n)}, \xi)d\xi\;]\; t_j^{(2m-1)}$$

$$+ \sum_{m=2}^{M_b} \Delta s_b^m/4 \; [\int_m (1+\xi)(\pi R)_{ij}^h(\mathbf{x}^{(n)}, \xi)d\xi \;] \; t_j^{(2m)}$$

$$- \sum_{m=2}^{M_b} \Delta s_b^m/4 \; [\int_m (1-\xi)(\pi c)_{ij}^h(\mathbf{x}^{(n)}, \xi)d\xi \;] \; u_j^{(m-1)}$$

$$- \sum_{m=2}^{M_b} \Delta s_b^m/4 \; [\int_m (1+\xi)(\pi c)_{ij}^h(\mathbf{x}^{(n)}, \xi)d\xi \;] \; u_j^{(m)}$$

$$+ \sum_{m=M_b+1}^{M_b+M_{c1}} \Delta s_c^m/4 \; [\int_m (1-\xi)(\pi c)_{ij}^h(\mathbf{x}^{(n)}, \xi)d\xi \;] \; \Delta u_j^{(m)} \qquad (2.2.12)$$

$$+ \sum_{m=M_b+1}^{M_b+M_{c1}-1} \Delta s_c^m/4 \; [\int_m (1+\xi)(\pi c)_{ij}^h(\mathbf{x}^{(n)}, \xi)d\xi \;] \; \Delta u_j^{(m+1)}$$

$$+ \sum_{m=M_b+M_{c1}+2}^{M_b+M_{c1}+M_{c2}+1} \Delta s_c^m/4 \; [\int_m (1-\xi)(\pi c)_{ij}^h(\mathbf{x}^{(n)}, \xi)d\xi \;] \; \Delta u_j^{(m)}$$

$$+ \sum_{m=M_b+M_{c1}+2}^{M_b+M_{c1}+M_{c2}} \Delta s_c^m/4 \; [\int_m (1+\xi)(\pi c)_{ij}^h(\mathbf{x}^{(n)}, \xi)d\xi \;] \; \Delta u_j^{(m+1)}$$

$$\pi_i^{(n)} = \sum_{m=2}^{M_b} \Delta s_b^m/4 \; [\int_m (1-\xi)(\pi R)_{ij}^h(\mathbf{x}^{(n)}, \xi)d\xi \;] \; t_j^{(2m-1)}$$

$$+ \sum_{m=2}^{M_b} \Delta s_b^m/4 \; [\int_m (1+\xi)(\pi R)_{ij}^h(\mathbf{x}^{(n)}, \xi)d\xi \;] \; t_j^{(2m)}$$

$$- \sum_{m=2}^{M_b} \Delta s_b^m/4 \; [\int_m (1-\xi)(\pi c)_{ij}^h(\mathbf{x}^{(n)}, \xi)d\xi \;] \; u_j^{(m-1)}$$

$$- \sum_{m=2}^{M_b} \Delta s_b^m/4 \; [\int_m (1+\xi)(\pi c)_{ij}^h(\mathbf{x}^{(n)}, \xi)d\xi \;] \; u_j^{(m)}$$

$$+ \sum_{m=M_b+1}^{M_b+M_{c1}} \Delta s_c^m/4 \; [\int_m (1-\xi)(\pi c)_{ij}^h(\mathbf{x}^{(n)}, \xi)d\xi \;] \; \Delta u_j^{(m)}$$

$$+ \sum_{m=M_b+1}^{M_b+M_{c1}-1} \Delta s_c^m/4 \; [\int_m (1+\xi)(\pi c)_{ij}^h(\mathbf{x}^{(n)}, \xi)d\xi \;] \; \Delta u_j^{(m+1)}$$

$$+ \sum_{m=M_b+M_{c1}+2}^{M_b+M_{c1}+M_{c2}+1} \Delta s_c^m/4 \left[\int_m (1-\xi)(\pi c)_{ij}^h(\mathbf{x}^{(n)}, \xi) d\xi \right] \Delta u_j^{(m)}$$

$$+ \sum_{m=M_b+M_{c1}+2}^{M_b+M_{c1}+M_{c2}} \Delta s_c^m/4 \left[\int_m (1+\xi)(\pi c)_{ij}^h(\mathbf{x}^{(n)}, \xi) d\xi \right] \Delta u_j^{(m+1)}$$

where $u_j^{(m)}$, $t_j^{(2m)}$, $t_j^{(2m+1)}$ are values at the external boundary nodal point m (m=1, ... M_b), $\Delta u_j^{(m)}$ are values at the crack nodal point m (m=M_b+1, ... M_b+M_{c1} , $M_b+M_{c1}+2$, ... $M_b+M_{c1}+M_{c2}+1$) ; $u_j^{(n)} = u_j(\mathbf{x}^{(n)})$, $\mathbf{x}^{(n)}$ being the location of the external boundary nodal point n, (n=1, ... M_b), and $\pi_i^{(n)} = \pi_i(\mathbf{x}^{(n)})$, $\mathbf{x}^{(n)}$ being the location of the crack element mid-point n, (n= M_b+1, ... M_b+M_{c1}, $M_b+M_{c1}+2$, ... $M_b+M_{c1}+M_{c2}+1$), in addition, we add two nodal points n= M_b+1, $M_b+M_{c1}+2$.

For an edge branch crack, we need to employ continuity conditions and equilibrium conditions, i.e.

$$\Delta u_j^{(M_b+M_{bk}+1)} = \Delta u_j^{(M_b+M_{c1}+2)} \tag{2.2.13}$$

$$F_j^{(M_b+M_{bk}+1)} = F_j^{(M_b+M_{bk}+1)} + F_j^{(M_b+M_{c1}+2)} \quad . \tag{2.2.14}$$

Then, eqs.(2.2.12) can be written in the following matrix form:

$$\begin{aligned}
&[UC]\left\{ u \right\} - [Q]\left\{ \Delta u^1 \right\} - [Q_1]\left\{ \Delta u^2 \right\} = [UR]\left\{ t \right\} \\
&[PC]\left\{ u \right\} - [X]\left\{ \Delta u^1 \right\} - [X_{12}]\left\{ \Delta u^2 \right\} = [PR]\left\{ t \right\} - \left\{ \pi^1 \right\} \\
&[PC_1]\left\{ u \right\} - [X_{21}]\left\{ \Delta u^1 \right\} - [X_2]\left\{ \Delta u^2 \right\} = [PR_1]\left\{ t \right\} - \left\{ \pi^2 \right\}
\end{aligned} \tag{2.2.15}$$

where

[UC] is $2M_b$ x $2M_b$, [Q] is $2M_b$ x $2M_{c1}$, $[Q_1]$ is $2M_b$ x $2M_{c2}$, [UR] is $2M_b$ x $4(M_b-1)$, [PC] is $2(M_{c1}+1)$ x $2M_b$, [X] is $2(M_{c1}+1)$ x $2M_{c1}$, $[X_{12}]$ is $2(M_{c1}+1)$ x $2M_{c2}$, [PR] is $2(M_{c1}+1)$ x $4(M_b-1)$, $[PC_1]$ is $2(M_{c2}+1)$ x $2M_b$, $[X_{21}]$ is $2(M_{c2}+1)$ x $2M_{c1}$, $[X_2]$ is $2(M_{c2}+1)$ x $2M_{c2}$ and $[PR_1]$ is $2(M_{c2}+1)$ x $4(M_b-1)$.

Thus

$$\begin{bmatrix} [UC] & -[Q] & -[Q_1] \\ [\Gamma_2][PC] & -[\Gamma_2][X] & -[\Gamma_2][X_{12}] \\ [\Gamma_{21}][PC_1] & -[\Gamma_{21}][X_{21}] & -[\Gamma_{21}][X_2] \end{bmatrix} \begin{Bmatrix} u \\ \Delta u^1 \\ \Delta u^2 \end{Bmatrix} = \begin{bmatrix} [UR] & [0] & [0] \\ [\Gamma_2][PR] & [I] & [0] \\ [\Gamma_{21}][PR_1] & [0] & [I] \end{bmatrix} \begin{Bmatrix} t \\ F^1 \\ F^2 \end{Bmatrix} \tag{2.2.16}$$

where, as in [76], we have defined nodal force matrices on the crack by

$$\left\{ F^1 \right\} = [\Gamma_2] \left\{ \pi^1 \right\}$$

$$\left\{ F^2 \right\} = [\Gamma_{21}] \left\{ \pi^2 \right\} \tag{2.2.17}$$

$$[\Gamma_2] = [\Gamma_{21}] = \begin{bmatrix} -I & I & 0 & 0 & 0 & 0 & 0 \\ 0 & -I & I & 0 & 0 & 0 & 0 \\ 0 & 0 & -I & I & 0 & 0 & 0 \\ \cdot & \cdot & \cdot & \cdot & \cdot & \cdot & \cdot \\ \cdot & \cdot & \cdot & \cdot & \cdot & \cdot & \cdot \\ 0 & 0 & 0 & 0 & 0 & -I & I \end{bmatrix} \tag{2.2.18}$$

I represents a 2x2 identity matrix, $[\Gamma_2]$ is $2M_{c1}x2(M_{c1}+1)$, and $[\Gamma_{21}]$ is $2M_{c2}x2(M_{c2}+1)$.

It is well-known that one can obtain the diagonal 2x2 blocks of [UC] in eqs.(2.2.8) or (2.2.16) from rigid-body considerations, as in the previous section.

Once eqs.(2.2.8) or (2.2.16) have been constructed, we must impose four conditions at each nodal point m on Γ_b involving the boundary values

$$u_1^{(m)}, \quad t_1^{(2m)}, \quad t_1^{(2m+1)},$$

$$u_2^{(m)}, \quad t_2^{(2m)}, \quad t_2^{(2m+1)},$$

and rearrange eqs.(2.2.8) or (2.2.16) accordingly to obtain

$$[A]\left\{ Z \right\} = \left\{ B \right\} \tag{2.2.19}$$

where $\{Z\}$ contains the unknown boundary displacements and tractions on Γ_b and the unknown matrix $\{\Delta u\}$.

Once we have obtained Δu_i at each crack nodal point, the displacement discontinuities normal and tangential to the crack surfaces at that point are

$$\Delta u_n = \Delta u_1 n_1 + \Delta u_2 n_2$$

$$\Delta u_t = \Delta u_2 n_1 - \Delta u_1 n_2 \tag{2.2.20}$$

and the stress intensity factors can be determined from

$$K_I|_{s=0} = \sqrt{\frac{\pi}{8\varepsilon}} G(1+\nu)\Delta u_n(\varepsilon)$$

$$K_{II}|_{s=0} = \sqrt{\frac{\pi}{8\varepsilon}} G(1+\nu)\Delta u_t(\varepsilon)$$

$$K_I|_{s=l} = \sqrt{\frac{\pi}{8\varepsilon}} G(1+\nu)\Delta u_n(l-\varepsilon) \tag{2.2.21}$$

$$K_{II}|_{s=l} = \sqrt{\frac{\pi}{8\varepsilon}} G(1+\nu)\Delta u_t(l-\varepsilon)$$

where $\varepsilon \rightarrow 0$, G, ν are the shear modulus and Possion's ratio, respectively, and l is the length of the crack.

2.2.3 Results

Here we employ the coupled model to find numerical solutions for some finite domain problems.

a) Single edge crack in a rectangular plate subjected to uniform uniaxial tesile stress.

A rectangular plate of height h and width w with a single edge crack of length a is loaded by a uniform tension acting over an interval of length L. The total force acting on the interval is denoted by constant σ, as shown in Figure 2.32. The crack line is modeled by 20 equal elements and the external boundary part Γ_{b1} is modeled by 45 equal elements. In Tables 2.16 and 2.17, the stress intensity factors, normalized with respect to $\sigma\sqrt{a}$, are given for various ratios of a/w and L/w and compared to those obtained in [93-96].

b) Single slanted edge crack in a rectangular plate subjected to uniform uniaxial tensile stress.

A rectangular plate of height 2.5w and width w, containing a single slanted edge crack of length a, is subjected to a uniform uniaxial tesile stress σ at the ends. The crack is located eccentrically a distance w from one end and inclined at an angle β towards the other end, as shown in Figure 2.33. The crack line is modeled by 25 equal elements and the external boundary part Γ_{b1} is modeled by 45 equal elements. In Table 2.18, the stress intensity factors, normalized with respect to $\sigma\sqrt{\pi a}$, are reported for various ratios a/w and various angles β and compared to those obtained in [84].

c) Single edge crack in a rectangular plate subjected to mixed mode loading.

A rectangular plate of height h and width w with a single edge crack of length a is subjected to a unit uniform tensile stress σ at one end and a sliding support on

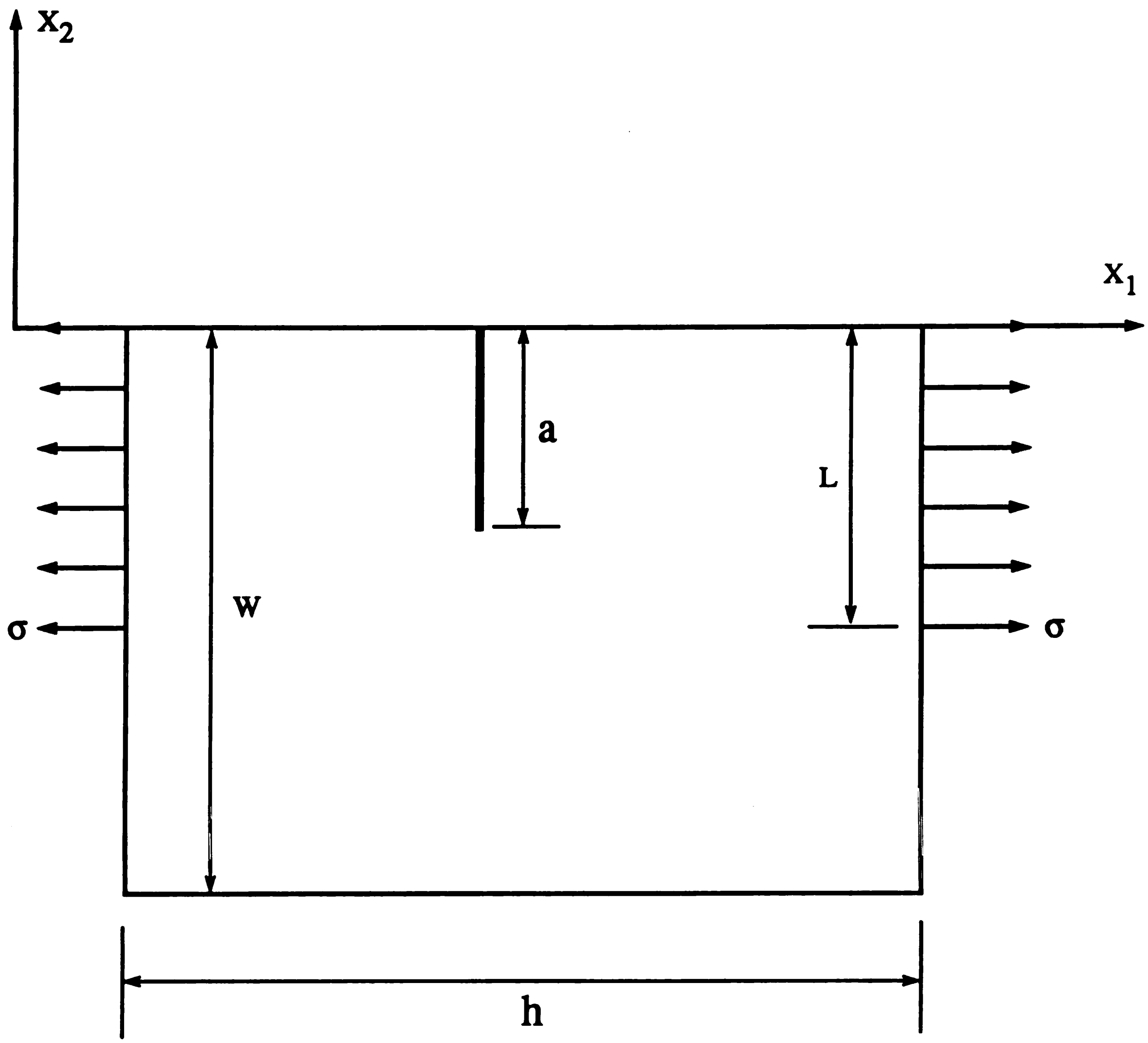

Figure 2.32 Geometry and loading of a rectangular plate with a single edge crack.

Table 2.16 Stress intensity factors for a single edge cracked plate under uniform tension.

a/w	0.1		0.2		0.3		0.4	
L/W	present	[93]	present	[93]	present	[93]	present	[93]
1.0	1.22	1.23	1.48	1.49	1.83	1.85	2.30	2.32
0.9	1.41	1.43	1.70	1.72	2.10	2.13	2.64	2.67
0.8	1.65	1.67	1.98	1.99	2.42	2.45	3.01	3.05
0.7	1.93	1.95	2.28	2.31	2.80	2.82	3.45	3.48
0.6	2.29	2.31	2.66	2.70	3.21	3.25	3.90	3.95
0.5	2.75	2.78	3.16	3.19	3.73	3.76	4.43	4.48
0.4	3.34	3.38	3.75	3.76	4.27	4.32	5.00	5.03
0.3	4.05	4.09	4.40	4.43	4.87	4.92	5.52	5.57
0.2	4.84	4.88	5.13	5.16	5.50	5.54	6.10	6.13
0.1	5.60	5.64	5.82	5.88	6.12	6.16	6.61	6.68

Table 2.16 Stress intensity factors for a single edge cracked plate under uniform tension.

a/w	0.5		0.6		0.7		0.8	
L/W	present	[93]	present	[93]	present	[93]	present	[93]
1.0	2.99	3.01	4.11	4.15	6.34	6.40	11.2	12.0
0.9	3.41	3.45	4.68	4.73	7.18	8.22	12.8	13.4
0.8	3.88	3.91	5.28	5.31	8.00	8.05	14.4	14.8
0.7	4.36	4.40	5.90	5.92	8.85	8.88	15.9	16.2
0.6	4.90	4.93	6.50	6.54	9.66	9.71	17.1	17.6
0.5	5.45	5.48	7.15	7.17	10.45	10.50	18.6	19.0
0.4	6.00	6.03	7.73	7.78	11.33	11.40	20.0	20.4
0.3	6.52	6.57	8.35	8.39	12.14	12.20	21.2	21.8
0.2	7.10	7.12	9.00	9.01	12.96	13.00	22.8	23.2
0.1	7.61	7.67	9.60	9.65	13.84	13.90	24.0	24.7

Table 2.17 Stress intensity factors for a single edge cracked plate under uniform tension, L/w=1.0.

	L/W=1.0				
a/w	present	[93]	[94]	[95]	[96]
0.125	1.28	---	1.26	1.27	1.299
0.150	1.35	---	1.30	1.34	1.362
0.200	1.48	1.49	1.40	1.48	1.505
0.300	1.83	1.85	1.67	1.82	1.867

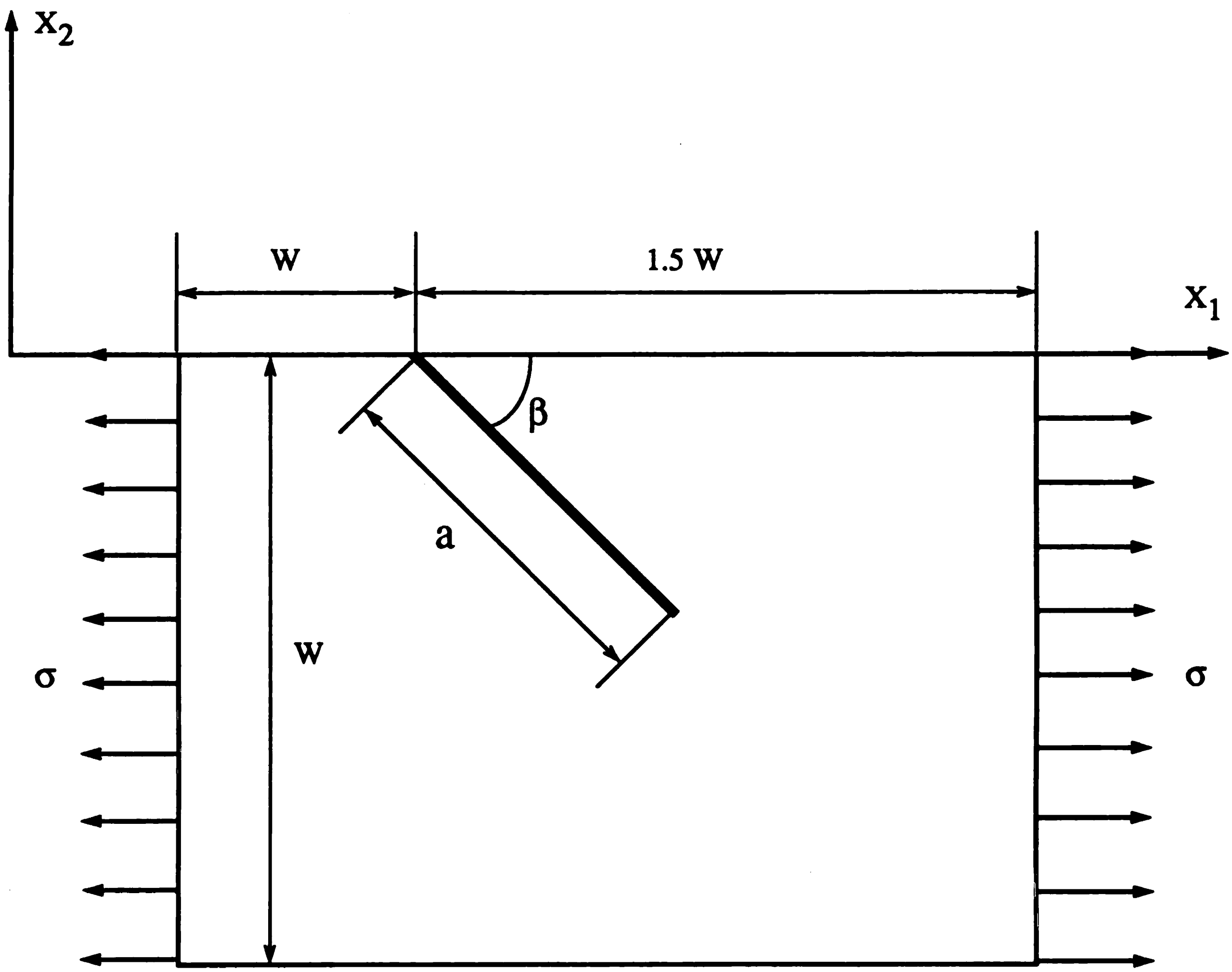

Figure 2.33 Geometry and loading of a rectangular plate with a single slanted edge crack.

Table 2.18 Stress intensity factors for a single slanted edge cracked plate.

a/W	$\beta = 45^o$				$\beta = 67.5^o$			
	present		**[84]**		**present**		**[84]**	
	$K_I/\sigma\sqrt{\pi a}$	$K_{II}/\sigma\sqrt{\pi a}$	$K_I/\sigma\sqrt{\pi a}$	$K_{II}/\sigma\sqrt{\pi a}$	$K_I/\sigma\sqrt{\pi a}$	$K_{II}/\sigma\sqrt{\pi a}$	$K_I/\sigma\sqrt{\pi a}$	$K_{II}/\sigma\sqrt{\pi a}$
0.30	0.89	0.443	0.89	0.443	1.43	0.342	1.43	0.342
0.35	0.95	0.472	0.95	0.473	1.58	0.370	1.58	0.370
0.40	1.01	0.502	1.02	0.504	1.76	0.402	1.77	0.404
0.45	1.08	0.534	1.10	0.536	1.99	0.440	2.00	0.441
0.50	1.20	0.570	1.20	0.571	2.27	0.491	2.28	0.494
0.55	1.30	0.608	1.32	0.612	2.60	0.562	2.62	0.565
0.60	1.40	0.658	1.43	0.662	3.03	0.658	3.06	0.662

the other opposite end as shown in Figure 2.34. The crack line is modeled by 30 equal elements and the external boundary part Γ_{b1} is modeled by 46 equal elements. In Table 2.19, the stress intensity factors are calculated and compared to those obtained in [97-99].

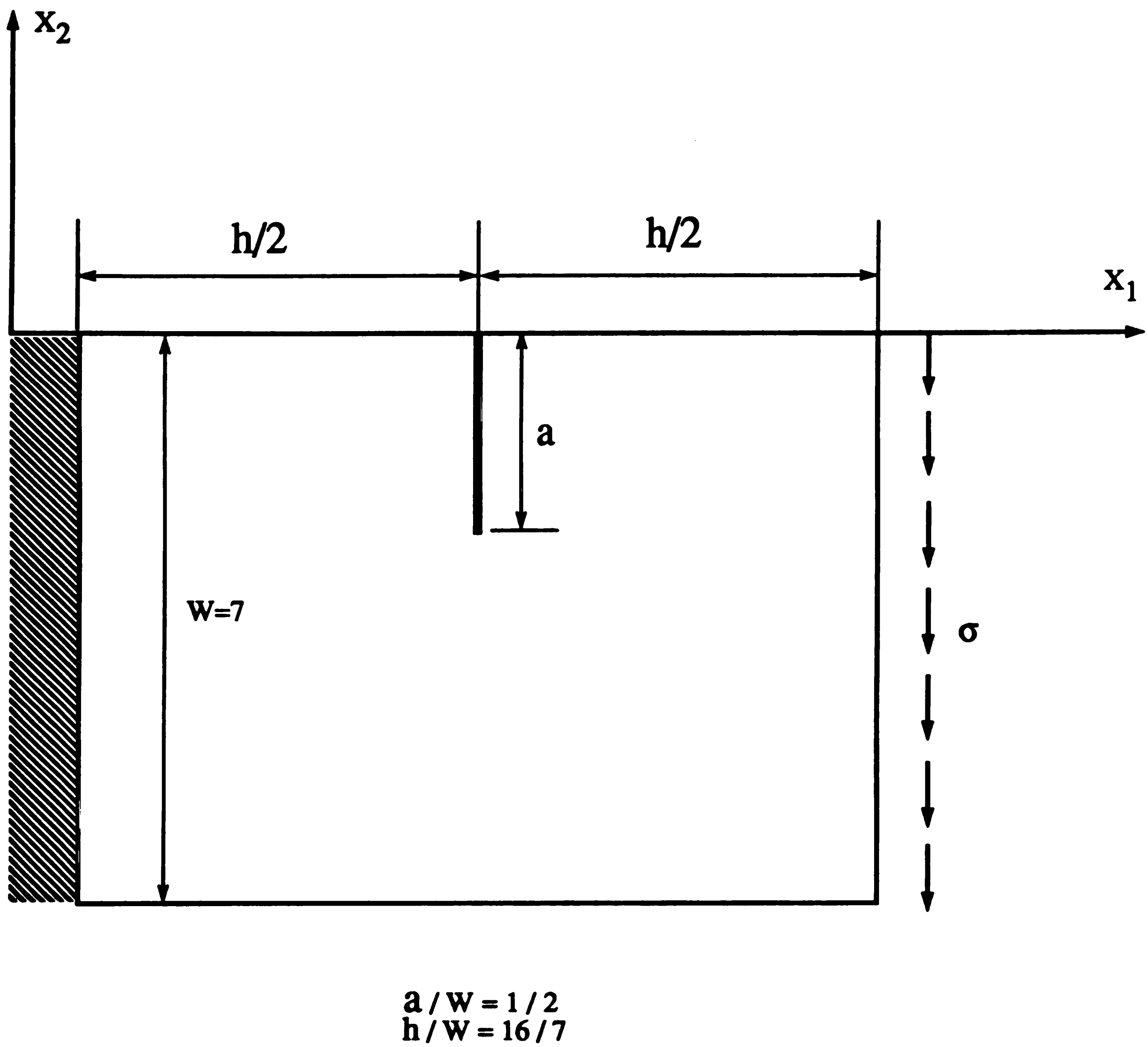

Figure 2.34 Geometry and loading of a rectangular plate with a single edge crack.

Table 2.19 Stress intensity factors for a single edge cracked plate as shown in Figure 2.34.

	present	[97]	[98]	[99]
K_I	32.6	34.0	33.20	33.1
K_{II}	4.38	4.55	4.50	4.36

Chapter 3

Mode III Crack Problems : Internal Cracks

3.1 Theoretical Development

Consider an infinite isotropic elastic plane in which there is a point, $\bar{\mathbf{x}}$, at which some "source" of stress is located and a point, $\mathbf{x}$, at which the stresses are to be computed. We will employ the following influence functions associted with antiplane strains:

$(uR)_{33}(\mathbf{x}, \bar{\mathbf{x}})$ = the displacement in the x_3 direction at $\mathbf{x}$ due to a unit force applied in the x_3 direction at $\bar{\mathbf{x}}$ in the infinite plane,

$(uc)_{33}(\mathbf{x}, \bar{\mathbf{x}})$ = the displacement in the x_3 direction at $\mathbf{x}$ due to a unit displacement discontinuity applied in the x_3 direction at $\bar{\mathbf{x}}$ in the infinite plane,

$(\pi R)_{33}(\mathbf{x}, \bar{\mathbf{x}})$ = the scalar π_3 in the x_3 direction at $\mathbf{x}$ due to a unit force applied in the x_3 direction at $\bar{\mathbf{x}}$ in the infinite plane,

$(\pi c)_{33}(\mathbf{x}, \bar{\mathbf{x}})$ = the scalar π_3 in the x_3 direction at $\mathbf{x}$ due to a unit displacement discontinuity applied in the x_3 direction in the infinite plane,

where π_3 is a stress function defined such that the stress components are

$$\sigma_{13} = \frac{\partial \pi_3}{\partial x_2}, \qquad \sigma_{23} = -\frac{\partial \pi_3}{\partial x_1}. \tag{3.1}$$

The influence functions are given in the Appendix C.

In Figure 2.2, suppose that Γ_c represents a crack, the surfaces of which are subjected to equal and opposite traction $t_3(s)$ given by

$$
\begin{aligned}
t_3 &= -\,(\,\sigma_{13}n_1 + \sigma_{23}n_2\,) \\
&= -\,(\,\frac{\partial\pi_3}{\partial x_2}\frac{dx_2}{ds} + \frac{\partial\pi_3}{\partial x_1}\frac{dx_1}{ds}\,) \\
&= -\,\frac{d\pi_3}{ds}
\end{aligned}
\tag{3.2}
$$

A plane elastic region Ω, with external boundary Γ_b, containing an internal piece-wise smooth crack Γ_c, as shown in Figure 2.2, or an internal piece-wise smooth branch crack or multiple cracks composed of Γ_{c1} and Γ_{c2}, as shown in Figures 2.3 and 2.4, is loaded by prescribed tractions t_3 on some part of the external boundary and prescribed displacements u_3 on the remainder of the external boundary. Then the direct boundary-integral equations and the crack integral equations developed as in [76] can be coupled as follows.

For a single smooth or kinked crack:

$$
\begin{aligned}
c_3(\mathbf{x})\,u_3(\mathbf{x}) &= \oint_{\Gamma_b}(uR)_{33}(\mathbf{x},\bar{\mathbf{x}})\,t_3(\bar{\mathbf{x}})\,ds(\bar{\mathbf{x}}) - \oint_{\Gamma_b}(uc)_{33}(\mathbf{x},\bar{\mathbf{x}})\,u_3(\bar{\mathbf{x}})\,ds(\bar{\mathbf{x}}) \\
&\quad + \int_{\Gamma_c}(uc)_{33}(\mathbf{x},\bar{\mathbf{x}})\,\Delta u_3(\bar{\mathbf{x}})\,ds(\bar{\mathbf{x}}) \qquad \mathbf{x} \text{ on } \Gamma_b
\end{aligned}
\tag{3.3}
$$

$$
\begin{aligned}
\pi_3(\mathbf{x}) &= \oint_{\Gamma_b}(\pi R)_{33}(\mathbf{x},\bar{\mathbf{x}})\,t_3(\bar{\mathbf{x}})\,ds(\bar{\mathbf{x}}) - \oint_{\Gamma_b}(\pi c)_{33}(\mathbf{x},\bar{\mathbf{x}})\,u_3(\bar{\mathbf{x}})\,ds(\bar{\mathbf{x}}) \\
&\quad + \int_{\Gamma_c}(\pi c)_{33}(\mathbf{x},\bar{\mathbf{x}})\,\Delta u_3(\bar{\mathbf{x}})\,ds(\bar{\mathbf{x}}) \qquad \mathbf{x} \text{ on } \Gamma_c\;.
\end{aligned}
$$

For a branch crack or multiple cracks:

$$c_3(\mathbf{x})\, u_3(\mathbf{x}) = \oint_{\Gamma_b} (uR)_{33}(\mathbf{x}, \overline{\mathbf{x}})\, t_3(\overline{\mathbf{x}})\, ds(\overline{\mathbf{x}}) - \oint_{\Gamma_b} (uc)_{33}(\mathbf{x}, \overline{\mathbf{x}})\, u_3(\overline{\mathbf{x}})\, ds(\overline{\mathbf{x}})$$

$$+ \sum_{k=1}^{2} \int_{\Gamma_{ck}} (uc)_{33}(\mathbf{x}, \overline{\mathbf{x}})\, \Delta u_3(\overline{\mathbf{x}})\, ds(\overline{\mathbf{x}}) \qquad \mathbf{x} \text{ on } \Gamma_b$$

$$\pi_3(\mathbf{x}) = \oint_{\Gamma_b} (\pi R)_{33}(\mathbf{x}, \overline{\mathbf{x}})\, t_3(\overline{\mathbf{x}})\, ds(\overline{\mathbf{x}}) - \oint_{\Gamma_b} (\pi c)_{33}(\mathbf{x}, \overline{\mathbf{x}})\, u_3(\overline{\mathbf{x}})\, ds(\overline{\mathbf{x}})$$

$$+ \sum_{k=1}^{2} \int_{\Gamma_{ck}} (\pi c)_{33}(\mathbf{x}, \overline{\mathbf{x}})\, \Delta u_3(\overline{\mathbf{x}})\, ds(\overline{\mathbf{x}}) \qquad \mathbf{x} \text{ on } \Gamma_{c1} \tag{3.4}$$

$$\pi_3(\mathbf{x}) = \oint_{\Gamma_b} (\pi R)_{33}(\mathbf{x}, \overline{\mathbf{x}})\, t_3(\overline{\mathbf{x}})\, ds(\overline{\mathbf{x}}) - \oint_{\Gamma_b} (\pi c)_{33}(\mathbf{x}, \overline{\mathbf{x}})\, u_3(\overline{\mathbf{x}})\, ds(\overline{\mathbf{x}})$$

$$+ \sum_{k=1}^{2} \int_{\Gamma_{ck}} (\pi c)_{33}(\mathbf{x}, \overline{\mathbf{x}})\, \Delta u_3(\overline{\mathbf{x}})\, ds(\overline{\mathbf{x}}) \qquad \mathbf{x} \text{ on } \Gamma_{c2} \quad .$$

In eqs.(3.3) and (3.4), $\Delta u_3 = u_3^- - u_3^+$ is the relative crack surface displacement in the x_3 direction and c_3 is a coefficient which depends on the smoothness at $\mathbf{x}$ on Γ_b.

3.2 Numerical Treatment

3.2.1 A single smooth or kinked crack

A simple numerical treatment of eqs.(3.3) is presented here in which the external boundary is approximated by M_b straight elements and the crack by M_c straight elements, as shown in Figure 2.5. For this model, eqs.(3.3) can then be written as

$$c_3(\mathbf{x})\, u_3(\mathbf{x}) = \sum_{m=1}^{M_b} \int_m [\, (uR)_{33}(\mathbf{x}, \overline{\mathbf{x}})\, t_3(\overline{\mathbf{x}}) - (uc)_{33}(\mathbf{x}, \overline{\mathbf{x}})\, u_3(\overline{\mathbf{x}})\,]\, ds(\overline{\mathbf{x}})$$

$$+ \sum_{m=M_b+1}^{M_b+M_c} \int_m (uc)_{33}(\mathbf{x}, \overline{\mathbf{x}})\, \Delta u_3(\overline{\mathbf{x}})\, ds(\overline{\mathbf{x}}) \qquad \mathbf{x} \text{ on } \Gamma_b$$

$$(3.5)$$

$$\pi_3(\mathbf{x}) = \sum_{m=1}^{M_b} \int_m [\, (\pi R)_{33}(\mathbf{x}, \overline{\mathbf{x}})\, t_3(\overline{\mathbf{x}}) - (\pi c)_{33}(\mathbf{x}, \overline{\mathbf{x}})\, u_3(\overline{\mathbf{x}})\,]\, ds(\overline{\mathbf{x}})$$

$$+ \sum_{m=M_b+1}^{M_b+M_c} \int_m (\pi c)_{33}(\mathbf{x}, \overline{\mathbf{x}})\, \Delta u_3(\overline{\mathbf{x}})\, ds(\overline{\mathbf{x}}) \qquad \mathbf{x} \text{ on } \Gamma_c \ .$$

The displacements, tractions and displacement discontinuities in the x_3 direction on each element can be linearly approximated by

$$\begin{aligned} u_3(\overline{\mathbf{x}}) &= N_1(\xi)u_3^{(m-1)} + N_2(\xi)u_3^{(m)} && \overline{\mathbf{x}} \text{ on element m of } \Gamma_b \\ t_3(\overline{\mathbf{x}}) &= N_1(\xi)t_3^{(2m-1)} + N_2(\xi)t_3^{(2m)} && \overline{\mathbf{x}} \text{ on element m of } \Gamma_b \qquad (3.6) \\ \Delta u_3(\overline{\mathbf{x}}) &= N_1(\xi)\Delta u_3^{(m)} + N_2(\xi)\Delta u_3^{(m+1)} && \overline{\mathbf{x}} \text{ on element m of } \Gamma_c \end{aligned}$$

where $u_3^{(m)}$, $t_3^{(2m)}$, $t_3^{(2m+1)}$ are values at the external boundary nodal point m (m=1, ... M_b), $\Delta u_3^{(m)}$ are values at the crack nodal point m (m=M_b+2, ... M_b+M_c), and

$$N_1(\xi) = (1-\xi)/2 \qquad N_2(\xi) = (1+\xi)/2 \qquad -1 \le \xi \le 1 \ . \qquad (3.7)$$

Furthermore

$$\overline{\mathbf{x}} = \begin{cases} N_1(\xi)\mathbf{x}^{(m-1)} + N_2(\xi)\mathbf{x}^{(m)} & \overline{\mathbf{x}} \text{ on element m of } \Gamma_b \\ N_1(\xi)\mathbf{x}^{(m)} + N_2(\xi)\mathbf{x}^{(m+1)} & \overline{\mathbf{x}} \text{ on element m of } \Gamma_c \end{cases} \qquad (3.8)$$

$$ds(\bar{\mathbf{x}}) = \begin{cases} [(s_b^{(m)} - s_b^{(m-1)})/2]\, d\xi = [\Delta s_b^m/2]\, d\xi & \bar{\mathbf{x}} \text{ on element m of } \Gamma_b \\ [(s_c^{(m+1)} - s_c^{(m)})/2]\, d\xi = [\Delta s_c^m/2]\, d\xi & \bar{\mathbf{x}} \text{ on element m of } \Gamma_c \end{cases} \tag{3.9}$$

where Δs_b^m is the length of the external boundary element m and Δs_c^m is the length of the crack element m.

Inserting eqs.(3.6) through (3.9) into eqs.(3.5), we obtain

$$\begin{aligned} c_3^{(n)} u_3^{(n)} = & \sum_{m=1}^{M_b} \Delta s_b^m/4 \, [\int_m (1-\xi)(uR)_{33}(\mathbf{x}^{(n)}, \xi) d\xi \,]\, t_3^{(2m-1)} \\ & + \sum_{m=1}^{M_b} \Delta s_b^m/4 \, [\int_m (1+\xi)(uR)_{33}(\mathbf{x}^{(n)}, \xi) d\xi \,]\, t_3^{(2m)} \\ & - \sum_{m=1}^{M_b} \Delta s_b^m/4 \, [\int_m (1-\xi)(uc)_{33}(\mathbf{x}^{(n)}, \xi) d\xi \,]\, u_3^{(m-1)} \\ & - \sum_{m=1}^{M_b} \Delta s_b^m/4 \, [\int_m (1+\xi)(uc)_{33}(\mathbf{x}^{(n)}, \xi) d\xi \,]\, u_3^{(m)} \\ & + \sum_{m=M_b+2}^{M_b+M_c} \Delta s_c^m/4 \, [\int_m (1-\xi)(uc)_{33}(\mathbf{x}^{(n)}, \xi) d\xi \,]\, \Delta u_3^{(m)} \\ & + \sum_{m=M_b+1}^{M_b+M_c-1} \Delta s_c^m/4 \, [\int_m (1+\xi)(uc)_{33}(\mathbf{x}^{(n)}, \xi) d\xi \,]\, \Delta u_3^{(m+1)} \end{aligned}$$

$$\tag{3.10}$$

$$\begin{aligned} \pi_3^{(n)} = & \sum_{m=1}^{M_b} \Delta s_b^m/4 \, [\int_m (1-\xi)(\pi R)_{33}(\mathbf{x}^{(n)}, \xi) d\xi \,]\, t_3^{(2m-1)} \\ & + \sum_{m=1}^{M_b} \Delta s_b^m/4 \, [\int_m (1+\xi)(\pi R)_{33}(\mathbf{x}^{(n)}, \xi) d\xi \,]\, t_3^{(2m)} \\ & - \sum_{m=1}^{M_b} \Delta s_b^m/4 \, [\int_m (1-\xi)(\pi c)_{33}(\mathbf{x}^{(n)}, \xi) d\xi \,]\, u_3^{(m-1)} \end{aligned}$$

$$- \sum_{m=1}^{M_b} \Delta s_b^m/4 \; [\int_m (1+\xi)(\pi c)_{33}(x^{(n)}, \xi) d\xi \;] \; u_3^{(m)}$$

$$+ \sum_{m=M_b+2}^{M_b+M_c} \Delta s_c^m/4 \; [\int_m (1-\xi)(\pi c)_{33}(x^{(n)}, \xi) d\xi \;] \; \Delta u_3^{(m)}$$

$$+ \sum_{m=M_b+1}^{M_b+M_c-1} \Delta s_c^m/4 \; [\int_m (1+\xi)(\pi c)_{33}(x^{(n)}, \xi) d\xi \;] \; \Delta u_3^{(m+1)}$$

where $u_3^{(n)} = u_3(x^{(n)})$, $x^{(n)}$ being the location of the external boundary nodal point n, (n=1, ... M_b), and $\pi_3^{(n)} = \pi_3(x^{(n)})$, $x^{(n)}$ being the location of the crack element mid-point n, (n= M_b+1, ... M_b+M_c).

Eqs.(3.10) can be written in the following matrix form:

$$[UC_3]\left\{ u_3 \right\} - [Q_3]\left\{ \Delta u_3 \right\} = [UR_3]\left\{ t_3 \right\}$$

$$[PC_3]\left\{ u_3 \right\} - [X_3]\left\{ \Delta u_3 \right\} = [PR_3]\left\{ t_3 \right\} - \left\{ \pi_3 \right\} \tag{3.11}$$

where $[UC_3]$ is M_bxM_b, $[Q_3]$ is M_bx(M_c−1), $[UR_3]$ is M_bx2M_b, $[PC_3]$ is M_cxM_b, $[X_3]$ is M_cx(M_c−1) and $[PR_3]$ is M_cx2M_b.

Thus

$$\begin{bmatrix} [UC_3] & -[Q_3] \\ [\Gamma_3][PC_3] & -[\Gamma_3][X_3] \end{bmatrix} \begin{Bmatrix} u_3 \\ \Delta u_3 \end{Bmatrix} = \begin{bmatrix} [UR_3] & [0] \\ [\Gamma_3][PR_3] & [I] \end{bmatrix} \begin{Bmatrix} t_3 \\ F_3 \end{Bmatrix} \tag{3.12}$$

where, as in [76], we have defined a nodal force matrix on the crack by

$$\left\{ F_3 \right\} = [\Gamma_3] \left\{ \pi_3 \right\} \tag{3.13}$$

where

$$[\Gamma_3] = \begin{bmatrix} -1 & 1 & 0 & 0 & 0 & 0 & 0 \\ 0 & -1 & 1 & 0 & 0 & 0 & 0 \\ 0 & 0 & -1 & 1 & 0 & 0 & 0 \\ \cdot & \cdot & \cdot & \cdot & \cdot & \cdot & \cdot \\ \cdot & \cdot & \cdot & \cdot & \cdot & \cdot & \cdot \\ 0 & 0 & 0 & 0 & 0 & -1 & 1 \end{bmatrix} \tag{3.14}$$

and $[\Gamma_3]$ is (M_c-1) x M_c.

3.2.2 A branch crack or multiple cracks

A simple numerical treatment of eqs.(3.4) is presented here in which the external boundary is approximated by M_b straight elements and the branch crack or multiple cracks by M_{c1}, M_{c2} straight elements, as shown in Figure 2.6 and Figure 2.7, respectively. Eqs.(3.4) can then be written as

$$c_3(\mathbf{x})\, u_3(\mathbf{x}) = \sum_{m=1}^{M_b} \int_m [\, (uR)_{33}(\mathbf{x}, \bar{\mathbf{x}})\, t_3(\bar{\mathbf{x}}) - (uc)_{33}(\mathbf{x}, \bar{\mathbf{x}})\, u_3(\bar{\mathbf{x}})\,]\, ds(\bar{\mathbf{x}})$$

$$+ \sum_{m=M_b+1}^{M_b+M_{c1}} \int_m (uc)_{33}(\mathbf{x}, \bar{\mathbf{x}})\, \Delta u_3(\bar{\mathbf{x}})\, ds(\bar{\mathbf{x}})$$

$$+ \sum_{m=M_b+M_{c1}+2}^{M_b+M_{c1}+M_{c2}+1} \int_m (uc)_{33}(\mathbf{x}, \bar{\mathbf{x}})\, \Delta u_3(\bar{\mathbf{x}})\, ds(\bar{\mathbf{x}}) \qquad \mathbf{x} \text{ on } \Gamma_b$$

$$\pi_3(\mathbf{x}) = \sum_{m=1}^{M_b} \int_m [\, (\pi R)_{33}(\mathbf{x}, \bar{\mathbf{x}})\, t_3(\bar{\mathbf{x}}) - (\pi c)_{33}(\mathbf{x}, \bar{\mathbf{x}})\, u_3(\bar{\mathbf{x}})\,]\, ds(\bar{\mathbf{x}})$$

$$+ \sum_{m=M_b+1}^{M_b+M_{c1}} \int_m (\pi c)_{33}(\mathbf{x}, \bar{\mathbf{x}})\, \Delta u_3(\bar{\mathbf{x}})\, ds(\bar{\mathbf{x}}) \tag{3.15}$$

$$+ \sum_{m=M_b+M_{c1}+2}^{M_b+M_{c1}+M_{c2}+1} \int_m (\pi c)_{33}(\mathbf{x}, \bar{\mathbf{x}})\, \Delta u_3(\bar{\mathbf{x}})\, ds(\bar{\mathbf{x}}) \qquad \mathbf{x} \text{ on } \Gamma_{c1}$$

$$\pi_3(\mathbf{x}) = \sum_{m=1}^{M_b} \int_m [\, (\pi R)_{33}(\mathbf{x}, \bar{\mathbf{x}})\, t_3(\bar{\mathbf{x}}) - (\pi c)_{33}(\mathbf{x}, \bar{\mathbf{x}})\, u_3(\bar{\mathbf{x}})\,]\, ds(\bar{\mathbf{x}})$$

$$+ \sum_{m=M_b+1}^{M_b+M_{c1}} \int_m (\pi c)_{33}(\mathbf{x}, \bar{\mathbf{x}})\, \Delta u_3(\bar{\mathbf{x}})\, ds(\bar{\mathbf{x}})$$

$$+ \sum_{m=M_b+M_{c1}+2}^{M_b+M_{c1}+M_{c2}+1} \int_m (\pi c)_{33}(\mathbf{x}, \bar{\mathbf{x}})\, \Delta u_3(\bar{\mathbf{x}})\, ds(\bar{\mathbf{x}}) \qquad \mathbf{x} \text{ on } \Gamma_{c2}\,.$$

The displacements, tractions and displacement discontinuities in the x_3 direction on each element can be linearly approximated by

$$u_3(\bar{\mathbf{x}}) = N_1(\xi)u_3^{(m-1)} + N_2(\xi)u_3^{(m)} \qquad \bar{\mathbf{x}} \text{ on element m of } \Gamma_b$$

$$t_3(\bar{\mathbf{x}}) = N_1(\xi)t_3^{(2m-1)} + N_2(\xi)t_3^{(2m)} \qquad \bar{\mathbf{x}} \text{ on element m of } \Gamma_b \tag{3.16}$$

$$\Delta u_3(\bar{\mathbf{x}}) = N_1(\xi)\Delta u_3^{(m)} + N_2(\xi)\Delta u_3^{(m+1)} \qquad \bar{\mathbf{x}} \text{ on element m of } \Gamma_{c1} \text{ or } \Gamma_{c2}$$

where $u_3^{(m)}$, $t_3^{(2m)}$, $t_3^{(2m+1)}$ are values at the external boundary nodal point m (m=1, ... M_b) and $\Delta u_3^{(m)}$ are values at the crack nodal point m. For multiple cracks, $m=M_b+2, \ldots M_b+M_{c1}$, $M_b+M_{c1}+3, \ldots M_b+M_{c1}+M_{c2}+1$. For a branch crack, $m=M_b+2, \ldots M_b+M_{c1}$, $M_b+M_{c1}+2, \ldots M_b+M_{c1}+M_{c2}+1$.

Furthermore

$$\bar{\mathbf{x}} = \begin{cases} N_1(\xi)\mathbf{x}^{(m-1)} + N_2(\xi)\mathbf{x}^{(m)} & \bar{\mathbf{x}} \text{ on element m of } \Gamma_b \\ N_1(\xi)\mathbf{x}^{(m)} + N_2(\xi)\mathbf{x}^{(m+1)} & \bar{\mathbf{x}} \text{ on element m of } \Gamma_{c1} \text{ or } \Gamma_{c2} \end{cases} \tag{3.17}$$

$$ds(\bar{\mathbf{x}}) = \begin{cases} [(s_b^{(m)} - s_b^{(m-1)})/2]\, d\xi = [\Delta s_b^m/2]\, d\xi & \bar{\mathbf{x}} \text{ on element m of } \Gamma_b \\ [(s_c^{(m+1)} - s_c^{(m)})/2]\, d\xi = [\Delta s_c^m/2]\, d\xi & \bar{\mathbf{x}} \text{ on element m of } \Gamma_{c1} \text{ or } \Gamma_{c2} \end{cases} \tag{3.18}$$

where Δs_b^m is the length of the external boundary element m and Δs_c^m is the length of the crack element m.

Inserting eqs.(3.16) through (3.18) into eqs.(3.15), we obtain

$$\begin{aligned} c_3^{(n)}u_3^{(n)} = & \sum_{m=1}^{M_b} \Delta s_b^m/4\ [\int_m (1-\xi)(uR)_{33}(\mathbf{x}^{(n)}, \xi)d\xi\ ]\ t_3^{(2m-1)} \\ & + \sum_{m=1}^{M_b} \Delta s_b^m/4\ [\int_m (1+\xi)(uR)_{33}(\mathbf{x}^{(n)}, \xi)d\xi\ ]\ t_3^{(2m)} \\ & - \sum_{m=1}^{M_b} \Delta s_b^m/4\ [\int_m (1-\xi)(uc)_{33}(\mathbf{x}^{(n)}, \xi)d\xi\ ]\ u_3^{(m-1)} \\ & - \sum_{m=1}^{M_b} \Delta s_b^m/4\ [\int_m (1+\xi)(uc)_{33}(\mathbf{x}^{(n)}, \xi)d\xi\ ]\ u_3^{(m)} \\ & + \sum_{m=M_b+2}^{M_b+M_{c1}} \Delta s_c^m/4\ [\int_m (1-\xi)(uc)_{33}(\mathbf{x}^{(n)}, \xi)d\xi\ ]\ \Delta u_3^{(m)} \\ & + \sum_{m=M_b+1}^{M_b+M_{c1}-1} \Delta s_c^m/4\ [\int_m (1+\xi)(uc)_{33}(\mathbf{x}^{(n)}, \xi)d\xi\ ]\ \Delta u_3^{(m+1)} \end{aligned}$$

$$+ \sum_{m=M_b+M_{c1}+2}^{M_b+M_{c1}+M_{c2}+1} \Delta s_c^m/4 \; [\int_m (1-\xi)(uc)_{33}(\mathbf{x}^{(n)}, \xi) d\xi \;] \; \Delta u_3^{(m)}$$

$$+ \sum_{m=M_b+M_{c1}+2}^{M_b+M_{c1}+M_{c2}} \Delta s_c^m/4 \; [\int_m (1+\xi)(uc)_{33}(\mathbf{x}^{(n)}, \xi) d\xi \;] \; \Delta u_3^{(m+1)}$$

$$\pi_3^{(n)} = \sum_{m=1}^{M_b} \Delta s_b^m/4 \; [\int_m (1-\xi)(\pi R)_{33}(\mathbf{x}^{(n)}, \xi) d\xi \;] \; t_3^{(2m-1)}$$

$$+ \sum_{m=1}^{M_b} \Delta s_b^m/4 \; [\int_m (1+\xi)(\pi R)_{33}(\mathbf{x}^{(n)}, \xi) d\xi \;] \; t_3^{(2m)}$$

$$- \sum_{m=1}^{M_b} \Delta s_b^m/4 \; [\int_m (1-\xi)(\pi c)_{33}(\mathbf{x}^{(n)}, \xi) d\xi \;] \; u_3^{(m-1)}$$

$$- \sum_{m=1}^{M_b} \Delta s_b^m/4 \; [\int_m (1+\xi)(\pi c)_{33}(\mathbf{x}^{(n)}, \xi) d\xi \;] \; u_3^{(m)}$$

$$+ \sum_{m=M_b+2}^{M_b+M_{c1}} \Delta s_c^m/4 \; [\int_m (1-\xi)(\pi c)_{33}(\mathbf{x}^{(n)}, \xi) d\xi \;] \; \Delta u_3^{(m)}$$

$$+ \sum_{m=M_b+1}^{M_b+M_{c1}-1} \Delta s_c^m/4 \; [\int_m (1+\xi)(\pi c)_{33}(\mathbf{x}^{(n)}, \xi) d\xi \;] \; \Delta u_3^{(m+1)} \qquad (3.19)$$

$$+ \sum_{m=M_b+M_{c1}+2}^{M_b+M_{c1}+M_{c2}+1} \Delta s_c^m/4 \; [\int_m (1-\xi)(\pi c)_{33}(\mathbf{x}^{(n)}, \xi) d\xi \;] \; \Delta u_3^{(m)}$$

$$+ \sum_{m=M_b+M_{c1}+2}^{M_b+M_{c1}+M_{c2}} \Delta s_c^m/4 \; [\int_m (1+\xi)(\pi c)_{33}(\mathbf{x}^{(n)}, \xi) d\xi \;] \; \Delta u_3^{(m+1)}$$

$$\pi_3^{(n)} = \sum_{m=1}^{M_b} \Delta s_b^m/4 \; [\int_m (1-\xi)(\pi R)_{33}(\mathbf{x}^{(n)}, \xi) d\xi \;] \; t_3^{(2m-1)}$$

$$+ \sum_{m=1}^{M_b} \Delta s_b^m/4 \; [\int_m (1+\xi)(\pi R)_{33}(\mathbf{x}^{(n)}, \xi) d\xi \;] \; t_3^{(2m)}$$

$$- \sum_{m=1}^{M_b} \Delta s_b^m/4 \; [\int_m (1-\xi)(\pi c)_{33}(\mathbf{x}^{(n)}, \xi) d\xi \;] \; u_3^{(m-1)}$$

$$- \sum_{m=1}^{M_b} \Delta s_b^m/4 \, [\int_m (1+\xi)(\pi c)_{33}(\mathbf{x}^{(n)}, \xi) d\xi \,] \, u_3^{(m)}$$

$$+ \sum_{m=M_b+2}^{M_b+M_{c1}} \Delta s_c^m/4 \, [\int_m (1-\xi)(\pi c)_{33}(\mathbf{x}^{(n)}, \xi) d\xi \,] \, \Delta u_3^{(m)}$$

$$+ \sum_{m=M_b+1}^{M_b+M_{c1}-1} \Delta s_c^m/4 \, [\int_m (1+\xi)(\pi c)_{33}(\mathbf{x}^{(n)}, \xi) d\xi \,] \, \Delta u_3^{(m+1)}$$

$$+ \sum_{m=M_b+M_{c1}+2}^{M_b+M_{c1}+M_{c2}+1} \Delta s_c^m/4 \, [\int_m (1-\xi)(\pi c)_{33}(\mathbf{x}^{(n)}, \xi) d\xi \,] \, \Delta u_3^{(m)}$$

$$+ \sum_{m=M_b+M_{c1}+2}^{M_b+M_{c1}+M_{c2}} \Delta s_c^m/4 \, [\int_m (1+\xi)(\pi c)_{33}(\mathbf{x}^{(n)}, \xi) d\xi \,] \, \Delta u_3^{(m+1)}$$

where $u_3^{(n)} = u_3(\mathbf{x}^{(n)})$, $\mathbf{x}^{(n)}$ being the location of the external boundary nodal point n, (n=1, ... M_b), and $\pi_3^{(n)} = \pi_3(\mathbf{x}^{(n)})$, $\mathbf{x}^{(n)}$ being the location of the crack element mid-point n. For multiple and branch cracks, n= M_b+1, ... M_b+M_{c1}, $M_b+M_{c1}+2$, ... $M_b+M_{c1}+M_{c2}+1$. In addition, for a branch crack, we add a nodal point n= $M_b+M_{c1}+2$.

Eqs.(3.19) can be written in the following matrix form:

$$\begin{aligned}
&[UC_3]\left\{ u_3 \right\} - [Q_3]\left\{ \Delta u_3^1 \right\} - [Q_{31}]\left\{ \Delta u_3^2 \right\} = [UR_3]\left\{ t_3 \right\} \\
&[PC_3]\left\{ u_3 \right\} - [X_3]\left\{ \Delta u_3^1 \right\} - [X_{32}]\left\{ \Delta u_3^2 \right\} = [PR_3]\left\{ t_3 \right\} - \left\{ \pi_3^1 \right\} \qquad (3.20) \\
&[PC_{31}]\left\{ u_3 \right\} - [X_{23}]\left\{ \Delta u_3^1 \right\} - [X_{33}]\left\{ \Delta u_3^2 \right\} = [PR_{31}]\left\{ t_3 \right\} - \left\{ \pi^2 \right\}.
\end{aligned}$$

For multiple cracks, the matrices in eqs.(3.20) have the following dimensions:

$[UC_3]$ is M_b x M_b , $[Q_3]$ is M_b x $(M_{c1}-1)$, $[Q_{31}]$ is M_b x $(M_{c2}-1)$, $[UR_3]$ is M_b x $2M_b$, $[PC_3]$ is M_{c1} x M_b , $[X_3]$ is M_{c1} x $(M_{c1}-1)$, $[X_{32}]$ is M_{c1} x $(M_{c2}-1)$, $[PR_3]$ is M_{c1} x $2M_b$, $[PC_{31}]$ is M_{c2} x M_b , $[X_{23}]$ is M_{c2} x $(M_{c1}-1)$, $[X_{33}]$ is M_{c2} x $(M_{c2}-1)$ and $[PR_{31}]$ is M_{c2} x $2M_b$.

For a branch crack, the matrices in eqs.(3.20) have the following dimensions:

$[UC_3]$ is M_b x M_b , $[Q_3]$ is M_b x $(M_{c1}-1)$, $[Q_{31}]$ is M_b x M_{c2} , $[UR_3]$ is M_b x $2M_b$, $[PC_3]$ is M_{c1} x M_b , $[X_3]$ is M_{c1} x $(M_{c1}-1)$, $[X_{32}]$ is M_{c1} x M_{c2} , $[PR_3]$ is M_{c1} x $2M_b$, $[PC_{31}]$ is $(M_{c2}+1)$ x M_b , $[X_{23}]$ is $(M_{c2}+1)$ x $(M_{c1}-1)$, $[X_{33}]$ is $(M_{c2}+1)$ x M_{c2} and $[PR_{31}]$ is $(M_{c2}+1)$ x $2M_b$.

Thus

$$\begin{bmatrix} [UC_3] & -[Q_3] & -[Q_{31}] \\ [\Gamma_3][PC_3] & -[\Gamma_3][X_3] & -[\Gamma_3][X_{32}] \\ [\Gamma_{31}][PC_{31}] & -[\Gamma_{31}][X_{31}] & -[\Gamma_{31}][X_{33}] \end{bmatrix} \begin{Bmatrix} u_3 \\ \Delta u_3^1 \\ \Delta u_3^2 \end{Bmatrix} = \begin{bmatrix} [UR_3] & [0] & [0] \\ [\Gamma_3][PR_3] & [I] & [0] \\ [\Gamma_{31}][PR_{31}] & [0] & [I] \end{bmatrix} \begin{Bmatrix} t_3 \\ F_3^1 \\ F_3^2 \end{Bmatrix} \tag{3.21}$$

where, as in [76], we have defined nodal force matrices on the crack by

$$\left\{ F_3^1 \right\} = [\Gamma_3]\left\{ \pi_3^1 \right\}$$

$$\left\{ F_3^2 \right\} = [\Gamma_{31}]\left\{ \pi_3^2 \right\} \tag{3.22}$$

$$[\Gamma_3] = [\Gamma_{31}] = \begin{bmatrix} -1 & 1 & 0 & 0 & 0 & 0 & 0 \\ 0 & -1 & 1 & 0 & 0 & 0 & 0 \\ 0 & 0 & -1 & 1 & 0 & 0 & 0 \\ \cdot & \cdot & \cdot & \cdot & \cdot & \cdot & \cdot \\ \cdot & \cdot & \cdot & \cdot & \cdot & \cdot & \cdot \\ 0 & 0 & 0 & 0 & 0 & -1 & 1 \end{bmatrix} . \tag{3.23}$$

For multiple cracks, $[\Gamma_3]$ is $(M_{c1}-1)$ x M_{c1} and $[\Gamma_{31}]$ is $(M_{c2}-1)$ x M_{c2}. For a branch crack, $[\Gamma_3]$ is M_{c1} x $(M_{c1}+1)$ and $[\Gamma_{31}]$ is M_{c2} x $(M_{c2}+1)$.

For a branch crack, we need to employ continuity conditions and equilibrium conditions, i.e.

$$\Delta u_3^{(M_b+M_{bk}+1)} = \Delta u_3^{(M_b+M_{c1}+2)} \tag{3.24}$$

$$F_3^{(M_b+M_{bk}+1)} = F_3^{(M_b+M_{bk}+1)} + F_3^{(M_b+M_{c1}+2)} \tag{3.25}$$

It is well-known that one can obtain the diagonal entries of $[UC_3]$ in eqs.(3.12) or (3.21) from rigid-body considerations. If we apply a rigid-body displacement, i.e.

$$u_3^{(1)} = u_3^{(2)} = u_3^{(3)} = \ .... \ = u_3^{(M_b)} = u_3 \tag{3.26}$$

then the body is stress-free. Thus

$$\left\{ t_3 \right\} = \left\{ 0 \right\} \qquad\qquad \left\{ \Delta u_3 \right\} = \left\{ 0 \right\}$$

and eqs.(3.12) or (3.21) reduce to

$$[UC_3]\begin{Bmatrix} u_3 \\ u_3 \\ \vdots \\ u_3 \end{Bmatrix} = \left\{ 0 \right\} \tag{3.27}$$

so that

$$UC_3^{(i)(i)} = -\sum_{\substack{j=1 \\ j\neq i}}^{M_b} UC_3^{(i)(j)} \tag{3.28}$$

Once eqs.(3.12) or (3.21) have been constructed, we must impose two conditions at each nodal point m on Γ_b involving the boundary values

$$u_3^{(m)}, \qquad t_3^{(2m)}, \qquad t_3^{(2m+1)}$$

and rearrange eqs.(3.12) or (3.21) accordingly to obtain

$$[A]\left\{ Z \right\} = \left\{ B \right\} \tag{3.29}$$

where $\{Z\}$ contains the unknown boundary displacements and tractions in the x_3 direction on Γ_b and the unknown matrix $\{\Delta u\}$.

Once we have obtained Δu_3 at each crack nodal point, the stress intensity factors can be determined from

$$K_{III}|_{s=0} = \sqrt{\frac{\pi}{8\varepsilon}} G\Delta u_3(\varepsilon)$$

$$K_{III}|_{s=l} = \sqrt{\frac{\pi}{8\varepsilon}} G\Delta u_3(l-\varepsilon) \tag{3.30}$$

where $\varepsilon \to 0$, G is the shear modulus, and l is the length of the crack.

It should be noted that, for a problem involving a traction free crack, $\{F_3\} = \{0\}$ and eqs.(3.12) or (3.21) reduce to

$$\begin{bmatrix} [UC_3] & -[Q_3] \\ [\Gamma_3][PC_3] & -[\Gamma_3][X_3] \end{bmatrix} \begin{Bmatrix} u_3 \\ \Delta u_3 \end{Bmatrix} = \begin{bmatrix} [UR_3] \\ [\Gamma_3][PR_3] \end{bmatrix} \begin{Bmatrix} t_3 \end{Bmatrix}. \tag{3.31}$$

or

$$\begin{bmatrix} [UC_3] & -[Q_3] & -[Q_{31}] \\ [\Gamma_3][PC_3] & -[\Gamma_3][X_3] & -[\Gamma_3][X_{32}] \\ [\Gamma_{31}][PC_{31}] & -[\Gamma_{31}][X_{31}] & -[\Gamma_{31}][X_{33}] \end{bmatrix} \begin{Bmatrix} u_3 \\ \Delta u_3^1 \\ \Delta u_3^2 \end{Bmatrix} = \begin{bmatrix} [UR_3] \\ [\Gamma_3][PR_3] \\ [\Gamma_{31}][PR_{31}] \end{bmatrix} \begin{Bmatrix} t_3 \end{Bmatrix} \tag{3.32}$$

respectively.

3.3 Results

Here we employ the coupled model to find numerical solutions for some finite domain problems.

1. Straight crack.

In all straight crack problems, the crack is modeled by 20 equal elements and the external boundary is modeled by 40 elements. The stress intensity factors, normalized with respect to $\sigma\sqrt{a}$, are calculated.

a) Straight central crack in a rectangular sheet subjected to anti-plane shear stress.

A rectangular sheet of height 2h and width 2b contains a straight central crack of length 2a. A uniform shear stress, σ, acts over the ends of the plate as shown in Figure 3.1. In Table 3.1, the stress intensity factors are given for various ratios of a/b and a/h and are compared to those obtained in [100].

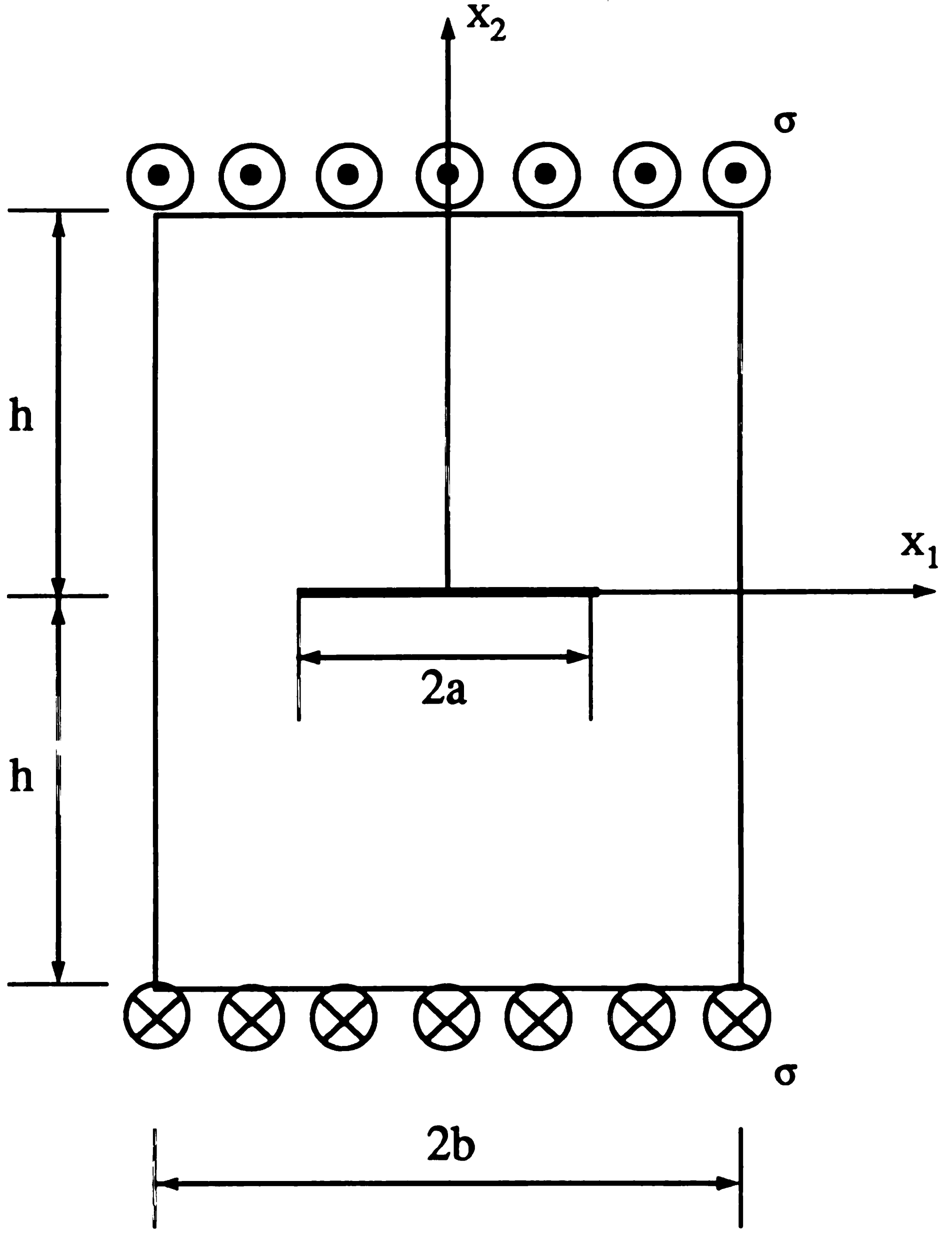

Figure 3.1 Geometry and loading for a straight central crack in a finite sheet under a uniformly distributed shear stress.

Table 3.1 Stress intensity factors for a straight central crack under a uniformly distributed shear stress as shown in Figure3.1.

a:b / a:h	1:1.2		1:1.4		1:1.6		1:2.0		1:∞	
	Present	[100]	Present	[100]	Present	[100]	Present	[100]	Present	[100]
1:0.25	1.897	1.900	1.780	1.782	1.771	1.773	1.770	1.772	1.770	1.772
1:0.5	1.723	1.725	1.460	1.463	1.399	1.401	1.377	1.379	1.375	1.377
1:1	1.689	1.691	1.369	1.370	1.254	1.256	1.176	1.178	1.147	1.149
1:2	1.686	1.689	1.359	1.361	1.233	1.235	1.127	1.130	1.046	1.047
1:4	1.686	1.689	1.358	1.360	1.233	1.235	1.126	1.128	1.012	1.013
1:∞	1.687	1.689	1.358	1.360	1.234	1.235	1.127	1.128	1.000	1.000

b) Straight central crack in a rectangular sheet subjected to anti-plane shear stress on the crack.

A rectangular sheet of height 2h and width 2b contains a straight central crack of length 2a. The crack is subjected to anti-plane shear stress σ. Three examples are considered for the problem of a rectangular sheet with fixed edges parallel to its crack, with fixed edges perpendicular to its crack and with four fixed edges as shown in Figures 3.2 throught 3.4, respectively. In Tables 3.2 throught 3.4, the stress intensity factors are given for various ratios of a/b and a/h and are compared to those obtained in [101].

2. Kinked crack.

In all kinked crack problems, both stress intensity factors, normalized with respect to $\sigma\sqrt{\pi a}$, and relative crack surface displacements are reported. G/σ = 200.

a) Symmetric V-shaped crack in a rectangular sheet subjected to anti-plane shear stress.

This example involves a symmetric V-shaped crack in a rectangular sheet subjected to a uniform anti-plane shear stress, as shown in Figure 3.5. The crack is modeled by 40 equal elements and the external boundary is modeled by 44 equal elements. For various angles α, the relative crack surface displacements are plotted in Figure 3.6 and the stress intensity factors are reported in Table 3.5.

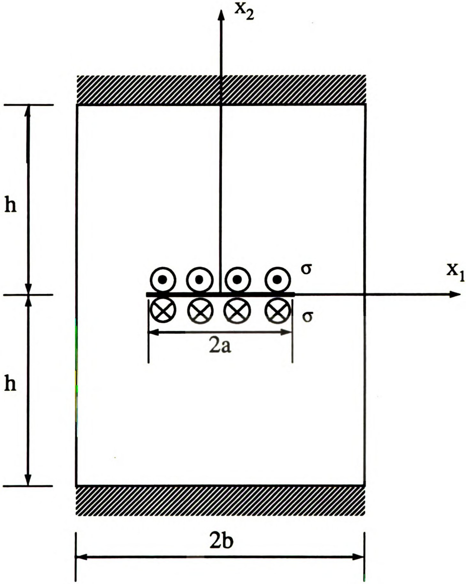

Figure 3.2 Geometry and loading for a straight central crack in a finite sheet with fixed edges parallel to the crack.

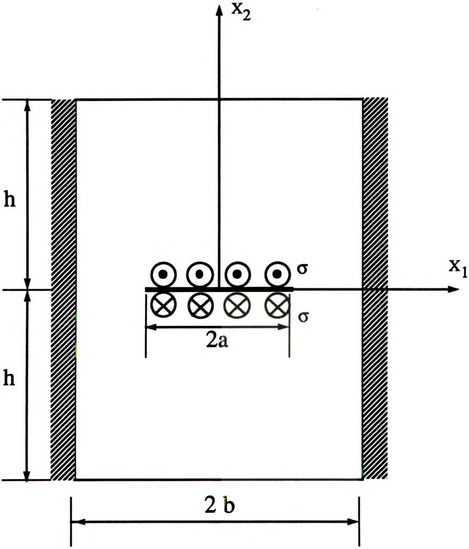

Figure 3.3 Geometry and loading for a straight central crack in a finite sheet with fixed edges perpendicular to the crack.

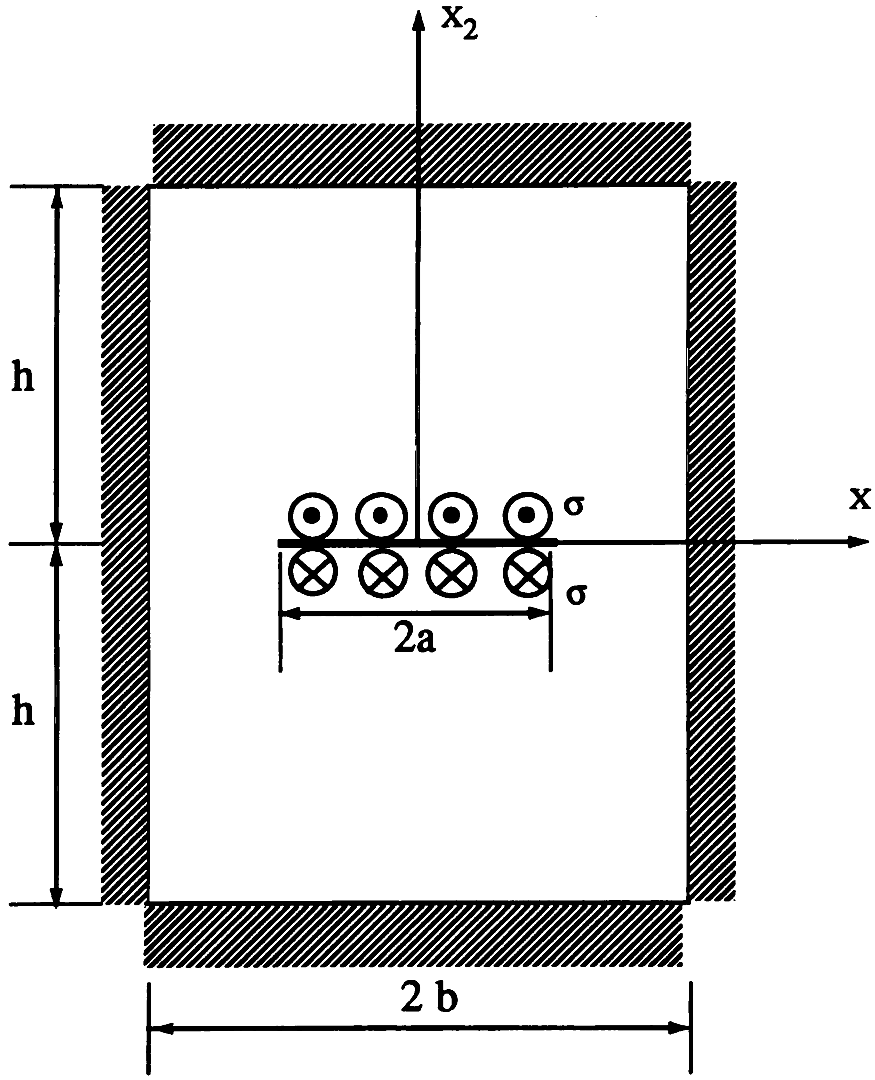

Figure 3.4 Geometry and loading for a straight central crack in a finite sheet with four fixed edges.

Table 3.2 Stress intensity factors for a straight central crack with fixed edges parallel to the crack as shown in Figure 3.2.

a:h \ a:b	1:1.2 Present	1:1.2 [101]	1:1.4 Present	1:1.4 [101]	1:1.6 Present	1:1.6 [101]	1:2.0 Present	1:2.0 [101]	1:∞ Present	1:∞ [101]
1:0.25	0.398	0.400	0.397	0.399	0.397	0.399	0.397	0.399	0.397	0.399
1:0.5	0.573	0.575	0.560	0.564	0.560	0.563	0.561	0.563	0.561	0.563
1:1	0.830	0.833	0.778	0.780	0.767	0.769	0.762	0.764	0.762	0.764
1:2	1.111	1.114	0.989	0.991	0.948	0.950	0.920	0.923	0.912	0.914
1:4	1.339	1.342	1.145	1.147	1.072	1.074	1.014	1.016	0.974	0.975
1:∞	1.687	1.689	1.358	1.360	1.234	1.235	1.127	1.128	1.000	1.000

Table 3.3 Stress intensity factors for a straight central crack with fixed edges perpendicular to ithe crack as shown in Figure 3.3.

a:h \ a:b	1:1.2 Present	1:1.2 [101]	1:1.4 Present	1:1.4 [101]	1:1.6 Present	1:1.6 [101]	1:2.0 Present	1:2.0 [101]	1:∞ Present	1:∞ [101]
1:0.25	1.650	1.653	1.759	1.760	1.769	1.771	1.770	1.772	1.770	1.772
1:0.5	1.177	1.180	1.295	1.298	1.351	1.354	1.373	1.375	1.375	1.377
1:1	0.844	0.847	0.981	0.984	1.055	1.058	1.120	1.122	1.147	1.149
1:2	0.772	0.775	0.868	0.871	0.920	0.922	0.977	0.979	1.046	1.047
1:4	0.767	0.770	0.856	0.859	0.899	0.901	0.941	0.943	1.012	1.013
1:∞	0.768	0.770	0.857	0.859	0.900	0.901	0.942	0.942	1.000	1.000

Table 3.4 Stress intensity factors for a straight central crack with four fixed edges as shown in Figure 3.4.

a:h \ a:b	1:1.2 Present	1:1.2 [101]	1:1.4 Present	1:1.4 [101]	1:1.6 Present	1:1.6 [101]	1:2.0 Present	1:2.0 [101]	1:∞ Present	1:∞ [101]
1:0.25	0.396	0.398	0.397	0.399	0.398	0.399	0.398	0.399	0.398	0.399
1:0.5	0.549	0.551	0.560	0.562	0.561	0.563	0.562	0.563	0.562	0.563
1:1	0.700	0.702	0.746	0.748	0.758	0.760	0.762	0.764	0.762	0.764
1:2	0.763	0.765	0.844	0.846	0.878	0.880	0.903	0.905	0.913	0.914
1:4	0.767	0.770	0.856	0.858	0.899	0.900	0.940	0.940	0.915	0.915
1:∞	0.768	0.770	0.857	0.859	0.900	0.901	0.942	0.942	1.000	1.000

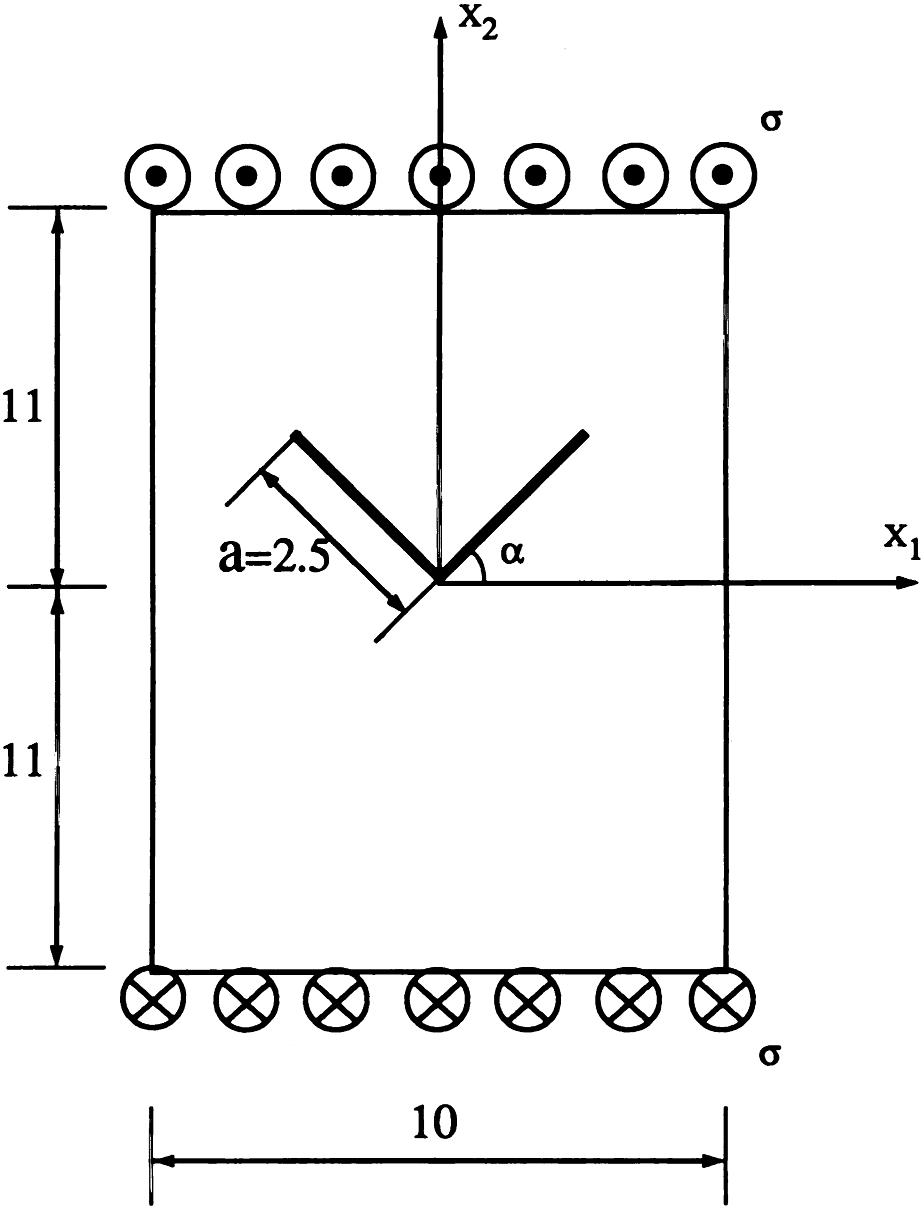

Figure 3.5 Geometry and loading for a symmetric V-shaped crack in a finite sheet under a uniformly distributed transverse shear stress.

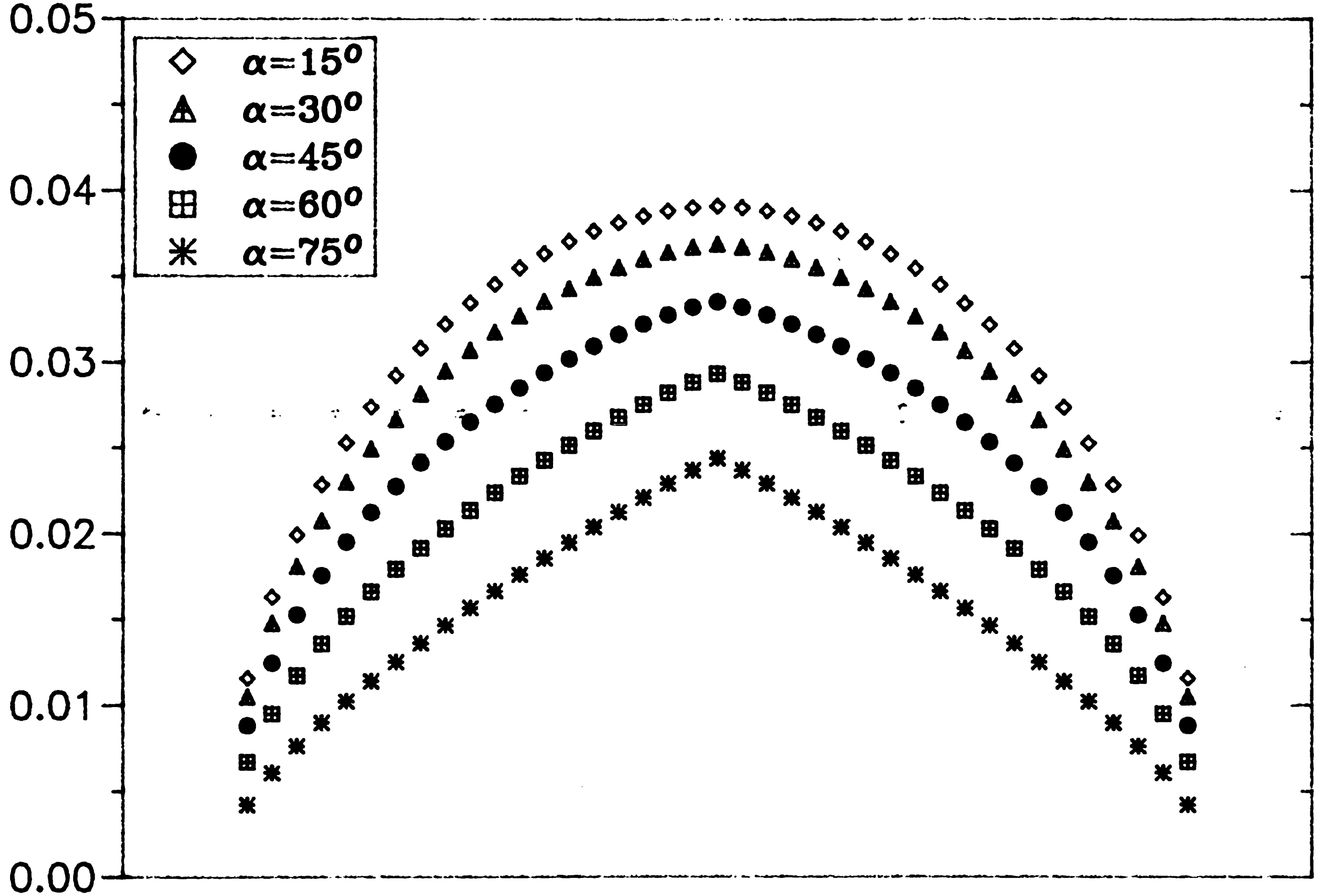

Figure 3.6 Relative crack surface displacement Δu_3 for a symmetric V–shaped crack.

b) Asymmetric kinked crack in a rectangular sheet subjected to anti-plane shear stress.

This example involves an asymmetric kinked crack in a rectangular sheet subjected to a uniform anti-plane shear stress, as shown in Figure 3.7. The crack is modeled by 30 equal elements and the external boundary is modeled by 44 equal elements. For various ratios L/2a, the relative crack surface displacements are plotted in Figure 3.8 and the stress intensity factors are reported in Table 3.6.

c) Anti-symmetric kinked crack in a rectangular sheet subjected to anti-plane shear stress.

This example involves an anti-symmetric kinked crack in a rectangular sheet subjected to a uniform anti-plane shear stress, as shown in Figure 3.9. The crack is modeled by 35 equal elements and the external boundary is modeled by 44 equal elements. For various angles α, the relative crack surface displacements are plotted in Figure 3.10 and the stress intensity factors are reported in Table 3.7.

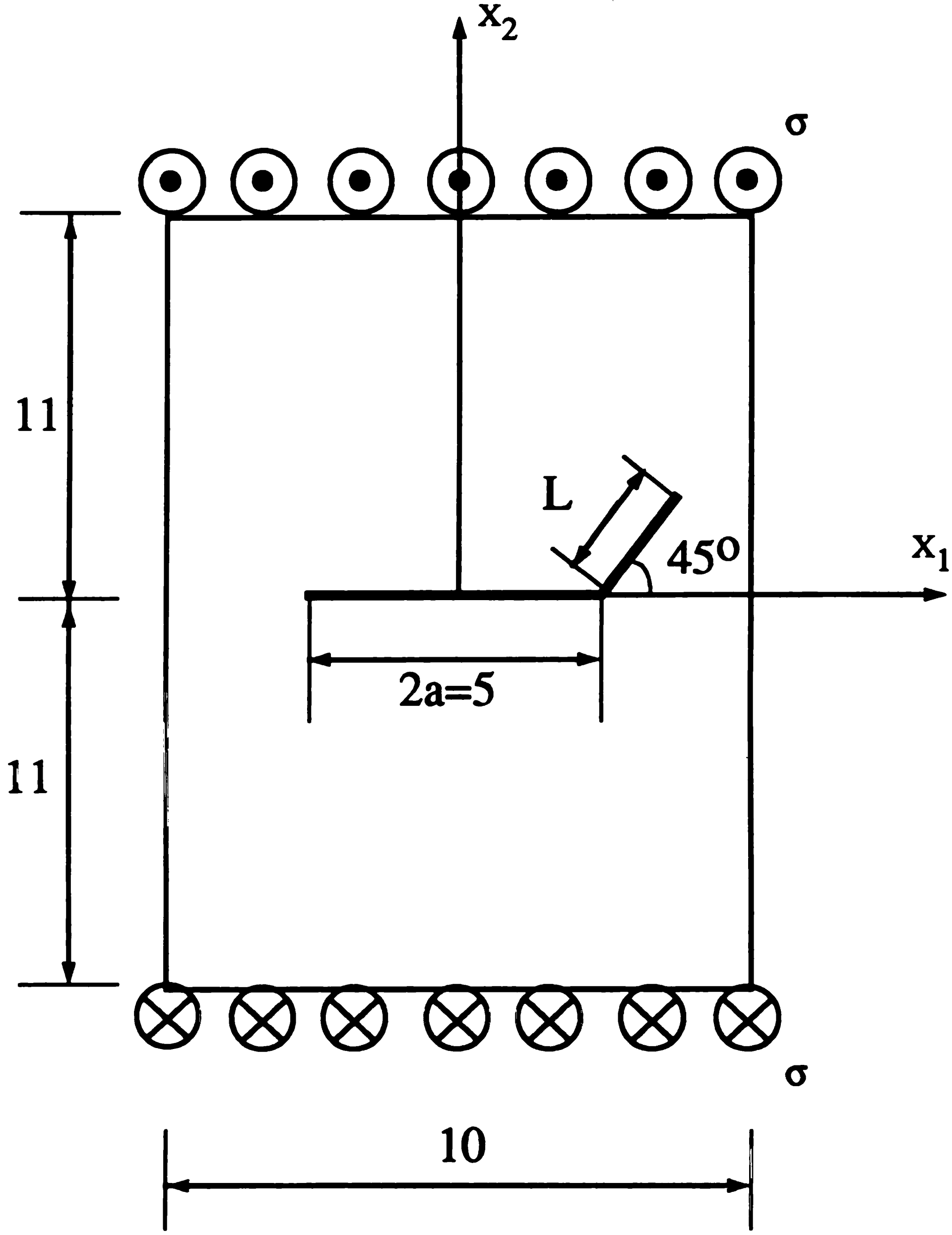

Figure 3.7 Geometry and loading for an asymmetric kinked crack in a finite sheet under a uniformly distributed transverse shear stresss.

Table 3.5 Stress intensity factors for a symmetric V-shaped crack under a uniformly distributed shear stress as shown in Figure 3.5.

α	15	30	45	60	75
$K_{III} / \sigma\sqrt{\pi a}$	2.0700	1.8743	1.5755	1.1965	0.7496

Table 3.6 Stress intensity factors for an asymmetric kinked crack under a uniformly distributed shear stress as shown in Figure 3.7.

L/2a	0.2	0.16	0.12	0.08	0.04
$K_{III} / \sigma\sqrt{\pi a}$	3.4359	3.9220	4.5877	5.6497	7.9809

Table 3.7 Stress intensity factors for an anti-symmetric kinked crack under a uniformly distributed shear stress as shown in Figure 3.9.

α	15	30	45	60	75
$K_{III} / \sigma\sqrt{\pi a}$	4.5605	4.3281	3.9757	3.5427	3.0664

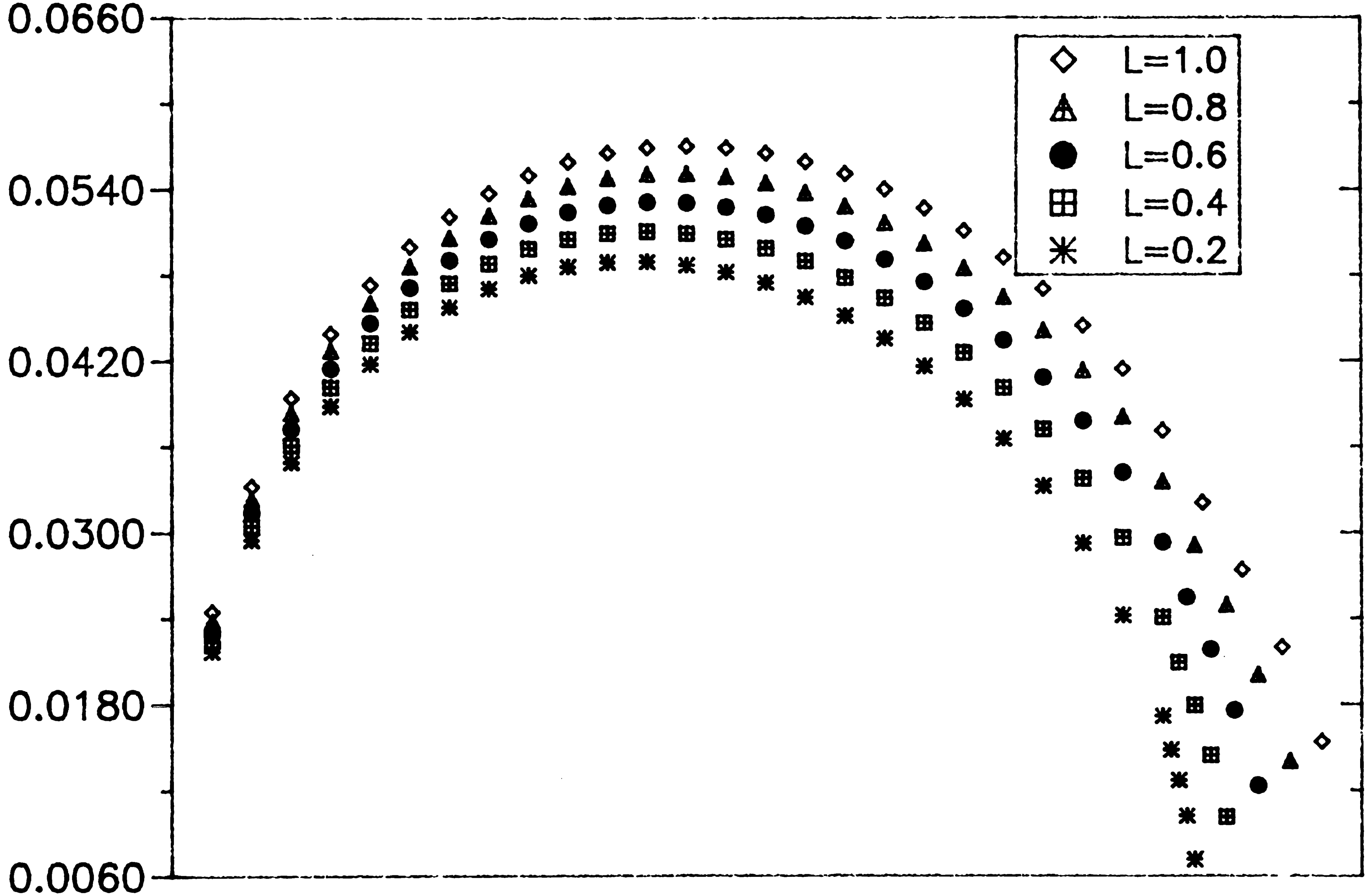

Figure 3.8 Relative crack surface displacement Δu_3 for an asymmertic kinked crack.

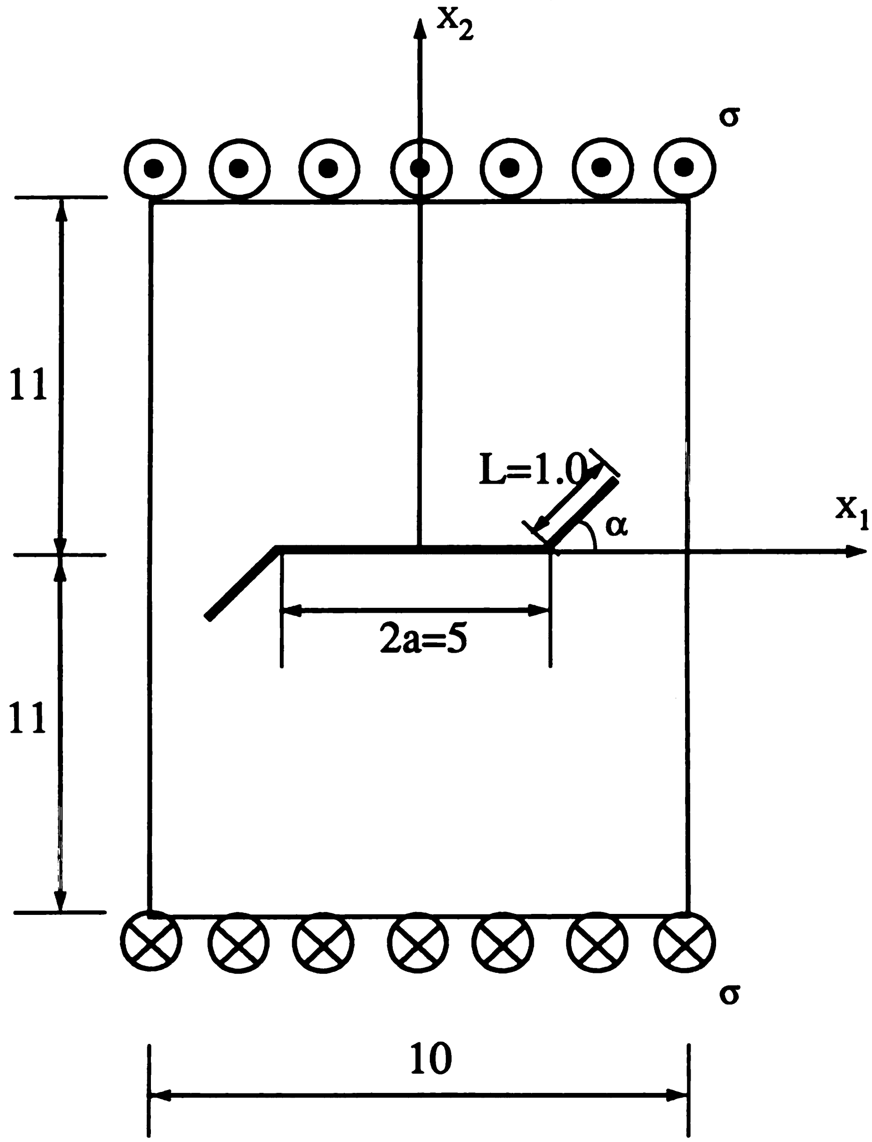

Figure 3.9 Geometry and loading for an anti-symmetric kinked crack in a finite sheet under a uniformly distributed trensverse shear stresss.

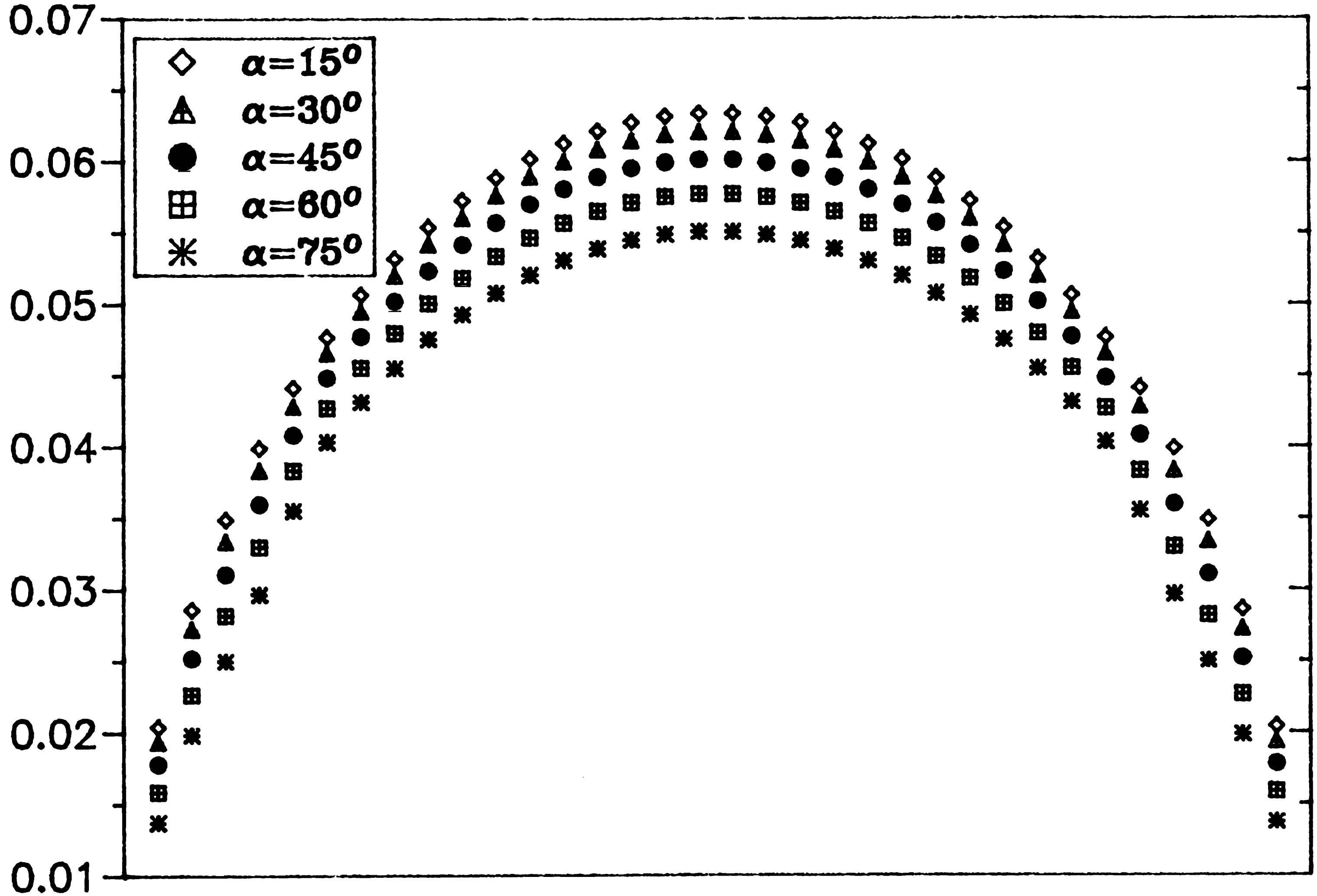

Figure 3.10 Relative crack surface displacemebt Δu_3 for an anti-symmetric kinked crack.

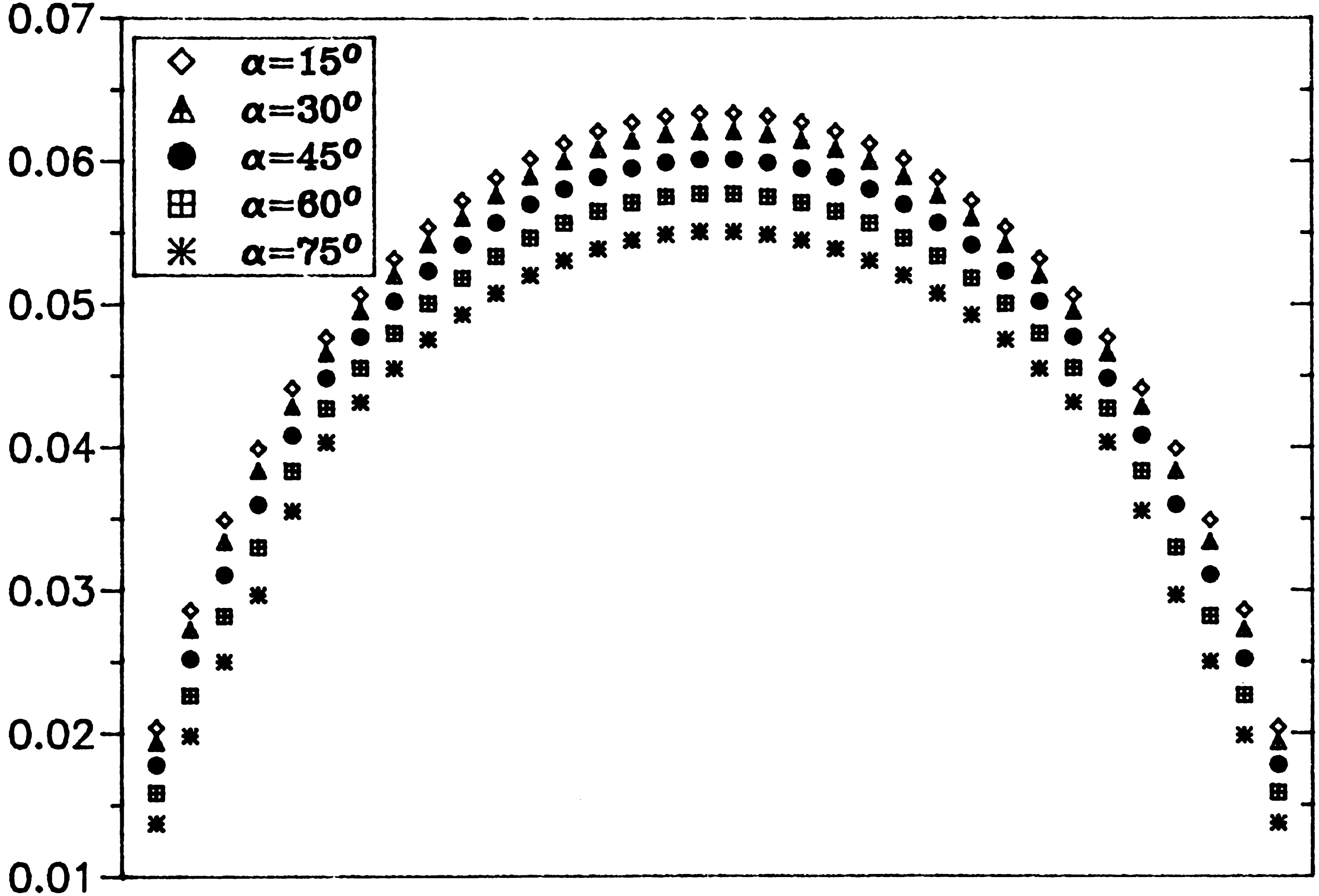

Figure 3.10 Relative crack surface displacemebt Δu_3 for an anti-symmetric kinked crack.

Chapter 4

Thermoelastic Problems Involving Cracks

4.1 Theoretical Development

In Chapters 2 and 3, an integral equation representation of cracks was developed and coupled to the direct boundary element method for treatment of smooth and/or kinked cracks in finite plane bodies. In these Chapters, the equations were written in terms of the displacement-discontinuity across the crack surfaces. The approach can be applied to arbitrary regions containing arbitrary cracks in a simple, straightforward manner. In Chapter 2, the coupling of the direct boundary-integral equations to crack integral equations were developed for modes I and II cracks. In Chapter 3, the analogous approach was developed for mode III crack problems.

The method outlined in the previous Chapters is here extended for application to steady-state thermal fields disturbed by arbitrary insulated internal smooth and/or kinked cracks in finite plane regions. In this approach, the divergence theorem is applied to transform the domain integrals to equivalent boundary integrals in order to treat the body force terms. The advantages of the boundary-only formulation is that only surface discretization is involved.

In the theory of uncoupled thermoelasticity, the steady-state problems can be solved separately from the elastic problem because thermal unknowns are independent of the elastic ones. The elastic fields (displacements and stresses), however, are generated by temperature gradients. Thus, steady-state heat conduction is considered first to determined the surface temperatures and heat flux distributions, then the resulting temperature fields are treated as body force terms in an elastostatic formulation.

A plane elastic region Ω, with external boundary Γ_b, containing an internal piece-wise smooth crack line Γ_c, as shown in Figure 4.1, is loaded by prescribed heat fluxes q_n on some part of the external boundary and prescribed temperatures T on the remainder of the external boundary. Because of the analogy between mode III elasticity and heat conduction, the steady-state heat conduction equations can be represented, as shown in Chapter 3, by replacing u_3, t_3, Δu_3 and π_3 by T, q_n, ΔT and Q, respectively

$$
\begin{aligned}
c_3(\mathbf{x})\, T(\mathbf{x}) &= \oint_{\Gamma_b} (uR)_{33}(\mathbf{x}, \bar{\mathbf{x}})\, q_n(\bar{\mathbf{x}})\, ds(\bar{\mathbf{x}}) - \oint_{\Gamma_b} (uc)_{33}(\mathbf{x}, \bar{\mathbf{x}})\, T(\bar{\mathbf{x}})\, ds(\bar{\mathbf{x}}) \\
&\quad + \int_{\Gamma_c} (uc)_{33}(\mathbf{x}, \bar{\mathbf{x}})\, \Delta T(\bar{\mathbf{x}})\, ds(\bar{\mathbf{x}}) \qquad \mathbf{x} \text{ on } \Gamma_b
\end{aligned}
$$

$$(4.1)$$

$$
\begin{aligned}
Q(\mathbf{x}) &= \oint_{\Gamma_b} (\pi R)_{33}(\mathbf{x}, \bar{\mathbf{x}})\, q_n(\bar{\mathbf{x}})\, ds(\bar{\mathbf{x}}) - \oint_{\Gamma_b} (\pi c)_{33}(\mathbf{x}, \bar{\mathbf{x}})\, T(\bar{\mathbf{x}})\, ds(\bar{\mathbf{x}}) \\
&\quad + \int_{\Gamma_c} (\pi c)_{33}(\mathbf{x}, \bar{\mathbf{x}})\, \Delta T(\bar{\mathbf{x}})\, ds(\bar{\mathbf{x}}) \qquad \mathbf{x} \text{ on } \Gamma_c
\end{aligned}
$$

where $\Delta T = T^- - T^+$ is the temperature jump across the crack, c_3 is a coefficient which depends on the smoothness of the boundary at **x** on Γ_b and

$$q_n = -\frac{dQ}{ds} \quad . \tag{4.2}$$

The influence functions in eqs.(4.1) are identical to those presented in Appendix C where G is replaced by k, the thermal conductivity. Following the same procedures as

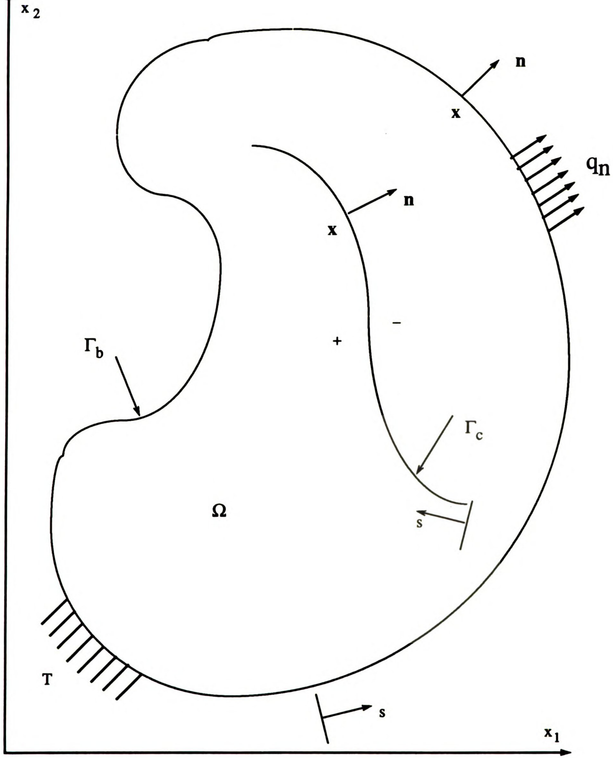

Figure 4.1 Heat transfer problem involving a crack.

shown in Chapter 3, we can obtain the temperatures T and heat fluxes q_n at each of the boundary nodal points and the temperature jumps ΔT at each of the crack nodal points for the insulated crack case.

Consider an infinite isotropic elastic plane in which there is a point, $\bar{\mathbf{x}}$, at which some "source" of stress is located and a point, $\mathbf{x}$, at which the stresses are to be computed. We will employ the following additional influence functions

$(uR)_{i3}(\mathbf{x}, \bar{\mathbf{x}})$ = the displacement in the i direction at $\mathbf{x}$ due to a unit heat source applied at $\bar{\mathbf{x}}$ in the infinite plane,

$(uc)_{i3}(\mathbf{x}, \bar{\mathbf{x}})$ = the displacement in the i direction at $\mathbf{x}$ due to a unit temperature jump applied at $\bar{\mathbf{x}}$ in the infinite plane,

$(\pi R)_{i3}(\mathbf{x}, \bar{\mathbf{x}})$ = the value of π_i at $\mathbf{x}$ due to a unit heat source applied at $\bar{\mathbf{x}}$ in the infinite plane,

$(\pi c)_{i3}(\mathbf{x}, \bar{\mathbf{x}})$ = the value of π_i at $\mathbf{x}$ due to a unit temperature jump applied at $\bar{\mathbf{x}}$ in the infinite plane,

where π_i, i=1,2, are stress functions defined as in eqs.(2.1.1).

A plane elastic region, as shown in Figure 4.2, is loaded by prescribed tractions t_j and/or heat fluxes q_n on some part of the external boundary and prescribed displacements u_j and/or temperatures T on the remainder of the external boundary. Then the direct boundary-integral equations and the integral equations developed in [76] can be coupled as follows:

$$c_{ij}(\mathbf{x})u_j(\mathbf{x}) + \oint_{\Gamma_b}[(uc)_{ij}(\mathbf{x},\bar{\mathbf{x}})u_j(\bar{\mathbf{x}}) - (uR)_{ij}(\mathbf{x},\bar{\mathbf{x}})t_j(\bar{\mathbf{x}})]ds(\bar{\mathbf{x}}) - \int_{\Gamma_c}(uc)_{ij}(\mathbf{x},\bar{\mathbf{x}})\Delta u_j(\bar{\mathbf{x}})ds(\bar{\mathbf{x}})$$

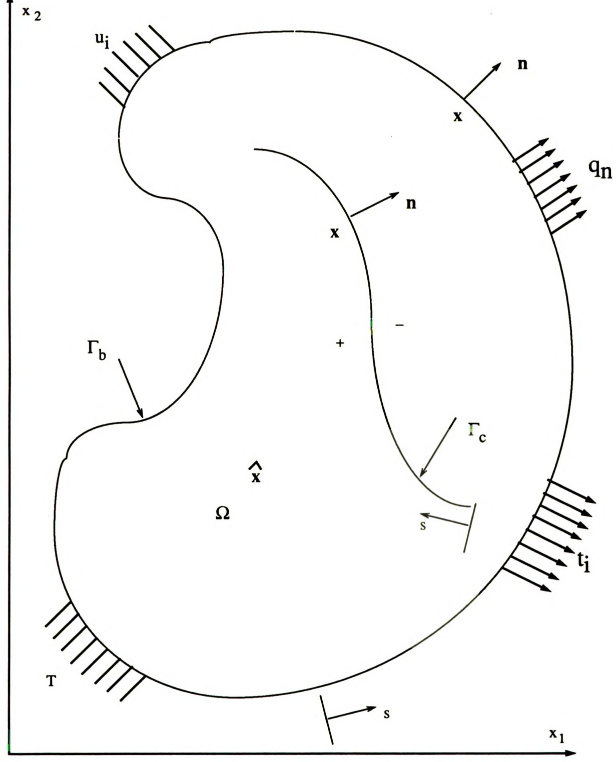

Figure 4.2 Thermoelasticity problem involving a crack.

$$= \int_{\Omega} (uR)_{ij}(\mathbf{x},\hat{\mathbf{x}}) b_j(\hat{\mathbf{x}}) dS(\hat{\mathbf{x}})$$

$$= \oint_{\Gamma_b} [(uc)_{i3}(\mathbf{x},\bar{\mathbf{x}})T(\bar{\mathbf{x}}) - (uR)_{i3}(\mathbf{x},\bar{\mathbf{x}})q_n(\bar{\mathbf{x}})]ds(\bar{\mathbf{x}}) - \oint_{\Gamma_b} (uR)_{ij}(\mathbf{x},\bar{\mathbf{x}})\gamma n_j(\bar{\mathbf{x}})T(\bar{\mathbf{x}})ds(\bar{\mathbf{x}})$$

$$- \int_{\Gamma_c} (uc)_{i3}(\mathbf{x},\bar{\mathbf{x}})\Delta T(\bar{\mathbf{x}})ds(\bar{\mathbf{x}}) \qquad \mathbf{x} \text{ on } \Gamma_{b,} \quad \hat{\mathbf{x}} \text{ in } \Omega$$

$$(4.3)$$

$$\pi_i(\mathbf{x}) + \oint_{\Gamma_b} [(\pi c)_{ij}(\mathbf{x},\bar{\mathbf{x}})u_j(\bar{\mathbf{x}}) - (\pi R)_{ij}(\mathbf{x},\bar{\mathbf{x}})t_j(\bar{\mathbf{x}})]ds(\bar{\mathbf{x}}) - \int_{\Gamma_c} (\pi c)_{ij}(\mathbf{x},\bar{\mathbf{x}})\Delta u_j(\bar{\mathbf{x}})ds(\bar{\mathbf{x}})$$

$$= \int_{\Omega} (\pi R)_{ij}(\mathbf{x},\hat{\mathbf{x}}) b_j(\hat{\mathbf{x}}) dS(\hat{\mathbf{x}})$$

$$= \oint_{\Gamma_b} [(\pi c)_{i3}(\mathbf{x},\bar{\mathbf{x}})T(\bar{\mathbf{x}}) - (\pi R)_{i3}(\mathbf{x},\bar{\mathbf{x}})q_n(\bar{\mathbf{x}})]ds(\bar{\mathbf{x}}) - \oint_{\Gamma_b} (\pi R)_{ij}(\mathbf{x},\bar{\mathbf{x}})\gamma n_j(\bar{\mathbf{x}})T(\bar{\mathbf{x}})ds(\bar{\mathbf{x}})$$

$$- \int_{\Gamma_c} (\pi c)_{i3}(\mathbf{x},\bar{\mathbf{x}})\Delta T(\bar{\mathbf{x}})ds(\bar{\mathbf{x}}) \qquad \mathbf{x} \text{ on } \Gamma_{c,} \quad \hat{\mathbf{x}} \text{ in } \Omega$$

where i=1, 2, j=1, 2, summation on repeated indices is implied, and $\Delta u_j = u_j^- - u_j^+$ are the relative crack surface thermal displacements.

In eqs. (4.3), we have inserted $b_j = -\gamma u_{3,j}$ and applied the divergence theorem as shown in Appendix D. It should be noted that the right sides of eqs.(4.3) are known functions.

4.2 Numerical Treatment

A simple numerical treatment of eqs.(4.3) is presented here in which the external boundary is approximated by M_b straight elements and the crack by M_c straight elements, as shown in Figure 2.5. Eqs.(4.3) can then be written as

$$c_{ij}(\mathbf{x})\ u_j(\mathbf{x}) + \sum_{m=1}^{M_b} \int_m [\ (uc)_{ij}(\mathbf{x}, \bar{\mathbf{x}})\ u_j(\bar{\mathbf{x}}) - (uR)_{ij}(\mathbf{x}, \bar{\mathbf{x}})\ t_j(\bar{\mathbf{x}})\ ]\ ds(\bar{\mathbf{x}})$$

$$- \sum_{m=M_b+1}^{M_b+M_c} \int_m (uc)_{ij}(\mathbf{x}, \bar{\mathbf{x}})\, \Delta u_j(\bar{\mathbf{x}})\, ds(\bar{\mathbf{x}})$$

$$= \sum_{m=1}^{M_b} \int_m [(uc)_{i3}(\mathbf{x}, \bar{\mathbf{x}})\, T(\bar{\mathbf{x}}) - (uR)_{i3}(\mathbf{x}, \bar{\mathbf{x}})\, q_n(\bar{\mathbf{x}})]\, ds(\bar{\mathbf{x}})$$

$$- \sum_{m=1}^{M_b} \int_m (uR)_{ij}(\mathbf{x}, \bar{\mathbf{x}}) \gamma n_j(\bar{\mathbf{x}}) T(\bar{\mathbf{x}})\, ds(\bar{\mathbf{x}})$$

$$- \sum_{m=M_b+1}^{M_b+M_c} \int_m (uc)_{i3}(\mathbf{x}, \bar{\mathbf{x}})\, \Delta T(\bar{\mathbf{x}})\, ds(\bar{\mathbf{x}}) \qquad \mathbf{x} \text{ on } \Gamma_b$$

$$(4.4)$$

$$\pi_i(\mathbf{x}) + \sum_{m=1}^{M_b} \int_m [\, (\pi c)_{ij}(\mathbf{x}, \bar{\mathbf{x}})\, u_j(\bar{\mathbf{x}}) - (\pi R)_{ij}(\mathbf{x}, \bar{\mathbf{x}})\, t_j(\bar{\mathbf{x}})\,]\, ds(\bar{\mathbf{x}})$$

$$- \sum_{m=M_b+1}^{M_b+M_c} \int_m (\pi c)_{ij}(\mathbf{x}, \bar{\mathbf{x}})\, \Delta u_j(\bar{\mathbf{x}})\, ds(\bar{\mathbf{x}})$$

$$= \sum_{m=1}^{M_b} \int_m [(\pi c)_{i3}(\mathbf{x}, \bar{\mathbf{x}}) T(\bar{\mathbf{x}}) - (\pi R)_{i3}(\mathbf{x}, \bar{\mathbf{x}}) q_n(\bar{\mathbf{x}})]\, ds(\bar{\mathbf{x}})$$

$$- \sum_{m=1}^{M_b} \int_m (\pi R)_{ij}(\mathbf{x}, \bar{\mathbf{x}}) \gamma n_j(\bar{\mathbf{x}}) T(\bar{\mathbf{x}}) ds(\bar{\mathbf{x}})$$

$$- \sum_{m=M_b+1}^{M_b+M_c} \int_m (\pi c)_{i3}(\mathbf{x}, \bar{\mathbf{x}})\, \Delta T(\bar{\mathbf{x}})\, ds(\bar{\mathbf{x}}) \qquad \mathbf{x} \text{ on } \Gamma_c \;.$$

The displacements, tractions, displacement discontinuities, temperatures, heat fluxes and temperature jumps on each element can be linearly approximated by

$$u_j(\bar{\mathbf{x}}) = N_1(\xi) u_j^{(m-1)} + N_2(\xi) u_j^{(m)} \qquad \bar{\mathbf{x}} \text{ on element m of } \Gamma_b$$

$$t_j(\bar{\mathbf{x}}) = N_1(\xi) t_j^{(2m-1)} + N_2(\xi) t_j^{(2m)} \qquad \bar{\mathbf{x}} \text{ on element m of } \Gamma_b$$

$$\Delta u_j(\bar{\mathbf{x}}) = N_1(\xi) \Delta u_j^{(m)} + N_2(\xi) \Delta u_j^{(m+1)} \qquad \bar{\mathbf{x}} \text{ on element m of } \Gamma_c$$

$$T(\bar{x}) = N_1(\xi)T^{(m-1)} + N_2(\xi)T^{(m)} \qquad \bar{x} \text{ on element } m \text{ of } \Gamma_b \qquad (4.5)$$

$$q_n(\bar{x}) = N_1(\xi)q_n^{(2m-1)} + N_2(\xi)q_n^{(2m)} \qquad \bar{x} \text{ on element } m \text{ of } \Gamma_b$$

$$\Delta T(\bar{x}) = N_1(\xi)\Delta T^{(m)} + N_2(\xi)\Delta T^{(m+1)} \qquad \bar{x} \text{ on element } m \text{ of } \Gamma_c$$

where $u_j^{(m)}$, $t_j^{(2m-1)}$, $t_j^{(2m)}$, $T^{(m)}$, $q_n^{(2m-1)}$, $q_n^{(2m)}$ are values at the external boundary nodal point m (m=1,... M_b), $\Delta u_j^{(m)}$ and $\Delta T^{(m)}$ are values at the crack nodal point (m) (m= M_b+2,... M_b+M_c), and

$$N_1(\xi) = (1-\xi)/2 \qquad N_2(\xi) = (1+\xi)/2 \qquad -1 \le \xi \le 1 \ . \qquad (4.6)$$

Furthermore

$$\bar{x} = N_1(\xi)x^{(m-1)} + N_2(\xi)x^{(m)} \qquad \bar{x} \text{ on element } m \text{ of } \Gamma_b \text{ and } \Gamma_c \qquad (4.7)$$

$$ds(\bar{x}) = [(s^{(m)} - s^{(m-1)})/2]\, d\xi = [\Delta s^m/2]\, d\xi \qquad \bar{x} \text{ on element } m \text{ of } \Gamma_b \text{ and } \Gamma_c \qquad (4.8)$$

where Δs^m is the length of the element m.

Inserting eqs.(4.5) through (4.8) into eqs.(4.4), we obtain

$$c_{ij}^{(n)}u_j^{(n)} + \sum_{m=1}^{M_b} \Delta s^m/4\, [\int_m (1-\xi)(uc)_{ij}(x^{(n)}, \xi)d\xi\ ]\ u_j^{(m-1)}$$

$$+ \sum_{m=1}^{M_b} \Delta s^m/4\, [\int_m (1+\xi)(uc)_{ij}(x^{(n)}, \xi)d\xi\ ]\ u_j^{(m)}$$

$$- \sum_{m=1}^{M_b} \Delta s^m/4 \left[\int_m (1-\xi)(uR)_{ij}(\mathbf{x}^{(n)}, \xi) d\xi \right] t_j^{(2m-1)}$$

$$- \sum_{m=1}^{M_b} \Delta s^m/4 \left[\int_m (1+\xi)(uR)_{ij}(\mathbf{x}^{(n)}, \xi) d\xi \right] t_j^{(2m)}$$

$$- \sum_{m=M_b+2}^{M_b+M_c} \Delta s^m/4 \left[\int_m (1-\xi)(uc)_{ij}(\mathbf{x}^{(n)}, \xi) d\xi \right] \Delta u_j^{(m)}$$

$$- \sum_{m=M_b+1}^{M_b+M_c} \Delta s^m/4 \left[\int_m (1+\xi)(uc)_{ij}(\mathbf{x}^{(n)}, \xi) d\xi \right] \Delta u_j^{(m+1)}$$

$$= \sum_{m=1}^{M_b} \Delta s^m/4 \left[\int_m (1-\xi)(uc)_{i3}(\mathbf{x}^{(n)}, \xi) d\xi \right] T^{(m-1)}$$

$$+ \sum_{m=1}^{M_b} \Delta s^m/4 \left[\int_m (1+\xi)(uc)_{i3}(\mathbf{x}^{(n)}, \xi) d\xi \right] T^{(m)}$$

$$- \sum_{m=1}^{M_b} \Delta s^m/4 \left[\int_m (1-\xi)(uR)_{ij}(\mathbf{x}^{(n)}, \xi) \gamma n_j(\xi) d\xi \right] T^{(m-1)}$$

$$- \sum_{m=1}^{M_b} \Delta s^m/4 \left[\int_m (1+\xi)(uR)_{ij}(\mathbf{x}^{(n)}, \xi) \gamma n_j(\xi) d\xi \right] T^{(m)}$$

$$- \sum_{m=M_b+2}^{M_b+M_c} \Delta s^m/4 \left[\int_m (1-\xi)(uc)_{i3}(\mathbf{x}^{(n)}, \xi) d\xi \right] \Delta T^{(m)}$$

$$- \sum_{m=M_b+1}^{M_b+M_c} \Delta s^m/4 \left[\int_m (1+\xi)(uc)_{i3}(\mathbf{x}^{(n)}, \xi) d\xi \right] \Delta T^{(m+1)}$$

$$- \sum_{m=1}^{M_b} \Delta s^m/4 \left[\int_m (1-\xi)(uR)_{i3}(\mathbf{x}^{(n)}, \xi) d\xi \right] q_n^{(2m-1)}$$

$$- \sum_{m=1}^{M_b} \Delta s^m/4 \left[\int_m (1+\xi)(uR)_{i3}(\mathbf{x}^{(n)}, \xi) d\xi \right] q_n^{(2m)} \qquad (4.9)$$

$$\pi_i^{(n)} + \sum_{m=1}^{M_b} \Delta s^m/4 \left[\int_m (1-\xi)(\pi c)_{ij}(\mathbf{x}^{(n)}, \xi) d\xi \right] u_j^{(m-1)}$$

$$+\sum_{m=1}^{M_b} \Delta s^m/4\ [\int_m (1+\xi)(\pi c)_{ij}(\mathbf{x}^{(n)}, \xi)d\xi\ ]\ u_j^{(m)}$$

$$-\sum_{m=1}^{M_b} \Delta s^m/4\ [\int_m (1-\xi)(\pi R)_{ij}(\mathbf{x}^{(n)}, \xi)d\xi\ ]\ t_j^{(2m-1)}$$

$$-\sum_{m=1}^{M_b} \Delta s^m/4\ [\int_m (1+\xi)(\pi R)_{ij}(\mathbf{x}^{(n)}, \xi)d\xi\ ]\ t_j^{(2m)}$$

$$-\sum_{m=M_b+2}^{M_b+M_c} \Delta s^m/4\ [\int_m (1-\xi)(\pi c)_{ij}(\mathbf{x}^{(n)}, \xi)d\xi\ ]\ \Delta u_j^{(m)}$$

$$-\sum_{m=M_b+1}^{M_b+M_c} \Delta s^m/4\ [\int_m (1+\xi)(\pi c)_{ij}(\mathbf{x}^{(n)}, \xi)d\xi\ ]\ \Delta u_j^{(m+1)}$$

$$=\sum_{m=1}^{M_b} \Delta s^m/4\ [\int_m (1-\xi)(\pi c)_{i3}(\mathbf{x}^{(n)}, \xi)d\xi\ ]\ T^{(m-1)}$$

$$+\sum_{m=1}^{M_b} \Delta s^m/4\ [\int_m (1+\xi)(\pi c)_{i3}(\mathbf{x}^{(n)}, \xi)d\xi\ ]\ T^{(m)}$$

$$-\sum_{m=1}^{M_b} \Delta s^m/4\ [\int_m (1-\xi)(\pi R)_{ij}(\mathbf{x}^{(n)}, \xi)\gamma n_j(\xi)d\xi\ ]\ T^{(m-1)}$$

$$-\sum_{m=1}^{M_b} \Delta s^m/4\ [\int_m (1+\xi)(\pi R)_{ij}(\mathbf{x}^{(n)}, \xi)\gamma n_j(\xi)d\xi\ ]\ T^{(m)}$$

$$-\sum_{m=M_b+2}^{M_b+M_c} \Delta s^m/4\ [\int_m (1-\xi)(\pi c)_{i3}(\mathbf{x}^{(n)}, \xi)d\xi\ ]\ \Delta T^{(m)}$$

$$-\sum_{m=M_b+1}^{M_b+M_c} \Delta s^m/4\ [\int_m (1+\xi)(\pi c)_{i3}(\mathbf{x}^{(n)}, \xi)d\xi\ ]\ \Delta T^{(m+1)}$$

$$-\sum_{m=1}^{M_b} \Delta s^m/4\ [\int_m (1-\xi)(\pi R)_{i3}(\mathbf{x}^{(n)}, \xi)d\xi\ ]\ q_n^{(2m-1)}$$

$$-\sum_{m=1}^{M_b} \Delta s^m/4\ [\int_m (1+\xi)(\pi R)_{i3}(\mathbf{x}^{(n)}, \xi)d\xi\ ]\ q_n^{(2m)}$$

where $u_j^{(n)} = u_j(x^{(n)})$, $x^{(n)}$ being the location of the external boundary nodal point n, (n=1, ... M_b), and $\pi_i^{(n)} = \pi_i(x^{(n)})$, $x^{(n)}$ being the location of the crack element mid-point n, (n= M_b+1, ... M_b+M_c).

Eqs.(4.9) can be written in the following matrix form:

$$[UC]\left\{u\right\} - [Q]\left\{\Delta u\right\} - [UR]\left\{t\right\} = [UC_{13}]\left\{T\right\} - [Q_{13}]\left\{\Delta T\right\} - [UR_{13}]\left\{q_n\right\}$$

$$[PC]\left\{u\right\} - [X]\left\{\Delta u\right\} - [PR]\left\{t\right\} + \left\{\pi\right\} = [PC_{13}]\left\{T\right\} - [X_{13}]\left\{\Delta T\right\} - [PR_{13}]\left\{q_n\right\} \tag{4.10}$$

where [UC] is $2M_b$ x $2M_b$, [Q] is $2M_b$ x $2(M_c-1)$, [UR] is $2M_b$ x $4M_b$, [PC] is $2M_c$ x $2M_b$, [X] is $2M_c$ x $2(M_c-1)$, [PR] is $2M_c$ x $4M_b$, $[UC_{13}]$ is $2M_b$ x M_b , $[Q_{13}]$ is $2M_b$ x (M_c-1) , $[UR_{13}]$ is $2M_b$ x $2M_b$, $[PC_{13}]$ is $2M_c$ x M_b , $[X_{13}]$ is $2M_c$ x (M_c-1) and $[PR_{13}]$ is $2M_c$ x $2M_b$.

Thus

$$\begin{bmatrix} [UC] & -[Q] \\ [\Gamma_2][PC] & -[\Gamma_2][X] \end{bmatrix} \begin{Bmatrix} u \\ \Delta u \end{Bmatrix} - \begin{bmatrix} [UR] & [0] \\ [\Gamma_2][PR] & [I] \end{bmatrix} \begin{Bmatrix} t \\ F \end{Bmatrix}$$

$$= \begin{bmatrix} [UC_{13}] & -[Q_{13}] \\ [\Gamma_2][PC_{13}] & -[\Gamma_2][X_{13}] \end{bmatrix} \begin{Bmatrix} T \\ \Delta T \end{Bmatrix} - \begin{bmatrix} [UR_{13}] \\ [\Gamma_2][PR_{13}] \end{bmatrix} \left\{ q_n \right\} \tag{4.11}$$

where, as in [76], we have defined a nodal force matrix on the crack by

$$\left\{ F \right\} = [\Gamma_2]\left\{ \pi \right\} \tag{4.12}$$

where

$$[\Gamma_2] = \begin{bmatrix} -I & I & 0 & 0 & 0 & 0 & 0 \\ 0 & -I & I & 0 & 0 & 0 & 0 \\ 0 & 0 & -I & I & 0 & 0 & 0 \\ \cdot & \cdot & \cdot & \cdot & \cdot & \cdot & \cdot \\ \cdot & \cdot & \cdot & \cdot & \cdot & \cdot & \cdot \\ 0 & 0 & 0 & 0 & 0 & -I & I \end{bmatrix} \tag{4.13}$$

I represents a 2x2 identity matrix, and $[\Gamma_2]$ is $2(M_c-1) \times 2M_c$.

It is well-known that one can obtain the diagonal 2x2 blocks of [UC] in eqs.(4.11) from rigid-body considerations. If we apply a rigid-body displacement, i.e.

$$u_j^{(1)} = u_j^{(2)} = u_j^{(3)} = \ldots\ldots\ldots = u_j^{(M_b)} = u_j \tag{4.14}$$

then the body is stress-free. Thus

$$\left\{ t \right\} = \left\{ 0 \right\} \qquad \left\{ \Delta u \right\} = \left\{ 0 \right\}$$

and eqs.(4.11) reduce to

$$[UC]\begin{Bmatrix} u_1 \\ u_2 \\ u_1 \\ u_2 \\ \cdot \\ \cdot \\ \\ u_1 \\ u_2 \end{Bmatrix} = \begin{Bmatrix} 0 \end{Bmatrix} \tag{4.15}$$

so that

$$UC^{(2i-1)(2i-1)} = -\sum_{\substack{j=0 \\ j\neq i}}^{M_b} UC^{(2i-1)(2j-1)}$$

$$UC^{(2i-1)(2i)} = -\sum_{\substack{j=0 \\ j\neq i}}^{M_b} UC^{(2i-1)(2j)}$$

(4.16)

$$UC^{(2i)(2i-1)} = -\sum_{\substack{j=0 \\ j\neq i}}^{M_b} UC^{(2i)(2j-1)}$$

$$UC^{(2i)(2i)} = -\sum_{\substack{j=0 \\ j\neq i}}^{M_b} UC^{(2i)(2j)} \quad .$$

Once eqs.(4.11) have been constructed, we must impose four conditions at each nodal point m on Γ_b involving the boundary values

$$u_1^{(m)}, \qquad t_1^{(2m)}, \qquad t_1^{(2m+1)},$$

$$u_2^{(m)}, \qquad t_2^{(2m)}, \qquad t_2^{(2m+1)},$$

and rearrange eqs.(4.11) accordingly to obtain

$$[A]\left\{ Z \right\} = \left\{ B \right\} \tag{4.17}$$

where $\{Z\}$ contains the unknown boundary thermal displacements and tractions on Γ_b and the unknown matrix $\{\Delta u\}$.

Once we have obtained Δu_i at each crack nodal point, the thermal displacement discontinuities normal and tangential to the crack surfaces at that point are

$$\Delta u_n = \Delta u_1 n_1 + \Delta u_2 n_2$$

$$\tag{4.18}$$

$$\Delta u_t = \Delta u_2 n_1 - \Delta u_1 n_2$$

and the thermal stress intensity factors can be determined from

$$K_I|_{s=0} = \sqrt{\frac{\pi}{8\varepsilon}} G(1+\nu)\Delta u_n(\varepsilon)$$

$$K_{II}|_{s=0} = \sqrt{\frac{\pi}{8\varepsilon}} G(1+\nu)\Delta u_t(\varepsilon)$$

(4.19)

$$K_I|_{s=l} = \sqrt{\frac{\pi}{8\varepsilon}}G(1+\nu)\Delta u_n(l-\varepsilon)$$

$$K_{II}|_{s=l} = \sqrt{\frac{\pi}{8\varepsilon}}G(1+\nu)\Delta u_t(l-\varepsilon)$$

where $\varepsilon \to 0$, G, ν are the shear modulus and Possion's ratio, respectively, and l is the length of the crack.

It should be noted that, for a problem involving a traction free crack, {F}={0} and eqs.(4.11) reduce to

$$\begin{bmatrix} [UC] & -[Q] \\ [\Gamma_2][PC] & -[\Gamma_2][X] \end{bmatrix} \begin{Bmatrix} u \\ \Delta u \end{Bmatrix} - \begin{bmatrix} [UR] \\ [\Gamma_2][PR] \end{bmatrix} \begin{Bmatrix} t \end{Bmatrix}$$

$$= \begin{bmatrix} [UC_{13}] & -[Q_{13}] \\ [\Gamma_2][PC_{13}] & -[\Gamma_2][X_{13}] \end{bmatrix} \begin{Bmatrix} T \\ \Delta T \end{Bmatrix} - \begin{bmatrix} [UR_{13}] \\ [\Gamma_2][PR_{13}] \end{bmatrix} \begin{Bmatrix} q_n \end{Bmatrix} \qquad (4.20)$$

4.3 Results

Here we employ the coupled model to find the numerical solution for a finite domain problem.

A rectangular plate of height 2h and width 2w contains a straight central crack of length 2a. The surface of the crack are assumed to be free of tractions and thermally insulated. Mechanical and thermal boundary conditions are shown in Figure 4.3. The crack is modeled by 20 equal elements and the external boundary is modeled by 40 elements. In Table 4.1, the thermal stress intensity factors are given for various ratios a/w and compared to those obtained in [57] and [61]. The relative crack surface thermal displacements are plotted in Figures 4.4 through 4.9 for $G = 8.4 \times 10^4$, $\nu = 0.3$ and $\alpha_t = 1.67 \times 10^{-5}$.

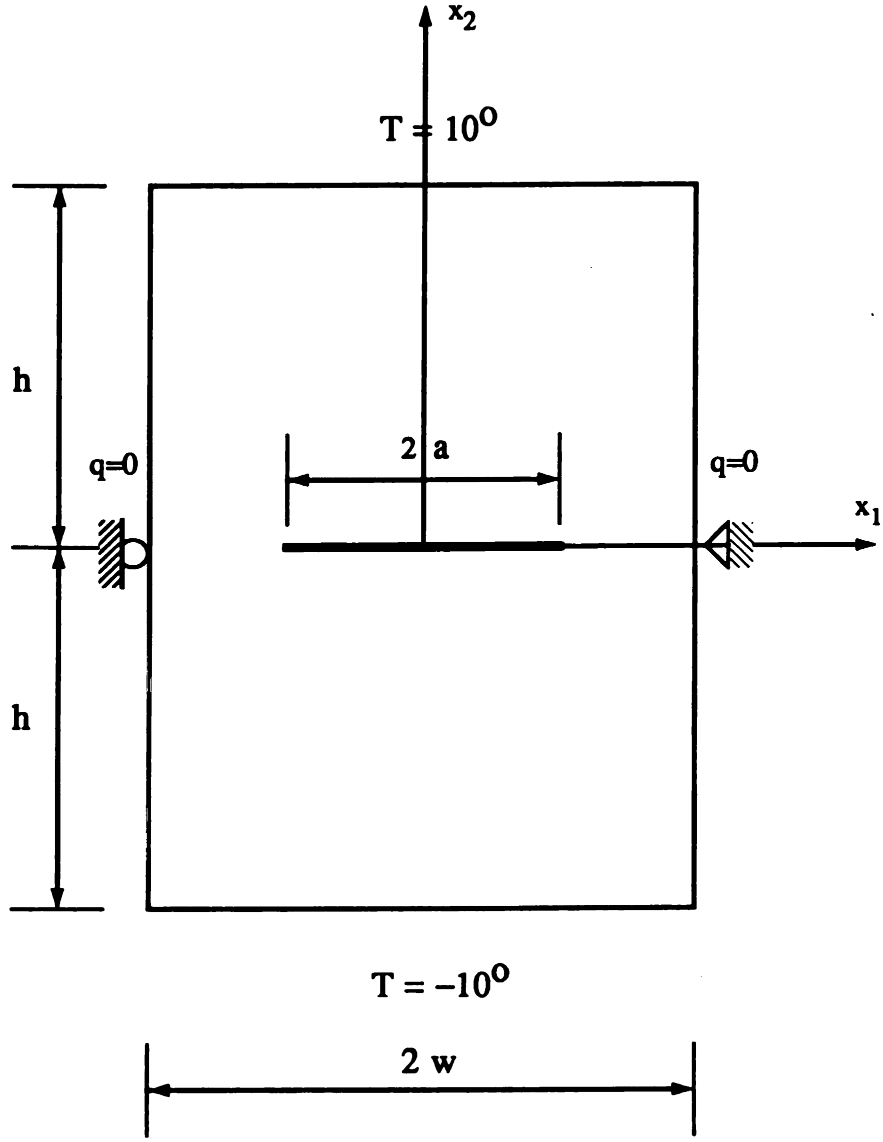

Figure 4.3 Geometry and thermal loading for an insulated straight central crack in a finite plate.

Table 4.1 Thermal stress intensity factors $K_{II}/\alpha_t\ ET\ (w)^{1/2}$ for an insulated straight central crack.

a/w	0.1	0.2	0.3	0.4	0.5	0.6
Present	0.6779	2.1587	3.8875	5.7308	7.6109	9.6078
[57]	0.6810	2.1643	3.8900	5.7314	7.6152	9.6190
[61]	0.6790	2.1500	3.8970	5.7600	7.7200	9.6800

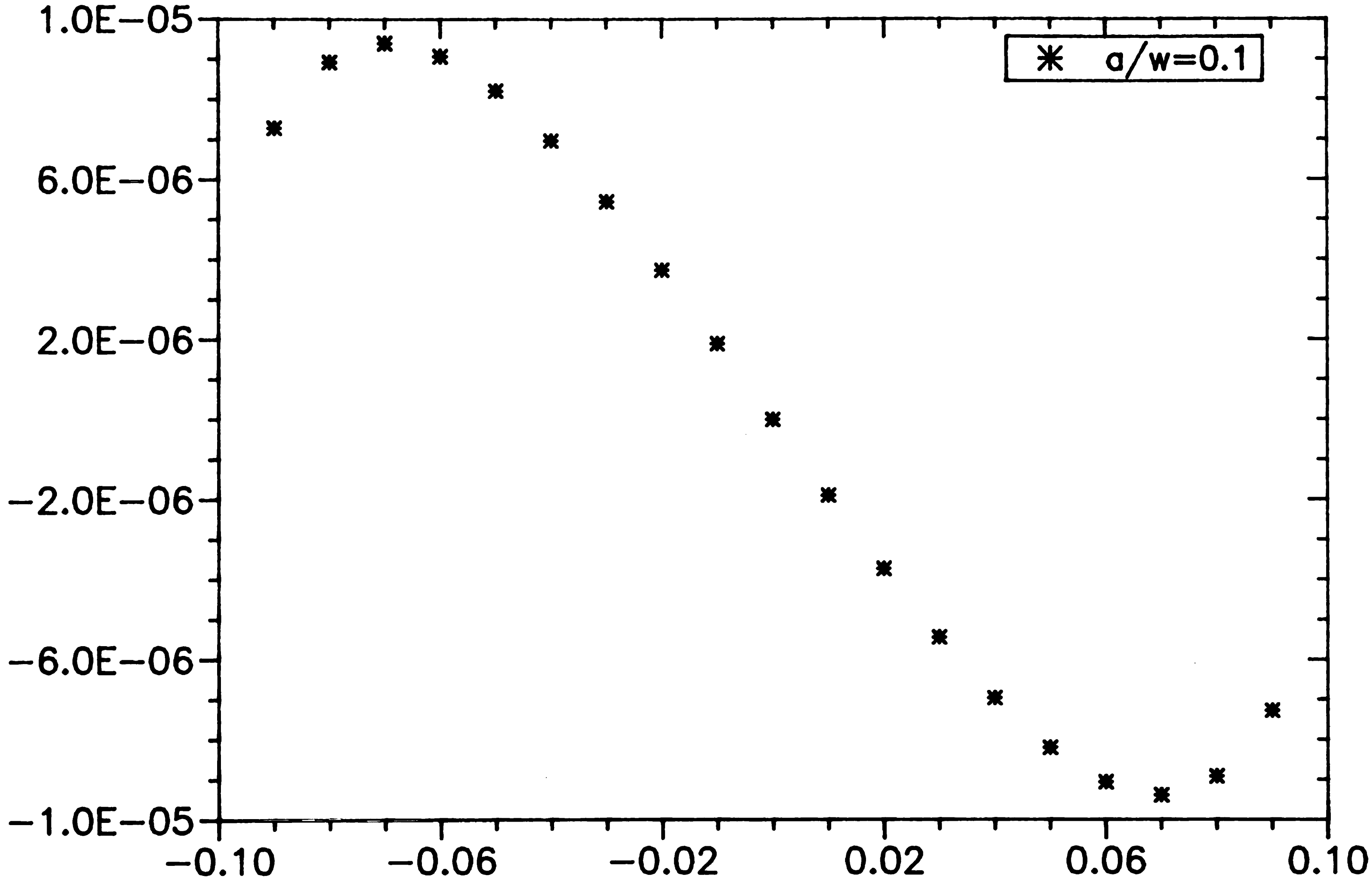

Figure 4.4 Relative crack surface thermal displacement Δu_t for a body containing an insulated straight central crack, a/w=0.1.

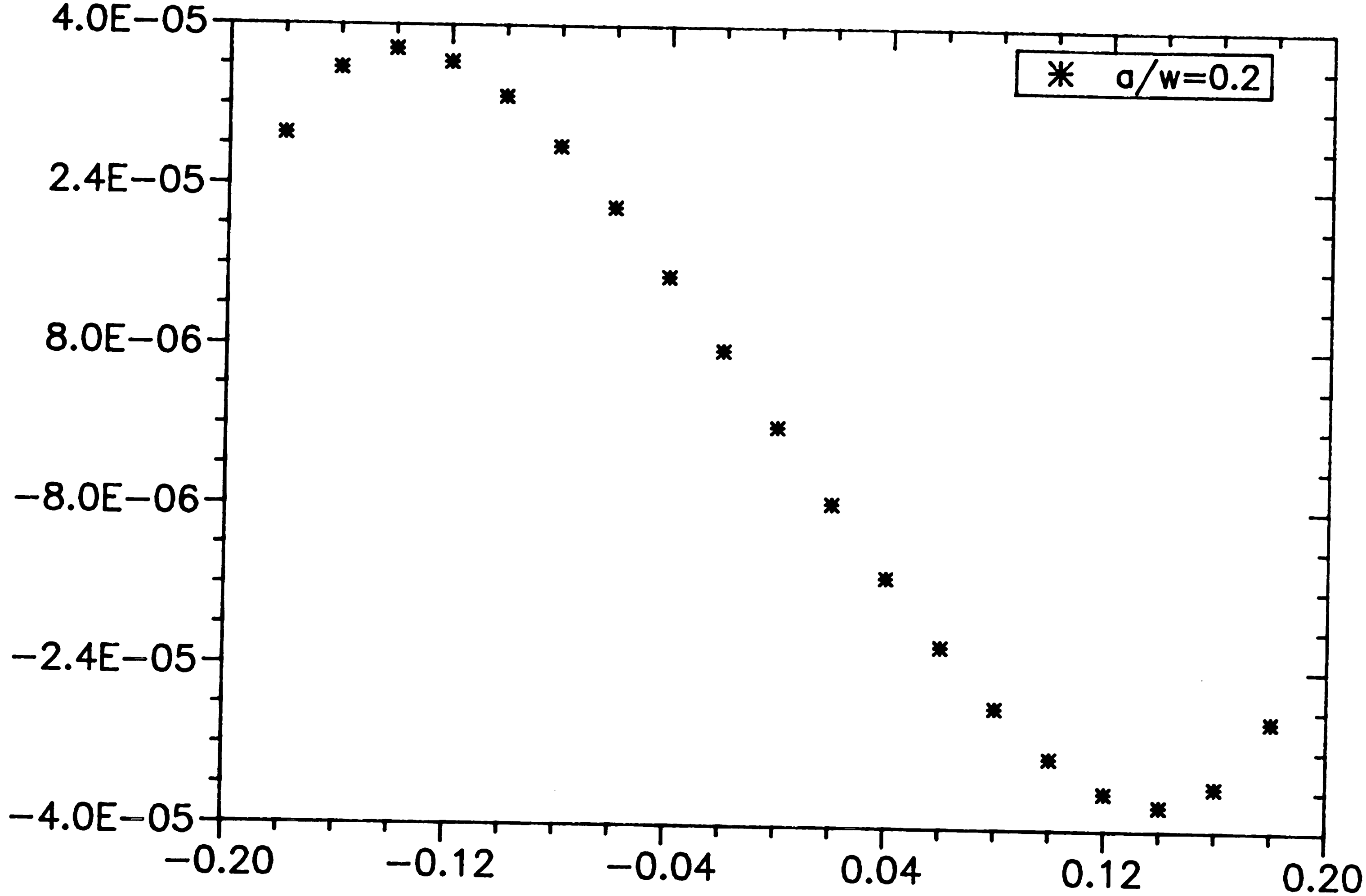

Figure 4.5 Relative crack surface thermal displacement Δu_t for a body containing an insulated straight central crack, a/w=0.2.

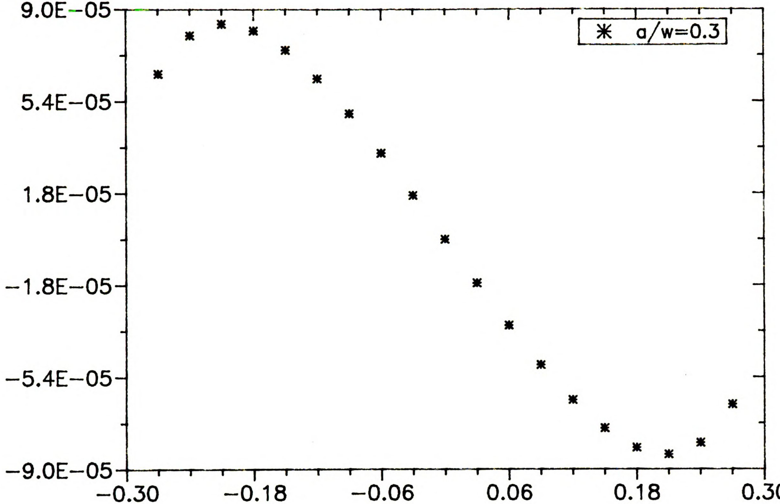

Figure 4.6 Relative crack surface thermal displacement Δu_t for a body containing an insulated straight central crack, a/w=0.3.

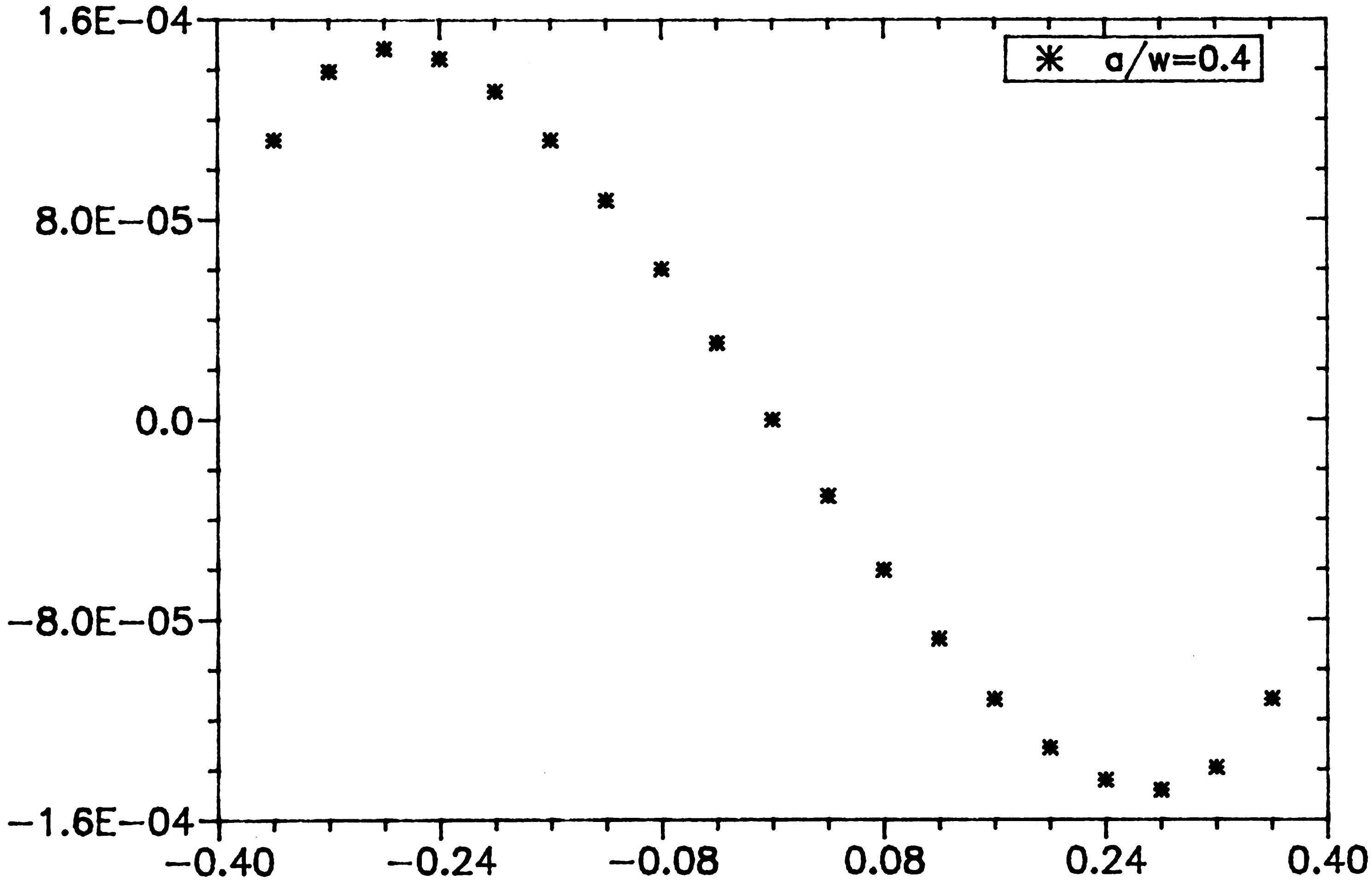

Figure 4.7 Relative crack surface thermal displacement Δu_t for a body containing an insulated straight central crack, a/w=0.4.

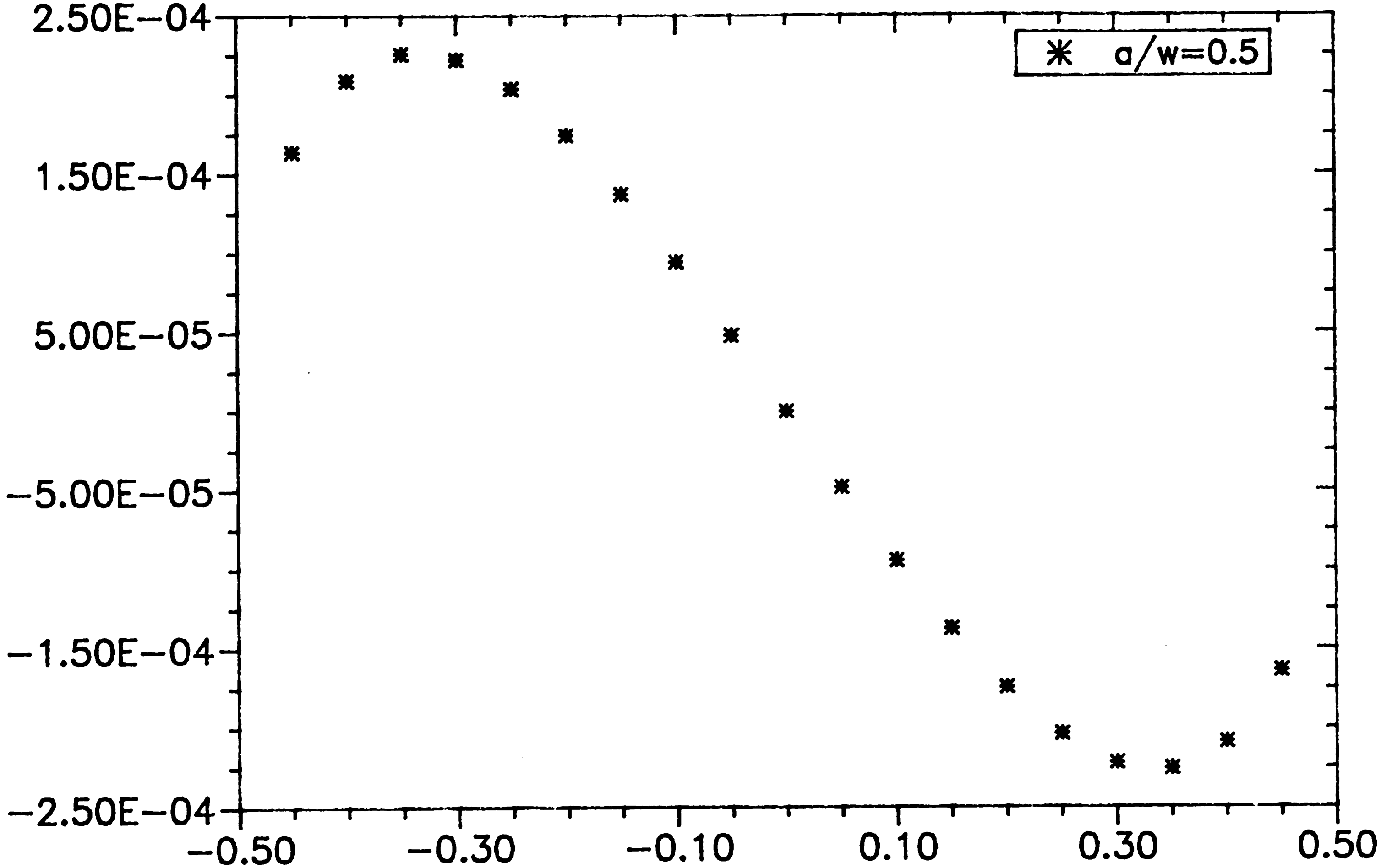

Figure 4.8 Relative crack surface thermal displacement Δu_t for a body containing an insulated straight central crack, a/w=0.5.

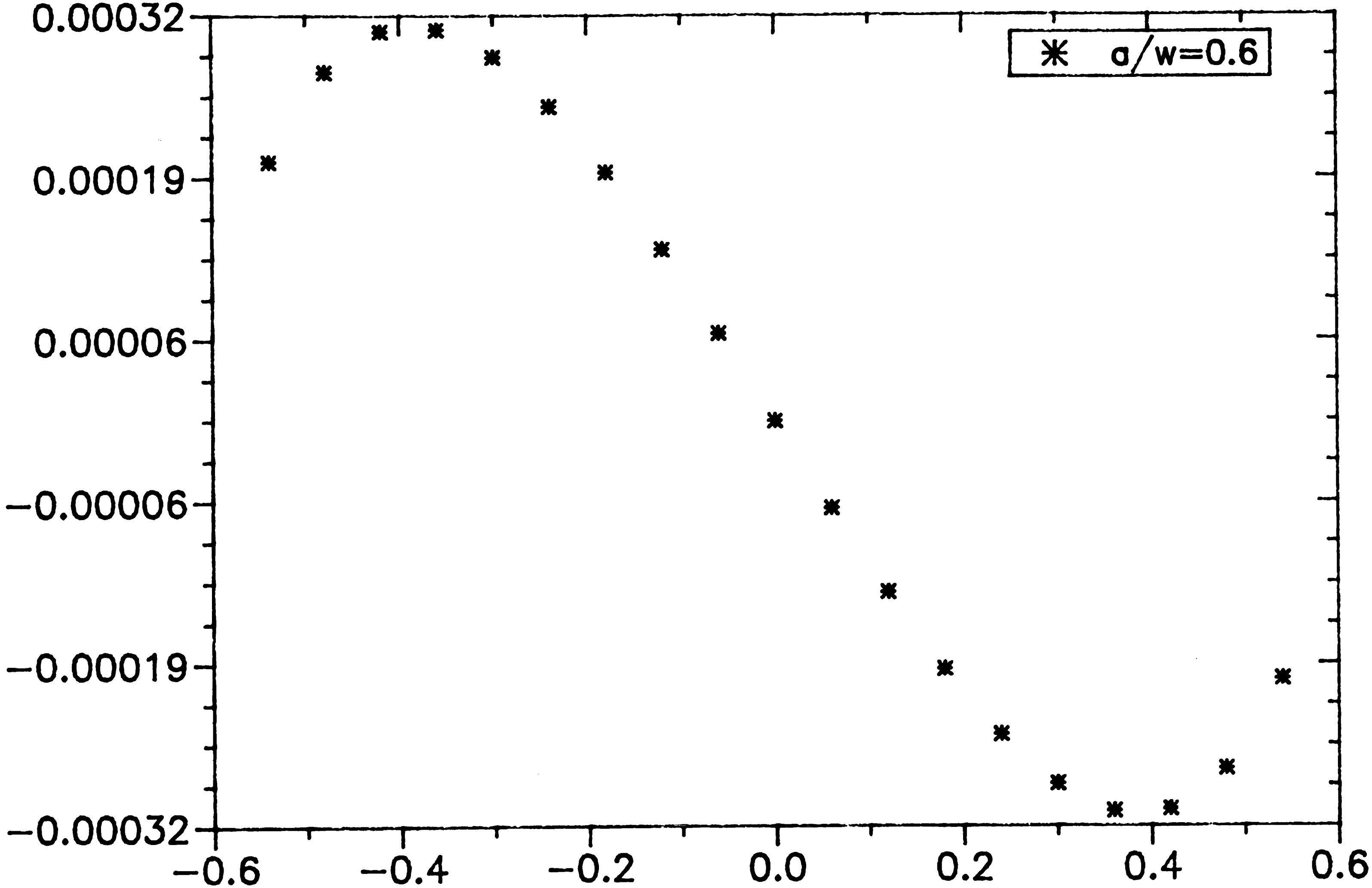

Figure 4.9 Relative crack surface thermal displacement Δu_t for a body containing an insulated straight central crack, a/w=0.6.

Chapter 5

Conclusions

An integral-equation representation for cracks in two-dimensional infinite regions [76] has been coupled to the well-known direct boundary element method so that cracks in finite plane bodies can be solved. The method has been further extended to include multiple cracks, branch cracks, edge cracks, mode III loading conditions and thermal conditions loading. In all cases, accurate results are obtained with small computational effort relative to other known methods.

In principle, this method is not confined to the classes of problems discussed in this dissertation. It is anticipated that this new method can be extended for use in the solution of thermoelasticity involving different thermal boundary conditions on the crack, electromagnetic problems, fiber reinforced composites, crack propagation studies and three-dimensional problems.

REFERENCES

[1] G. C. Sih, On the singular character of thermal stresses near a crack tip, *Journal of Applied Mechanics* **29**, 587-589 (1962).

[2] T. Koizumi, K. Takakuda, T. Shibuya and T. Nishizawa, An infinite plate with a flaw and subjected to uniform heat flow, *Journal of Thermal Stresses* **2**, 341-351 (1979).

[3] H. Sekine, Thermal stress problem for a ribbonlike inclusion, *Letters in Applied Engineering Sciences* **5**, 51-61 (1977).

[4] A. L. Florence and J. N. Goodier, The linear thermoelastic problem of uniform heat flow disturbed by a penny-shaped insulated crack, *International Journal of Engineering Sciences* **1**, 533-540 (1963).

[5] Z. Olesiak and I. N. Sneddon, The distribution of thermal stress in an infinite elastic solid containing a penny-shaped crack, *Archives for Rational Mechanics Analysis* **4**, 238-254 (1960).

[6] R. Shail, Some steady-state thermoelastic stress distributions in the vicinity of an external crack in an infinite solid, *International Journal of Engineering Sciences* **6**, 685-694 (1968).

[7] L. Rubenfeld, Non-axisymmetric thermoelastic stress distribution in a solid containing an external crack, *International Journal of Engineering Sciences* **8**, 499-509 (1970).

[8] J. R. Barber, Steady-state thermal stresses in an elastic solid containing an insulated penny-shaped crack, *Journal of Strain Analysis* **10**, 19-24 (1975).

[9] W. F. Williams, A solution of the steady-state thermoelastic equations, *Zeitschroft fuer Angewandte Mathematik and Physik* **12**, 452-255 (1961).

[10] J. R. Barber, The disturbance of a uniform steady-state heat flux by a partially conducting plane crack, *International Journal of Heat and Mass Transfer* **19**, 956-958 (1976).

[11] J. R. Barber, Steady-state thermal stress caused by an imperfectly conducting penny-shaped crack in an elastic solid, *Journal of Thermal Stresses* **3**, 77-83 (1980).

[12] A. Atsumi, Y. Mori and Y. Shindo, Thermal stresses in a circular cylinder with a circumferential edge crack under uniform heat flow, *Journal of Thermal Stresses* **2**, 425-436 (1979).

[13] K. Anzai, Y. Shindo and A. Atsumi, Linear thermoelastic problem of a uniform heat flow disturbed by an infinite row of parallel circumferential edge cracks along a cylindrical cavity, *Engineering Fracture Mechanics* **15**, 275-282 (1981).

[14] A. Atsumi and Y. Shindo, Peripheral edge crack around a spherical cavity under uniaxial tension field, *International Journal of Engineering Sciences* **21**, 269-278 (1981).

[15] A. L. Florence and J. N. Goodier, Thermal stress at spherical cavities and circular holes in uniform heat flow, *ASME Journal of Applied Mechanics* **26**, 293-294 (1959).

[16] K. Nakazono, Y. Shindo and A. Atsumi, Thermal singular stresses near a circumferential edge crack in a spherical cavity under uniform axial heat flow, *Journal of Thermal Stresses* **7**, 163-174 (1984).

[17] T. Koizumi and H. Niwa, Transient thermal stress problem in a semi-infinite plate with an edge crack perpendicular to the edge surface, *Transcations. Japan Society of Mechanical Engineers* **43**, 442-447 (1977).

[18] H. Abe, H. Sekine and Y. Shibuya, *Transcations. Japan Society of Mechanical Engineers* **48**, 899-903 (1982).

[19] H. Abe, H. Sekine and Y. Shibuya, *Transcations. Japan Society of Mechanical*

Engineers **49**, 1300-1305 (1983).

[20] V. C. Ting and H. R. Jacobs, Stress intensity factors for transient stress loadings of a semi-infinite medium, *Journal of Thermal Stresses* **2**, 1-13 (1979).

[21] H. F. Nied and F. Erdogan, Transient thermal stress problem for a circumferentially cracked hollow cylinder, *Journal of Thermal Stresses* **6**, 1-14 (1983).

[22] H. F. Nied, Thermal shock fracture in an edge-cracked plate, *Journal of Thermal Stresses* **6**, 217-229 (1983).

[23] N. Noda and N. Sumi, Stress intensity factor for transient thermal stress of a thin plate with a Griffith crack, *Journal of Thermal Stresses* **8**, 173-182 (1985).

[24] N. Noda, Y. Matsunaga and H. Nyuko, Stress intensity factor for transient thermal stresses in an infinite elastic body with external crack, *Journal of Thermal Stresses* **9**, 119-131 (1986).

[25] S. N. Maiti and J. C. Misra, Thermal stresses in a finite aeolotropic cylinder due to thermal crack, *Revue Roumaine des Sciences Techniques* **21**, 339-351 (1976).

[26] K. Murata and A. Atsumi, Thermal stresses in a transversely isotropic cylinder containing a penny-shaped crack, *Letters in Applied and Engineering Sciences* **5**, 173-185 (1977).

[27] Y. M. Tsai, Thermal stresses in a transversely isotropic medium containing a penny-shaped crack, *Journal of Applied Mechanics* **50**, 24-28 (1983).

[28] Y. M. Tsai, Transversely isotropic thermoelastic problem of uniform heat flow disturbed by a penny-shaped crack, *Journal of Thermal Stresses* **6**, 379-389 (1980).

[29] D. K. Ram, H. K. Parhi and A. K. Paul, Thermal stresses in a transversely isotropic solid containing an annular crack, *Indian Journal of Technology* **18**, 437-443 (1980).

[30] N. Noda and F. Ashida, Stress intensity factors for a transversely isotropic infinite solid containing an annular crack, *Journal of Thermal Stresses* **11**, 39-55

(1988).

[31] Y. M. Tsai, Orthotropic thermoelastic stress intensity factor for a pair of central cracks, Iowa State University, Engineering Research Institute preprint ERI-86179, (1985).

[32] Y. M. Tsai, Orthotropic thermoelastic problem of uniform heat flow disturbed by a central crack, *Journal of Composite Materials* **18**, 122-131 (1984).

[33] Y. M. Tsai, Thermal stress in an Orthotropic plate containing a pair of coplanar central cracks, *Journal of Thermal Stresses* **9**, 225-235 (1986).

[34] J. L. Nowinski, *Theory of Thermoelasticity with Applications*, p. 118, Sijthoff & Noordhoff, The Netherlands, (1978).

[35] R. M. Christensen, *Mechanics of Composite Materials*, p. 311, Wiley, New York, (1979).

[36] F. J. Rizzo and D. J. Shippy, An advanced boundary integral equation method for three-dimensional thermoelasticity, *International Journal for Numerical Methods in Engineering* **11**, 1753-1768 (1977).

[37] T. A. Cruse, D. W. Snow and R. B. Wilson, Numerical solutions in axisymmetric elasticity, *Computers and Structures* **7**, 445-451 (1977).

[38] V. Sladek and J. Sladek, Boundary integral equation method in thermoelasticity Part I: General analysis, *Applied Mathematical Modeling* **7**, 241-253 (1983).

[39] V. Sladek and J. Sladek, Boundary integral equation method in thermoelasticity Part II: Crack Analysis, *Applied Mathematical Modeling* **8**, 27-36 (1984).

[40] V. Sladek and J. Sladek, Boundary integral equation method in thermoelasticity Part III: Uncoupled thermoelasticity, *Applied Mathematical Modeling* **8**, 413-418 (1984).

[41] V. Sladek and J. Sladek, Boundary integral equation method in two-dimensional thermoelasticity, *Engineering Analysis* **1**, 135-148 (1984).

[42]] V. Sladek and J. Sladek, Boundary element method in micropolar thermoelastici-

ty, *Engineering Analysis* **2**, 155-162 (1985).

[43] M. Tanaka and K. Tanaka, Boundary element approach to dynamic problems in coupled thermoelasticity-part I: Integral equation formulation, *Solid Mechanics Archives* **6**, 467-491 (1981).

[44] M. Tanaka, H. Togoh and M. Kikuta, An application of boundary element method to thermoelastic problems, *Proceedings of the fifth International Conference on Boundary Elements (C. A. Brebbia, T. Futagami and M. Tanaka, eds.)*, 417-426 (1983).

[45] M. Tanaka, H. Togoh and M. Kikuta, Boundary element method applied to 2-D thermoelastic problems in steady and non-steady states, *Engineering Analysis* **1**, 13-19 (1984).

[46] M. Tanaka, H. Togoh and M. Kikuta, A boundary element investigation of 3-D thermoelastic problems in transient heat conduction states, *Proceedings of the seventh International Conference on Boundary Elements (C. A. Brebbia and G. Maier, eds.)*, 3-16 (1985).

[47] A. Chaudouet, Three-dimensional transient thermoelastic analysis by the BIE method, *International Journal for Numerical Methods in Engineering* **24**, 24-45 (1987).

[48] J. Masinda, Application of the boundary elements method to 3D problems of non-stationary thermoelasticity, *Engineering Analysis* **1**, 66-69 (1984).

[49] S. Sharp and S. L. Crouch, Boundary integral methods for thermoelasticity problems, *Journal of Applied Mechanics* **53**, 298-302 (1986).

[50] P.K Banerjee, R. Butterfield and G. R. Tomlin, Boundary element methods for two-dimensional problems of transient ground water flow, *International Journal for Numerical and Analytical Methods in Geomechanics* **5**, 15-31 (1981).

[51] G. F. Dargush and P. K. Banerjee, Advanced development of the boundary element method for steady-state heat conduction, *International Journal for Numeri-*

cal Methods in Engineering **28**, 2123-2142 (1989).

[52] G. F. Dargush and P. K. Banerjee, Development of a boundary element method for time-dependent planar thermoelasticity, *International Journal of Solids and Structures* **25**, 999-1021 (1989).

[53] D. W. Smith and J. R. Booker, Boundary integral analysis of transient thermoelasticity, *International Journal for Numerical and Analytical Methods in Geomechanics* **13**, 283-302 (1989).

[54] V. Sladek and J. sladek, Computation of thermal stresses in quasistatic non-stationary thermoelasticity using boundary elements, *International Journal for Numerical Methods in Engineering* **28**, 1131-1144 (1989).

[55] H. Nakanishi, S. Tani, M. Suzuki and N. Sumi, Orthotropic rectangular plates with an eccentric crack and an inclined crack in steady-state temperature fields, *Transcations. Japan Society of Mechanical Engineers* **51**, 2094-2101 (1985).

[56] T. K. Hellen, F. Cesari and A. Maitan, The application of fracture mechanics in thermally stressed structures, *International Journal of Pressure Vessels and Piping* **10**, 181-204 (1982).

[57] N. Sumi, Thermal stress singularities at tips of a Griffith crack in finite rectangular plate, *Nuclear Engineering and Design* **60**, 389-394 (1980).

[58] E. Emmel and H. Stamm, Calculation of stress intensity factors of thermally loaded cracks using the finite element method, *International Journal of Pressure and Vessels and Piping* **19**, 1-17 (1985).

[59] V. Sladek and J. Sladek, Computation of the stress intensity factor in 2-D stationary thermoelasticity using the BEM, *Acta Technica CSAV* **2**, 217-229 (1987).

[60] K. Y. Lee and H. S. Choi, Determination of thermal stress intensity factors for traction free cusp cracks under uniform heat flow, *Engineering Fracture Mechanics* **32**, 183-193 (1989).

[61] K. Y. Lee and Y. H. Cho, Boundary element analysis of thermal stress intensity

factors for cusp cracks, *Engineering Fracture Mechanics* **37** , 787-798 (1990).

[62] C. A. Brebbia, J. Telles and L. Wrobel, *Boundary Element Techniques - Theory and Applications in Engineering*, Springer-Verlag, (1984).

[63] D. Nardini and C. A. Brebbia, A new approach to free vibration analysis using boundary elements, *Boundary Element Methods in Engineering* (C. A. Brebbia, ed.), Springer-Verlag, (1982).

[64] D. Nardini and C. A. Brebbia, Boundary integral formulation of mass matrices for dynamics analysis, *Topics in Boundary Element Research*, Vol. **2**, Springer-Verlag, (1985).

[65] C. A. Brebbia and L. C. Wrobel, The solution of parabolic problems using the dual reciprocity boundary element, *Proceedings of the IUPAM Symp.* (T. A. Cruse, ed.), Springer-Verlag, Heidelberg, 55-73, (1987).

[66] C. A. Loeffler and W. L. Mansur, Analysis of time integration schemes for boundary element applications to transient wave propagation problems, *Boundary Element Techniques: Applications in Stress Analysis and Heat Transfer* (C. A. Brebbia and W. S. Venturini, eds.), Computational Mechanics Publications, Southampton, 105-122, (1987).

[67] S. M. Niku and C. A. Brebbia, Dual reciprocity boundary element formulation for potential problems with arbitrarily distributed sources, *Engineering Analysis* **5**, 46-48 (1987).

[68] L. C. Wrobel and C. A. Brebbia, Boundary elements for non-linear heat conduction problems, *Communications in Applied Numerical Methods* **4**, 617-622 (1988).

[69] M. M. Aral and Y. Tang, A boundary only procedure for time dependent diffusion equations, *Applied Mathematical Modeling* **4**, 617-622 (1988).

[70] W. Tang, Transforming domain integrals into boundary integrals in **BEM** - A generalized approach, *Lecture Notes in Engineering* (C. A. Brebbia and S. A.

Orszag, eds.), Springer-Verlag, (1988).

[71] M. Itagaki and C. A. Brebbia, Boundary element method applied to neutron diffusion problems, *Proceedings of the tenth BEM Conference*, Southampton, (C. A. Brebbia, ed.), Springer-Verlag, **2**, 45-53 (1988).

[72] J. P. S. Azevedo and C. A. Brebbia, An efficient technique for reducing domain integrals to the boundary, *Proceedings of the tenth BEM Conference*, Southampton, (C. A. Brebbia, ed.), Springer-Verlag, **1**, 347-363 (1988).

[73] A. J. Nowak and C. A. Brebbia, The multiple-reciprocity method. A new approach for transforming **BEM** domain integrals to the boundary, *Engineering Analysis with Boundary Elements*, 6, 164-167, (1989).

[74] A. J. Nowak, Temperature fields in domains with heat sources using boundary-only formulation, *Proceedings of the tenth BEM Conference*, Southampton, (C. A. Brebbia, ed.), Springer-Verlag, **2**, 233-247 (1988).

[75] D. A. Pape and P. K. Banerjee, Treatment of body forces in 2D elastostatic **BEM** using particular integrals, *Journal of Applied Mechanics* **54**, 866-871 (1987).

[76] U. Sur and N. J. Altiero, An alternative integral equation approach for curved and kinked cracks, *International Journal of Fracture* **38**, 25-41 (1988).

[77] N. Liu, N. J. Altiero and U. Sur, An alternative integral equation approach applied to kinked cracks in finite plane bodies, *Computer Methods in Applied Mechanics and Engineering* **84**, 211-226 (1990).

[78] N. Liu and N. J. Altiero, Multiple cracks and branch cracks in finite plane bodies, *Mechanics Research Communications*, **18**, 233-244 (1991).

[79] N. Liu and N. J. Altiero, An integral equation method applied to mode III crack problems, *Engineering Fracture Mechanics*, to appear (1991)

[80] C. F. Sheng, Boundary element methods by dislocation distribution, *Journal of Applied Mechanics* **54**, 105-109 (1987).

[81] W. L. Zang and P. Gudmundson, A boundary integral method for internal piece-wise smooth crack problems, *International Journal of Fracture* **38**, 275-294 (1988).

[82] Y. K. Chueng and Y. Z. Chen, Solutions of branch crack problems in plane elsticity by using a new integral equation approach, *Engineering Fracture Mechanics* **28**, 31-41 (1987).

[82] Y. K. Chueng and Y. Z. Chen, New integral equation for plane elasticity crack problems, *Theoretical and Applied Fracture Mechanics* **7**, 177-185 (1987).

[83] W. L. Zang and P. Gudmundson, An integral equation method based on resultant forces on a piece-wise smooth crack in a finite plate, *Advances in Fracture Research* (K. Salama *et al.*, eds.), Pergamon, Oxford, **3**, 2127-2134 (1989).

[84] D. P. Rooke and D. J. Cartwright, *Compendium of Stress Intensity Factors*, Her Majesty's Stationery Office, London, (1975).

[85] K. Y. Lee, D. S. Won and H. J. Choi, Boundary element analysis of stress intensity factors for Z-shaped cracks, *Engineering Fracture Mechanics* **27**, 75-82 (1987).

[86] Y. Z. Chen, Multiple crack problems for finite plate with arbitrary contour configuration, *Engineering Fracture Mechanics* **31**, 289 (1988).

[87] W. A. Xie, *Shanghai Mechanics* **5**, 48 (1984).

[88] H. Terata and T. Yixita, *Report of Aviation Institute* TR-436 (1975).

[89] A. Mehdi-soozan, I. Miskioglu, C. P. Burger and T. J. Rudolphi, Stress intensity factors for interacting cracks, *Engineering Fracture Mechanics* **27**, 345 (1987).

[90] P. S. Theocaris, G. Tsamasphyros and E. E. Throtokoglou, An alternating coupling of finite elements and singular integral equations for the solution of branched cracks in finite sheets, *Engineering Fracture Mechanics* **20**, 583-589 (1984).

[91] G. W. Ye and T. Sawada, Some numerical properties of boundary element analy-

sis using half-plane fundamental solutions in 2-d elastostatics, *Computational Mechanics* **4**, 161-164 (1989).

[92] J. C. F. Telles and C. A. Brebbia, Boundary element solution for half-plane problems, *International Journal of Solid Structure* **17**, 1149-1158 (1981).

[93] O. L. Bowie, Solutions of plane crack problems by mapping techniques, *Methods of Analysis and Solutions of Crack Problems* (George C. Sih ed.), Noordhoff, 1-55 (1973).

[94] B. S. Annigeri and M. P. Cleary, Quasi-static fracture propagation using the surface integral finite element hybird method, *Computational Fracture Mechanics - Nonliear and 3-D problems* (P. B. Hiltio and L. N. Gifford, eds.), PVP -Vol. **85**, AMD - Vol. **81**, ASME (1984).

[95] T. A. Cruse and R. B. Wilsion, Advanced applications of boundary-integral equation methods, *Nuclear Engineering and Design* **46**, 223-234 (1987).

[96] N. Fares and V. C. Li, An indirect boundary element method for 2-D finite/infinite regions with multiple displacement discontinuities, *Engineering Fracture Mechanics* **26**, 127-141 (1987).

[97] W. K. Wilson, *Combined mode fracture mechanics*, Ph.D dissertation, University of Pittsburgh (1969).

[98] M. Stern, E. B. Becker and R. S. Dunham, A contour integral computation of mixed-mode stress intensity factors, *International Journal of Fracture* **12**, 359-368 (1976).

[99] G. Ogen and B. Schiff, Stress intensity factors for two-dimensional crack problems using constrained finite elements, *International Journal of Fracture* **28**, 55-68 (1985).

[100] S. W. Ma, A central crack in a rectangular sheet where its boundary is subjected to an arbitrary anti-plane load, *Engineering Fracture Mechanics* **30**, 435-443 (1988).

[101] S. W. Ma, A central crack of mode III in a rectangular sheet with fixed edges, *International Journal of Fracture* **39**, 323-329 (1989).

[102] W. Zang, *Crack kinks and crack closure modeled by integral equation methods*, Ph.D Dissertation, Royal Institute of Technology, Sweden, (1990).

Appendix A In-plane Elasticity Influence Functions

The Kelvin influence functions for plane stress can be written as in [77]

$$(uR)_{ij} = [-(3-\nu)\,\delta_{ij}\log\rho + (1+\nu)\,q_i\,q_j\,]/8\pi G \tag{a.1}$$

$$(uc)_{11} = [2(1+\nu)(\bar{n}_1 q_1^3-\bar{n}_2 q_2^3)+(1-\nu)\bar{n}_1 q_1+(3+\nu)\bar{n}_2 q_2\,]/4\pi\rho$$

$$(uc)_{12} = [2(1+\nu)(-\bar{n}_2 q_1^3-\bar{n}_1 q_2^3)+(1+3\nu)\bar{n}_2 q_1+(3+\nu)\,\bar{n}_1 q_2\,]/4\pi\rho$$

$$\tag{a.2}$$

$$(uc)_{21} = [2(1+\nu)(-\bar{n}_2 q_1^3-\bar{n}_1 q_2^3)+(3+\nu)\bar{n}_2 q_1+(1+3\nu)\,\bar{n}_1 q_2\,]/4\pi\rho$$

$$(uc)_{22} = [-2(1+\nu)(\bar{n}_1 q_1^3-\bar{n}_2 q_2^3)+(1-\nu)\bar{n}_2 q_2+(3+\nu)\bar{n}_1 q_1\,]/4\pi\rho$$

$$(\pi R)_{11} = [-2\hat{\theta} - (1+\nu)\,q_1 q_2\,]/4\pi$$

$$(\pi R)_{12} = [(1-\nu)\,\log\rho + (1+\nu)\,q_1^2\,]/4\pi$$

$$\tag{a.3}$$

$$(\pi R)_{21} = [-(1-\nu)\,\log\rho - (1+\nu)\,q_2^2\,]/4\pi$$

$$(\pi R)_{22} = [-2\hat{\theta} + (1+\nu)\,q_1 q_2\,]/4\pi$$

$$(\pi c)_{11} = \frac{G(1+\nu)}{2\pi\rho}\,[2\bar{n}_2 q_1^3 + 2\bar{n}_1 q_2^3 - \bar{n}_2 q_1 - 3\,\bar{n}_1 q_2\,]$$

$$(\pi c)_{12} = (\pi c)_{21} = \frac{G(1+\nu)}{2\pi\rho}\,[2\bar{n}_1 q_1^3 - 2\bar{n}_2 q_2^3 - \bar{n}_1 q_1 + \bar{n}_2 q_2\,] \tag{a.4}$$

$$(\pi c)_{22} = \frac{G(1+\nu)}{2\pi\rho}\,[-2\bar{n}_2 q_1^3 - 2\bar{n}_1 q_2^3 + 3\bar{n}_2 q_1 + \bar{n}_1 q_2\,]$$

where

$$\rho_1 = x_1 - \bar{x}_1 \qquad \rho_2 = x_2 - \bar{x}_2 \tag{a.5}$$

$$\rho = [(x_1 - \bar{x}_1)^2 + (x_2 - \bar{x}_2)^2]^{1/2} \tag{a.6}$$

$$q_1 = \frac{x_1 - \bar{x}_1}{\rho}, \qquad q_2 = \frac{x_2 - \bar{x}_2}{\rho} \tag{a.7}$$

$$\hat{\theta} = \arctan\left[\frac{q_2\bar{n}_1 - q_1\bar{n}_2}{q_1\bar{n}_1 + q_2\bar{n}_2}\right] \tag{a.8}$$

and G, ν are the shear modulus and Poisson's ratio, respectively. For plane strain, ν must be replaced by $\nu/(1-\nu)$.

Appendix B Complementary Elasticity Influence Functions

The complementary expressions for plane stress can be written as in [102]

$$(uR)^c_{11} = \frac{1}{8\pi G}[[(3-\nu)-\frac{8}{1+\nu}]\log\rho^*+[(3-\nu)-2(1+\nu)\frac{x_2\bar{x}_2}{\rho^{*2}}]q_1^{*2}+2(1+\nu)\frac{x_2\bar{x}_2}{\rho^{*2}}q_2^{*2}]$$

$$(uR)^c_{12} = \frac{1}{8\pi G}[-4\frac{1-\nu}{1+\nu}\theta-4(1+\nu)\frac{x_2\bar{x}_2}{\rho^{*2}}q_1^*q_2^*+(3-\nu)q_1^*q_2]$$

$$\tag{b.1}$$

$$(uR)^c_{21} = \frac{1}{8\pi G}[+4\frac{1-\nu}{1+\nu}\theta+4(1+\nu)\frac{x_2\bar{x}_2}{\rho^{*2}}q_1^*q_2^*+(3-\nu)q_1^*q_2]$$

$$(uR)^c_{22} = \frac{1}{8\pi G}[[(3-\nu)-\frac{8}{1+\nu}]\log\rho^*-2(1+\nu)\frac{x_2\bar{x}_2}{\rho^{*2}}q_1^{*2}+[(3-\nu)+2(1+\nu)\frac{x_2\bar{x}_2}{\rho^{*2}}]q_2^{*2}]$$

$$(uc)^c_{11} = \frac{1}{4\pi\rho^*}[3(1-\nu)+2(1+\nu)q_1^{*2}+4(1+\nu)\frac{x_2\bar{x}_2}{\rho^{*2}}(1-4q_1^{*2})+4(1-\nu)\frac{\bar{x}_2}{\rho^*}q_2^*]q_n^*$$

$$+\frac{1}{4\pi\rho^*}[-4(1+\nu)\frac{x_2\rho_2}{\rho^{*2}}q_1^*\bar{n}_1+2(1-\nu)\frac{x_2}{\rho^*}\bar{n}_2]$$

$$(uc)^c_{12} = \frac{1}{4\pi\rho^*}[[2(1+\nu)(1-8\frac{x_2\bar{x}_2}{\rho^{*2}})q_1^*q_2^*-4(1-\nu)\frac{\bar{x}_2}{\rho^*}q_1^*]q_n^*+[(1-\nu)-4(1+\nu)\frac{x_2^2}{\rho^{*2}}]\bar{n}_2q_1^*]$$

$$+\frac{1}{4\pi\rho^*}[[-(1-\nu)+4(1+\nu)\frac{x_2\bar{x}_2}{\rho^{*2}}]\bar{n}_1q_2^*-2(1-\nu)\frac{x_2}{\rho^*}\bar{n}_1]$$

$$\tag{b.2}$$

$$(uc)^c_{21} = \frac{1}{4\pi\rho^*}[[2(1+\nu)(1+8\frac{x_2\bar{x}_2}{\rho^{*2}})q_1^*q_2^*+4[(1+\nu)\frac{x_2}{\rho^*}-(1-\nu)\frac{\bar{x}_2}{\rho^*}]q_1^*]q_n^*-2(1-\nu)\frac{x_2}{\rho^*}\bar{n}_1]$$

$$+\frac{1}{4\pi\rho^*}[[(1-\nu)+4(1+\nu)\frac{x_2^2}{\rho^{*2}}]\bar{n}_1q_2^*-[(1-\nu)+4(1+\nu)\frac{x_2\bar{x}_2}{\rho^{*2}}]\bar{n}_2q_1^*]$$

$$(uc)^c_{22} = \frac{1}{4\pi\rho^*}[-(1-\nu)+2(1+\nu)q_2^{*2}+4(1+\nu)\frac{x_2\bar{x}_2}{\rho^{*2}}(1-4q_1^{*2})-4(1-\nu)\frac{\bar{x}_2}{\rho^*}q_2^*]q_n^*$$

$$+\frac{1}{4\pi\rho^*}[-4(1+\nu)\frac{x_2\rho_2}{\rho^{*2}}q_1^*\bar{n}_1-2(1-\nu)\frac{x_2}{\rho^*}\bar{n}_2]$$

$$(\pi R)^c_{11} = \frac{1}{4\pi}[2\theta+(1+\nu)(1-4\frac{x_2\bar{x}_2}{\rho^{*2}})q_1^*q_2^*-2(1-\nu)\frac{x_2}{\rho^*}q_1^*]$$

$$(\pi R)^c_{12} = \frac{1}{4\pi}[-(1-\nu)\log\rho^*+2(1+\nu)\frac{x_2\bar{x}_2}{\rho^{*2}}q_1^{*2}+2(1+\nu)(1-2\frac{x_2\bar{x}_2}{\rho^{*2}})q_2^{*2}+4\frac{x_2}{\rho^*}q_2^*]$$

(b.3)

$$(\pi R)^c_{21} = \frac{1}{4\pi}[+(1-\nu)\log\rho^*-(1+\nu)(1+2\frac{x_2\bar{x}_2}{\rho^{*2}})q_1^{*2}+2(1+\nu)\frac{x_2\bar{x}_2}{\rho^{*2}}q_2^{*2}+4\frac{x_2}{\rho^*}q_2^*]$$

$$(\pi R)^c_{22} = \frac{1}{4\pi}[2\theta-(1+\nu)(1+4\frac{x_2\bar{x}_2}{\rho^{*2}})q_1^*q_2^*+2(1-\nu)\frac{x_2}{\rho^*}q_1^*]$$

$$(\pi c)^c_{11} = \frac{G(1+\nu)}{2\pi\rho^*}[2(1-8\frac{x_2\bar{x}_2}{\rho^{*2}})q_1^*q_2^*q_n^*+(-1+4\frac{x_2\bar{x}_2}{\rho^{*2}})\bar{n}_2q_1^*]$$

$$+\frac{G(1+\nu)}{2\pi\rho^*}[(1+4\frac{x_2\bar{x}_2}{\rho^{*2}})\bar{n}_1q_2^*-2\frac{x_2}{\rho^*}\bar{n}_1(q_1^{*2}-q_2^{*2})]$$

$$(\pi c)^c_{12} = \frac{G(1+\nu)}{2\pi\rho^*}[-(q_1^{*2}-q_2^{*2})q_n^*-16\frac{x_2\bar{x}_2}{\rho^{*2}}(\bar{n}_1q_1^*q_2^{*2}-\bar{n}_2q_1^{*2}q_2^*)]$$

$$+\frac{G(1+\nu)}{2\pi\rho^*}[4\frac{x_2\bar{x}_2}{\rho^{*2}}(\bar{n}_1q_1^*-\bar{n}_2q_2^*)-2\frac{x_2}{\rho^*}\bar{n}_2(q_1^{*2}-q_2^{*2})]$$

(b.4)

$$(\pi c)^c_{21} = \frac{G(1+\nu)}{2\pi\rho^*}[-(q_1^{*2}-q_2^{*2})q_n^*+16\frac{x_2\bar{x}_2}{\rho^{*2}}(\bar{n}_1q_1^*q_2^{*2}-\bar{n}_2q_1^{*2}q_2^*)]$$

$$+\frac{G(1+\nu)}{2\pi\rho^*}[-4\frac{x_2\bar{x}_2}{\rho^{*2}}(\bar{n}_1q_1^*-\bar{n}_2q_2^*)-2\frac{x_2}{\rho^*}(\bar{n}_2q_1^{*2}-4\bar{n}_1q_1^*q_2^*-\bar{n}_2q_2^*s)]$$

$$(\pi c)^c_{22} = \frac{G(1+\nu)}{2\pi\rho^*}[-2(1+8\frac{x_2\bar{x}_2}{\rho^{*2}})q_1^* q_2^* q_n^* + (-1+4\frac{x_2\bar{x}_2}{\rho^{*2}})\bar{n}_2 q_1^*]$$

$$+ \frac{G(1+\nu)}{2\pi\rho^*}[(1+4\frac{x_2\bar{x}_2}{\rho^{*2}})\bar{n}_1 q_2^* - 2\frac{x_2}{\rho^*}\bar{n}_1(q_1^{*2} - q_2^{*2})]$$

where

$$\rho_1^* = x_1 - \bar{x}_1 \qquad \rho_2^* = -x_2 - \bar{x}_2 \tag{b.5}$$

$$\rho^{*2} = \rho_1^{*2} + \rho_2^{*2} \tag{b.6}$$

$$q_1^* = \frac{x_1 - \bar{x}_1}{\rho^*} \qquad q_2^* = \frac{-x_2 - \bar{x}_2}{\rho^*} \tag{b.7}$$

$$q_n^* = \frac{\rho_1^* \bar{n}_1 + \rho_2^* \bar{n}_2}{\rho^*} \tag{b.8}$$

$$\theta = \arctan \frac{\rho_2^*}{\rho_1^*} \tag{b.9}$$

and G, ν are the shear modulus and Poisson's ratio, respectively. For plane strain, ν must be replaced by $\nu/(1-\nu)$.

The half-plane influence functions $(\ )^h$ can be written as

$$(\ )^h = (\ ) + (\ )^c$$

where ( ) are given in Appendix A.

Appendix C Anti-plane Elasticity Influence Functions

The influence functions associted with antiplane strains can be written as in [79]

$$(uR)_{33} = -\frac{1}{2\pi G}\log\rho \tag{c.1}$$

$$(uc)_{33} = \frac{1}{2\pi\rho}[\bar{n}_1 q_1 + \bar{n}_2 q_2] \tag{c.2}$$

$$(\pi R)_{33} = -\frac{1}{2\pi}\hat{\theta} \tag{c.3}$$

$$(\pi c)_{33} = \frac{G}{2\pi\rho}[-\bar{n}_1 q_2 + \bar{n}_2 q_1] \tag{c.4}$$

where

$$\rho = [(x_1 - \bar{x}_1)^2 + (x_2 - \bar{x}_2)^2]^{1/2} \tag{c.5}$$

$$q_1 = \frac{x_1 - \bar{x}_1}{\rho}, \qquad q_2 = \frac{x_2 - \bar{x}_2}{\rho} \tag{c.6}$$

$$\hat{\theta} = \arctan\left[\frac{q_2\bar{n}_1 - q_1\bar{n}_2}{q_1\bar{n}_1 + q_2\bar{n}_2}\right] \tag{c.7}$$

and G is the shear modulus.

Appendix D Reduction of Domain Integrals to Boundary Integrals

Here we remove the domain integrals involving the temperature gradient. According to the Divergence Theorem and Green's Second Identity, i.e.

$$\int_{\Omega} f_{,j}\, dS = \oint_{\Gamma_b} f\, n_j\, ds \tag{d.1}$$

$$\int_{\Omega} (f\nabla^2 g - g\nabla^2 f)\, dS = \oint_{\Gamma_b - \Gamma_c} (f\frac{\partial g}{\partial n} - g\frac{\partial f}{\partial n})\, ds \tag{d.2}$$

the domain integral terms in eqs.(4.3) can be transformed to boundary integral terms as follows,

$$\begin{aligned}
&\int_{\Omega} (uR)_{ij}(\mathbf{x},\hat{\mathbf{x}})[-\gamma T_{,j}(\hat{\mathbf{x}})]\, dS(\hat{\mathbf{x}}) \\
&= \int_{\Omega} [(uR)_{ij,j}(\mathbf{x},\hat{\mathbf{x}})\gamma T(\hat{\mathbf{x}}) - [(uR)_{ij}(\mathbf{x},\hat{\mathbf{x}})\gamma T(\hat{\mathbf{x}})]_{,j}]\, dS(\hat{\mathbf{x}}) \\
&= \int_{\Omega} [T(\hat{\mathbf{x}})\nabla^2 (uR)_{i3}(\mathbf{x},\hat{\mathbf{x}}) - (uR)_{i3}(\mathbf{x},\hat{\mathbf{x}})\nabla^2 T(\hat{\mathbf{x}})]\, dS(\hat{\mathbf{x}}) - \oint_{\Gamma_b} (uR)_{ij}(\mathbf{x},\bar{\mathbf{x}})\gamma n_j T(\bar{\mathbf{x}})\, ds(\bar{\mathbf{x}}) \\
&= \oint_{\Gamma_b - \Gamma_c} [T(\bar{\mathbf{x}})\frac{\partial}{\partial n}(uR)_{i3}(\mathbf{x},\bar{\mathbf{x}}) - (uR)_{i3}(\mathbf{x},\bar{\mathbf{x}})\frac{\partial}{\partial n}T(\bar{\mathbf{x}})]\, ds(\bar{\mathbf{x}}) - \oint_{\Gamma_b} (uR)_{ij}(\mathbf{x},\bar{\mathbf{x}})\gamma n_j T(\bar{\mathbf{x}})\, ds(\bar{\mathbf{x}}) \\
&= \oint_{\Gamma_b - \Gamma_c} [(uc)_{i3}(\mathbf{x},\bar{\mathbf{x}})T(\bar{\mathbf{x}}) - (uR)_{i3}(\mathbf{x},\bar{\mathbf{x}})q_n(\bar{\mathbf{x}})]\, ds(\bar{\mathbf{x}}) - \oint_{\Gamma_b} (uR)_{ij}(\mathbf{x},\bar{\mathbf{x}})\gamma n_j T(\bar{\mathbf{x}})\, ds(\bar{\mathbf{x}})
\end{aligned} \tag{d.3}$$

where

$$(uR)_{ij,j}(\mathbf{x},\hat{\mathbf{x}}) = \nabla^2 (uR)_{i3}(\mathbf{x},\hat{\mathbf{x}}) \qquad \nabla^2 T(\hat{\mathbf{x}}) = 0$$

$$q_n(\bar{\mathbf{x}}) = \frac{\partial}{\partial n} T(\bar{\mathbf{x}}) \qquad (uc)_{i3}(\mathbf{x},\bar{\mathbf{x}}) = \frac{\partial}{\partial n} (uR)_{i3}(\mathbf{x},\bar{\mathbf{x}}) \ . \tag{d.4}$$

All the problems discussed in this Dissertation involve a finite region with a crack. The boundary Γ consists of two parts, namely the external boundary Γ_b and the crack surface Γ_c. The upper face Γ_c^+ and the lower face Γ_c^- of the crack surface differ only in their normal, so that $n^+ = - n^-$. We make use of the apparent relations of symmetry:

$$T^-(\bar{\mathbf{x}}) = T^+(\bar{\mathbf{x}}) \qquad q_n^-(\bar{\mathbf{x}}) = - q_n^+(\bar{\mathbf{x}})$$

$$(uc)_{i3}^-(\mathbf{x},\bar{\mathbf{x}}) = - (uc)_{i3}^+(\mathbf{x},\bar{\mathbf{x}}) \qquad (uR)_{i3}^-(\mathbf{x},\bar{\mathbf{x}}) = (uR)_{i3}^+(\mathbf{x},\bar{\mathbf{x}}) \ . \tag{d.5}$$

The first integral in eqs.(d.3) can be expressed as follows,

$$\begin{aligned}
&\oint_{\Gamma_b - \Gamma_c} [(uc)_{i3}(\mathbf{x},\bar{\mathbf{x}})T(\bar{\mathbf{x}}) - (uR)_{i3}(\mathbf{x},\bar{\mathbf{x}})q_n(\bar{\mathbf{x}})]\, ds(\bar{\mathbf{x}}) \\
&= \oint_{\Gamma_b} [(uc)_{i3}(\mathbf{x},\bar{\mathbf{x}})T(\bar{\mathbf{x}}) - (uR)_{i3}(\mathbf{x},\bar{\mathbf{x}})q_n(\bar{\mathbf{x}})]\, ds(\bar{\mathbf{x}}) \\
&- \oint_{\Gamma_c^-} [(uc)_{i3}^-(\mathbf{x},\bar{\mathbf{x}})T^-(\bar{\mathbf{x}}) - (uR)_{i3}^-(\mathbf{x},\bar{\mathbf{x}})q_n^-(\bar{\mathbf{x}})]\, ds(\bar{\mathbf{x}}) \\
&- \oint_{\Gamma_c^+} [(uc)_{i3}^+(\mathbf{x},\bar{\mathbf{x}})T^+(\bar{\mathbf{x}}) - (uR)_{i3}^+(\mathbf{x},\bar{\mathbf{x}})q_n^+(\bar{\mathbf{x}})]\, ds(\bar{\mathbf{x}}) \\
&= \oint_{\Gamma_b} [(uc)_{i3}(\mathbf{x},\bar{\mathbf{x}})T(\bar{\mathbf{x}}) - (uR)_{i3}(\mathbf{x},\bar{\mathbf{x}})q_n(\bar{\mathbf{x}})]\, ds(\bar{\mathbf{x}}) - \oint_{\Gamma_c^-} (uc)_{i3}^-(\mathbf{x},\bar{\mathbf{x}})\Delta T(\bar{\mathbf{x}})\, ds(\bar{\mathbf{x}}) \\
&= \oint_{\Gamma_b} [(uc)_{i3}(\mathbf{x},\bar{\mathbf{x}})T(\bar{\mathbf{x}}) - (uR)_{i3}(\mathbf{x},\bar{\mathbf{x}})q_n(\bar{\mathbf{x}})]\, ds(\bar{\mathbf{x}}) - \oint_{\Gamma_c} (uc)_{i3}(\mathbf{x},\bar{\mathbf{x}})\Delta T(\bar{\mathbf{x}})\, ds(\bar{\mathbf{x}}) \ .
\end{aligned} \tag{d.6}$$

Following the same approach as above, the domain integral terms in eqs.(4.3) can be expressed as follows,

$$\int_{\Omega}(\pi R)_{ij}(\mathbf{x},\hat{\mathbf{x}})[-\gamma T_{,j}(\hat{\mathbf{x}})]\, dS(\hat{\mathbf{x}})$$

$$= \oint_{\Gamma_b} [(\pi c)_{i3}(\mathbf{x},\bar{\mathbf{x}})T(\bar{\mathbf{x}}) - (\pi R)_{i3}(\mathbf{x},\bar{\mathbf{x}})q_n(\bar{\mathbf{x}})]\, ds(\bar{\mathbf{x}}) \tag{d.7}$$

$$- \oint_{\Gamma_c} (\pi c)_{i3}(\mathbf{x},\bar{\mathbf{x}})\Delta T(\bar{\mathbf{x}})\, ds(\bar{\mathbf{x}}) - \oint_{\Gamma_b}(\pi R)_{ij}(\mathbf{x},\bar{\mathbf{x}})\gamma n_j T(\bar{\mathbf{x}})\, ds(\bar{\mathbf{x}})$$

where

$$(\pi R)_{ij,j}(\mathbf{x},\hat{\mathbf{x}}) = \nabla^2(\pi R)_{i3}(\mathbf{x},\hat{\mathbf{x}}) \qquad (\pi c)_{i3}(\mathbf{x},\bar{\mathbf{x}}) = \frac{\partial}{\partial n}(\pi R)_{i3}(\mathbf{x},\bar{\mathbf{x}}) \ . \tag{d.8}$$

Appendix E Heat Transfer Influence Functions

The influence functions for plane stress can be written as in [59]

$$(uR)_{i3} = \frac{(1+\nu)\alpha_t}{8\pi}[1+2\log\rho]\rho_i \tag{e.1}$$

$$(uc)_{i3} = \frac{(1+\nu)\alpha_t}{8\pi}[(1+2\log\rho)\bar{n}_i+2q_iq_k\bar{n}_k] \tag{e.2}$$

$$(\pi R)_{13} = -\frac{\gamma}{8\pi}[4\rho_1\hat{\theta}+(4\nu\log\rho - (1-\nu))\rho_2]$$

$$(\pi R)_{23} = +\frac{\gamma}{8\pi}[(4\nu\log\rho - (1-\nu))\rho_1+4\rho_2\hat{\theta}] \tag{e.3}$$

$$(\pi c)_{13} = -\frac{\gamma}{8\pi}[(4\nu\rho_2q_1+4\hat{\theta}-4\rho_1\rho_2)\bar{n}_1+(4\nu\log\rho-(1-\nu)+4\nu\rho_2q_2+4\rho_1^2)\bar{n}_2]$$

$$(\pi c)_{23} = +\frac{\gamma}{8\pi}[(4\nu\log\rho-(1-\nu)+4\nu\rho_1q_1-4\rho_2^2)\bar{n}_1+(4\nu\rho_1q_2+4\hat{\theta}+4\rho_1\rho_2)\bar{n}_2] \tag{e.4}$$

where

$$\rho_1 = x_1 - \bar{x}_1 \qquad \rho_2 = x_2 - \bar{x}_2 \tag{e.5}$$

$$\rho = [(x_1 - \bar{x}_1)^2 + (x_2 - \bar{x}_2)^2]^{1/2} \tag{e.6}$$

$$q_1 = \frac{x_1 - \bar{x}_1}{\rho}, \quad q_2 = \frac{x_2 - \bar{x}_2}{\rho} \tag{e.7}$$

$$\hat{\theta} = \arctan\left[\frac{q_2\bar{n}_1 - q_1\bar{n}_2}{q_1\bar{n}_1 + q_2\bar{n}_2}\right] \tag{e.8}$$

$$\gamma = 2G\frac{1+\nu}{1-\nu}\alpha_t \tag{e.9}$$

and G, ν , α_t are the shear modulus, Poisson's ratio and thermal expansion coefficient, respectively. For plane strain, ν must be replaced by $\nu/(1-\nu)$ and α_t must be replaced by $(1+\nu)\alpha_t$.

$$(\pi R)_{i3} = -G\int_0^s [(uR)_{i3'n} + (uR)_{k3,i3}n_k + \frac{2\nu}{1-\nu}(uR)_{k3'k3}n_i]\, ds$$

(e.10)

$$(\pi c)_{i3} = \frac{\partial}{\partial n}(\pi R)_{i3} \quad .$$

Appendix F Computer Program for Matrices

```
C CCCCCCCCCCCCCCCCCCCCCCCCCCCCCCCCCCCCCCCCCCCCCCCCCCCCCCCCCCCCCCCCCCCCCC
C
C COMPUTE MATRICES [X] ; [Q] ; [UC] [UR] ; [PC] [PR]
C
C CCCCCCCCCCCCCCCCCCCCCCCCCCCCCCCCCCCCCCCCCCCCCCCCCCCCCCCCCCCCCCCCCCCCCC
C
C                    ****************************
C                    *                          *
C         1.         *          CRACK           *
C                    *                          *
C                    ****************************
C
C ----- MESH LOOP ON CRACK
      DO 1101 J=1,N
      DO 1101 K=1,2
      JK=J-2+K
      IF(JK.EQ.0) JK=N
C ---  THE COLUMN OF THE COEFFICIENT MATRIX
      JK2=2*JK
      JK1=JK2-1
C ----- MESH LOOP ON CRACK
      DO 1101 I=1,N
      II2=2*I
      II1=II2-1
C ---  FIELD POINTS (MID-POINT OF CRACK MESH)
```

```
      XM1=(XB(I)+XB(I+1))/2.
      YM1=(YB(I)+YB(I+1))/2.
C ----- LOOP ON GAUSS POINTS
      DO 1103 L=1,12
      X=0.
      Y=0.
      DX=0.
      DY=0.
C ---  SOURCE POINTS AND THEIR DIFFERENTIATIONS
      DO 1107 KK=1,2
      JKK=J-1+KK
      X=X+XB(JKK)*PHI(KK,L)
      Y=Y+YB(JKK)*PHI(KK,L)
      DX=DX+XB(JKK)*DPHI(KK,L)
1107  DY=DY+YB(JKK)*DPHI(KK,L)
C
      RR=(XM1-X)**2+(YM1-Y)**2
      RR=DSQRT(RR)
      QX=(XM1-X)/RR
      QY=(YM1-Y)/RR
      QX3=QX*QX*QX
      QY3=QY*QY*QY
C ---  INFLUENCE FUNCTIONS
      C11=G*(1.+PR)/(2.*PI)
      CON1=C11*(-2.*DX*QX3+2.*DY*QY3+DX*QX-3.*DY*QY)/RR
```

```
      CON2=C11*(2.*DY*QX3+2.*DX*QY3-DY*QX-DX*QY)/RR
      CON3=C11*(2.*DX*QX3-2.*DY*QY3-3.*DX*QX+DY*QY)/RR
C ---  ENDPOINT EXCEPT CRACK TIPS
      IF(JK.EQ.N) GOTO 1101
      A1(II1,JK1)=A1(II1,JK1)+W(L)*PHI(K,L)*CON1
      A1(II1,JK2)=A1(II1,JK2)+W(L)*PHI(K,L)*CON2
      A1(II2,JK1)=A1(II2,JK1)+W(L)*PHI(K,L)*CON2
      A1(II2,JK2)=A1(II2,JK2)+W(L)*PHI(K,L)*CON3
C
1103  CONTINUE
1101  CONTINUE
C
C                    *****************************
C                    *                           *
C          2.        *       CRACK FIELD         *
C                    *                           *
C                    *****************************
C
C ----- MESH LOOP ON THE CLOSED BOUNDARY
      DO 1104 I=1,M
      II2=2*I
      II1=II2-1
C ----- MESH LOOP ON CRACK
      DO 1104 J=1,N
      DO 1104 K=1,2
```

```
      JK=J-2+K
      IF(JK.EQ.0) JK=N
      JK2=JK*2
      JK1=JK2-1
      DO 1106 L=1,12
      X=0.
      Y=0.
      DX=0.
      DY=0.
      DO 1108 KK=1,2
      JKK=J-1+KK
      X=X+XB(JKK)*PHI(KK,L)
      Y=Y+YB(JKK)*PHI(KK,L)
      DX=DX+XB(JKK)*DPHI(KK,L)
1108  DY=DY+YB(JKK)*DPHI(KK,L)
C
      RR=(XF(I)-X)**2+(YF(I)-Y)**2
      RR=DSQRT(RR)
      QX=(XF(I)-X)/RR
      QY=(YF(I)-Y)/RR
      QX3=QX*QX*QX
      QY3=QY*QY*QY
C
      C1=1.+PR
      C2=1.-PR
```

```
      C3=3.+PR
      C4=3.-PR
      C5=1.+3.*PR
C
      T11=(2.*C1*(DY*QX3+DX*QY3)+C2*DY*QX-C3*DX*QY)/(4.*PI*RR)
      T21=(2.*C1*(DX*QX3-DY*QY3)-C5*DX*QX+C3*DY*QY)/(4.*PI*RR)
      T12=(2.*C1*(DX*QX3-DY*QY3)-C3*DX*QX+C5*DY*QY)/(4.*PI*RR)
      T22=(2.*C1*(-DY*QX3-DX*QY3)+C3*DY*QX-C2*DX*QY)/(4.*PI*RR)
C
      IF(JK.EQ.N) GOTO 1104
      Q(II1,JK1)=Q(II1,JK1)+W(L)*PHI(K,L)*T11
      Q(II1,JK2)=Q(II1,JK2)+W(L)*PHI(K,L)*T21
      Q(II2,JK1)=Q(II2,JK1)+W(L)*PHI(K,L)*T12
      Q(II2,JK2)=Q(II2,JK2)+W(L)*PHI(K,L)*T22
1106  CONTINUE
1104  CONTINUE
C
C                    ******************************
C                    *                            *
C        3.          *          ELASLIN           *
C                    *                            *
C                    ******************************
C
C ----- MESH LOOP ON BOUNDARY (SOURCE POINTS)
      DO 2101 J=1,M
```

```
      JJ=J-2
      DO 2101 K=1,2
      JK=JJ+K
      JKJ=JK+J
      IF(JK.EQ.0) JK=M
C ---  THE COLUMN OF THE COEFFICIENT MATRIX
      JK2=2*JK
      JKJ2=2*JKJ
      JKJ1=JKJ2-1
C ----- MESH LOOP ON BOUNDARY (FIELD POINTS)
      DO 2101 I=1,M
      II2=2*I
      II1=II2-1
C ---  LOOP ON GAUSS POINTS
      DO 2103 L=1,12
      X=0.
      Y=0.
      DX=0.
      DY=0.
C ---  SOURCE POINTS AND THEIR DIFFERENTIATIONS
      DO 2107 KK=1,2
      JKK=JJ+KK
      IF(JKK.EQ.0) JKK=M
      X=X+XF(JKK)*PHI(KK,L)
      Y=Y+YF(JKK)*PHI(KK,L)
```

```
      DX=DX+XF(JKK)*DPHI(KK,L)
2107  DY=DY+YF(JKK)*DPHI(KK,L)
C
      DS=DSQRT(DX*DX+DY*DY)
      IF(I.EQ.JK) GOTO 2108
C
      RR=(XF(I)-X)**2+(YF(I)-Y)**2
      RR=DSQRT(RR)
      QX=(XF(I)-X)/RR
      QY=(YF(I)-Y)/RR
      QX3=QX*QX*QX
      QY3=QY*QY*QY
C
      T11=(2.*C1*(DY*QX3+DX*QY3)+C2*DY*QX-C3*DX*QY)/(4.*PI*RR)
      T21=(2.*C1*(DX*QX3-DY*QY3)-C5*DX*QX+C3*DY*QY)/(4.*PI*RR)
      T12=(2.*C1*(DX*QX3-DY*QY3)-C3*DX*QX+C5*DY*QY)/(4.*PI*RR)
      T22=(2.*C1*(-DY*QX3-DX*QY3)+C3*DY*QX-C2*DX*QY)/(4.*PI*RR)
C
      UC(II1,JK1)=UC(II1,JK1)+W(L)*PHI(K,L)*T11
      UC(II1,JK2)=UC(II1,JK2)+W(L)*PHI(K,L)*T21
      UC(II2,JK1)=UC(II2,JK1)+W(L)*PHI(K,L)*T12
      UC(II2,JK2)=UC(II2,JK2)+W(L)*PHI(K,L)*T22
C
      GOTO 2109
C
```

```
C ---  SINGULARITY INTEGREL NONSINGULARITY TERMS
C
2108   J1=J-1
       IF(J1.EQ.0) J1=M
       RR=(XF(J)-XF(J1))**2+(YF(J)-YF(J1))**2
       RR=DSQRT(RR)
       QX=(XF(J)-XF(J1))/RR
       QY=(YF(J)-YF(J1))/RR
C
C ---  NONSINGULARITY INTEGREL
C
2109   U11=(-C4*LOG(RR)+C1*QX*QX)*DS/(8.*PI*G)
       U12=C1*QX*QY*DS/(8.*PI*G)
       U22=(-C4*LOG(RR)+C1*QY*QY)*DS/(8.*PI*G)
C
       UR(II1,JKJ1)=UR(II1,JKJ1)+W(L)*PHI(K,L)*U11
       UR(II1,JKJ2)=UR(II1,JKJ2)+W(L)*PHI(K,L)*U12
       UR(II2,JKJ1)=UR(II2,JKJ1)+W(L)*PHI(K,L)*U12
2103   UR(II2,JKJ2)=UR(II2,JKJ2)+W(L)*PHI(K,L)*U22
C
       IF(I.NE.JK) GOTO 2101
C
C ---  SINGULARITY INTEGERL SINGULARITY TERMS
C
       DO 2118 L=1,12
```

```
C
      X=0.
      Y=0.
      DX=0.
      DY=0.
      DO 2117 KK=1,2
      JKK=JJ+KK
      IF(JKK.EQ.0) JKK=M
      X=X+XF(JKK)*PHIL(K,KK,L)
      Y=Y+YF(JKK)*PHIL(K,KK,L)
      DX=DX+XF(JKK)*DPHIL(K,KK,L)
2117  DY=DY+YF(JKK)*DPHIL(K,KK,L)
C
      DS=DSQRT(DX*DX+DY*DY)
      UR(II1,JKJ1)=UR(II1,JKJ1)+WL(L)*PHIL(K,K,L)*C4*DS/(8.*PI*G)
      UR(II2,JKJ2)=UR(II2,JKJ2)+WL(L)*PHIL(K,K,L)*C4*DS/(8.*PI*G)
2118  CONTINUE
2101  CONTINUE
C
C ---  COMPUTE DIAGONAL ENTRIES OF UC
C
      DO 2140 I=1,M
      II2=2*I
      II1=II2-1
      DO 2140 K=1,M
```

```
      IF(K.EQ.I) GOTO 2140
      KK2=2*K
      KK1=KK2-1
      UC(II1,II1)=UC(II1,II1)-UC(II1,KK1)
      UC(II1,II2)=UC(II1,II2)-UC(II1,KK2)
      UC(II2,II1)=UC(II2,II1)-UC(II2,KK1)
      UC(II2,II2)=UC(II2,II2)-UC(II2,KK2)
2140  CONTINUE
C
C                       ******************************
C                       *                            *
C         4.            *      ELASLIN   FIELD       *
C                       *                            *
C                       ******************************
C
C ----- MESH LOOP ON CRACK (FIELD POINTS)
      DO 2113 I=1,N
      II2=2*I
      II1=II2-1
      I3=3*I
      I2=I3-1
      I1=I3-2
C ---  FIELD POINTS (MID-POINT OF CRACK MESH)
      XBM=(XB(I)+XB(I+1))/2.
      YBM=(YB(I)+YB(I+1))/2.
```

```
C ----- MESH LOOP ON BOUNDARY (SOURCE POINTS)
      DO 2113 J=1,M
      JJ=J-2
      DO 2113 K=1,2
      JK=JJ+K
      JKJ=JK+J
      IF(JK.EQ.0) JK=M
      JK2=2*JK
      JK1=JK2-1
      JKJ2=2*JKJ
      JKJ1=JKJ2-1
C ---  LOOP ON GAUSS POINTS
      DO 2115 L=1,12
      X=0.
      Y=0.
      DX=0.
      DY=0.
C ---  SOURCE POINTS
      DO 2116 KK=1,2
      JKK=JJ+KK
      IF(JKK.EQ.0) JKK=M
      X=X+XF(JKK)*PHI(KK,L)
      Y=Y+YF(JKK)*PHI(KK,L)
      DX=DX+XF(JKK)*DPHI(KK,L)
2116  DY=DY+YF(JKK)*DPHI(KK,L)
```

```
C
      DS=DSQRT(DX*DX+DY*DY)
      RNX=+DY/DS
      RNY=-DX/DS
      RR=(XBM-X)**2+(YBM-Y)**2
      RR=DSQRT(RR)
      QX=(XBM-X)/RR
      QY=(YBM-Y)/RR
      QX2=QX*QX
      QY2=QY*QY
      QX3=QX2*QX
      QY3=QY2*QY
C
      TT11=C1*G*(-2.*DX*QX3+2.*DY*QY3+DX*QX-3.*DY*QY)/(2.*PI*RR)
      TT12=C1*G*(2.*DY*QX3+2.*DX*QY3-DY*QX-DX*QY)/(2.*PI*RR)
      TT22=C1*G*(2.*DX*QX3-2.*DY*QY3-3.*DX*QX+DY*QY)/(2.*PI*RR)
C
      UC1(II1,JK1)=UC1(II1,JK1)+W(L)*PHI(K,L)*TT11
      UC1(II1,JK2)=UC1(II1,JK2)+W(L)*PHI(K,L)*TT12
      UC1(II2,JK1)=UC1(II2,JK1)+W(L)*PHI(K,L)*TT12
      UC1(II2,JK2)=UC1(II2,JK2)+W(L)*PHI(K,L)*TT22
C
      TH=DATAN((QY*RNX-QX*RNY)/(QX*RNX+QY*RNY))
      UU11=(-2.*TH-C1*QX*QY)*DS/(4.*PI)
      UU12=(+C2*LOG(RR)+C1*QX2)*DS/(4.*PI)
```

```
      UU21=(-C2*LOG(RR)-C1*QY2)*DS/(4.*PI)
      UU22=(-2.*TH+C1*QX*QY)*DS/(4.*PI)
C
      UR1(II1,JKJ1)=UR1(II1,JKJ1)+W(L)*PHI(K,L)*UU11
      UR1(II1,JKJ2)=UR1(II1,JKJ2)+W(L)*PHI(K,L)*UU12
      UR1(II2,JKJ1)=UR1(II2,JKJ1)+W(L)*PHI(K,L)*UU21
      UR1(II2,JKJ2)=UR1(II2,JKJ2)+W(L)*PHI(K,L)*UU22
C
2115  CONTINUE
2113  CONTINUE
C
C CCCCCCCCCCCCCCCCCCCCCCCCCCCCCCCCCCCCCCCCCCCCCCCCCCCCCCCCCCCCCCCCCCCC
C
C CREATE MATRIX GAMMA2
C MULTIPLICATIONS ( [A]=[GAM]*[X]; [A21]=[GAM]*[PC]; [GY]=[GAM]*[PR] )
C
C CCCCCCCCCCCCCCCCCCCCCCCCCCCCCCCCCCCCCCCCCCCCCCCCCCCCCCCCCCCCCCCCCCCC
C
      DO 1202 I=1,NN2M2
      DD=1.
      GAM(I,I)=+DD
      GAM(I,I+2)=-DD
1202  CONTINUE
C
      DO 1204 I=1,NN2M2
```

```
      DO 1204 J=1,NN2M2
      A(I,J)=0.
      DO 1203 K=1,NN2
1203  A(I,J)=A(I,J)-GAM(I,K)*A1(K,J)
1204  CONTINUE
C
      DO 230 I=1,NN2M2
      DO 230 J=1,MM2
      J2=2*J
      J1=J2-1
      A21(I,J)=0.
      GY(I,J1)=0.
      GY(I,J2)=0.
      DO 225 K=1,NN2
      A21(I,J)=A21(I,J)+GAM(I,K)*UC1(K,J)
      GY(I,J1)=GY(I,J1)+GAM(I,K)*UR1(K,J1)
225   GY(I,J2)=GY(I,J2)+GAM(I,K)*UR1(K,J2)
230   CONTINUE
C
C CCCCCCCCCCCCCCCCCCCCCCCCCCCCCCCCCCCCCCCCCCCCCCCCCCCCCCCCCCCCCCCCCCCCCCCC
C
C COMPUTE RIGHT HAND SIDE METRIX [RR1] AND COEFFICIENT MATRIX [COEF]
C
C CCCCCCCCCCCCCCCCCCCCCCCCCCCCCCCCCCCCCCCCCCCCCCCCCCCCCCCCCCCCCCCCCCCCCCCC
C
```

```
      DO 310 I=1,MM2
      DO 310 J=1,MM2
      J2=J*2
      J1=J2-1
      RR1(I,J1)=UR(I,J1)
      RR1(I,J2)=UR(I,J2)
310   COEF(I,J)=UC(I,J)
C
      DO 330 I=1,MM2
      DO 330 J=1,NN2M2
      I2=I*2
      I1=I2-1
      RR1(J+MM2,I1)=GY(J,I1)
      RR1(J+MM2,I2)=GY(J,I2)
      COEF(I,J+MM2)=-Q(I,J)
330   COEF(J+MM2,I)=A21(J,I)
C
      DO 350 I=1,NN2M2
      DO 350 J=1,NN2M2
      RR1(I+MM2,I+MMR)=-1.
350   COEF(I+MM2,J+MM2)=A(I,J)
C
```